Dynamic Operability Assessment: A Mathematical Programming Approach Based on Q-Parametrization

by

Roderick Ross

Submitted in fulfilment of the requirements for the degree of

PHILOSOPHIAE DOCTOR

in the Department of Chemical Engineering
University of Cape Town, South Africa.

Promoter: Dr C.L.E. Swartz

July 1997

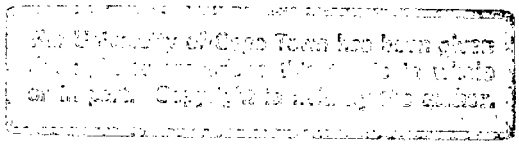

Abstract

The ability of a process plant to guarantee high product quality, in terms of low variability, is emerging as a defining feature when distinguishing between alternative suppliers. The extent to which this can be achieved is termed a plant's dynamic operability and is a function of both the plant design and the control system design. In the limit, however, the closed-loop performance is determined by the properties inherent in the plant. This realization of the interrelationship between a plant design and its achievable closed-loop performance has motivated research toward systematic techniques for screening inherently inferior designs.

Pioneering research in the early 1980's identified right-half-plane transmission zeros, time delays, input constraints and model uncertainty as factors that limit the achievable closed-loop performance of a process. Quantifying the performance-limiting effect of combinations of these factors has proven to be a challenging problem, as reflected in the literature. It is the aim of this thesis to develop a systematic procedure for dynamic operability assessment in the presence of combinations of performance-limiting factors.

The approach adopted in this thesis is based on the Q-parametrization of stabilizing linear feedback controllers and involves posing dynamic operability assessment as a mathematical programming problem. In the proposed formulation, a convex objective function, reflecting a measure of closed-loop performance, is optimized over all stable Q, subject to a set of constraints on the closed-loop behavior, which for many specifications of interest is convex. A discrete-time formulation is chosen so as to allow for the convenient handling of time delays and time-domain constraints. An important feature of the approach is that, due to the convexity, global optimality is guaranteed. Furthermore, the fact that Q parametrizes all stabilizing linear feedback controllers implies that the performance at the optimum represents the best possible performance for any such controller. The results are thus not biased by controller type or tuning, apart from the requirement that the controller be linear.

In addition to calculating closed-loop performance limits, the Q-parametrization approach also allows the incorporation of economic considerations into the problem. The basic premise is that the proximity of the operating point to the process constraints affects both the economics and the dynamic operability. The proposed formulation involves including the process setpoints as decision variables together with Q and optimizing an economic objective subject to constraints on the quality of the closed-loop behavior. In this manner, the unfavorable economic consequences of having poor dynamic operability may be quantified. Competing designs are now compared according to a common economic basis, facilitating the screening of design alternatives.

One of the key aspects of this dissertation is the treatment of structured model uncertainty for multivariable systems. The model uncertainty is assumed to be nonlinear and/or time-varying. This assumption is reasonable at the process design stage where limited information may be available regarding the nature of the uncertainty. By allowing for the uncertainty to have structure, independent sources of model error may be treated in a nonconservative manner. The resulting optimization problem is nonconvex and a hybrid solution strategy involving a combination of convex quadratic programming and standard nonlinear programming is implemented.

The optimization problems in the different formulations mentioned above are generally large and require considerable computational effort. To address this, methods are presented which exploit features of the formulations and enable reduced solution times. Particular attention is paid to exploiting the structure and sparsity of each problem and significant computational improvements have been achieved in this manner. As a result, it is now possible to determine performance limits for larger, more complicated systems.

Application of the Q-parametrization approach to a number of illustrative examples is presented in order to demonstrate the relevant problem formulation and to highlight important themes of the thesis. The importance of considering the effect of combinations of performance-limiting factors is shown in many of these examples. In particular, application of the Q-parametrization approach to multivariable distillation columns containing all four performance-limiting factors highlights the non-intuitive role that time delays may play in multivariable systems. A detailed case study involving the dynamic operability assessment of alternative three-bank flotation circuits is also presented. The purpose of the study is to use dynamic operability in conjunction with steady-state economic considerations to screen out inherently inferior flowsheets. Two different implementations of the Q-parametrization approach are applied to the problem and the results obtained are compared and discussed. The study illustrates a number of important points involving the trade-off between economics and dynamic operability, as well as the importance of clearly defining control objectives.

It is recommended that future research in this field should target the issue of nonlinear control, particularly its ability to improve both dynamic operability and steady-state economics. Finally, research should focus on developing methods to detect process bottlenecks systematically, to improve the operability of given designs and, ultimately, to synthesize designs which are both operable and economical.

Acknowledgments

I should like to thank Dr Chris Swartz for his excellent supervision of this research project from the conceptual stages through to its completion. I am most grateful to have had a supervisor of his caliber and I have learned much under his guidance. Thank you very much for your encouragement and friendly nature, both of which considerably enhanced the learning experience.

Next, I should like to thank my parents, my sister and my immediate family for all their thoughts, encouragement and prayers. In particular, I should like to thank my dad for helping me check the final drafts of this thesis. I really appreciate the interest that you, my family, have taken in my studies and thank you for the opportunities which have been made possible to me as a result of your foresight and planning.

A grateful word of acknowledgment goes to all those involved indirectly with my research at UCT. To Bill Randall, Craig Balfour and Granville de la Cruz for their assistance with hardware and software issues. To my fellow students in the Process Systems group: Trevor Hadley, Jarrod Hart, Clifford Meyer, Mark Seager and Julian Young; thank you for all your help and kind assistance and for making the office a fruitful environment in which to work. Thanks go, in particular, to Jarrod Hart for his expert assistance with graphics-related issues. Thanks also go to Rolf Poser for his endless patience and excellent assistance with regard to the administration of our UNIX workstations and for providing significant motivation during the latter stages of this project.

Special thanks go to Mintek for generous financial support of this research project and to Joachim Schubert for his comments regarding flotation circuit modelling. I should also like to thank the Foundation for Research Development for providing financial support for this project and, in particular, for funding my attendance at a Robust Control Professional Program held at the Massachusetts Institute of Technology (MIT). The insights which I gained and the contacts which I made at that course were most beneficial to my studies and I am dearly grateful for these.

I should like to thank Professors Ragu Balakrishnan, Eric Feron and Stephen Hall for their excellent course on Linear Matrix Inequalities which I attended at MIT. I am also indebted to Professor Gill for kindly allowing me to have a beta version of his excellent software for solving sparse optimization problems; and to Professors Margaret Wright and Michael Saunders for pointing me in the direction of Professor Gill and for their explanations regarding the merits of various LSSOL routines. I should also like to thank Irv Lustig for his recommendations

with regard to the formulation of sparse constrained least-squares problems.

To *all* my friends who have been by my side through the duration of this project - thank you for your support and kindness. I really appreciate all the phone calls and e-mails of encouragement. Thank you also for granting me the freedom to be myself and for continuing to love me despite that.

I should also like to thank my favorite guitarist, Phil Keaggy, for his excellent CDs which helped me to "get beyond midnight" and which lifted my spirits.

Lastly, I would like to thank God Almighty for being the source of my energy and ability and for keeping the following promise to me throughout my life:

> *I the Lord Your God hold your future in the palm of my hands. As you continue to step out in the paths before you I will bless you. Don't be afraid, for I am before you, and behind you and alongside you. I have seen your heart and I know your desires and I will place my seal upon them.*

Contents

Appendices

List of Figures

List of Tables

Chapter 1

Introduction

Plant operability is concerned with the issues involved in the day-to-day operation of chemical engineering processes. It is a broad term used to cover aspects such as plant safety, reliability, start-up, shut-down, flexibility and dynamic operability. Of these issues, dynamic operability forms the focus of this thesis.

Dynamic operability is a measure of the quality of control that can be achieved for a plant by feedback (Morari, 1983). While dynamic operability is a post-design phenomenon it is an implicit result of the plant design and should be given attention during all stages of design. Historically, plants have been designed in a sequential manner, with process design preceding control system design. The weakness with this approach is that often the expected economic performance cannot be achieved due to operational difficulties. In other cases, sophisticated control technology is needed to treat operability problems which could have been alleviated with simple design modifications had they been given attention in the early design stages (Downs and Doss, 1991).

The importance of systematically assessing dynamic operability is growing as plants are being pushed toward their limits and have little additional capability to deal with process upsets. This is a consequence of the modern production environment where greater process integration, tighter design margins, stricter environmental regulations and the requirement for decreased product variability have all placed increased pressure on plant control systems.

Pioneering research by Morari (1983) made use of the Internal Model Control framework to show that the factors which limit the achievable closed-loop performance of a process are right-half-plane zeros, time delays, input constraints and model uncertainty. Subsequent

research attempted to quantify the performance limits for individual performance-limiting factors. Determining a limit of performance in the presence of combinations of these factors has proved to be a challenging problem, as reflected in the literature, and is the focus of this thesis.

The approach adopted is based on Q-parametrization and poses dynamic operability assessment as a mathematical programming problem. An important feature of this formulation, which distinguishes it from other approaches, is that the optimization problem, for many specifications of interest, is convex and thus global optimality is ensured. Furthermore, the fact that Q parametrizes all stabilizing linear feedback controllers implies that the performance at the optimum represents a limit of achievable closed-loop performance for any such controller. The results are thus not biased by controller type or tuning, apart from the fact that the controller is linear.

In addition to determining performance limits at fixed operating conditions, the Q-parametrization approach facilitates the incorporation of economic considerations into the problem formulation. This is done by including the operating conditions as decision variables together with Q and optimizing an economic performance objective subject to constraints on the quality of the closed-loop behavior. The constraints include both time-domain bounds on the inputs and outputs as well as a weighted sum-of-square-error bound on the output behavior. As a result, competing designs may be compared on a common economic basis, facilitating the screening of inferior designs.

The thesis is structured as follows: Chapter 2 provides a review of systematic approaches to plant operability assessment and provides motivation for research in this field. Chapter 3 treats the application of the Q-parametrization approach to dynamic operability assessment in the absence of model uncertainty. A background to Q-parametrization theory is provided and the details of the mathematical programming formulation are presented. Extensions of the basic formulation to include economic considerations are also dealt with. Illustrative application examples are presented to highlight some of the important issues introduced during the course of the thesis.

The treatment of performance limits in the presence of structured model uncertainty is the focus of Chapter 4. A background to robust control theory is provided and three commonly used approaches to robust control are discussed; namely the structured singular value framework, the framework of the passivity theorem with multipliers, and the ℓ_1 robust control framework. The applicability and suitability of each of these frameworks to dynamic operability assessment is also discussed. It is argued that the ℓ_1 approach is very suitable due to

its assumptions regarding the nature of the expected model uncertainty and its mathematical convenience. The mathematical formulation of the dynamic operability assessment problem in the presence of structured model uncertainty is presented, solution strategies are discussed and its application demonstrated on an example problem.

Chapter 5 deals in greater detail with the different problem formulations and shows how special features of the problem structure may be exploited to reduce solution time. It is shown how, in the absence of model uncertainty, the Q-parametrization framework may be posed in an open-loop manner. The theoretical and computational implications of the open-loop formulation are discussed and highlighted through illustrative examples. An alternative measure of dynamic operability, namely the maximum tolerable disturbance range, is introduced and its applicability to certain problems is discussed. The possible benefits of nonlinear control are explored briefly using the open-loop formulation. Finally, a multi-rate formulation is presented which allows for approximate solutions to be calculated very rapidly.

In Chapter 6, the application of the Q-parametrization approach to the screening of alternative three-bank flotation circuits is examined. Two different formulations of the Q-parametrization approach are applied to the problem. The first approach assesses a limit achievable control performance at a fixed operating point and uses this in conjunction with a steady-state economic measure to generate a noninferior set of flowsheets. In this manner circuits which have both poor economics and dynamic operability are screened from further consideration. The second approach involves determining the operating conditions which maximize some economic measure subject to constraints on the quality of the closed-loop performance. This enables a comparison of alternative circuits according to a common economic basis and facilitates the screening of design alternatives. The two approaches are closely related and the results obtained are compared and discussed. Throughout the study the trade-off between the different performance-limiting factors, as well as the importance of specifying an appropriate performance objective, are explored.

Finally, in Chapter 7 conclusions are drawn and recommendations for future research in this field are made.

Chapter 2

Systematic Approaches to Plant Operability Assessment - A Review

2.1 Background

In the modern production environment there is a growing need to guarantee product quality despite operational uncertainties. To achieve this goal in an economically efficient manner, it has been argued that control and operability issues should be considered simultaneously with the plant design. Such considerations are not unique to control, as the use of waste minimization strategies in environmental engineering has shown that waste prevention, through correct and thoughtful design, is far more cost effective than waste treatment. Plant operability analysis is thus simply another application of the philosophy that "prevention is better than cure".

Plant operability is increasing in importance and is expected to remain a critical issue in process design (Downs and Doss, 1991). Some of the main factors that have contributed to the growing need for incorporating operability into the plant design are:

1. The quality revolution which started in the consumer products industries has effected the supply chain and quality is now being defined both in terms of specifications on absolute levels and in terms of product variability (Downs and Doss, 1991; Downs and Ogunnaike, 1995).

2. Uncertain markets have meant that a plant design must be capable of handling a wide

range of operating conditions.

3. Strict environmental regulations pertaining to emissions and waste, including off-specification products, have meant that plants have to operate consistently at their desired conditions.

The achievement of designs meeting the above criteria is made difficult by the fact that economic considerations would tend to force designs in the "opposite direction". Examples of the modern economic issues resulting in designs with operational difficulties are:

1. Increases in raw material and energy costs have led to the need for greater process integration. This has resulted in operability problems as variability in certain streams now has a greater zone of effect than would previously have been the case. In other words, process upsets now propagate more freely throughout the plant.

2. Forces present in the capital arena have pushed to minimize the upfront capital cost of a plant and have led to tighter design margins, fewer surge tanks and less surplus capacity to deal with process upsets. The result is that process equipment cannot handle as wide a range of operating conditions as before and so infeasible operation is more likely.

A trade-off thus exists between steady-state economic considerations and plant operability. While this is true, it should be noted that in order for the anticipated economic benefit to be achievable, a plant must be operable. Furthermore, optimizing a plant's economic performance during operation requires both good regulatory control behavior, termed dynamic operability, as well as good supervisory control behavior, termed flexibility (Mathisen and Skogestad, 1992). Therefore it is not entirely fair to view operability considerations as being negative from an economical point of view. Just as waste minimization may have economic benefits for a process, so too can good operability be of economic benefit.

The need for good operability in the current design environment has placed considerable pressure on plants' control systems. In dealing with this issue, two fundamentally different approaches may be adopted, namely:

1. to develop advanced control strategies and algorithms to achieve satisfactory closed-loop performance despite the above-mentioned adverse conditions, and/or

2. to develop systematic methods to analyze and deal with the sources of the operability problems rather than merely treating their symptoms.

The latter approach has been proposed by industrial practitioners and academic researchers alike (Grossmann and Morari, 1984; Benson, 1987; Downs and Doss, 1991) who argue that only after it has been attempted to design out operational difficulties should one resort to advanced control strategies. The need is thus to integrate process design and control system design; the ultimate aim being to synthesize processes that are economically optimal and inherently easy to control. In order to achieve this goal, research has been carried out over the last decade toward developing methods that are able to:

1. predict and rule out designs with inherently inferior operability properties,
2. highlight the sources of the operability problems,
3. systematically improve the operability of a given design without seriously worsening its steady-state economics, and finally
4. synthesize designs that are optimal from an economic and operations perspective.

As synthesis will aim to achieve an optimal trade-off between economics and operability, it is essential to be able to quantify operability or to associate a cost with poor operability. In this chapter, quantitative measures of operability are reviewed for both operability analysis and synthesis. Particular emphasis is given to the issue of dynamic operability assessment, as this forms the focus of the thesis. Before continuing with a quantitative analysis of operability, two examples will first be presented to motivate further the importance of systematic procedures for operability assessment.

2.1.1 Case Studies Motivating the Need for Systematic Operability Assessment

The following two case studies deal with flexibility and dynamic operability. The aim is to highlight the importance of systematically assessing the operability of a given design.

Flexibility case study

Plant flexibility represents the ability of a plant to operate over a range of conditions while satisfying certain performance specifications (Swaney and Grossmann, 1985a). A traditional method of overcoming flexibility problems in a plant is to introduce empirical overdesign

factors. The major drawbacks associated with this approach are as follows (Grossmann and Morari, 1984):

1. The resulting flexibility is in general uncertain due the non-intuitive manner in which process interactions may affect flexibility.
2. By optimizing the plant design at a given set of operating conditions, no guarantee is available regarding the plant performance over a range of different conditions.
3. No understanding is gained on the conditions limiting plant flexibility (the process bottlenecks) and these may be overlooked due to complex interactions between units.
4. The trade-off between economics and flexibility is not quantified and the resulting design may be inferior from both an operability standpoint and an economic one.

These points are best illustrated by considering the heat exchanger network shown in Figure 2.1 (Grossmann and Morari, 1984). The goal of the network is to maintain the outlet temperatures of streams H and C_2 from Exchanger 2 at the values shown in the figure ($T_{C_2} \geq 430$ °C and $T_H \leq 410$ °C). It is assumed that the areas of Exchangers 1 and 2 are first designed using nominal values for the heat transfer coefficients of $U_1 = U_2 = 800\,\mathrm{W.m^{-2}.K^{-1}}$ and then oversized by 20% to (supposedly) improve operability.

Now, suppose that uncertainty in the estimation of the nominal heat transfer coefficients results in U_1 being 20% higher and U_2 being 20% lower than their respective nominal values. On the basis of the above assumptions, the resulting stream temperatures are shown in Figure 2.2 (Grossmann and Morari, 1984). From the figure it is clear that stream C_2 violates its requirement of $T_{C_2} \geq 430$ °C, resulting in infeasible operation.

Grossmann and Morari (1984) show that if *both* U_1 and U_2 are 20% lower than their nominal design value, corresponding to the intuitive "worst-case" condition, the network actually meets its specifications. Furthermore, if the goal of the network is to meet the temperature specifications despite variations of $\pm 20\,\%$ in the nominal values of U_1 and U_2, then this could be achieved by overdesigning Exchanger 2 by 23 % and *underdesigning* Exchanger 1 by 16 %.

From the above, it is clear that process interactions can make empirical overdesign techniques unreliable and that the identification of the "worst-case" operating conditions is not always intuitively obvious. Furthermore, it is seen that empirical overdesign techniques, apart from being economically inferior, can actually worsen operability. This suggests the need for systematic approaches to ensure flexible plant operation.

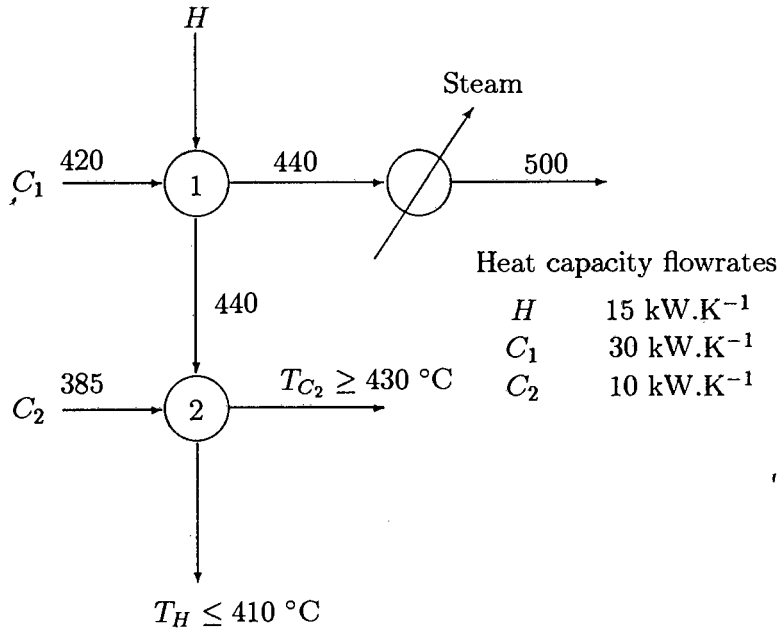

Figure 2.1: Heat exchanger network with specifications for stream C_2 and stream H.

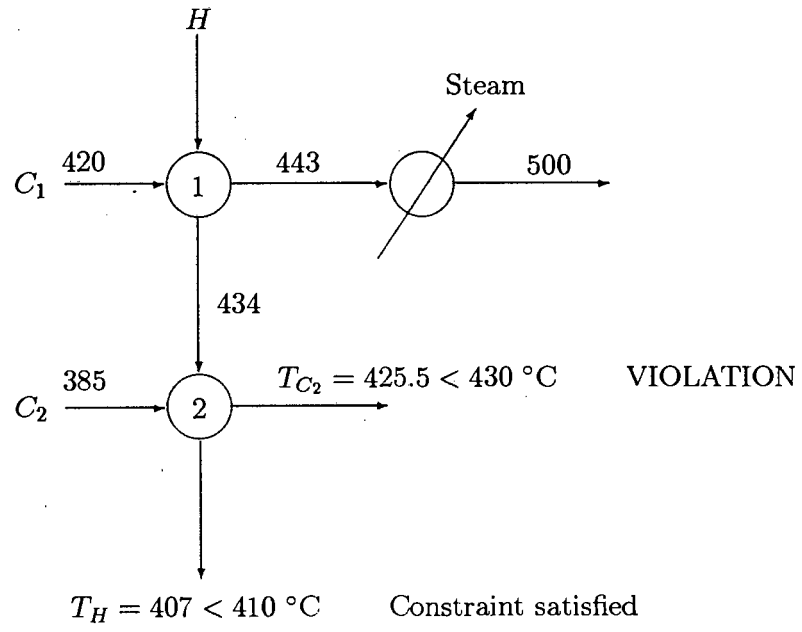

Figure 2.2: Actual performance obtained by the network as a result of uncertainty in the estimation of the heat transfer coefficients.

Dynamic operability case study

Dynamic operability is a measure of the quality of closed-loop performance achievable for a plant by feedback (Morari, 1983). The simple case study below, from Arkun (1986), serves as an introduction to the impact of model uncertainty on dynamic operability and demonstrates how some designs may be inherently more sensitive to model uncertainty. It also highlights the conflicting requirements of steady-state economics and dynamic operability. The system under consideration is the heat-integrated reactor shown in Figure 2.3 (Georgakis and Worthey, 1978; Arkun, 1986), where the parameter η denotes the extent of heat integration.

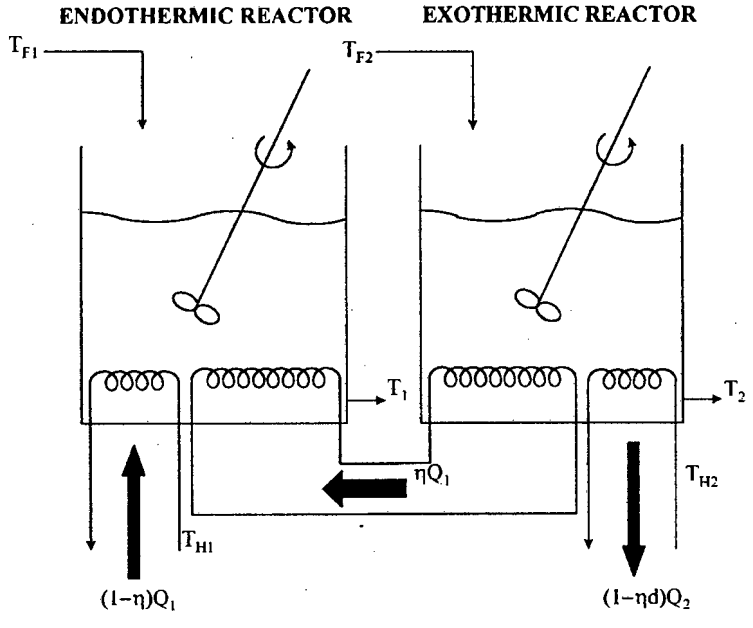

Figure 2.3: Heat integration between an exothermic and an endothermic reactor (Arkun, 1986). Here $Q_1 < Q_2$ $(d < 1)$ and $0 < \eta < 1$.

The aim of the control system is to regulate the reactor outlet temperatures by manipulating the temperature of the heating and cooling coils. Possible sources of uncertainty in the dynamic model are (i) a poor knowledge of the reaction mechanism and the reaction rate constants, as well as (ii) variations in the feed composition during operation (Arkun, 1986). Two alternative process designs are considered, differing only in the design parameters (T_{f_2} and V_2) of the exothermic reactor. Optimally tuned Internal Model Controllers are used throughout the study to prevent bias due to tuning. The tuning parameters for the nominal designs (perfect models) are referred to as the nominal tuning parameters.

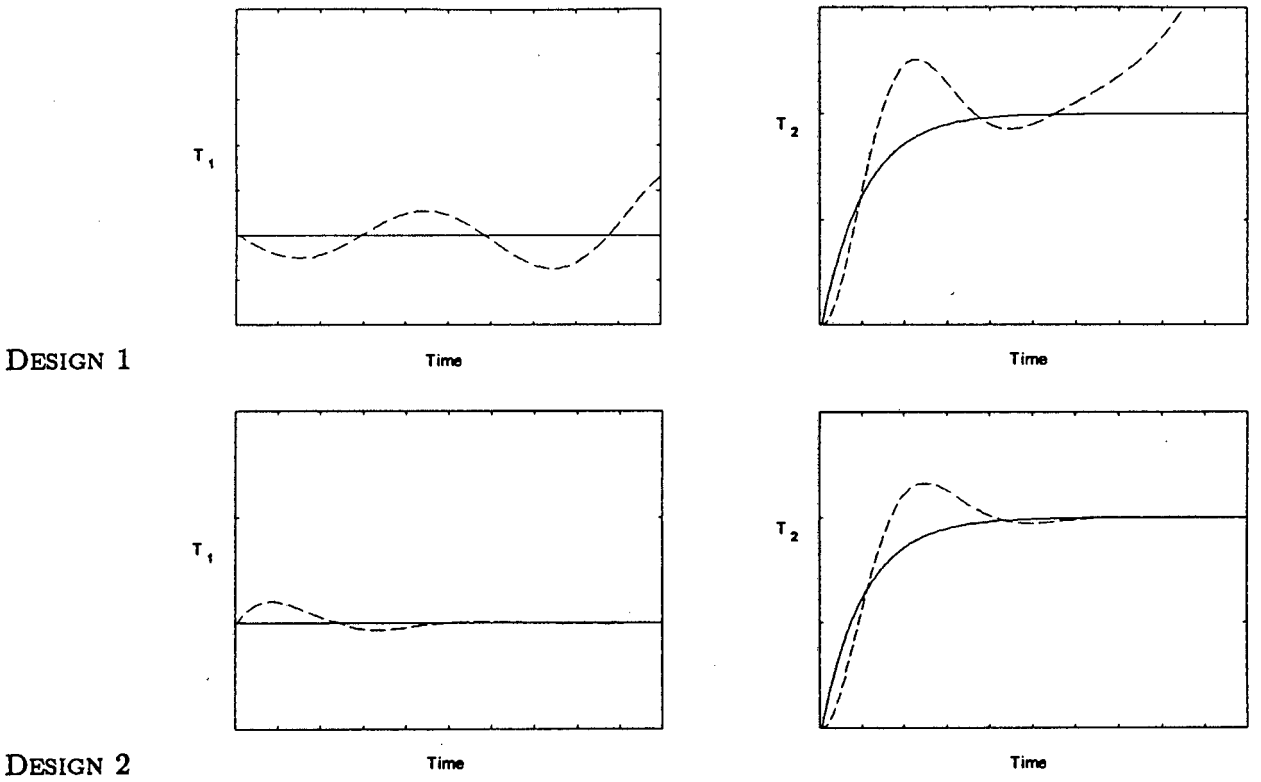

Figure 2.4: Dynamic responses of Design 1 and 2 with model error (- -) and without (-), for a unit step change in the setpoint of T_2 (Arkun, 1986).

Figure 2.4 shows the simulation results achieved for each design at a fixed degree of heat integration ($\eta = 0.2$), for a step in the temperature setpoint of the exothermic reactor, both with and without uncertainty in the reaction rate constant. From the simulation it is clear that if the dynamic models are perfect then both designs perform equally well. However, if uncertainty in the reaction rate is included, then Design 2 performs significantly better than Design 1, at the nominal tuning parameters. In fact, the closed-loop performance of Design 1 is seen to be unstable in the presence of model uncertainty. While stability could be regained by detuning the controller, this will result in Design 1 having inferior nominal performance as compared to Design 2. From the simulations above, Design 2 is seen to be inherently less sensitive than Design 1 to errors in the rate constant. Design engineers equipped with this sort of information at the early design stages are able to prevent costly modifications from being made at a later stage of the design.

Another design parameter which influences the sensitivity to model uncertainty is the degree of heat integration. Figure 2.5 (Arkun, 1986) shows the dynamic performance of Design 2, with uncertainty in the reaction rate constant, for different degrees of heat integration. It is clear from the simulations that the quality of the dynamic performance decreases with

increasing heat integration. The process thus becomes more sensitive to model uncertainty as increasing energy savings are sought.

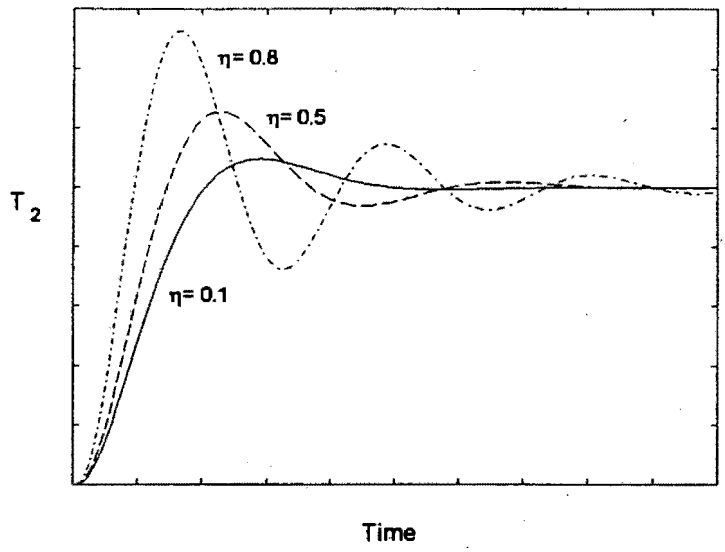

Figure 2.5: Dynamic responses of Design 2, with various degrees of heat integration η, for a unit step change in the setpoint of T_2 (Arkun, 1986).

This case study has thus shown that the sensitivity of dynamic performance to model uncertainty is a function of the process design parameters T_{f_2}, V_2 and η (Arkun, 1986). The conflict between dynamic operability and steady-state economics has also been highlighted.

Having provided a background to the importance of considering operability issues in parallel with the plant design, a review of the systematic approaches that have been developed for this purpose follows. Plant safety and reliability are dealt with first, followed by flexibility and dynamic operability.

2.2 Assessment of Plant Safety and Reliability

In this section the important operational needs of safety and reliability are discussed. Plant safety is concerned with the hazards and consequences of equipment failure and abnormal operating conditions. Plant reliability, on the other hand, deals with the probability of normal operation given that equipment failure can occur (Swaney and Grossmann, 1985a). Plant safety is of paramount importance in the modern production environment and is clearly a

function of both the process design (plant layout, choice of equipment and operating conditions) and the reliability of the individual units.

2.2.1 Plant Safety

There is an increasing need to evaluate the safety of a process at the early design stage. Such a need is motivated by both external and internal pressures. External pressures for plant safety include stricter government regulations and increased public pressure on safety and environmental issues (Heikkila *et al.*, 1996). Internal pressures include the need to improve system effectiveness (Asbjornsen, 1989) by reducing the costs associated with redesign at the later phases of design when detailed Hazard and Operability (HAZOP) studies are conducted.

Process safety can be categorized into inherent (internal) safety and external safety. Inherent safety pertains to the intrinsic aspects of the process, such as the type of chemicals used, the operating conditions and the unit operations selected. The goal in designing for inherent safety is to avoid or to remove hazards rather than to control them by add-on protective systems (Benson, 1987; Kletz, 1991). Inherent safety is best considered in the early, conceptual stages of design when the choice of process route is made. External safety is related to process control systems and piping and equipment details and is mostly carried out during the detailed engineering stages with the aid of computerized HAZOP analysis tools (Venkatasubramanian and Vaidhyanathan, 1994).

Total plant safety is a combination of inherent safety and external safety. Since the final designs of chemical processes must be safe, the challenge facing the designer is to reach the required safety level at the minimum cost in terms of capital and design time. It is argued (Kletz, 1991) that inherently safe plants require fewer modifications to improve safety and are thus simpler and cheaper.

Methods of estimating inherent process safety include the Dow Index and the Mond Index, but these indices only estimate the risks associated with explosion and fire. Edwards and Lawrence (1993) present an inherent safety index for analyzing the choice of process route, that is, the choice of raw materials and reactions steps. Their method, however, is mainly concerned with reactor safety and does not properly consider the other parts of the process, even though these usually represent the majority of the equipment.

To overcome this, Heikkila *et al.* (1996) proposed a new inherent safety index which considers a wide range of factors affecting the inherent safety of a process. The index is divided into

two main categories, namely the chemical inherent safety index, I_{CI}, and the process inherent safety index, I_{PI}.

The chemical inherent safety index describes the effect of the choice of raw materials and other chemicals on process safety. It considers aspects such as the heat of the main reaction I_{RM}, the heat of side reactions I_{RS}, flammability I_{FL}, explosiveness I_{EX}, toxicity I_{TOX}, corrosiveness I_{COR} and the potential reaction hazards I_{INT} associated with accidental mixing of chemicals. It is formally calculated as:

$$I_{CI} = I_{RM,\max} + I_{RS,\max} + (I_{FL} + I_{EX} + I_{TOX})_{\max} + I_{COR,\max} + I_{INT,\max} \tag{2.1}$$

where the subindices are assigned a given value in a range depending on their associated risk. Large databases of information pertaining to the safety of past designs and known risks are used for this purpose.

The process inherent safety index describes the effect of the type of process equipment and operating conditions on the inherent safety. It considers aspects such as temperature I_T, pressure I_P, equipment safety I_{EQ}, safety of the process structure I_{ST} and storage facilities I_I. It is formally calculated as:

$$I_{PI} = I_{T,\max} + I_{P,\max} + I_{EQ,\max} + I_{ST,\max} + I_I \tag{2.2}$$

As before, the values of the subindices are determined from large databases of information.

The total inherent safety index I_{TI} is calculated for each process step as $I_{TI} = I_{CI} + I_{PI}$. Different process alternatives may now be compared on the basis of their total inherent safety indices. Process designers may weight the subindexes which they wish to emphasize in a given application. Heikkila *et al.* (1996) show the application of this approach in assessing the inherent safety of a liquid-phase methanol carbonylation process.

The advantage of the above inherent safety index is that it is easy to determine, given the database of information. It provides a simple screening tool at the conceptual design stage to avoid designs which are inherently unsafe. As the design proceeds, safety considerations need to be included concurrently at each step. In the detailed engineering phase of the design, modern tools for computerized integrated Fault Tree/Event Tree/HAZOP analysis have been developed (Kuo *et al.*, 1997). The aim of these tools is not to remove the engineer from the safety analysis but rather to remove the repetitive tasks and provide information and decision making abilities to the design engineer. The developments in this regard have aimed at artificial intelligence approaches which act more as "advisors" than "auditors" (Preston *et al.*, 1996). It should be noted though that purely "auditor-type" tools are still

of great importance as they reduce the burden of demonstrating compliance with regulatory requirements on process safety.

Preston *et al.* (1996) also argue that, apart from developing tools for assessing inherent safety and for providing automated safety assessment, there is still a need to provide thorough operator training through simulation schemes which teach operators how to respond correctly to emergency process situations.

2.2.2 Plant Reliability

According to Asbjornsen (1989), production system effectiveness has three main components, namely:

1. Reliability, which is the probability of a piece of equipment being in working order.
2. Availability, which is the probability of a piece of equipment being available for production.
3. Performance, which is the probability of producing product to the required quality tolerance.

Of the above issues, reliability and availability are dealt with in this section. The issue of performance will be dealt with in the sections pertaining to flexibility and dynamic operability.

Process and equipment reliability are often measured by failure distribution models. A commonly used measure of reliability is the mean time between failures, denoted $MTBF$ (Asbjornsen, 1989). Reliability is clearly a function of the design decisions with regard to equipment selection and process layout. Reliability may be improved by using better quality equipment and/or by providing hot parallel standbys for critical components (Asbjornsen, 1989). Either of these options increases capital costs, which must be traded off against the costs of poor reliability. The costs of an unreliable plant are frequent trips and stoppages, which result in a loss in product and which may propagate down the plant and cause safety hazards due to abnormal operating conditions. A further cost of poor reliability is the additional maintenance personnel needed as well as the equipment and storage costs of the spare parts required.

Process and equipment availability is related to reliability but incorporates the time needed to repair faulty equipment. The repair time is particularly important and can mean that a

process with lower reliability but shorter repair time is preferred over a process with slightly higher reliability and longer repair times. Asbjornsen (1989) defines availability, A, as follows:

$$A = \frac{MTBF}{MTTS + MTTSD + MTTR} \tag{2.3}$$

Availability is thus a function of reliability ($MTBF$), the start-up and shut-down times ($MTTS$ and $MTTSD$ respectively) and the mean time to repair ($MTTR$). From the above expression we see that process start-up and shut-down are important aspects of plant operability. The modern trend is toward on-line development of start-up and shut-down procedures, particularly for the cases where the situation at hand is different from that for which documentation is available (Pradubsripetch *et al.*, 1996).

Plant availability becomes increasingly important when other plants are dependent on the availability of the current plant. Therefore, the supplier is usually bound by a contract liability to maintain a certain level of availability.

Having briefly dealt with the issues of plant safety and reliability, the next section considers another important aspect of plant operability, namely operational flexibility. It will also be shown how reliability and availability considerations may be combined with flexibility to obtain a more realistic assessment of plant flexibility (Pistikopoulos and Mazzuchi, 1990).

2.3 Flexibility Analysis

Plant flexibility represents the ability of a design to operate at steady-state over a range of conditions while satisfying performance specifications. Mathematically, flexibility may be described as the range of variations in uncertain operating parameters that can be tolerated without violating mass and energy balance constraints and any relevant steady-state design specifications (Swaney and Grossmann, 1985a). The variations in operating conditions experienced by a plant may be due to internal or external sources. External sources of variation include changes in throughput, feed quality, product requirements, ambient conditions and utility fluctuations. Internal sources of variability include changes in heat exchanger fouling factors and catalyst deactivation. Flexibility is primarily concerned with slow variations in these parameters whereas high frequency variations and their associated dynamics are treated using the concept of dynamic operability.

The conventional approach to provide for flexibility is to choose a conservative set of operating conditions as the design basis and then to introduce additional units and empirical

overdesign factors to improve flexibility. The disadvantages of such a procedure have already been mentioned in the flexibility case study presented earlier in this chapter. In order to overcome these problems, research efforts have focussed on developing systematic approaches for both flexibility assessment and for synthesizing flexible designs. The aim of this section is to highlight the approaches that have been presented in the literature for this purpose. Particular emphasis will be given to the pioneering work by Swaney and Grossmann (1985a&b). Extensions of their approach as well as alternative approaches will be presented in less detail.

2.3.1 Development of a Mathematical Formulation for Plant Flexibility

Pioneering research by Swaney and Grossmann (1985a&b) aimed to provide the design engineer with the capability to:

1. evaluate the flexibility of a given or proposed design,
2. determine the operating conditions, or process bottlenecks, which limit the flexibility of a design,
3. compare the degree of flexibility of different designs or design configurations for screening purposes, and
4. quantify the trade-off between plant flexibility and steady-state economics.

In order to achieve these goals a scalar index for operational flexibility was proposed, the development of which follows. The physical steady-state performance of a process may be defined in terms of the following relations:

$$h(d, z, x, \theta) = 0 \tag{2.4}$$

$$g(d, z, x, \theta) \leq 0 \tag{2.5}$$

where h is a vector of the mass, energy and equilibrium equations applicable to steady-state process operation and g is a vector of inequalities pertaining to physical operating limits and/or product specifications. The vector d contains all the fixed design variables and z is a vector of all control variables, representing the degrees of freedom available during operation. The vector x contains the state variables (same dimension as h) and θ is the set of uncertain parameters whose values are expected to vary over the lifetime of the project or during normal operation.

The vector θ may include, for example, throughput, rate constants, catalyst activity and heat exchanger fouling factors. Typically bounds exist on θ of the form:

$$\theta_j^N - \Delta\theta_j^- \leq \theta_j \leq \theta_j^N + \Delta\theta_j^+ \tag{2.6}$$

where $\Delta\theta_j^+$ and $\Delta\theta_j^-$ are the expected positive and negative deviations of the jth element of θ from the nominal design value θ_j^N. The uncertain parameters are expected to vary independently of each other and if this is not the case then the existing set θ should be reduced to an independent set.

For a given plant design d and any realization of the uncertain parameters θ, the state variables x may be expressed as an implicit function of d, z and θ:

$$h(d, z, x, \theta) = 0 \quad \Rightarrow \quad x = x(d, z, \theta) \tag{2.7}$$

As a result, it is possible to eliminate the state variables from the formulation and thereby describe the process operation by the following reduced inequality constraints:

$$g(d, z, x(d, z, \theta), \theta) = f(d, z, \theta) \leq 0 \tag{2.8}$$

Thus, for feasible operation we require (2.8) to be satisfied. The region of feasible operation in the space of the uncertain parameters θ can now be classified formally as:

$$\mathcal{R} = \{\theta \mid [\exists\, z \mid f(d, z, \theta) \leq 0]\} \tag{2.9}$$

In order to describe the feasible region in a more mathematically useful way, Swaney and Grossmann (1985a) used a scaled hyperrectangle $\mathcal{T}$ defined, in terms of a nonnegative scalar variable δ, as follows:

$$\mathcal{T}(\delta) = \left\{\theta \mid \theta^N - \delta\ \Delta\theta^- \leq \theta \leq \theta^N + \delta\ \Delta\theta^+\right\} \tag{2.10}$$

The flexibility index F for a given set of design parameters d is defined as the maximum value that δ can take without $\mathcal{T}$ containing any infeasible points. That is, $\mathcal{T}$ is the largest scaled hyperrectangle, whose ratios are set by the designer, that can fit inside the region of feasible operation. This corresponds to the solution of the following semi-infinite programming problem:

$$\begin{aligned} F &= \max\ \delta \\ \text{s.t.}\quad \{\forall\ \theta &\in \mathcal{T}(\delta) \mid \exists\, z \mid f(d, z, \theta) \leq 0\} \end{aligned} \tag{2.11}$$

It should be noted that, when $F \geq 1$, the proposed design allows for feasible operation over the range of parameter uncertainties originally specified or expected by the designer.

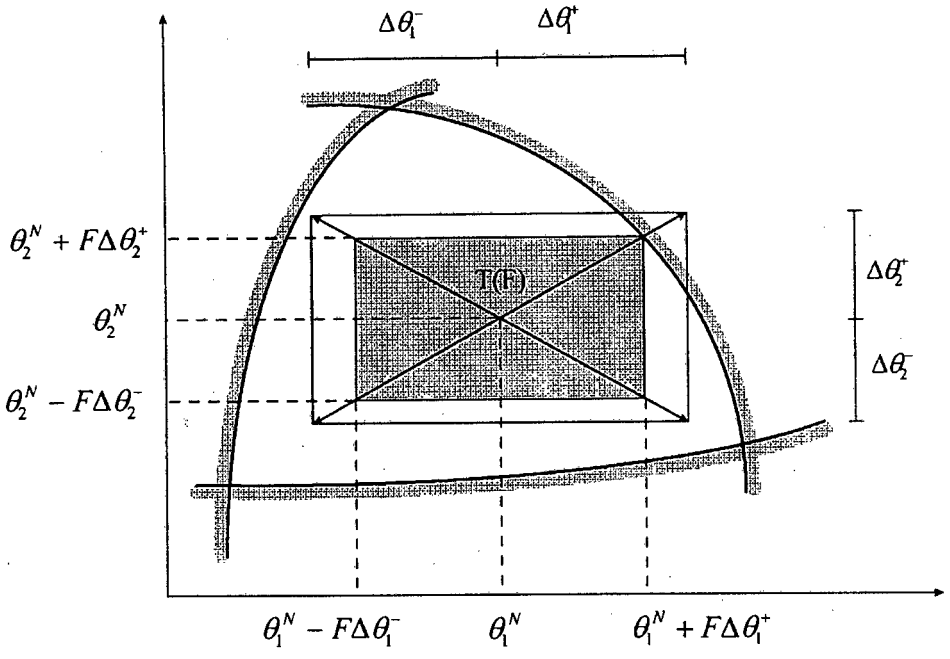

Figure 2.6: Geometrical interpretation of the feasible region and the flexibility index F for a two-dimensional uncertain parameter set θ.

The point θ^* corresponding to the case where $f_i(d, z, \theta^*) = 0$ is known as a critical point. Its importance lies in the fact that it corresponds to a so-called "worst-case" operating condition as described earlier in the motivational example. The constraints that are limiting at this point can be thought of as the bottlenecks in the given design. The above concepts are illustrated graphically in Figure 2.6 for the case where the uncertain parameter set θ has two elements.

Halemane and Grossmann (1983) have shown that the feasibility constraint in (2.11) is mathematically equivalent to the following max-min-max constraint:

$$\max_{\theta \in T(\delta)} \min_{z} \max_{i \in I} f_i(d, z, \theta) \leq 0 \tag{2.12}$$

An equivalent formulation for the flexibility index is thus given by:

$$\begin{aligned} F &= \max\ \delta \\ \text{s.t.} &\quad \max_{\theta \in T(\delta)} \min_{z} \max_{i \in I} f_i(d, z, \theta) \leq 0 \\ \text{where} \quad T(\delta) &= \left\{ \theta \,|\, \theta^N - \delta\ \Delta\theta^- \leq \theta \leq \theta^N + \delta\ \Delta\theta^+ \right\} \end{aligned} \tag{2.13}$$

In the present form the problem is still very difficult to solve due to the max-min-max constraint and its semi-infinite nature. According to Grossmann *et al.* (1983), the max-

min-max constraints can lead to a non-differentiable global optimization problem. Swaney and Grossmann (1985a) have shown that, for the special case where the constraint functions $f(d, z, \theta)$ are jointly quasi-convex in z and one-dimensional quasi-convex in θ, the solution to (2.13) lies at a vertex of the hyperrectangle $\mathcal{T}(\delta)$. The problem can then be decomposed into a two-stage optimization problem where a δ^k is determined for each vertex direction and the minimum one is chosen. Grossmann and Floudas (1987) developed an active constraint solution strategy for flexibility analysis that does not rely on the assumption that the solution of (2.13) lies at a vertex. Ovstrovsky *et al.* (1996) provide a mixed integer nonlinear programming (MINLP) solution strategy to the above flexibility analysis problem and report that in some cases it has computational advantages over the methods mentioned above.

Pistikopoulos and Mazzuchi (1989 and 1990) extended the method of Swaney and Grossmann to consider the case where the uncertainty in the parameters θ is represented by probability distribution functions rather than bounds. They assume a Gaussian distribution model for the uncertain parameters with the idea being that θ is most likely to be near θ_j^N. The result enables a stochastic flexibility index to be determined.

Straub and Grossmann (1990) developed an expected stochastic flexibility measure for analyzing the flexibility of a design to withstand stochastic uncertainty in the continuous parameters as well as discrete state uncertainty. The treatment of discrete state uncertainty is typically associated with reliability assessment where a unit is either operating or has failed (Dhillon and Rayapati, 1988). Therefore, the measure provides a framework for integrating flexibility and reliability and accurately accounts for the interactions between these important aspects of operability.

Dimitriadis and Pistikopoulos (1995) developed an approach for assessing the feasibility and flexibility of *dynamic* systems in the presence of time-varying uncertain parameters. The formulation for both the dynamic feasibility and dynamic flexibility problems is an extension of the steady-state flexibility analysis framework discussed thus far. The difference is that in the dynamic case the feasible region and the flexibility index vary with time. A dynamic flexibility index is now defined as the largest scaled deviation that can be tolerated while remaining feasible over a given time horizon. If the critical points limiting feasibility are assumed to lie at the vertices of the time-varying uncertainty space, then both the dynamic feasibility and flexibility problems reduce to differential algebraic optimization problems. These problems are solved using the DAEOPT optimal control code of Vassiliadis *et al.* (1994a&b).

When the above simplifying assumption is not valid, orthogonal collocation is used to discretize the differential algebraic equation system and an active constraint strategy (Grossmann and Floudas, 1987) is used to transform both problems into MINLP problems. Mohideen *et al.* (1996) show how the above approach has application in control structure selection and controller tuning for dynamic chemical processes. Details of their approach are provided later in this chapter, in the section pertaining to the synthesis of operable plants.

Chacon-Mondragon and Himmelblau (1988) adopt an alternative approach to flexibility analysis. The fundamental difference lies in the fact that they assess flexibility as the size of the set of control variables that satisfy the feasibility constraints rather than in terms of the size of the feasible region. Intuitively, the more "options" available for achieving feasibility, the more flexible the plant design. In order to assess the size of this set, they linearize the feasibility constraints in (2.8) with respect to the control variables and calculate the so-called m-dimensional volume of the polyhedron formed by the intersections of the linear constraints in the space of the control variables. If this volume is positive, then there exists a set of control variables which result in feasible operation. Chacon-Mondragon and Himmelblau (1994) extend their approach to treat the synthesis problem in a multi-objective fashion whereby a pareto-optimal trade-off is achieved between economics (in the form of minimized cost) and flexibility.

2.4 Systematic Approaches To Dynamic Operability Assessment

In this section the different approaches that have been proposed for both dynamic operability assessment and for the synthesis of dynamically operable plants are reviewed. A number of terms are currently used in the literature for what is termed dynamic operability in this thesis. Other regularly used terms include (dynamic) resiliency and controllability. Although a number of different definitions are used in the literature, the common thread is that dynamic operability is a measure of the quality of closed-loop control performance that can be achieved for a plant via feedback (Morari, 1983). Clearly, the quality of control performance depends on the type of controller used, the tuning parameters, the choice of measured and manipulated variables (control structure) and the process itself. In order not to bias the results by the choice of controller or tuning parameters, Morari (1983) proposed that dynamic operability be determined as a limit of achievable control performance. In this way, it is only a function of the inherent properties of the process design and the control structure.

The impact that a plant design has on its closed-loop control performance was stated explicitly as early as 1943 by Ziegler and Nichols (1943). They devoted an entire paper to this topic, an excerpt of which appears below:

> "In the application of automatic controllers, it is important to realize that the controller and the process form a unit; credit or discredit for results obtained are attributable to one as much as the other. A poor controller is often able to perform acceptably on a process which is easily controlled. The finest controller made, when applied to a miserably designed process, may not deliver the desired performance. True, on badly designed processes, advanced controllers are able to eke out better results than older models, but on these processes there is a definite end point which can be approached by instrumentation and it falls short of perfection."

Ziegler and Nichols (1943) also introduced a "recovery factor" to classify processes in terms of their dynamic operability or controllability, regardless of the controller used. Though not theoretically rigorous, the recovery factor does express reasonably accurately the performance achievable for single-input single-output (SISO) processes, even when using current sophisticated control hardware (Morari and Perkins, 1995).

One of the earliest industrial examples illustrating the importance of considering the dynamic aspects of a process at its design stage is given by Anderson (1966). This study considered an improperly designed feed-effluent heat-exchanger system. The recycle of energy introduced positive feedback and destabilized the system at high throughputs. Only after shutdown and a complete re-design was it possible to run the plant at its design capacity.

A number of papers appeared subsequently, discussing the impact of plant design on dynamics and control (Silverstein and Shinnar, 1977; Georgakis and Worthey, 1978). Uppal *et al.* (1974) considered the influence of design parameters on the dynamic behavior of CSTRs and Lee *et al.* (1972) did so for heat exchangers. However, the first systematic and general approach for including operability considerations into process design was due to Nishida and Ichikawa (1975) and Nishida *et al.* (1976). Their method involves a min-max optimal control formulation, reported to be too complex to be applicable for larger systems.

Despite the above mentioned research, it is primarily since the early 1980s that quantitative measures have been developed to assess dynamic operability. The remainder of this section focuses on these approaches. Unless otherwise mentioned, the plant and controller will be assumed to be linear time-invariant.

The discussion begins with the Internal Model Control (IMC) framework used in the pioneering work by Morari (1983) to determine the factors limiting the achievable closed-loop performance of a process. Care is taken in describing each of these factors and detailing how the IMC approach enables a limit of performance to be determined without bias due to controller type or tuning. The IMC approach will be treated fairly thoroughly since much of the work in this field is based on these initial ideas and since the Q-parametrization approach, used in this thesis, is closely related to the IMC framework.

Following the IMC approach, methods due to Perkins and coworkers (Perkins and Wong, 1985; Russell and Perkins, 1987; Cao *et al.*, 1994) based on controllability analysis are presented. The controllability approach is based on the idea of output reproducibility and is seen to involve similar conditions for perfect control as those determined in the IMC framework. It will be shown in Chapter 5 that the Q-parametrization approach is also closely related to the concept of functional controllability.

Following the above two approaches is the research due to Psarris and Floudas (1991a&b) which simultaneously treats the effect of right-half-plane transmission (RHPT) zeros and time delays on dynamic operability. Thereafter further heuristic indicators of dynamic operability are reviewed. The incorporation of economic aspects is discussed next, followed by methods for synthesizing plants that have both good steady-state economics and good dynamic operability.

2.4.1 Internal Model Control Framework

Since dynamic operability is a closed-loop property it is very difficult to assess without some bias due to the particular controller (Arkun, 1986; Morari, 1983). This is especially true when working in the classical feedback control framework.

An intuitive approach to dynamic operability assessment would be to select a particular controller structure and to optimize a scalar closed-loop performance measure subject to the relevant closed-loop constraints in order to determine the optimal tuning parameters. The result obtained can then be used to judge the performance of the system under closed-loop control. Unfortunately, the resulting optimization problem is notoriously nonconvex, with multiple local minima. Thus, if a solution is obtained no guarantees are available regarding its global optimality; furthermore, one cannot be sure of the quality of control achievable with a more sophisticated controller. Poor control performance could be due to sub-optimal tuning and/or a sub-optimal controller structure and/or an inherently inferior process design.

Unfortunately, it is difficult to isolate the cause(s) of the problem. If no solution is obtained then this could either be a consequence of numerical difficulties, or it could be that no controller is able to meet the constraints. An added difficulty with this approach is the problem of ensuring that the controller parameters used in the optimization do not lead to instability.

In order to remedy this situation, Morari (1983) proposed the use of the Internal Model Control framework to represent the closed-loop properties of a system independent of the controller structure and thereby isolate the sources of the inherent control problems. Figure 2.7 shows the IMC structure and how it is obtained from the classical feedback structure by the addition of two blocks, each containing the plant model $\tilde{G}(s)$ in such a way that their effects cancel each other out (Morari and Zafiriou, 1989).

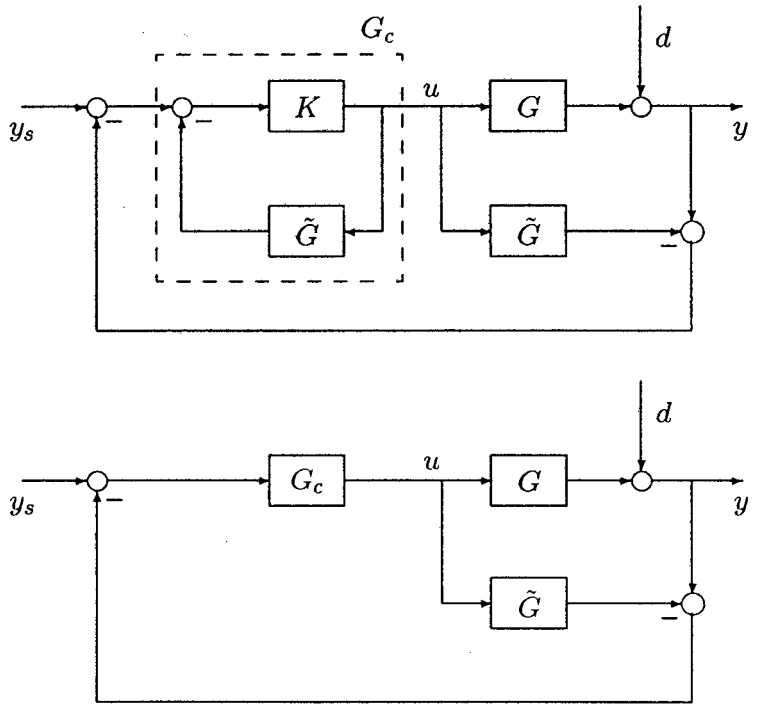

Figure 2.7: Development of the IMC structure from the classical feedback structure.

In performing this transformation no generality is lost, as is apparent from the following equations relating the IMC controller G_c to the classical controller K.

$$G_c = K(I + \tilde{G}K)^{-1} \quad \Leftrightarrow \quad K = G_c(I - \tilde{G}G_c)^{-1} \tag{2.14}$$

Although the two representations are equivalent, the IMC structure is more useful for the analysis of dynamic operability, as will be shown next.

Using block-diagram algebra, the closed-loop expression for the outputs y as a function of the actual plant G, the plant model $\tilde{G}$ and the IMC controller G_c is given by

$$y = GG_c(I + (G - \tilde{G})G_c)^{-1}(y_s - d) + d \tag{2.15}$$

where y_s is the vector of setpoint changes and d is the disturbance to the system.

An important property of the IMC formulation is that, if the model is perfect ($G = \tilde{G}$), then the closed-loop system is internally stable if and only if the plant and the IMC controller are each stable. As alluded to earlier, this property is especially useful in optimal controller design because, for a stable plant and a stable IMC controller, closed-loop stability is ensured.

A property of great importance to dynamic operability assessment is that, for a perfect model ($G = \tilde{G}$) and a stable IMC controller, perfect control can be achieved if the IMC controller can be chosen as the right inverse of the plant model. This is best understood by noting that, in the absence of model uncertainty, the closed-loop expression for y in (2.15) reduces to:

$$y = \tilde{G}G_c(y_s - d) + d \tag{2.16}$$

Now, by choosing the IMC controller such that $\tilde{G}G_c = I$, or if the plant model is square, $G_c = \tilde{G}^{-1}$, it is clear that $y(t) = y_s(t)$ for all time t and for all disturbances d. This situation corresponds to perfect control, which, although not achievable in practice, provides a useful criterion to test the inherent performance limitations of a plant.

In order for G_c to be implementable it must be causal, realizable and stable. Morari (1983) argued that the following factors, if present in a plant, prevent one from implementing the inverse of the plant model as the IMC controller and hence prevent the achievement of perfect control:

1. Right-half-plane transmission (RHPT) zeros - since these would result in unstable poles in the controller G_c.

2. Time delays - since these would require prediction (noncausal behavior) by the controller.

3. Input constraints - since most physical plants are strictly proper and implementing the model inverse would result in an improper controller and infinite input signals to the process. Any input constraints limit the degree to which the IMC controller can approximate the inverse of the plant model, while still remaining proper, and thus limit the achievable closed-loop performance.

4. Model uncertainty - since the above discussion relied on the assumption of a perfect model. It will be shown later, using the IMC framework, that model uncertainty limits the frequency range over which perfect control is possible.

If any of these performance-limiting factors are present in a plant, then the IMC approach for dynamic operability assessment involves factorizing the plant model $\tilde{G}$ into an invertible part $\tilde{G}_-$ and a non-invertible part $\tilde{G}_+$, so that $\tilde{G} = \tilde{G}_+\tilde{G}_-$. The IMC controller is then chosen as the right inverse of $\tilde{G}_-$, that is, $\tilde{G}_-G_c = I$. Substitution of this controller into the expression for the closed-loop response of y, in the absence of model uncertainty yields:

$$y = \tilde{G}_+(y_s - d) + d \tag{2.17}$$

It is thus clear that the properties of the non-invertible part of the plant $\tilde{G}_+$ will determine the achievable closed-loop performance. Ideally we desire $\tilde{G}_+ = I$ but, as has been mentioned earlier, this is not always possible. Choosing $\tilde{G}_+$ such that $\tilde{G}_+(s = 0) = I$ will result in offset-free control performance and typically $\tilde{G}_+$ is chosen such that it has unity norm, $||\tilde{G}_+|| = 1$.

It should be noted that the number of possible factorizations of the plant model is infinite and thus a factorization which is optimal in some specified sense is sought. A commonly used measure of performance is the minimum integral-square-error (ISE) of the output response. Another point to note is that the classical controller has effectively been removed from the problem and dynamic operability is dependent only on $\tilde{G}_+$, which is a function of the plant model only. In the discussion below it is shown how optimal factorizations of the plant model have been obtained analytically by researchers when studying the individual impact of the performance-limiting factors on dynamic operability.

Effect of RHPT zeros on dynamic operability

For single-input single-output (SISO) systems, the zeros are the roots of the numerator polynomial of the transfer function. For multi-input multi-output (MIMO) systems the *transmission* zeros are defined as those values of s for which the rank of $\tilde{G}(s)$ drops below its nominal rank (MacFarlane and Karcanias, 1976). Holt and Morari (1985b) show that, for an open-loop stable system, the RHPT zeros are the roots of the numerator of the determinant that are in the right-half-plane.

Some important properties of RHPT zeros are (Holt and Morari, 1985b):

1. They lead to an initial inverse response behavior in SISO systems (if there are an odd number present). This behavior is common in boiler drums, simple distillation columns and coupled distillation columns. For multivariable systems, the presence of RHPT zeros is not necessarily shown by inverse response behavior. In addition, in MIMO systems it is possible to generate "inverse" response-type behavior by appropriate manipulation of the inputs, even though there are no RHPT zeros present.

2. They possess a transmission blocking property in that there can exist an exponentially growing input and a set of initial conditions for which the output remains unchanged. This property is the reason why for multivariable systems they are called RHP *transmission* zeros.

3. Transmission zeros are invariant under state and output feedback (Kwakernaak and Sivan, 1972). They can therefore not be moved into the left-half-plane by clever controller design. However, by modifying the process it is sometimes possible to eliminate the presence of RHPT zeros, as will be demonstrated later in the work of Psarris and Floudas (1991a&b).

4. Inverting plant models that contain RHPT zeros results in the presence of RHP poles, which are unstable.

Because of the above it is clear that RHPT zeros adversely affect the closed-loop performance of a system. The extent to which they do this depends on their number and their location and is discussed next. The discussion will be divided into the SISO case and the MIMO case.

SISO case In the discussion which follows it is assumed that the system is stable, has no time-delays, that no input constraints are present and that there is no model uncertainty. Consider a SISO process $\tilde{G}(s)$, with m RHP zeros $(z_1, ..., z_m)$, given by:

$$\tilde{G}(s) = \frac{\left(-\frac{1}{z_1}s+1\right)\dots\left(-\frac{1}{z_m}s+1\right)\left(\frac{1}{\tau_1}s+1\right)\dots\left(\frac{1}{\tau_\ell}s+1\right)}{\left(\frac{1}{\rho_1}s+1\right)\dots\left(\frac{1}{\rho_n}s+1\right)} \quad , \quad z_i,\, \tau_i,\, \rho_i > 0 \qquad (2.18)$$

Kwakernaak and Sivan (1972) have shown that, to minimize the integral square error (ISE) to step inputs, $\tilde{G}_+$ in (2.17) must be chosen as follows:

$$\tilde{G}_+(s) = \prod_{i=1}^{m} \frac{(-\frac{1}{z_i}s+1)}{(\frac{1}{z_i}s+1)} \qquad (2.19)$$

The closed-loop poles should thus be placed at the mirror images of the open-loop RHP zeros.

The resulting minimal ISE for a system with real zeros, subject to a unit step in y_s, is given by (Frank, 1974):

$$\text{ISE} = \sum_{i=1}^{m} \frac{2}{z_i} \tag{2.20}$$

The conclusion is that the more RHP zeros there are, and the closer they lie to the imaginary axis, the worse the resulting closed-loop performance. Hence, for good dynamic operability, systems with "small" RHP zeros should be avoided.

It should be noted that the optimal factorization of $\tilde{G}(s)$ depends on the choice of inputs as well as the performance measure. Frank (1974) developed a procedure to determine $\tilde{G}_+(s)$ that minimizes the ISE for different types of inputs. Holt and Morari (1985b) provide optimal factorizations for step inputs where the performance measure is the minimum integral absolute error (IAE). Despite the different performance measures or input types, the results still show that RHP zeros near the origin cause control difficulties.

MIMO case For multivariable systems Holt and Morari (1985b) show that RHPT zeros are a characteristic only of square systems and that, except in rare cases corresponding to so-called "pinned zeros" (Bristol, 1980), the RHPT zeros can affect all the outputs of the system.

For multivariable systems the optimal factorization of $\tilde{G}(s)$ depends on the performance index, the type of input and the relative importance of the outputs (expressed as weights in the performance index). Frank (1974) provides a procedure for determining $\tilde{G}_+(s)$ which minimizes the weighted ISE performance measure, but the procedure is reported to be extremely complicated and of little practical significance (Holt and Morari, 1985b).

As the optimal $\tilde{G}_+(s)$ is a function of the infinite number of possible choices of performance weights, Holt and Morari considered two special cases, namely that of dynamic decoupling and where the effect of the RHPT zero is shifted onto the least important output.

Dynamic decoupling Consider a square MIMO system of dimension n, with m RHPT zeros. If we require the outputs to be dynamically decoupled then the $\tilde{G}_+$ which generates an ISE-optimal response to step inputs is given by:

$$\tilde{G}_+(s) = \text{diag}\left\{ \prod_{i=1}^{m} \frac{(-\frac{1}{zi}s+1)}{(\frac{1}{zi}s+1)}, \prod_{i=1}^{m} \frac{(-\frac{1}{zi}s+1)}{(\frac{1}{zi}s+1)}, \ldots, \prod_{i=1}^{m} \frac{(-\frac{1}{zi}s+1)}{(\frac{1}{zi}s+1)} \right\} \tag{2.21}$$

Using this factorization means that the RHPT zeros affect every output. The degradation in closed-loop performance can be seen on the same basis as the SISO results and is inversely

proportional to the location of the RHPT zeros. This factorization is never optimal in an ISE sense since each RHPT zero contributes n times to the overall ISE instead of simply once, as required for optimality by Kwakernaak and Sivan (1972). Hence, for MIMO systems with RHPT zeros near the origin, dynamic decoupling is not a good control strategy and some form of interaction is preferable.

Shifting effect of zero onto least important output Shifting the effect of RHPT zeros onto the least important output is complicated by the presence of "pinned zeros" (Bristol, 1980) which make it impossible to shift the effect of a RHPT zero from a particular output. However, Holt and Morari (1985b) argue that for experimentally determined models it is virtually impossible to find pinned zeros, with a notable exception being the case of block triangular matrices where certain matrix elements are structurally equal to zero.

Holt and Morari (1985b) showed that for a square stable system of dimension n with m RHPT zeros and no pinned zeros, it is possible to obtain perfect control on any set of $n-1$ outputs, with the remaining output exhibiting no steady-state offset. The form of $\tilde{G}_+$ satisfying this theorem is as follows:

$$\tilde{G}_+(s) = \begin{bmatrix} 1 & 0 & 0 & 0 \\ 0 & \ddots & \vdots & \vdots \\ \vdots & \cdots & 1 & 0 \\ \frac{s\,a_1(s)}{b_1(s)} & \cdots & \frac{s\,a_{n-1}(s)}{b_{n-1}(s)} & \prod_{i=1}^{m} \frac{(-\frac{1}{z_i}s+1)}{(\frac{1}{z_i}s+1)} \end{bmatrix} \tag{2.22}$$

The form of the $a_i(s)$ and $b_i(s)$ terms in the above expression are yet to be determined. Using a result of Kwakernaak and Sivan (1972), Holt and Morari show that the poles of the off-diagonal terms of $\tilde{G}_+$, namely the roots of $b_i(s)$, need to be at the mirror images of the RHPT zeros. It is, however, unclear how the poles should be distributed among the $b_i(s)$ terms. For the case of a single RHPT zero z, Holt and Morari (1985b) provide the following optimal factorization:

$$\tilde{G}_+(s) = \begin{bmatrix} 1 & 0 & 0 & 0 \\ 0 & \ddots & \vdots & \vdots \\ \vdots & \cdots & 1 & 0 \\ \frac{s\,\beta_1}{(\frac{1}{z}s+1)} & \cdots & \frac{s\beta_{n-1}}{(\frac{1}{z}s+1)} & \frac{(-\frac{1}{z}s+1)}{(\frac{1}{z}s+1)} \end{bmatrix} \tag{2.23}$$

where the β_i are given by:

$$\beta_i = -\frac{2\hat{g}_{ji}(s=z)}{z\hat{g}_{jn}(s=z)} \quad , \quad \text{for arbitary } j \in \{1,...,n\} \tag{2.24}$$

and $\hat{g}_{ji}$ represents the (j,i) element of the inverse of $\tilde{G}$.

While the above approach provides valuable insight into the effect of RHPT zeros on achievable closed-loop performance, it is unable to treat multiple zeros for MIMO systems rigorously. As mentioned in the assumptions, it does not consider the performance-limiting effects of input constraints, time delays and model uncertainty nor is it able to consider the case where different outputs are equally important and decoupling is not desired.

Morari *et al.* (1987) use the concept of zero-directions to assess the benefits of partial decoupling and extend some of the results of Holt and Morari (1985b). Their method provides a convenient tool to judge the feasibility of alternative forms of decouplers. In particular, it is shown that for MIMO plants where a zero direction is predominantly aligned with one output, the best overall performance is achieved by preserving this alignment in the closed-loop transfer matrix.

Effect of time delays on dynamic operability

Time delays occur frequently in industrial process models due to the piping of fluids and the fact that high order systems, such as distillation columns, may be approximated as having time delays. For this reason it is important that the performance-limiting effect of time delays be quantified. Clearly, for SISO systems, the larger the time delay, the worse the ISE. In fact, for a SISO process containing a time delay θ and m RHP zeros, Kwakernaak and Sivan (1972) showed that the ISE in response to step inputs is minimized by selecting:

$$\tilde{G}_+(s) = \prod_{i=1}^{m} \frac{(-\frac{1}{z_i}s+1)}{(\frac{1}{z_i}s+1)} e^{-\theta s} \tag{2.25}$$

where z_i is the ith RHP zero.

For MIMO systems the problem is complicated by the fact that both the magnitudes and the distribution of the time delays within the transfer matrix are important. The most significant research in this regard has been by Holt and Morari (1985a), Perkins and Wong (1985), Russell and Perkins (1987) and Psarris and Floudas (1991a&b). Of these researchers, only Holt and Morari used the IMC approach and hence only their approach will be considered in this subsection. The other approaches will be discussed in later sections.

In order to consider the performance-limiting effects of deadtimes, Holt and Morari (1985a) assume a square, perfect transfer matrix model of dimension n, unlimited controller power and a stable inverse. Under these assumptions, determining $\tilde{G}_+$ involves finding the smallest

delays such that $G_c = \tilde{G}_-^{-1} = \tilde{G}^{-1}\tilde{G}_+$ is causal. That is, G_c is required to contain no terms in $e^{\tau s}$ where $\tau > 0$. In general, $\tilde{G}_+$ cannot be determined uniquely as it is a function of the weighting of the outputs in the performance index, as well as the type of input used. Holt and Morari (1985a) provide lower and upper bounds on the performance index by considering the minimum possible response time both with and without dynamic decoupling. These two bounds are discussed next.

Minimum response time without dynamic decoupling - an upper bound on dynamic operability A lower bound for the settling time of output i is given by:

$$\tau_i = \min_j \, p_{ij} \tag{2.26}$$

where p_{ij} is the minimum delay in the numerator of element (i,j) of $\tilde{G}(s)$. Proof of the above result is direct since no input can effect a change in output i faster than that given by τ_i. An upper bound on the dynamic operability is thus obtained by choosing $\tilde{G}_+$ as follows:

$$\tilde{G}_+ = \text{diag}\,(e^{-\tau_1 s}, ..., e^{-\tau_n s}) \tag{2.27}$$

In general this upper bound is not achievable and off-diagonal elements need to be added and/or the delays of certain diagonal elements need to be increased in order for $G_c = \tilde{G}_-^{-1} = \tilde{G}^{-1}\tilde{G}_+$ to be causal.

Minimum response time with dynamic decoupling - lower bound on dynamic operability While the upper bound on dynamic operability may not always be achievable, the following lower bound is always possible and corresponds to the minimum delay associated with each output when the system is dynamically decoupled. According to Theorem 2 in Holt and Morari (1985a), the diagonal matrix G_+^d, corresponding to a decoupled response, with the smallest time delay terms such that $G_c = \tilde{G}_-^{-1} = \tilde{G}^{-1}G_+^d$ is realizable, has the following form:

$$G_+^d = \text{diag}(e^{-\tau_{11} s}, ..., e^{-\tau_{nn} s}) \tag{2.28}$$

where τ_{ii} is given by

$$\tau_{ii} = \max_j(\max(0, (\hat{q}_{ji} - \hat{p}_{ji}))) \,, \tag{2.29}$$

In the above, $\hat{p}_{ji}$ is the minimum delay in the numerator of element (j,i) of $\tilde{G}^{-1}$ and $\hat{q}_{ji}$ is the minimum delay in the denominator of element (j,i) of $\tilde{G}^{-1}$.

Holt and Morari (1985a) provide a simple rearrangement test to determine whether G_+^d for a dynamically decoupled system is ISE optimal. The test involves determining whether, by

appropriate column interchanges, it is possible for the minimum delay in each row to appear on the diagonal. If the rearrangement test is satisfied then the upper and lower bounds coincide and the lower bound is referred to as being optimal. Clearly, in this case the upper bound is achievable.

When the outputs are of different relative importance it is always possible to design a G_+ such that the most important output settles in the minimum time predicted by τ_i in (2.26). However, when this happens, at least one output will not be able to settle faster than the bound on the response time as determined in (2.28) and (2.29).

Illustrative example Consider the following simple example from Holt and Morari (1985a), where $\tilde{G}$ is given by:

$$\tilde{G} = \begin{bmatrix} 0 & e^{-2s} \\ -e^{-2s} & 1 \end{bmatrix} \tag{2.30}$$

The minimum possible response time is given by the vector $(2,0)$, which corresponds to $\tilde{G}_+ = \text{diag}(e^{-2s}, 1)$. As mentioned earlier, this response time may not necessarily be achievable.

If dynamic decoupling is required, then $\tilde{G}_+^d = \text{diag}(e^{-4s}, e^{-2s})$, which is clearly worse from an ISE perspective, but is definitely achievable. If the first output is more important, it is possible to make it settle in the minimum response time given by $\tau_1 = 2$, but the result is that the second output cannot settle faster than the time given by $\tilde{G}_+^d$, namely a delay of two units. Alternately, if the second output is more important then it can settle immediately, but the first output will not be able settle faster than a delay of four units.

Screening alternative designs Having shown how the time delay bounds may be evaluated, it is useful to mention how they may be applied to the screening of alternative designs. The basic idea is that designs having smaller time delay elements in the bounds are preferable. Unfortunately, there are several difficulties associated with this. The first difficulty is that the vector nature of these bounds, with each output having an associated delay, makes it difficult to choose between alternatives. Perkins and Wong (1985) argued that a single scalar measure would be more beneficial. More importantly perhaps is the fact that the upper bound is not necessarily achievable whereas the lower bound is achievable but not necessarily desirable. If alternative designs have upper and lower bounds which overlap, it becomes particularly difficult to rank them in an unambiguous manner based on their dynamic operability.

One issue that has not yet been dealt with in this section is the fact that time delays may introduce an infinite number of RHPT zeros into $\tilde{G}$ (Morari, 1983; Psarris and Floudas, 1991a&b) and thus not only limit perfect control due to prediction but also due to stability requirements on G_c. This issue will be dealt with when the research of Psarris and Floudas is reviewed in section 2.4.3 of this chapter.

Effect of input constraints on dynamic operability

Input constraints play an important part in assessing dynamic operability, as every physical system has actuator limits. As mentioned earlier, this imposes a restriction on the level of closed-loop control performance that can be achieved. A very simple approach to determining the effect input constraints have on achievable performance is developed in the IMC framework (Morari, 1983) and is discussed below.

Considering a perfect plant model ($G = \tilde{G}$); from block-diagram algebra applied to the IMC framework, where $G_c = \tilde{G}^{-1}\tilde{G}_+$, we obtain the following:

$$\begin{aligned} u &= G_c(y_s - d) \\ &= \tilde{G}^{-1}\tilde{G}_+(y_s - d) \end{aligned} \tag{2.31}$$

The factorization of $\tilde{G}$ is typically done in such a fashion that $||\tilde{G}_+|| = 1$. The ℓ_2-induced matrix norm will be used in the remainder of this section and is defined as follows:

$$\begin{aligned} ||\tilde{G}||_2 &= \sigma_M(\tilde{G}) \\ &= \sqrt{\lambda_{\max}(\tilde{G}^*\tilde{G})} \end{aligned} \tag{2.32}$$

where σ_M is the maximum singular value, $\lambda_{\max}$ is the maximum eigenvalue, and $\tilde{G}^*$ is the complex conjugate transpose of $\tilde{G}$. Using the fact that $||\tilde{G}^{-1}||_2 = \sigma_m^{-1}(\tilde{G})$, where σ_m is the minimum singular value of $\tilde{G}$ and is defined in an analogous manner to σ_M (except that the minimum eigenvalue is indicated), we see from (2.31) that

$$||u||_2 \geq \sigma_m^{-1}(\tilde{G})\,||\,y_s - d\,||_2 \tag{2.33}$$

Therefore, the constraint $||\,u\,||_2 \leq ||\,u_{\max}\,||_2$ will not be violated if we require:

$$||\,y_s - d\,||_2 \leq \sigma_m(\tilde{G})\,||\,u_{\max}\,||_2 \tag{2.34}$$

For SISO systems with u appropriately scaled so that $u_{\max} = 1$, the requirement (2.34) reduces to

$$|y_s - d| \leq \left|\tilde{G}(j\omega)\right| \tag{2.35}$$

where $|\tilde{G}(j\omega)|$ is the open-loop amplitude ratio. Therefore, for SISO systems, the open-loop amplitude ratio plot of $|\tilde{G}|$ is a measure of the maximum disturbance amplitude that the system can handle without input saturation. For example, if the disturbance exceeds $|\tilde{G}(\omega = 0)|$ at steady-state, then there will be offset due to the saturation of the manipulated variable. Thus one desires systems with large values of $|\tilde{G}(\omega = 0)|$.

In order for the above approach to be applicable for multivariable systems it requires scaling so that all the manipulated variables are subjected to similar constraints. Nevertheless, we see that large values of $\sigma_m(\tilde{G})$ are beneficial. It should also be noted that the above measures are not expressed naturally in terms of time domain bounds on input signals, nor do they consider the impact of other performance-limiting factors.

The above discussion has focussed on the performance-limiting effect of input constraints. Zafiriou and Chiou (1994) look at the interaction between *output* constraints and RHP zeros using Model Predictive Control theory. They show that if the transfer matrix has elements or sub-blocks containing RHP zeros then instabilities may occur when enforcing hard output constraints.

Effect of model uncertainty on dynamic operability

As has been illustrated in the motivational example earlier in this chapter, the sensitivity of a plant to model uncertainty is a strong function of the plant design. As most mathematical models only approximate the actual process dynamics, the issue of model uncertainty is always important and its effect on the inherent "controllability" of a process needs to be quantified. At present, most models used for the control of continuous processes are linear time-invariant (LTI) models. In general, the sources of model uncertainty in such models could be due to any of the following (Arkun, 1986; Skogestad and Morari, 1987):

1. Unmodelled high-frequency dynamics.
2. Linearization of a nonlinear model about a particular operating point.
3. Different operating conditions leading to changes in the model parameters, even if the process is fairly linear. For example, increases in flowrates lead to shorter deadtimes and time constants.
4. True uncertainties such as imperfect knowledge of model parameters and the order of a model at high frequencies.

One typically therefore works with a model of the plant (nominal plant) and a set of plants (uncertainty set) lying in a norm-bounded region about the nominal plant, which is thought to contain the actual plant. In assessing the effect of model uncertainty on achievable control performance, researchers have generally addressed one or more of the following problems (Skogestad and Morari, 1987):

1. How does the requirement that all plants in the uncertainty set remain stable limit the achievable closed-loop performance of the nominal plant?
2. How does the requirement that all plants in the uncertainty set satisfy a given performance criterion limit the achievable nominal performance?
3. What is the best achievable performance for *all* plants in the uncertainty set?

It will be seen in Chapter 4 that if the performance requirements are specified in an appropriate form, then the second issue is a special case of the first. The exact problem that the designer chooses to address depends very much on the application and on the confidence in the plant model. Considering problem 3 is far more complicated and may be overly conservative in certain situations to design for the worst-case performance. For example, in cases where the plant "operates" close to its nominal point for most of the time, with occasional perturbations, it may be more appropriate to consider problem 1 (Skogestad and Morari, 1987).

Early work by Morari (1983) used the IMC framework to identify the plant condition number as a measure of the plant's sensitivity to (unstructured) model uncertainty. Consider for example the case where the actual process is thought to lie in the following norm-bounded region about the nominal plant

$$G(s) = \tilde{G}\,(I + L_I(s)) \tag{2.36}$$

The above description corresponds to multiplicative input uncertainty where L_I is the plant perturbation and is bounded as follows:

$$\|L_I(j\omega)\|_2 \leq \ell\,(\omega) \tag{2.37}$$

The bound $\ell(\omega)$ on the perturbation L_I usually increases with frequency and exceeds one at high frequencies for any practical process control problem (Morari, 1983). Using the small-gain theorem (to be discussed in Chapter 4), the closed-loop system is stable for all plants in the uncertainty set defined by (2.36) and (2.37) if and only if

$$\left\|G_c\tilde{G}(j\omega)\right\|_2 < \frac{1}{\ell(\omega)} \quad , \quad \forall\,\omega \tag{2.38}$$

Now, since $\ell(\omega)$ exceeds unity at high frequencies, the above requirement for robust stability prevents one from choosing $G_c = \tilde{G}^{-1}$. Therefore, model uncertainty limits the frequency range over which perfect control can be achieved.

In order to satisfy the above requirement, the IMC Robust Control design methodology (Morari and Zafiriou, 1989) involves the introduction of a filter $F(s)$ which essentially detunes the control performance at high frequencies to allow for robustness. The IMC controller then has the form:

$$G_c(s) = \tilde{G}_-^{-1}(s)F(s) \tag{2.39}$$

where the filter is chosen such that $F(s = 0) = I$. The robust stability requirement now becomes:

$$\gamma(\omega) \equiv \left\|\tilde{G}^{-1}(j\omega)\right\|_2 \left\|\tilde{G}(j\omega)\right\|_2 = \frac{\sigma_M(\tilde{G})}{\sigma_m(\tilde{G})} < \frac{1}{\sigma_M(F)\ell(\omega)} \quad , \quad \forall\, \omega\,. \tag{2.40}$$

From the above we see that the condition number γ is a measure of the sensitivity of the control performance to model uncertainty. Processes having small condition numbers are beneficial. The condition number is a system inherent property and is independent of the controller used. Unfortunately the condition number is very sensitive to scaling and thus, when comparing alternative designs, care must be taken to avoid incorrect conclusions. The most common approach to overcome this problem is to use the minimized condition number. However, Skogestad and Morari (1987) report that scaling can distort conclusions regarding the sensitivity of a plant to model uncertainty.

It should be noted that no mention has been made thus far regarding the structure of the model uncertainty. For uncertainty in the manipulated inputs, the inputs are generally independent of each other and thus the perturbation matrix is actually diagonal. The appropriate robust stability condition is then derived in the framework of the structured singular value, in which case it is impossible to eliminate the controller from the formulation. Skogestad and Morari (1987) provide some useful results on the use of open-loop measures to analyze robustness. As these measures do not directly employ the IMC framework, they are discussed later in section 2.4.4 of this chapter.

An alternative approach, which aims at exploiting information regarding the uncertainty structure is due to Arkun and coworkers (Palazoglu *et al.*, 1985; Palazoglu and Arkun, 1986; Arkun, 1986). Their approach makes use of the IMC framework to derive a sufficient condition for robust stability in the presence of model uncertainty. From this condition it is seen that certain "robustness indices" are particularly convenient for modifying a design to improve robustness. They also include these indices together with economic measures to pose a multiobjective optimization problem whereby economics and robustness are traded-off

against each other. The details of their formulation follows.

One of the key features of the approach of Arkun and coworkers is the use of symbolic logic algorithms to carry the design and uncertain parameters in the nonlinear state-space model through to the transfer function representation. This procedure facilitates sensitivity analysis and thus enables design modifications to be made in a systematic manner.

Consider the following transfer function description of a process, obtained by a linear sensitivity analysis about a nominal operating point:

$$G(s,\phi,\beta) = C(\phi,\beta)\,[sI - A(\phi,\beta)]\,B(\phi,\beta) + D(\phi,\beta) \quad , \quad \forall\,\beta \in \mathcal{D} \tag{2.41}$$

where ϕ is a vector containing the process design parameters and β is a vector of uncertain model parameters for which only upper and lower bounds are known through the set $\mathcal{D}$. By using symbolic logic languages such as MACSYMA, Arkun and coworkers are able to perform the necessary parametric operations involving analytic differentiation with excellent accuracy.

Now, using the error multiplicative form to express the actual plant $G(s,\phi,\beta)$ as a function of the known nominal plant model $\tilde{G}(s,\phi,\beta^o)$, we have:

$$G(s,\phi,\beta) = [I + \mathbf{L}(s,\beta)]\,\tilde{G}(s,\phi,\beta^o) \tag{2.42}$$

In the above expression, $\mathbf{L}(s,\beta)$ is the structured model-error matrix, which is a function of the uncertain parameter β and is bounded such that $\sigma_M\,[\mathbf{L}(s,\beta)] \leq \ell_m(\omega)$. Guruswamy (1983) provides an efficient method for determining the uncertainty bound $\ell_m(\omega)$.

Using the IMC framework with G_c chosen as in (2.39), Palazoglu *et al.* (1985) show that the closed-loop system is robustly stable (that is, stable for all $\mathbf{L}(s,\beta)$ such that $\sigma_M\,[\mathbf{L}(s,\beta)] \leq \ell_m(\omega)$), if the following condition holds:

$$(1-\alpha)\frac{1}{\epsilon_1\left[\tilde{G}\right]\,\epsilon_2\left[\tilde{G}\right]} + \alpha\frac{1}{\left(\epsilon_1\left[\tilde{G}\right]\right)^2} > \left(\ell_m(\omega)\sigma_M\left[\tilde{G}_+\right]\,\sigma_M\,[F]\right)^2 \quad \forall\,\omega \tag{2.43}$$

where ϵ_1 and ϵ_2 are the first and second *robustness indices* respectively, and are given by

$$\epsilon_1(\omega,\phi) \equiv \frac{\sigma_M\left[\tilde{G}(j\omega,\phi,\beta^o)\right]}{\sigma_m\left[\tilde{G}(j\omega,\phi,\beta^o)\right]} \tag{2.44}$$

$$\epsilon_2(\omega,\phi) \equiv \frac{\sigma_{M,2}\left[\tilde{G}(j\omega,\phi,\beta^o)\right]}{\sigma_m\left[\tilde{G}(j\omega,\phi,\beta^o)\right]} \tag{2.45}$$

In the above expression $\sigma_{M,2}$ refers to the second largest singular value. All of the above quantities are easily computed by the Singular Value Decomposition techniques (Klema and Laub, 1980).

The parameter α ($0 \leq \alpha \leq 1$) in (2.43) is a measure of the structural information available on the modelling errors. Palazoglu *et al.* (1985) show how α may be determined from the projection of the model error $\mathbf{L}$ onto the "most sensitive" direction of the operator $\tilde{G}_+ F$. When $\alpha = 1$, no information is known regarding the structure of the model uncertainty.

The condition in (2.43) was derived by requiring the projection of the error matrix $\mathbf{L}$ onto the "most sensitive direction" of the IMC structure to be small. Projections onto other "less sensitive directions" may also be incorporated into the formulation. What results is that as more projections are made small, more robustness indices are required in the denominator of the left hand side of (2.43). A system of dimension n has n robustness indices available for this purpose, with the ith one being defined in a similar manner to (2.45) except that the ith largest singular value is used in the numerator. Since $\epsilon_n \equiv 1$, only $n-1$ of the robustness indices are available for analysis.

It is useful to note that the first robustness index ϵ_1 is the process condition number. If the error is completely unstructured, with only a bound on its magnitude and no information available regarding its error projection ($\alpha = 1$), then (2.43) reduces to:

$$\frac{1}{\epsilon_1} > \ell_m(\omega)\, \sigma_M \left[\tilde{G}_+\right] \sigma_M [F] \tag{2.46}$$

which is equivalent to the result derived by Morari (1983) in (2.40), under the assumption that $\sigma_M (\tilde{G}_+) = 1$.

Since the robustness indices depend only on the open-loop plant design and not on the controller or the filter, Arkun and coworkers use them to compare the relative robust dynamic operability of different plant designs. The basic principle is that plant designs with robustness indices close to unity over a wide range of frequencies will be less sensitive to model uncertainty. As different designs may have different error bounds $\ell_m(\omega)$, these can be included in the analysis. Generally, designs having the smallest product $\epsilon_1 \epsilon_2 \ell_m^2$ are regarded as being more favorable from a robust dynamic operability standpoint. The motivation behind this criterion is seen by setting $\alpha = 0$ in (2.43). Care should however be taken since ϵ_1, ϵ_2 and ℓ_m are scaling dependent. Palazoglu *et al.* (1985) scale $\tilde{G}$ to minimize the product of the robustness indices and the error bound. The resulting optimal scaling problem is a min-max semi-infinite optimization problem for which efficient computational techniques exist (Guruswamy, 1983; Arkun *et al.*, 1985).

It should be noted that the approach of Arkun and coworkers does not explicitly test for robust stability but rather chooses designs that are more robust than the other alternatives. Since the filter F is not designed, no guarantee can be made that (2.43) is satisfied. On the other hand, (2.43) is potentially conservative and thus the robustness indices alone are not the only indications of a system's robustness. Good designs may be rejected due to inferior robustness indices even though they might be robust, when measured with more accurate measures of robustness, such as the structured singular value (Skogestad and Morari, 1987). A subtle point to note is that for a system of dimension n there are only $n-1$ robustness indices available for analysis. Therefore, for a 2×2 system we only have the condition number, known to be a potentially conservative measure of the sensitivity to model errors. Despite this weakness, the robustness indices provide an elegant means of improving system robustness, as will be discussed next.

Since the robustness indices are expressed explicitly in terms of the design parameters, it is possible to perform a sensitivity analysis to evolve the current design into a more robust one. This is done by using the mathematical theory of singular value sensitivities (Freudenberg *et al.*, 1982). Palazoglu *et al.* (1985) define the kth robustness index sensitivity of $\tilde{G}(j\omega, \phi)$ with respect to ϕ_i as:

$$\nabla_{\phi_i} \epsilon_k \left[\tilde{G}\right] = \frac{1}{\sigma_m \left[\tilde{G}\right]} \left(\nabla_{\phi_i} \sigma_{M,k} \left[\tilde{G}\right] - \epsilon_k \left[\tilde{G}\right] \nabla_{\phi_i} \sigma_m \left[\tilde{G}\right] \right) \tag{2.47}$$

where $\sigma_{M,k}$ is the kth largest singular value. Use is made of symbolic logic languages to calculate $\nabla_{\phi_i} \tilde{G}(j\omega, \phi)$ at each frequency of interest. On the basis of these sensitivities, the key design parameters can be modified in such a manner so as to improve robustness. Clearly, no design modification should be made without considering its effect on the steady-state economics of the process.

Palazoglu and Arkun (1986) use a multiobjective optimization approach to treat both steady-state economics and robust dynamic operability simultaneously, where the robustness indices are used as measures of dynamic operability. Further details of this are provided in section 2.4.5 of this chapter.

2.4.2 Controllability Analysis Framework

An alternative approach to the IMC method for dynamic operability assessment was proposed by Perkins and coworkers (Perkins and Wong, 1985; Russell and Perkins, 1987; Cao *et al.*, 1994). The approach draws, in particular, on the concept of functional controllability,

introduced by Rosenbrock (1970). As with the IMC approach, the invertibility of the plant model is seen to be essential for perfect control.

Functional controllability is concerned with output reproducibility and is defined as follows (Rosenbrock, 1970; Russell and Perkins, 1987):

> A system with polynomial transfer function matrix $G(s)$ will be called functionally controllable if it satisfies the following condition. Given any output trajectory y which is zero for $t < 0$ and which satisfies certain smoothness conditions, there exists an input trajectory u such that, with the state vector x satisfying $x(0) = 0$, u generates y.

Rosenbrock (1970) showed that a system with a polynomial transfer function matrix $G(s)$ is functionally controllable if and only if $G(s)$ is non-singular, that is invertible. Sufficiency of this condition is obvious since

$$u(s) = G^{-1}(s)y(s) \tag{2.48}$$

is the input trajectory which generates the required output trajectory.

As was established using the IMC framework, we see that perfect control is limited by:

1. RHPT zeros - since these would result in an unstable input trajectory.
2. Time delays - since an input cannot affect an output faster than the smallest time delay in the row corresponding to that output.
3. Input constraints - since these limit the region over which output reproducibility is possible.
4. Model uncertainty - since perfect control requires the inverse of the actual plant, which is unknown if model uncertainty (error) is present.

As was the case with the IMC approach, the concept of functional controllability removes the controller from the evaluation of dynamic operability and shows that performance is limited by the inherent properties of the plant. The controllability approach has been used to determine the effects of each of the above performance-limiting factors on dynamic operability. Details of its application are discussed next.

Nonminimum phase characteristics Rosenbrock (1970) considered the effect of RHP zeros on functional controllability. Perkins and Wong (1985) characterize the effect of time delays on functional controllability with the aid of a parameter $\tau_{\min}$, which is the minimum necessary delay needed before the outputs can be independently specified. The motivation behind their work is that the measures developed by Holt and Morari (1985a) for multivariable time delay systems involve vectors of delay times, which can be awkward to use when ranking process alternatives. The goal of their research was thus to develop a scalar measure for the impact of time delays on controllability (dynamic operability).

Use is made of the z-transform to facilitate the treatment of time delays. The following theorem of Rosenbrock (1970) is central to their work:

> Given a transfer function matrix $G(z)$ with McMillan degree p, and a sequence of outputs $0, ..., 0, y_p, y_{p+1}, ...$, then there exists a sequence of inputs $u_0, u_1, ...$ which generates the output sequence, given $x_0 = 0$, if and only if
>
> $$\det [G(z)] \neq 0 \tag{2.49}$$

The period of time p over which the output is not required to change is an attempt by Rosenbrock to define a delay time for the multivariable system and it is the time that must pass before the output vector can be specified independently. Perkins and Wong (1985) suggested that the scalar delay time p may be used as a measure of control performance for multivariable delay systems. In general though, the McMillan degree p is very conservative and overestimates the minimum necessary delay time. To overcome this, Perkins and Wong provide an algorithm for calculating the minimum necessary delay $\tau_{\min}$ to allow independent specification of all the outputs. The result obtained is equivalent to the largest delay term in G_+^d for a dynamically decoupled response, as obtained using the theorem of Holt and Morari (1985a) and equations (2.28) and (2.29). This was noted by Russell and Perkins (1987) and is easy to see by definition. While the minimum necessary delay is a convenient scalar measure, its utility is limited by the fact that dynamic decoupling for time-delay systems has been shown to be a sub-optimal control strategy (Holt and Morari, 1985a). Therefore, the measure does not strictly correspond to a limit of performance.

Russell and Perkins (1987) also consider the effect of time delays on dynamic operability, but propose an approach that is able to predict the design changes necessary to improve operability. A controllability measure is developed based on a time-domain analysis for systems represented by mixed sets of differential and algebraic equations with time-delays. Direct application of the theory to the time-domain system representation, as opposed to the

input-output representation in Laplace or z-domains, allows insight into the physical cause of control problems. The approach thus has goals similar in some respects to those of Arkun and coworkers (Palazoglu *et al.*, 1985; Palazoglu and Arkun, 1986; Arkun, 1986) where one relates the results of a dynamic operability analysis to identifiable features of the system.

The approach makes use of the concept of structural controllability (Lin, 1974) in conjunction with functional controllability and the theory is extended to delayed differential-algebraic equation (D_{DAE}) systems. Rigorous conditions for controllability are shown to imply the existence of feasible cause and effect paths in the delayed system. The details of the approach are discussed below.

Consider the process system described by a D_{DAE} system, with a non-negative delay associated with each variable in the equation system:

$$f(t, x, \dot{x}, z, u) = 0 \tag{2.50}$$

In the above, t is time, x is a vector of variables whose time derivatives appear in the model, z is a vector of unknowns whose time derivatives do not appear and u is the set of inputs whose time behavior is given. Provided the above model is of index 1, it can be linearized and rearranged to give the state-space form:

$$\dot{x} = Ax + Bu \tag{2.51}$$

where x and u are now perturbation variables about a given steady-state.

A delay occurrence matrix D is now defined, in which the equations in (2.50) are represented by rows, with the columns corresponding to the unknown variables x, $\dot{x}$ and z. The equations in (2.50) are first augmented by the implicit relations between the states x and their derivatives $\dot{x}$ in order to make D square. The sparse matrix D has non-negative time delays associated with each occurrence of a variable in an equation. The proposed control system is now included by augmenting D with columns corresponding to the manipulated inputs and rows corresponding to the equations defining the desired outputs. The resulting structural matrix is denoted by $D(A)$.

Russell and Perkins (1987) define the generic minimum time-delay τ_{ming} of a system with delay occurrence matrix D, as the lowest minimum necessary delay achievable for any system with the same delay matrix D. In other words, the generic minimum delay is determined purely by the delay structure of the delayed DAE system and not by the other aspects of its dynamics. Now, by combining the concepts of structural controllability and minimum necessary delay (determined from a functional controllability argument), it is possible to derive an expression for τ_{ming} of the delayed DAE system.

The condition for generic functional controllability of a delayed DAE with a state-space representation as in (2.51) is that $D(A)$ is structurally non-singular. This implies the existence of cause-and-effect paths in the delay operator $D(A)$. Using the cause-and-effect paths it is possible to determine the minimum necessary delay and to identify the parts of the system that contribute to control problems.

While the above approach is useful for determining sources of control difficulties, it ignores the effects of RHPT zeros, input bounds and model uncertainty. Also, it uses the generic minimum necessary delay as a rating tool, which may be overly conservative as one does not necessarily require independent specification of the outputs.

The concept of structural controllability has more recently been used in a prototype software system which enables the design engineer to expose systems that suffer from poor controllability as a result of inherent structural characteristics (Srinophakhun and Lant, 1996).

Input constraints Since functional controllability deals with output reproducibility and the associated input trajectories, it is not surprising that it lends itself to determining the effect of input constraints on achievable closed-loop performance. Early forms of analysis in this regard (Narraway *et al.*, 1991) used singular value decomposition (SVD) arguments for this purpose. It can be shown that (Morari, 1983; Maciejowski, 1989):

$$\sigma_m(G)\,\|u(j\omega)\|_2 \leq \|y(j\omega)\|_2 \leq \sigma_M(G)\,\|u(j\omega)\|_2 \tag{2.52}$$

where σ_m and σ_M are the respective minimum and maximum singular values of $G(s)$. In the presence of input constraints, the above relation gives the bounds on the reproducible output region when u varies within the manipulated constraint region (Cao *et al.*, 1994). Thus, the larger the singular values, the larger the size of the output region for which trajectories can be specified (Narraway *et al.*, 1991).

Another useful property is the two-norm condition number of $G(s)$:

$$\gamma_2(\omega) \equiv \frac{\sigma_M(G)}{\sigma_m(G)} \tag{2.53}$$

The output trajectories of processes with large condition numbers are very sensitive to the directionality of the inputs. This deforms the shape of the output region and limits the specification of achievable output trajectories. Biss and Perkins (1993) show that in order to describe adequately the effect of input constraints on controllability (dynamic operability), one needs to consider σ_m, σ_M and the two-norm condition number γ_2. It is desirable to have systems with large singular values (σ_m and σ_M) and a condition number γ_2 close to unity over all frequencies.

More recent work by Cao *et al.* (1994) uses a modified singular value analysis technique and an optimization-based approach to asses the effect of input constraints on achievable dynamic performance. As the singular value decomposition is scaling dependent, Cao *et al.* (1994) propose scaling the state and output variables, in the linearized state-space model, by their associated steady-state values. In order to compare results between different processes, the inputs are scaled to be in the range $[-1, 1]$ by dividing every manipulated variable in u by a scaling factor s:

$$s = \min(u^U - u_{sp}, u_{sp} - u^L) \tag{2.54}$$

where u^U and u^L are the upper and lower bounds on the manipulated variables and u_{sp} is the steady-state input level.

A weakness of the singular value decomposition is that it requires any nonlinear process model to be linearized about a particular operating point. The second method considered by Cao *et al.* (1994) requires no such linearization and uses the dynamic model directly. The method determines the best achievable dynamic performance of a given plant and control structure (defined using the integral-square-error (ISE) measure) by solving the following manipulated variable constrained optimization (MVCO), over the time horizon $t = 0$ to $t = t_f$:

$$\begin{aligned} J &= \min_u \int_0^{t_f} (y - y_{sp})^T W (y - y_{sp})\, dt \qquad (2.55)\\ \text{s.t.}\quad f(\dot{x}, x, y, u, t) &= 0 \\ x(0) &= x_0 \\ u^L &\leq u \leq u^U \\ \dot{x}(t_f) &= 0 \\ y(t_f) &= y_{sp} \end{aligned}$$

where y_{sp} is the set of step functions representing the desired output trajectory, W is a diagonal weighting matrix, x is the system states and x_0 is the initial states of the system. The manipulated variables u are constrained between upper and lower bounds u^U and u^L respectively. The software DAEOPT (Vassiliadis, 1992) is used to handle the differential-algebraic nature of the ISE optimization problem.

Model uncertainty Perkins and Wong (1985) show how the condition number emerges naturally as a measure of robustness to unstructured model error using the framework of functional controllability. Given a specified output trajectory y, it is necessary to solve

$$Gu = y \tag{2.56}$$

to determine the required input trajectory. Now, given errors in the model G, the standard estimate of implied errors in u gives:

$$\frac{\|\delta u\|}{\|u\|} \leq \gamma(G) \leq \frac{\|\delta G\|}{\|G\|} \tag{2.57}$$

where $\gamma(G) = \|G\| . \|G^{-1}\|$ is the condition number of G, determined from the appropriate norm on G. The above measure indicates the sensitivity to unstructured model uncertainty since the entire matrix G is perturbed (δG) as opposed to simply perturbing the individual elements of G which cause the model error. Processes with large condition numbers may thus be sensitive to unstructured model uncertainty since, for small errors in the transfer matrix, the implied error in the input trajectory could be large.

Since the condition number is not scale invariant, it is necessary to remove the possible effects of scaling before using it to compare the controllability of alternative designs. Perkins and Wong (1985) recommend using either the optimally scaled ℓ_1-induced or the optimally scaled ℓ_∞-induced condition numbers. The optimal scaling problem for the ℓ_2-induced condition number, proposed by Morari (1983), has not been solved. While scaling the condition number makes intuitive sense, Skogestad and Morari (1987) showed subsequently that minimizing the condition number by input and output scaling tends to distort any conclusions on model error sensitivity and this procedure should therefore be used with caution.

2.4.3 Psarris and Floudas Approach to Dynamic Operability Assessment

Psarris and Floudas (1991a&b) consider the dynamic operability of multivariable systems containing both time delays and right-half-plane transmission (RHPT) zeros. The problem is tackled by realizing that time-delays in multivariable systems play a non-intuitive role, due to the following three (often competing) effects:

1. Time-delays cause a purely delay effect and limit the minimum time before input action is witnessed in the outputs.

2. Time-delays can result in an infinite number of RHPT zeros due to the transcendental nature of the characteristic equation. This point was also noted by Morari (1983) but not considered in the analysis of Holt and Morari (1985a).

3. For systems with an infinite number of RHPT zeros, it is possible to reduce the number present to a finite amount by *increasing* the time delays of certain elements.

The first part of their study involves calculating the zeros of multivariable time-delay systems. For multivariable systems with rational polynomial elements and no time delays, only a finite number of zeros are present and the QZ algorithm (Moler and Stewart, 1973; Laub and Moore, 1978) is a reliable and robust tool for the computation of these zeros. When time delays are present, the algorithm can no longer be applied directly to the system in the frequency-domain. Some researchers have suggested the use of Padé approximations to overcome this problem, but Psarris and Floudas (1991a&b) report that even very high order Padé approximations are not guaranteed to provide accurate information on all the zeros present and may even falsely indicate the presence of zeros. Another approach is to apply the QZ algorithm to a discrete state-space system representation, but the results are sensitive to the sampling time used and are unreliable for large systems. To overcome these difficulties (Psarris and Floudas, 1991a) consider an alternative approach that looks directly at the roots of the characteristic equation.

Consider a linear multivariable system of dimension n with time delays:

$$G(s) = \begin{bmatrix} g_{11}(s)e^{-a_{11}s} & \dots & g_{1n}(s)e^{-a_{1n}s} \\ \vdots & & \vdots \\ g_{n1}(s)e^{-a_{n1}s} & \dots & g_{nn}(s)e^{-a_{nn}s} \end{bmatrix} \tag{2.58}$$

where

$$g_{ij}(s) = \frac{p_{ij}(s)}{q_{ij}(s)} \tag{2.59}$$

with $p_{ij}(s)$ and $g_{ij}(s)$ polynomials in s.

The zeros of such a system are the roots of an equation of the form:

$$H(s) = h(s, e^s) = 0 \tag{2.60}$$

where $h(s, e^s)$ is an exponential polynomial or *quasi-polynomial.* Though (2.60) can be solved by numerical methods, this procedure is impractical for systems containing an infinite number of zeros By exploiting the rich mathematical theory regarding the distribution of the roots of (2.60) (Langer, 1931; Pontryagin, 1942; Bellman and Cook, 1963), Psarris and Floudas were able to:

1. identify systems containing an infinite number of RHPT zeros, and
2. develop asymptotic formulas for their computation without explicitly solving (2.60).

Having determined the location of the RHPT zeros, it is possible to assess the implication that these will have on dynamic operability by using the results of Holt and Morari (1985b).

The idea is that the closer the RHPT zeros are to the origin, the worse will be the achievable closed-loop performance. By combining these results with the upper and lower bounds on the effect of time delays on dynamic operability (Holt and Morari, 1985a), Psarris and Floudas (1991a) attempt to treat simultaneously the performance-limiting effects of time delays and RHPT zeros. Caution should be used however, since the results of Holt and Morari (1985b) were incomplete for multivariable systems containing *multiple* RHPT zeros. Furthermore, the time delay bounds have already been shown to be potentially ambiguous, especially if dynamic decoupling is not desired. Nevertheless, their approach provides valuable insight into the behavior of multivariable delay systems and also allows for a systematic means to enhance the dynamic operability of such systems (Psarris and Floudas, 1991b).

If a system contains an infinite number of RHPT zeros, some of which are near the origin, then it will suffer from poor operability. Psarris and Floudas (1991b) show how the theory of the distribution of zeros of quasi-polynomials may be used to formulate a linear programming problem which identifies those delays of a process that need to be increased, and by how much, in order to obtain a system with a finite number of RHPT zeros.

Clearly, a trade-off is involved between the advantages of fewer RHPT zeros and the disadvantages of larger time delays in certain elements of the transfer matrix. This trade-off is further complicated by the fact that, for decoupled control, it is sometimes beneficial to increase the delays of certain elements (Holt and Morari, 1985a). In fact, Psarris and Floudas (1990) showed that if a system fails the rearrangement test (Holt and Morari, 1985a) then there is room for improvement in the lower response bound, corresponding to the case of dynamic decoupling. They show that an optimal lower bound, which coincides with the upper bound, can be achieved by increasing the delays of a system in a manner determined by the solution of a mixed integer linear programming problem (MILP).

For systems that contain an infinite number of RHPT zeros and for which a sub-optimal lower bound exists (that is, one that fails the rearrangement test), Psarris and Floudas (1991b) propose a MILP framework to identify whether *both* (1) the infinite RHPT zeros can be removed, and (2) an optimum lower bound, can be achieved.

While the approach allows greater insight into the behavior of time-delay systems, it still does not provide one with a clear method for trading off the benefits of reducing or eliminating the number of RHPT zeros with the disadvantage of having larger time delays. Furthermore, it cannot be guaranteed that a system with a finite number of RHPT zeros is better than one with an infinite number if its RHPT zeros are much closer to the origin. Psarris and Floudas (1991b) attempt to use the response time bounds of Holt and Morari (1985a) for this

purpose, but as has been mentioned, these bounds are potentially ambiguous. Moreover, the method does not incorporate the effect of input constraints and model uncertainty.

2.4.4 Further Indicators of Dynamic Operability

Using the IMC framework, controllability analysis and other theoretical results, a number of open-loop measures have been developed for dynamic operability assessment. Some measures are more theoretically rigorous than others, but all simply aim to provide one with an approximation of the expected quality of control achievable. The motivation behind the use of these measures is to facilitate rapid and easy screening of design alternatives at the early stages of design. We review some of the commonly used measures in this section. The implementation of many of these open-loop measures in an X-Windows based software package, referred to as the Process Controllability ToolBox (PCTB), is discussed in Fararooy *et al.* (1993). Indicators such as RHPT zeros and time delay bounds have already been discussed and are not treated in this section.

Measures derived from singular values decomposition

The ability of MIMO systems to display directionality is one of the key differences between such systems and SISO systems. Essentially "directionality" refers to the fact that the amplification of a vector input signal by a system is a function of the relative size of the elements of that vector.

Singular value decomposition (SVD) is a useful way of quantifying the directionality of a multivariable system. Given an $\ell \times m$ complex matrix $G(j\omega)$, its singular value decomposition at a given frequency ω may be written as:

$$G = U\Sigma V^* \tag{2.61}$$

In the above, Σ is an $\ell \times m$ matrix with $k = \min\{\ell, m\}$ non-negative singular values σ_i arranged in descending order along its diagonal, with the remaining entries being zero. The matrix U is an $\ell \times \ell$ unitary matrix of output singular column vectors u_i and V is an $m \times m$ unitary matrix of input singular column vectors v_i. Being unitary, U satisfies the requirement that $U^* = U^{-1}$, with all its singular values being one. Clearly the same applies to V.

The column vectors of U are orthogonal and of unit length (orthonormal) and represent

output directions of the plant. In other words they satisfy:

$$\begin{aligned} ||u_i||_2 &= \sqrt{|u_{i1}|^2 + \ldots |u_{i\ell}|^2} = 1 \\ u_i^* u_i &= 1 \\ u_i^* u_j &= 0 \quad \forall\, i \neq j \end{aligned} \tag{2.62}$$

In a similar manner the column vectors of V are orthonormal and represent the input directions of the system. Care should be taken not to confuse the output singular vectors u_i with the standard notation to represent the input signal in process control.

The input and output directions, v_i and u_i respectively, are related through the singular value σ_i. This is best seen by noting that since V is unitary ($V^*V = I$), we have $GV = U\Sigma$. For column i this becomes:

$$Gv_i = \sigma_i u_i \tag{2.63}$$

Thus, given an input in the direction v_i, the output is in the direction u_i. By noting that $||v_i||_2 = ||u_i||_2 = 1$, we see that σ_i gives the gain of the matrix G in the direction of the input v_i. The singular values of a transfer function are thus measures of the gains of the process in different directions. The maximum singular value σ_M is the largest gain for *any* input direction and the minimum singular value σ_m is the smallest gain for any input direction. The output and input vectors associated with σ_M are denoted u_M and v_M respectively. Similarly, the vectors u_m and v_m relate to the minimum singular value σ_m.

As an example, consider the following system where G is a constant real matrix given by (Skogestad and Postlethwaite, 1996):

$$G = \begin{bmatrix} 5 & 4 \\ 3 & 2 \end{bmatrix} \tag{2.64}$$

The singular value decomposition of G is:

$$G = \underbrace{\begin{bmatrix} 0.872 & 0.490 \\ 0.490 & -0.872 \end{bmatrix}}_{U} \underbrace{\begin{bmatrix} 7.343 & 0 \\ 0 & 0.272 \end{bmatrix}}_{\Sigma} \underbrace{\begin{bmatrix} 0.794 & -0.608 \\ 0.608 & 0.794 \end{bmatrix}}_{V^*} \tag{2.65}$$

The largest gain occurs for the input direction $v_1 = \begin{bmatrix} 0.794 & 0.608 \end{bmatrix}^T$ and is of magnitude 7.343. The smallest gain of 0.272 is for an input direction $v_2 = \begin{bmatrix} -0.608 & 0.794 \end{bmatrix}$. From the relatively large difference between the largest and smallest singular values it is clear that certain combinations of the inputs have a strong effect on the outputs whereas other combinations have a weak influence.

In the context of dynamic operability one desires plants that are able to achieve good control of the outputs with little input effort. This is particularly the case when input constraints are present.

Therefore, a plant with large maximum and minimum singular values, σ_M and σ_m respectively, is desirable as it means that all input directions will have significant effects on the outputs. As a result, the effect of input constraints on achievable closed-loop performance is reduced. In addition to requiring large singular values one also requires the process condition number, the ratio between maximum and minimum singular values, to be close to unity over all frequencies. If this is not the case then the plant is said to be "ill-conditioned" and sensitive to the direction of inputs.

In many cases "ill-conditioned" plants are sensitive to model uncertainty, especially if the model uncertainty changes the directionality of the plant (Skogestad *et al.*, 1988). Stated differently, processes for which the presence of model uncertainty significantly changes the way in which input signals are amplified, should be avoided. However, great care should be taken in rejecting a plant with a large condition number on the basis of its sensitivity to model uncertainty as the relation between the condition number and closed-loop stability and performance is sufficient but not necessary (Morari and Zafiriou, 1989). It can therefore be very conservative and acceptable designs may be unfairly rejected.

Disturbance condition number

For a single disturbance acting directly on the outputs, with $y = g_d d$, the disturbance direction is defined as:

$$y_d = \frac{g_d}{\|g_d\|_2} \tag{2.66}$$

If $y_d = u_M$, where u_M is as defined earlier in the SVD of G, the disturbance lies in the output direction in which the plant has the largest gain. As a result, such a disturbance is relatively easy to reject. On the other hand, if $y_d = u_m$, it lies in the output direction for which the process has the smallest gain and can only be rejected with large input action. This may be problematic if tight input constraints are present.

Associated with the disturbance direction is the disturbance condition number γ_d defined as:

$$\gamma_d = \frac{\|G^{-1}G_d\|}{\|G_d\|}\sigma_M(G) \tag{2.67}$$

where G_d is the disturbance transfer matrix corresponding to disturbances acting directly on the output. The disturbance condition number is a function of frequency and may vary

between unity and the process condition number. When used in conjunction with the condition number γ, it reveals whether the disturbances lie in the most critical directions of the plant. Plants for which γ_d is close to unity over all frequencies are likely to be easy to control. Plants for which $\gamma_d \simeq \gamma$ are likely to suffer from poor control because the disturbance is in the direction corresponding to low plant gain.

Frequency dependent relative gain array

The steady-state relative gain array (RGA) was originally proposed by Bristol (1966) as a means of assessing interaction problems and recommending possible pairings for decentralized controllers. It is defined as follows:

$$RGA = G(0) \times \left[G(0)^{-1}\right]^T \tag{2.68}$$

where $\times$ denotes element-by-element multiplication and the matrix $G(0)$ is the steady-state gain matrix of the process.

Morari and Perkins (1995) report that the steady-state RGA is often erroneously used in industry as a controllability indicator. Skogestad and Morari (1987) showed that the steady-state RGA is a reliable indicator of closed-loop sensitivity to element uncertainty only if the relative errors of the transfer matrix elements are independent and have similar magnitudes. Indiscriminate use of the RGA for robustness analysis can lead to very misleading results (Skogestad *et al.*, 1990).

The frequency-dependent RGA is a simple extension of the RGA, whereby the RGA is evaluated as a function of frequency. Skogestad and Postlethwaite (1996) provide many useful control-related properties of the frequency-dependent RGA. These include indications of sensitivity to diagonal input uncertainty, the presence of RHP zeros in $G(s)$ or some subsystem of $G(s)$ and an indication of diagonal dominance. In addition to these properties, Skogestad *et al.* (1991) have shown the frequency-dependent RGA to be a reliable measure of robustness when used in conjunction with the closed-loop disturbance gain (discussed subsequently).

Performance relative gain array (PRGA)

The performance relative gain array Γ may be thought of as a scaled inverse of the plant model. It is defined as follows:

$$\Gamma(s) = G_{\text{diag}}(s)\, G^{-1}(s) \tag{2.69}$$

where G_{diag} is a diagonal matrix containing the diagonal elements of G. The diagonal elements of Γ are equal to those of the *RGA*, defined earlier. Skogestad and Postlethwaite (1996) show that for good decentralized control performance it is desirable to have *small* elements in Γ, at least at frequencies where feedback is effective. At frequencies closer to the crossover frequency, stability is the major issue and it is desirable to have the diagonal elements of Γ close to unity. This result is based on the assumption that G is arranged such that the ith input is used to control the ith output. For different sets of pairings of manipulated variables and controlled variables, the plant transfer matrix has to be rearranged accordingly and the performance relative gain array recalculated.

Closed-loop disturbance gain and relative disturbance gain

The closed-loop disturbance gain (CLDG or $\tilde{G}_d$), introduced by Hovd and Skogestad (1992), may be defined in terms of Γ as follows:

$$\tilde{G}_d(s) = \Gamma(s)\, G_d(s) \tag{2.70}$$

where G_d is the disturbance transfer matrix for disturbances acting directly on the output. The CLDG depends on both input and output scaling. For a single disturbance, $\tilde{G}_d$ is a vector whose ith element gives the apparent disturbance gain as seen from loop i when the system is controlled using decentralized control (Skogestad and Postlethwaite, 1996).

For a single disturbance g_d acting directly on the output, the relative disturbance gain β is defined as follows (Stanley *et al.*, 1985):

$$\beta_i = \frac{\tilde{G}_d}{g_d} \tag{2.71}$$

By definition, the effect of the disturbance on the ith output with no control is $g_{d\,i}$. Thus, the relative disturbance gain can be viewed as the ratio of the disturbance effect on a measurement with and without (decentralized) control. It is desirable to keep β_i small since this means that control loop interactions are such that they reduce the effect of the disturbance (Skogestad and Postlethwaite, 1996).

2.4.5 Incorporation of Economic Considerations

A shortcoming of the approaches treated thus far is their inability to consider all the performance-limiting factors simultaneously. A further disadvantage is that the economics associated with good or poor control performance is difficult to quantify. This section will focus primarily on reviewing approaches that have been developed to treat the latter issue. Two key methods for exploring the interrelationship between economics and dynamic operability will be addressed. The first involves a multiobjective analysis where a pareto-optimal set of designs is selected from a number of alternatives. In this manner those designs that have inherently inferior economics and dynamic operability are eliminated from further consideration. The second treatment makes use of a more direct quantification of the benefits of good control and aims to compare designs on a common economic basis. At this stage the discussion is limited to the analysis of given alternative designs, with the issue of synthesis being treated in the following section.

Multiobjective approaches

Early work on the simultaneous consideration of economic and dynamic aspects in process design is due to Lenhoff and Morari (1982). Their approach involved the determination of a pareto-optimal set of design alternatives where an economic performance index (EPI) is optimally traded-off against a dynamic performance index (DPI). The approach is illustrated on a heat-integrated distillation column example where the goal is to select column configurations, column designs and control structures with the most favorable operational characteristics.

The EPI is chosen as the vapor boilup rate as this is directly related to the operating expenses (utility usage), which usually dominate the steady-state economic analysis of such columns. As the capital expenses for distillation columns are usually small compared to the operating expenses, and because the three alternative configurations considered use almost identical pieces of equipment, these issues are neglected in the EPI. Designs having a lower EPI are favorable from a steady-state economic viewpoint. The selection of measured and manipulated variables (the control structure) has no influence on the EPI since measurement and instrumentation costs are not considered. The choice of control structure may, however, have a significant effect on the DPI. An integral square error (ISE) measure is used as the DPI, with lower values being favorable. An output feedback controller of a fixed structure is used, with the tuning parameters included as search parameters in the optimization.

A key to this approach is the efficient calculation of a lower bound on the DPI. In order to reduce the complexity of the problem, a lower bound is determined by analyzing the subsystems formed by a decomposition of the original system. In this way, the modular structure of typical processing systems is exploited. This decomposition technique and certain bounding properties of the Lagrangian enable larger, more complicated systems to be analyzed. Application of this approach to the heat-integrated distillation column problem identified those steady-state designs which are inherently inferior in both economic and dynamic aspects.

Palazoglu and Arkun (1986) also use a multiobjective optimization approach to study the interrelationship between steady-state economics and dynamic operability. The robustness indices developed by Palazoglu *et al.* (1985) are used as a measure of dynamic operability. Use is made of the ε-constraint method of Haimes *et al.* (1975) to treat the multiobjective nature of the problem. Essentially, the dynamic operability criterion is included as a constraint and the overall nonlinear programming problem solved for a number of different values for the bound on the dynamic operability measure. Since the robustness indices are frequency-dependent, a semi-infinite nonlinear program results for each value of the dynamic operability bound. A discretization strategy is suggested by Palazoglu and Arkun (1986) and an interactive ellipsoid algorithm is used to allow the user to recover manually from local optima, which occur readily due to the nonconvex nature of the problem. Applying this procedure yields pareto-optimal trade-off curves between steady-state economics and dynamic operability, which can be used by the designer to screen alternative designs.

Economic assessment of process disturbances

In contrast to the multiobjective approaches discussed above, the approaches in this section attempt to quantify the economic benefits of good control directly. The pioneering research in this regard is due to Perkins (1989) and is outlined in an exploratory paper by Narraway *et al.* (1991). The basic concept is summarized in Figure 2.8 and discussed below.

The conventional approach to optimization-based process design involves determining the set of steady-state operating conditions which optimize an economic measure subject to a set of equality (process model) constraints and a set of inequality (operational) constraints. The optimal steady-state point determined in this fashion usually lies at the intersection of (active) process constraints, as shown in Figure 2.8. In practice it is not possible to operate the plant on these active constraints as process disturbances will result in constraint violations. In order to ensure feasible operation in the presence of disturbance-induced fluctuations, it is necessary to move the steady-state operating point away from the active constraints.

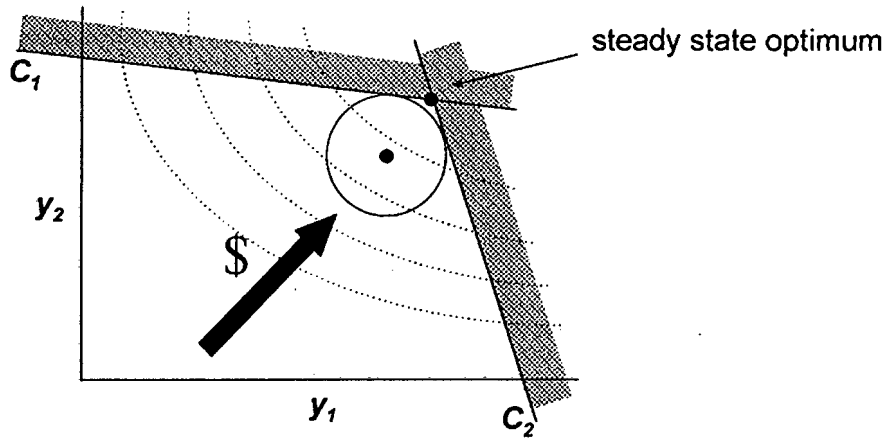

Figure 2.8: The economics of process control.

The disturbance-induced fluctuations are indicated by the "ball" in Figure 2.8. The size of the "ball" around the steady-state operating condition is a function of the disturbance regime and the control system. The steady-state operating point should be chosen such that economic performance is optimized without any point in the ball violating the operating constraints. Clearly, the smaller the effect of disturbances on the process, the closer one can operate to the desired steady-state optimum and the less one needs to sacrifice economics. Since the sensitivity of a plant to disturbances is closely related to its dynamic operability, it is evident that the above procedure allows one to quantify the economics associated with good dynamic operability.

Narraway *et al.* (1991) use linear frequency-response techniques and pose a linear programming problem to determine the "back-off" required in order to prevent constraint violation in the presence of sinusoidal disturbances. The frequency domain analysis is based on asymptotic behavior and does not consider the initial transient behavior. While the approach only approximates the back-off necessary, it nevertheless provides valuable insight into the economic benefits associated with processes that are inherently easy to control.

Narraway and Perkins (1993a&b) extend the above approach to consider the problem of control structure synthesis for linear and nonlinear dynamic models. Given a set of candidate manipulated variables and measurements, their associated instrumentation costs and a specified disturbance regime, an optimal control structure is sought which minimizes the economic give-away implied by the ball-size analysis and the cost of control instrumentation.

Narraway and Perkins (1993a) consider a linear analysis where both the dynamic model

and the economic objective are assumed to be linear. Furthermore, it is assumed that the control performance may be approximated via the perfect control hypothesis. That is, the disturbance effects do not appear in the measured variables but only in the manipulated variables. Using a frequency-response analysis, the resulting optimization problem is almost a mixed-integer linear program (MILP) with the only nonlinearity being associated with the calculation of the ball-size. This nonlinearity includes discontinuities in the first derivatives due to the calculation of the moduli of complex variables. A special algorithm which takes these properties into account in the solution procedure is presented. Application of the approach to case studies revealed that the resulting control structure is critically dependent on the disturbance regime assumed. Furthermore, the relationship between the disturbances and the control structure is not simple. It is reported that examples exist in which increasing levels of disturbance require a less sophisticated control structure (Narraway, 1992).

Narraway and Perkins (1993b) address the issue of nonlinear systems and include realistic controller models. Multiloop PI controllers are used, where the required pairings have to be selected in the optimization as well. To reduce the computational burden, only a single sinusoidal disturbance is considered. The resulting mixed-integer nonlinear programming (MINLP) problem is solved by a version of the outer-approximation augmented penalty algorithm of Viswanathan and Grossmann (1990). Application of the approach revealed significant nonconvexities, which resulted in multiple local minima. Nevertheless, the method consistently suggested good structures, although they were not optimal.

Lear *et al.* (1995) propose an approach for simultaneously assessing the impact of process dynamics, model uncertainty and controller complexity on process economics. The approach considers linear systems where an economic objective is optimized subject to bounds on the input and output responses. The key feature of the method is that the steady-state input and output constraints are modified in order to compensate for disturbance-induced variations. In this way the optimal operating point is moved away from the bounds to prevent constraint violation as a result of input manipulation and output variation in the presence of disturbances.

The approach utilizes the fundamental insight that control systems seek to transform variability (disturbances) in one stream to variability in another (Downs and Doss, 1991). For the open-loop case, sinusoidal disturbances result in output variability, with the inputs remaining constant. If perfect control is possible then all of the variation introduced by the disturbance is transferred to variation in the inputs and the outputs remain constant at their desired levels. Due to the presence of process constraints it may not always be economically optimal to transfer all the disturbance variability onto either the input or the output. In

some cases it is beneficial, from an economic viewpoint, to tolerate less than perfect control in the outputs in order to spread the disturbance effect more evenly between the inputs and outputs. Lear *et al.* (1995) term this partial control and introduce a partial control factor k to determine the best level of control to be used.

The deviations in the inputs and outputs are calculated from steady-state frequency-response methods and depend on the disturbances encountered and the controller used. Lear *et al.* (1995) adopt a numerical approach to determine the maximum magnitudes of the input and output deviations as a function of the partial control factor k and the controller being used. The deviations are then used to adjust the bounds and the optimal economic performance is calculated. In order to consider the effect of model uncertainty, the IMC approach is used to design an H_∞ controller. The benefit of using such a controller in the analysis is that it is advanced, but is still realistic (implementable) and is able to consider model uncertainty. Application of their approach to a simple SISO problem illustrated its utility as well as the economic benefits achievable with the use of sophisticated H_∞ controllers.

Bandoni *et al.* (1994) consider the economic impact of disturbances at steady-state when no control action is taken (open-loop). The result provides a measure of the economic incentive for a well designed control system. In order to characterize the necessary back-off, they define a region of variation for the uncertain disturbances. It is assumed that the disturbances acting on the process are step-like and satisfy the following relation:

$$\Gamma = \left\{ d \,|\, d^N - d^- \leq d \leq d^N + d^+ \right\} \tag{2.72}$$

where d^N corresponds to the known nominal disturbance level and d^+ and d^- are deviations in the positive and negative directions about d^N. It is assumed that any choice of $d \in \Gamma$ is equally probable. The optimal steady-state operating conditions that have sufficient open-loop back-off to ensure feasibility are given through the solution of the following semi-infinite optimization problem:

$$\begin{aligned} & \min_m \Phi(m, x, d^N) \\ \text{s.t.} \quad & h(m, x, d) = 0 \qquad \forall\, d \in \Gamma \\ & g(m, x, d) \leq 0 \qquad \forall\, d \in \Gamma \\ & m_L \leq m \leq m_U \end{aligned} \tag{2.73}$$

where Φ is the steady-state economic objective to be optimized, h includes the model equations and equality specifications and g comprises the inequality constraints associated with operational specifications. The vector m contains the independent (optimization) variables or process degrees of freedom. In the open-loop back-off problem, m is any physical input

and is bounded from above and below by m_U and m_L respectively. The vector x is the set of dependent (state) variables which, through h, are functions of the degrees of freedom m and the disturbances d.

Due to the continuous disturbance description in (2.72), an infinite number of constraints must be satisfied. Bandoni *et al.* (1994) employ an extension of the cutting-plane algorithm of Bandoni and Romagnoli (1989) and Gonzaga and Polak (1979) to solve the resulting semi-infinite optimization problem. It should be noted that the above problem is conceptually similar to the steady-state flexibility analysis introduced earlier. The difference lies in the fact that the objective function is an economic criterion, with the degree of flexibility being specified by the constraints.

Figueroa *et al.* (1994a) introduced the concept of maximum percentage recovery (MPR) as a tool for comparing the economic merit of alternative controller types. The MPR is defined as follows:

$$MPR = 100\frac{\Phi_C - \Phi_B}{\Phi_A - \Phi_B} \tag{2.74}$$

Here, Φ_A corresponds to the situation where perfect regulatory control is achieved and no back-off is required (provided there is sufficient input rangeability to reject the disturbances). Φ_B corresponds to the steady-state open-loop case, namely the solution of (2.73), while Φ_C depends on the type of closed-loop controller used.

Figueroa *et al.* (1994b) extended the steady-state ideas of Bandoni *et al.* (1994) to the closed-loop dynamic case. The first part of their analysis involves determining the dynamic open-loop back-off necessary to ensure feasibility despite disturbance-induced dynamics. The problem formulation is similar to that of Bandoni *et al.* (1994) except that the dynamic model is included in the problem formulation, resulting in a differential-algebraic optimization problem.

Having established a measure of dynamic open-loop back-off, Figueroa *et al.* (1994b) make use of the maximum percentage recovery to determine the economic benefits associated with a particular controller. The formulation of the dynamic closed-loop back-off calculation, to determine Φ_C, is as for the dynamic open-loop problem, with the inclusion of the controller tuning parameters as search variables and the inclusion of the differential equations defining the controllers.

2.4.6 Synthesis of Dynamically Operable Plants

The synthesis of plants that are both economical and operable has received relatively little attention in the literature. In this section we review some of the important developments in this regard. We first consider a heuristic approach to the synthesis of controllable plants, which is an extension of the systematic synthesis procedure of Douglas (1985). Thereafter we explore optimization-based approaches which either use a multiobjective formulation or which directly use an economic assessment of the effect of disturbances.

Heuristic approach

Douglas and coworkers (Fisher *et al.*, 1985, 1988a,b&c) propose a systematic procedure for assessing dynamic operability at the early design stages. The approach is based on steady-state arguments whereby the economics associated with control is used as an additional tool for screening alternative designs. The goal of their approach is to develop a preliminary control structure (set of measured and manipulated variables) that provides a starting point for subsequent dynamic studies.

By using a steady-state analysis to determine flowsheet and equipment modifications that enhance controllability, they are able to eliminate the following important sources of poor control quickly and efficiently:

1. Insufficient manipulated variables to accomplish the control objectives;
2. Insufficient control action available to achieve these objectives;
3. Neglecting important interactions caused by recycle loops or other arrangements of coupled equipment.

In order to determine a good control structure, two preliminary studies are conducted at the early design stage. The first involves generating an adequate number of manipulated variables to achieve the economic and non-economic control objectives (Fisher *et al.*, 1988a). The second involves an adequate overdesign of "bottleneck" equipment (Fisher *et al.*, 1988b). In each of these studies, use is made of the hierarchical decision procedure for flowsheet synthesis developed by Douglas (1985). The above two issues are thus considered at each of the following process design decision levels:

1. Batch versus continuous
2. Input-output structure of the flowsheet
3. Recycle structure of the flowsheet
4. Separation system - general structure
   (a) Vapor recovery system
   (b) Liquid recovery system
5. Heat exchanger network

Having carried out these two studies, the next step is the determination of the control structure. Fisher *et al.* (1988c) provide a heuristic approach for determining of a control structure that will provide near-optimal steady-state performance after dynamic transients have decayed. The basic methodology is to select as controlled variables the constrained operating variables and those variables which correspond to active constraints in a steady-state optimization. Manipulated variables are chosen as those variables which need to be free in order for the process constraints to be satisfied and/or the operating costs to be kept low over the expected range of disturbances.

Clearly, such a steady-state analysis is insufficient for the design of a dynamic control system. For this reason, Douglas and coworkers propose that above mentioned procedure should form a starting point from which dynamic control studies can be performed.

In terms of the terminology of this thesis, the approach of Douglas and coworkers uses heuristic steady-state arguments to treat both flexibility and dynamic operability issues in a combined fashion. The determination of process bottlenecks is typical of flexibility studies, whereas the determination of control structure is usually the focus of dynamic operability studies.

The methods discussed above aim to address a large class of chemical processes. In contrast to this, Luyben (1993) introduced an approach for designing operable jacketed, perfectly mixed chemical reactors. The conflicts between steady-state economic design and dynamic process control in jacket-cooled continuous stirred-tank reactors (CSTRs) are explored through simple examples. These examples show that the conflict between design and control affects not only capital costs but also product yield in systems with more complex kinetics. Having gained insights from these examples, a design methodology is proposed which attempts to resolve these conflicts in a quantitative manner. Important design parameters

for CSTRs include the reactor temperature, the feed flowrate and the coolant temperature. The goal is thus to choose these in such a way that one has good operability and steady-state economics.

An essential element of the approach proposed by Luyben (1993) is the use of a controllability index R_Q, defined as the ratio of the maximum heat-removal rate to the nominal design heat-removal rate. The designer selects a desired value of R_Q, typically in the range 1.5 to 3, based on the need for tight temperature control, the expected disturbances and the accuracy of kinetic, thermodynamic and transport data. Clearly, lumping all these considerations into a single parameter is perhaps simplistic and Luyben states that future work in this regard will involve a more careful determination of acceptable values for R_Q.

By choosing a desired value for the controllability index R_Q and any two of the three design parameters mentioned earlier, the procedure enables the remaining design parameter to be determined. The economics associated with this design choice may then be calculated. If no feasible solution exists, then different design parameters should be chosen or the desired level of controllability should be loosened.

Optimization-based approaches

Very few algorithmic synthesis techniques exist for the design of processes that are both economical and operable or where economics is optimally traded-off against operability. Early work looking at the interaction between design and control involved that of Nishida *et al.* (1976) who used the framework of optimal control to pose the synthesis problem as a min-max optimization problem.

The fundamental starting point for such mathematical programming-based synthesis procedures is the construction of a process superstructure that incorporates all possible design alternatives of interest. This superstructure contains both discrete decisions regarding the existence of units, and continuous decisions about the values of process variables. The resulting mathematical model requires both binary and continuous variables and leads naturally to a MINLP of the form:

$$\begin{aligned} & \min \ f(x,y) \\ \text{s.t.} \quad & h(x,y) = 0 \\ & g(x,y) \leq 0 \\ & x \in \mathcal{X} \end{aligned} \tag{2.75}$$

$$y \in \{0,1\}$$

Here, x represents continuous variables such as flowrates, compositions, pressures and temperatures. The binary variables y denote the existence of particular units or structures within the overall process superstructure. A single objective function $f(x,y)$ is chosen to describe the economics associated with a particular design. The equality constraints $h(x,y)$ typically include material and energy balances as well as thermodynamic relations. The inequality constraints $g(x,y)$ include constraints on process variables as well as logical constraints regarding the existence of units and their associated variables.

Solution methods for (2.75) include the Generalized Benders Decomposition (Paules and Floudas, 1989) and the Outer Approximation/Equality Relaxation/Augmented Penalty approach (Viswanathan and Grossmann, 1990). Due to nonconvexity, no guarantee regarding global optimality is possible.

Multiobjective approach Luyben and Floudas (1994a&b) use a multiobjective MINLP approach to study the trade-off between various steady-state controllability measures and economics in the context of process synthesis. The controllability measures include the maximum and minimum singular values, the plant condition number, the disturbance condition number and the relative gain array. The advantage of these measures is that they depend only on the process itself and not on the controller. However, their steady-state nature makes inferences on dynamic aspects tenuous at best.

Due to the multiple objectives relating to economic aspects and the controllability measures, the resulting mathematical problem leads naturally to a multiobjective MINLP of the form:

$$\begin{aligned} & \min\ U\left[f_1(x,y),...,f_P(x,y)\right] \\ \text{s.t.}\quad & h(x,y) = 0 \\ & g(x,y) \leq 0 \\ & x \in \mathcal{X} \\ & y \in \{0,1\} \end{aligned} \tag{2.76}$$

where $f_i(x,y)$ are the individual objective functions relating to the steady-state economic aspects and the controllability measures. It should be noted that $g(x,y)$ in (2.76) may also include constraints on the controllability measures. The integer variables y are used to define the space of alternative process structures, while the continuous variables x define the associated design parameters. The purpose is to determine a set of plant layouts and design parameters that provides a noninferior trade-off between the multiple objectives in U.

The utility function U is, in general, unknown. If it were known explicitly, (2.76) would simply involve a conventional scalar optimization problem similar in form to (2.75). Although each objective function can be individually minimized, together they are in conflict. As a result, one obtains a set of solutions in which one objective can only be improved at the expense of one or more of the other objectives. This is the noninferior solution set, also termed the efficient, nondominated or pareto-optimal set.

Luyben and Floudas (1994a&b) make use of the ε-constraint method (Haimes *et al.*, 1975) for determining the noninferior set, by adding inequality constraints to the scalar optimization of a single objective. The best-compromise solution between the competing design and control objectives is determined on the basis of the partial derivative information from the noninferior set, using a multiobjective algorithm based on cutting planes.

Economic assessment of process disturbances Mohideen *et al.* (1996) propose a unified synthesis framework for obtaining plant designs and control systems which are economically optimal while being able to cope with process variations. The approach makes direct use of the nonlinear differential-algebraic model equations and considers both low frequency time-varying uncertain process parameters and high frequency time-varying disturbances. Both the control structure and the controller design are part of the optimization problem and a robust stability criterion is included to account for the destabilizing effects of the uncertain parameters.

An objective function is chosen which accounts for the average expected operating costs as well as the capital costs of process units and controllers. The inclusion of a term in the objective function relating to control loop costs allows for a comparison of alternative control structures on a common economic basis.

The constraints include path constraints on the dynamic behavior of the system, which have to be satisfied throughout the period of operation for any combination of uncertain parameters and disturbances. Furthermore, a set of constraints is introduced for the definition of an appropriate, optimally tuned, multi-loop PI control scheme. In addition, a constraint is included which enforces the stability of the nonlinear time-varying system by means of a bound on the induced vector norm of the Jacobian matrix of the nonlinear system.

The above, mixed-integer stochastic optimization problem is solved via an efficient decomposition algorithm which involves the following:

1. Orthogonal collocation on finite elements is used to convert the infinite dimensional

mixed-integer optimal control problem into a finite dimensional one.

2. Successive solution of:

   (a) a multi-period design/control subproblem with explicit stability requirements in order to provide an optimal set of design variables and a control structure which is stable and can accommodate uncertainty and disturbances at specified periods, and

   (b) a combined feasibility-stability analysis over time subproblem which provides a new set of critical periods to be further included in the multi-period problem.

The method is able to treat binary variables corresponding to both alternative process operations and alternative measured or manipulated variables. Furthermore, it accounts for the problem of robust stability in the presence of uncertain process parameters and includes the controller tuning parameters as optimization variables. While it is likely to be extremely computationally intensive for large systems, it does provide an excellent approach upon which further studies can be based.

Another systematic approach to the synthesis of economically optimal and operable process designs is due to Bahri (1996). The approach introduces both flexibility and dynamic operability aspects into the design procedure and poses synthesis as a dynamic MINLP with uncertainty. The method is an extension of the research of Bahri *et al.* (1995) which involved optimizing economic performance while satisfying constraints on the regulatory performance in the form of bounds on the peak response of the system to disturbances. Figueroa *et al.* (1996) consider a similar problem, but with the design fixed.

Bahri (1996) extends the approach of Bahri *et al.* (1995) to include more sophisticated measures of regulatory performance (dynamic operability). The measures include bounds on the squared errors between the outputs and their setpoints as well as bounds on the response time of the system. The worst-case disturbances are also calculated automatically.

To summarize, the method selects a process and control structure together with operating conditions so that the resulting plant:

1. has a steady-state operating point at the minimum possible distance from the optimum, without violating feasibility requirements,

2. takes the least time to reach its original steady-state after a disturbance acts on the system, and

3. responds to the disturbances smoothly and has an acceptable squared-error behavior.

2.5 Conclusion

In this chapter we have reviewed a number of the systematic approaches that have been developed for the assessment of plant operability. Particular attention has been paid to the issue of dynamic operability assessment.

The majority of the methods for dynamic operability assessment are either analytical or involve numerical calculation of an open-loop controllability measure. As such, they are not suitable for the simultaneous consideration of all the performance-limiting factors in an unambiguous manner. It was seen that optimization-based approaches are able to include actual performance requirements and obtain a less ambiguous ranking of process alternatives. Furthermore, nonlinear dynamic models may often be handled directly, without linearization.

Recent developments in the synthesis of dynamically operable plants show that considerable progress has been made since the early research of the 1980's. Nevertheless, there are still some unresolved issues which this thesis aims to address. The first is the rigorous assessment of a limit of achievable closed-loop performance in the presence of *all* the performance-limiting factors. The second is the inclusion of economic aspects into the formulation without simplifying assumptions being made as to the quality of control achievable. The approach adopted in this thesis is based on the Q-parametrization of all stabilizing linear feedback controllers and is discussed in the chapters to follow.

Chapter 3

The Q-Parametrization Approach to Dynamic Operability Assessment

3.1 Introduction

As mentioned in the previous chapter, dynamic operability is a measure of the quality of closed-loop control performance that can be achieved for a plant via feedback (Morari, 1983). The quality of control clearly depends on the plant design, the selection of measured and manipulated variables (control structure) and the controller design. In order not to bias the results by the choice of controller type or tuning parameters, Morari proposed that dynamic operability be determined as a limit of achievable control performance. In this way it is a function of the inherent limitations present in the process design and the selected control structure.

Using the Internal Model Control (IMC) framework, Morari (1983) argued that the factors that limit the achievable control performance of a system are right-half-plane transmission (RHPT) zeros, time delays, input constraints and model uncertainty. In order to assess the effect of these factors on dynamic operability, a number of alternative measures have been developed in the literature. These approaches were discussed in Chapter 2, and may be summarized as follows (Ross and Swartz, 1997b):

1. The Internal Model Control (IMC) framework: An alternative controller parametrization is used to show that time delays, right-half-plane transmission (RHPT) zeros, input constraints and model uncertainty limit the achievable closed-loop performance

of a system. These limits of performance may be determined analytically for certain special cases (Holt and Morari, 1985a&b).

2. The controllability analysis framework: The ability of a process to follow a desired output trajectory is related to properties in the plant model (Perkins and Wong, 1985; Russell and Perkins, 1987). Rather than seeking an optimal controller (or plant factorization), an optimal input trajectory is sought (Cao *et al.*, 1994).

3. Open-loop measures: Theoretical and heuristic arguments are used to derive simple measures of dynamic operability which aim to be consistent with the results achieved using a more rigorous analysis of the problem (Skogestad *et al.*, 1991).

4. Optimization-based approaches: Mathematical programming is used to address both dynamic operability analysis and the synthesis of operable plants (Bahri, 1996; Mohideen *et al.*, 1996). The economic benefits associated with good control are assessed by determining the economic back-off required to ensure dynamic feasibility in the presence of disturbances.

A shortcoming of the first three approaches listed above is their inability to consider all of the performance limiting factors *simultaneously*. Furthermore, the economics associated with good or poor control performance is difficult to quantify. The optimization-based approaches are able to assess combinations of performance limiting factors and quantify the economic benefits associated with good control. However, the majority of such optimization-based approaches make simplifying assumptions regarding the controller and the achievable control performance. Furthermore, no guarantee of global optimality is possible for the resulting non-convex optimization problems.

In this chapter, an approach to dynamic operability assessment, based on the Q-parametrization of stabilizing linear feedback controllers is presented. The method was first proposed by Swartz (1994) and closely follows that of Boyd and coworkers (Boyd *et al.*, 1988, 1990, 1991) who considered the issue of control system design. It is also similar in concept to the IMC approach of Morari (1983) in that both methods involve alternative controller parametrizations and seek to determine limits of achievable control performance, independent of controller type or tuning. However, whereas Morari and coworkers follow an analytical approach, Swartz formulates dynamic operability assessment as a numerical convex optimization problem. This permits the simultaneous treatment of performance limiting factors, with the convexity property guaranteeing global optimality. The fact that Q parametrizes all stabilizing linear feedback controllers implies that the performance at the global optimum represents a limit of achievable performance for any such controller. Thus, the results are not biased by

controller type or tuning, apart from the requirement that the controller be linear.

In addition to calculating limits of performance, it will be shown how the Q-parametrization approach facilitates the incorporation of economic considerations into the problem. This is done by including the process setpoints as decision variables together with Q and optimizing an economic objective subject to constraints on the quality of the closed-loop behavior (Young *et al.*, 1996). The approach of Young *et al.* (1996) is extended to include a quadratic constraint on the quality of the output behavior, to enforce rapid disturbance rejection. Inclusion of the quadratic constraint permits a deeper understanding of the interrelationship between steady-state economics and dynamic operability, since dynamic operability is typically quantified in terms of such a measure. An illustrative example is presented wherein these ideas are explored.

In this chapter it is assumed that no model uncertainty is present. The incorporation of model uncertainty into the problem formulation is dealt with in Chapter 4.

3.2 Outline of Q-Parametrization Approach For Calculating Limits of Performance

Boyd *et al.* (1990) consider the following fundamental control system design problem:

> **Fundamental Controller Design Problem:** Given a specific system to be controlled, a control configuration, and a set of control performance specifications, either find a suitable control law that meets these design specifications, or determine that none exists.

The above problem is extremely difficult to solve in a general sense. However, by restricting the process to be linear time invariant and restricting the set of control performance specifications to be closed-loop convex, Boyd *et al.* (1990) used a theoretical result of Vidyasagar (1985), together with the power of numerical convex optimization to solve the Fundamental Controller Design Problem. The details of the approach are discussed next.

3.2.1 The General Feedback Framework

Consider the general feedback structure shown in Figure 3.1. The negative sign before the controller K reflects the convention that feedback should be negative. The inputs are partitioned into two vector signals, namely:

1. The *actuator* or control signal vector u, which includes all the inputs to the plant that can be manipulated by the controller.
2. The *exogenous* input vector w, which consists of all other input signals, such as disturbances and/or setpoints.

The output consists of two vector signals defined as follows:

1. The *sensor* or measured signal vector y, which comprises those signals that are accessible to the controller.
2. The *regulated* signal vector z, which consists of signals required to meet given performance specifications. The vector z may, for example, contain elements of u and y which the designer may wish to constrain in some fashion.

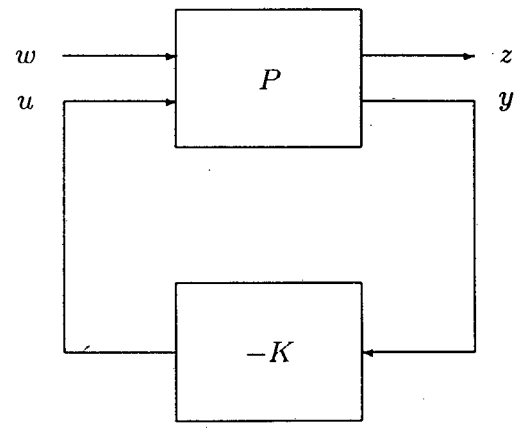

Figure 3.1: The general feedback framework of Boyd and coworkers.

It should thus be clear that, in general, P is not the plant model of the classical control framework, but rather a composite plant mapping all inputs of interest to all outputs of

interest. That is, P is defined such that

$$\begin{bmatrix} z \\ y \end{bmatrix} = P \begin{bmatrix} w \\ u \end{bmatrix} \tag{3.1}$$

In order to solve the Fundamental Controller Design Problem, Boyd *et al.* (1990) confine the plant P and the controller K to be linear time-invariant (LTI) and lumped. This is clearly a restrictive assumption as most chemical engineering processes are nonlinear and the use of nonlinear and/or adaptive controllers is becoming more popular. However, many researchers (Roat *et al.*, 1986; Oglesby *et al.*, 1992; Perkins and Walsh, 1994) agree that, despite the assumptions made in a linear analysis, the results obtained are still very useful and facilitate a deeper understanding of the issues involved in the trade-off between design and control. It is also argued that a linear assumption is reasonable provided the system is kept near to its steady-state operating point. Despite much progress in nonlinear analysis and nonlinear control, these fields are still not fully developed and are not as commonly used in practice. For this reason, the majority of methods for dynamic operability assessment are based on a linear analysis. The following chapter illustrates how process nonlinearities may, for example, be included in the form of nonlinear and/or time-varying uncertainty. Chapter 5 briefly deals with some of the issues pertaining to nonlinear control and its benefits over linear control, when treating a range of disturbances.

As a result of the assumptions regarding the process and controller, the plant P can be described by the set of transfer functions from each of the inputs to each of the outputs, organized in the form of a transfer matrix and partitioned as follows:

$$P = \begin{bmatrix} P_{zw} & P_{zu} \\ P_{yw} & P_{yu} \end{bmatrix} \tag{3.2}$$

The partitioning is such that, for example, P_{zw} is the transfer matrix from the elements of w to the elements of z.

With the controller K in operation, the closed-loop transfer matrix from w to z is given by:

$$H_{zw} = P_{zw} - P_{zu}K\,(I + P_{yu}K\,)^{-1}P_{yw} \tag{3.3}$$

Observe that the controller K appears in a linear fractional form in the above expression. Of central importance to the Q-parametrization approach is that H_{zw} should contain all the closed-loop transfer functions of interest. Therefore it is essential, when formulating a problem, that all exogenous inputs and all outputs of interest are included in w and z respectively.

Transformation of the classical control framework to the general feedback framework

Consider the classical control framework shown in Figure 3.2. Assuming that it is desired to place performance specifications on the responses of the classical input u and output y' to setpoint changes and disturbances, then, in terms of Figure 3.1, one would choose:

$$z = \begin{bmatrix} y' \\ u \end{bmatrix} \quad , \quad w = \begin{bmatrix} y_{set} \\ d \end{bmatrix} \quad , \quad y = [-e] \quad \text{and} \quad u = [u] \tag{3.4}$$

The transformation of the classical control framework into the general feedback control framework is shown in Figure 3.3. In terms of the partitioning of P we have:

$$\left[\begin{array}{c} y' \\ u \\ \hline -e \end{array}\right] = \left[\begin{array}{cc|c} 0 & G_d & G_P \\ 0 & 0 & I \\ \hline -I & G_d & G_P \end{array}\right] \left[\begin{array}{c} y_{set} \\ d \\ \hline u \end{array}\right] \tag{3.5}$$

3.2.2 Geometry of Design Specifications

The next step in solving the fundamental problem is to change the focus from finding a suitable controller to that of finding a closed-loop transfer matrix H_{zw} that meets the control performance specifications, or to determine that none exists. In this regard it is necessary to view the controller design specifications as sets. For this reason it is essential to include all closed-loop mappings of interest in H_{zw}.

Let $\mathcal{H}$ denote the set of all $n_z \times n_w$ transfer matrices, where n_z is the number of regulated outputs z and n_w is the number of exogenous inputs w. With each controller design specification $\mathcal{D}_i$, there is the associated set $\mathcal{H}_i \subseteq \mathcal{H}$ of all $n_z \times n_w$ transfer matrices that meet the design specification $\mathcal{D}_i$.

Now, simultaneous satisfaction of design specifications corresponds to the intersection of the associated sets of acceptable closed-loop transfer matrices. Therefore, if the design specifications are $\mathcal{D}_1, ..., \mathcal{D}_L$, then the set of closed-loop transfer matrices which satisfy all these specifications is given by:

$$\mathcal{H}_{\text{spec}} = \mathcal{H}_1 \cap ... \cap \mathcal{H}_L \tag{3.6}$$

In many cases the design specifications have a simple geometric form, in that they are either affine or convex. Noting that $\mathcal{H}$ is a vector space with addition and scalar multiplications

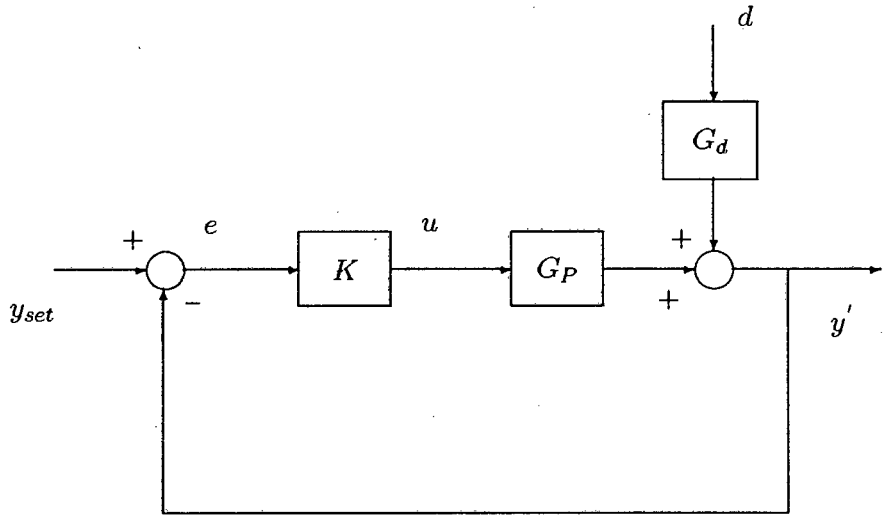

Figure 3.2: The classical feedback control structure for a one-degree-of-freedom controller.

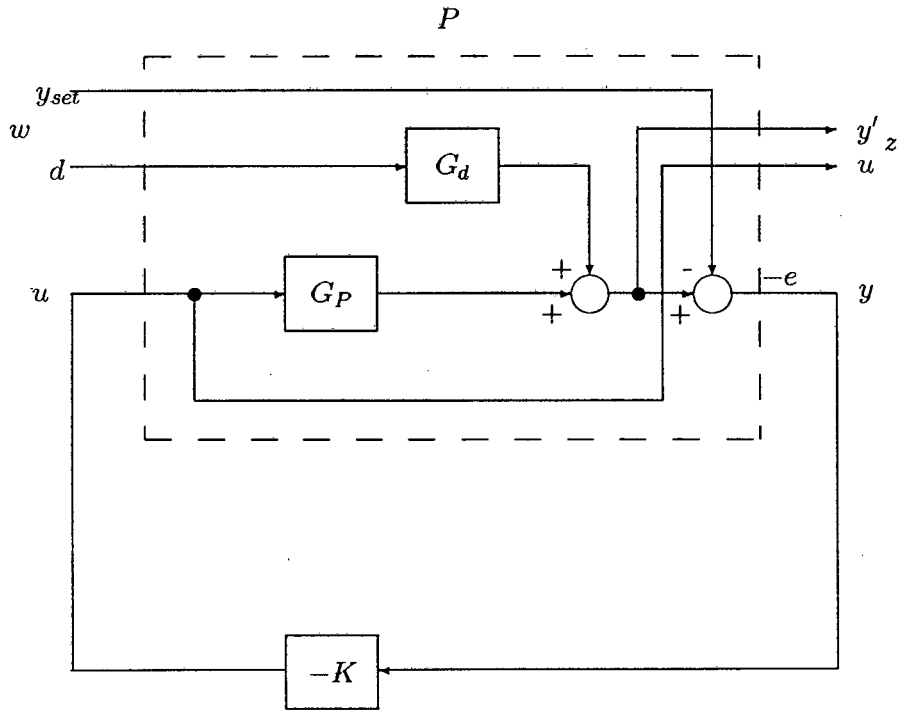

Figure 3.3: Transformation between the classical feedback structure and the general one used by Boyd and coworkers.

appropriately defined, we now define what is meant by an affine and a convex vector space (according to standard set theory), as well as a *closed-loop convex* performance specification.

Definition 1 *A subset $\mathcal{C}$ of a vector space $\mathcal{V}$ is said to be affine if, whenever two distinct points are in the set, then so is the entire line passing through them. More precisely, $\mathcal{C} \subseteq \mathcal{V}$ is affine if, for any c_1, $c_2 \in \mathcal{C}$ and any $\lambda \in \Re$, then $\lambda c_1 + (1-\lambda)\, c_2 \in \mathcal{C}$.*

Definition 2 *A subset $\mathcal{C}$ of a vector space $\mathcal{V}$ is said to be convex if, whenever two distinct points are in the set, then so is the entire line segment between them. More precisely, $\mathcal{C} \subseteq \mathcal{V}$ is affine if, for any c_1, $c_2 \in \mathcal{C}$ and any $\lambda \in [0,1]$, then $\lambda c_1 + (1-\lambda)\, c_2 \in \mathcal{C}$.*

Definition 3 *A controller design specification $\mathcal{D}_i$ is closed-loop convex if the set of transfer matrices, $\mathcal{H}_i$, that satisfy it is convex.*

Examples of closed-loop convex performance specifications

Boyd *et al.* (1988, 1990) have shown that many important control performance specifications in the time or frequency domain are closed-loop convex.

Closed-loop stability We firstly consider the essential controller design requirement of closed-loop (internal) stability. Let $\mathcal{H}_{\text{stab}}$ denote the set of all H_{zw}'s achievable with stabilizing controllers. It has been shown (Vidyasagar, 1985; Youla *et al.*, 1976a&b) that a free parametric representation of $\mathcal{H}_{\text{stab}}$ can be derived using stable coprime factorization theory:

$$\begin{aligned} \mathcal{H}_{\text{stab}} &= \{H_{zw} \,|\, \text{the system is closed-loop stable}\} \\ &= \left\{H_{zw} = P_{zw} - P_{zu}K(I + P_{yu}K)^{-1}P_{yw} \,|\, \text{ for some } K \text{ that stabilizes } P\right\} \\ &= \{H_{zw} = T_1 + T_2 Q T_3 \,|\, Q \text{ stable}\} \end{aligned} \tag{3.7}$$

In the above Q is any stable transfer matrix and is the free parameter in the corresponding equation. The T_i are stable transfer matrices determined from coprime factorizations of the plant model P_{yu} and a nominal stabilizing controller, details of which are provided in a subsequent section.

The word *parameter* in this case refers to the fact that Q parametrizes all stable closed-loop maps as opposed to meaning that it is some unspecified controller tuning parameter. An

important point to note is that the set of closed-loop stable H_{zw} is affine in Q. Thus, any closed-loop specifications that are convex in H_{zw} are convex in Q. This is not true of the classical controller K which appears in a linear fractional (nonconvex) fashion in the above expression.

In addition to the fundamental requirement for closed-loop stability, many other important controller design specifications are also closed-loop convex. Some examples which are likely to be used in dynamic operability analysis are discussed next.

Time domain bounds In order to place a constraint on the response of a signal to a given input, that signal needs to be included in the vector of regulated variables z and the input needs to be included in the vector w. Having done so, it is relatively easy to show that placing lower and upper bounds on the behavior of the signal is a closed-loop convex constraint.

Consider, for example, the time-domain response of the first element of the vector z (denoted z_1) to a step in the second element of the vector w (denoted w_2). Let $s_{12}(t)$ denote the step response from w_2 to z_1. It should be noted from (3.7) that the step response s_{zw} is convex in Q. Consider the following constraints on the behavior of s_{12}:

$$s_{12\,\min}(t) \leq s_{12}(t) \leq s_{12\,\max}(t) \quad \text{for } t \geq 0 \tag{3.8}$$

The set of closed-loop transfer matrices $\mathcal{H}_{\text{bound}}$ which meet the constraint (3.8) is given by:

$$\mathcal{H}_{\text{bound}} = \{H_{zw} \in \mathcal{H} \mid s_{12\,\min}(t) \leq s_{12}(t) \leq s_{12\,\max}(t) \quad \text{for } t \geq 0\} \tag{3.9}$$

Let $H, \tilde{H} \in \mathcal{H}_{\text{bound}}$ be transfer matrices such that the corresponding step responses $s_{12}(t)$ and $\tilde{s}_{12}(t)$ satisfy (3.8). It is easy to see that, if $0 \leq \lambda \leq 1$, then $s_{\lambda 12}(t) = \lambda s_{12}(t) + (1-\lambda)\tilde{s}_{12}(t)$ also satisfies (3.8). Thus $H_\lambda \in \mathcal{H}_{\text{bound}}$ and the set $\mathcal{H}_{\text{bound}}$ is closed-loop convex. As a result, time-domain bounds on the step response are closed-loop convex controller performance specifications on H_{zw}, and thus on Q.

The requirement for dynamically decoupled behavior may be enforced in a similar manner by simply stipulating that one command has no effect on the other regulated outputs. Thus, if we desire w_2 to have no effect on z_1 then we can simply set $s_{12\,\max} = s_{12\,\min} = 0$ for all $t \geq 0$.

Other important performance specifications that are closed-loop convex include bounds on the slew rate of an actuator signal (or any regulated output), asymptotic tracking of steps, ramps or parabolic inputs, as well as upper bounds on both the ITAE and ISE controller performance measures.

Important nonconvex performance specifications

Very few robustness specifications are closed-loop convex. One important exception is the robustness to *unstructured* norm-bounded LTI model uncertainty, which Boyd *et al.* (1990) show to be a closed-loop convex constraint. In the presence of structured model uncertainty, however, the appropriate robust stability criterion is a bound on the structured singular value (Doyle, 1982), which is a *nonconvex* closed-loop constraint. Treating the problem of robust performance involves the use of the structured singular value and is thus also a nonconvex requirement on Q.

Further important examples of closed-loop controller design specification which are not convex include the specification of controller order as well as the requirement for a decentralized controller. This is unfortunate as it would be desirable to quantify performance limits for controllers of given complexity. Also, when considering large systems it may be more appropriate to use decentralized controllers. Stated differently, for many systems it may be beneficial to quantify the benefits associated with multivariable control. Recent research (Sourlas and Manousiouthakis, 1995) has shown how, despite the nonconvexity, such a performance limit may be calculated for decentralized controllers.

3.2.3 Relationship Between the Q-Parametrization and IMC frameworks

Before continuing with the assessment of closed-loop performance limits, it is useful to highlight the relationship between Q-parametrization and the IMC framework. To this end, it is necessary to firstly show how the T_i matrices in (3.7) may determined from coprime factorizations of the plant model P_{yu} and a nominal stabilizing controller K_{nom}.

Given a nominal stabilizing controller K_{nom}, let the following be left stable coprime factorizations of K_{nom} and P_{yu} respectively:

$$\begin{aligned} K_{\text{nom}} &= Y^{-1}X \\ P_{yu} &= \tilde{D}^{-1}\tilde{N} \end{aligned} \tag{3.10}$$

In the above, $\tilde{D}$ and $\tilde{N}$ are stable and coprime, with an equivalent condition holding for Y and X. Stability implies that $\tilde{N}$ contains all the right-half-plane transmission (RHPT) zeros of P_{yu} and $\tilde{D}$ contains, as RHPT zeros, all the RHPT poles of P_{yu}. The requirement that $\tilde{D}$ and $\tilde{N}$ be coprime means that they have no common RHPT zeros. Mathematically this is equivalent to the requirement that there exist stable matrices $U_\ell(s)$ and $V_\ell(s)$ such that

the following Bezout identity is satisfied:

$$\tilde{D}U_\ell + \tilde{N}V_\ell = I \tag{3.11}$$

Similar conditions hold for Y and X.

Now, given the coprime factorizations in (3.10), then a controller K stabilizes P if and only if K has the following form (Vidyasagar, 1985):

$$K = (Y - Q\tilde{N})^{-1}(X + Q\tilde{D}) \quad , \quad Q \text{ stable} \tag{3.12}$$

Since K_{nom} stabilizes P_{yu}, there is also a right stable coprime factorization of $P_{yu} = ND^{-1}$ with the Bezout identity map $XN + YD = I$ (Francis, 1987). Substitution of (3.12) into (3.7) and use of the Bezout identity reveals, after some algebraic manipulation, that T_1, T_2 and T_3 are given by:

$$\begin{aligned} T_1 &= P_{zw} - P_{zu}DXP_{yw} \\ T_2 &= -P_{zu}D \\ T_3 &= \tilde{D}P_{yw} \end{aligned} \tag{3.13}$$

For a stable plant, no feedback control is required to ensure stability and hence we can choose $K_{\text{nom}} = 0$. This allows one to set $\tilde{D} = D = Y = I$, $\tilde{N} = N = P_{yu}$ and $X = 0$, giving:

$$\begin{aligned} T_1 &= P_{zw} \\ T_2 &= -P_{zu} \\ T_3 &= P_{yw} \end{aligned} \tag{3.14}$$

As a result, *all* closed-loop stable H_{zw} are parametrized as follows:

$$\begin{aligned} H_{zw} &= T_1 + T_2QT_3 \\ &= P_{zw} - P_{zu}QP_{yw} \quad , \quad Q \text{ stable} \end{aligned} \tag{3.15}$$

Furthermore, from (3.12) all stabilizing controllers have the form:

$$K = (I - QP_{yu})^{-1}Q \quad , \quad Q \text{ stable} \tag{3.16}$$

Comparison of (3.15) with (3.7) and noting the form of the above equation shows that there is a one-to-one relationship between all stabilizing controllers K and Q:

$$\begin{aligned} K &= (I - QP_{yu})^{-1}Q \\ &\Leftrightarrow \; Q = K(I + P_{yu}K)^{-1} \end{aligned} \tag{3.17}$$

This is exactly the relation given by the IMC framework and thus, for stable plants, the IMC and the Q-parametrization frameworks are equivalent.

The difference between the IMC parametrization and the Q-parametrization is that the latter encompasses all stabilizing controllers, even for unstable MIMO plants, which is not true of the IMC parametrization. Assumptions are made in the IMC framework which restrict the type of unstable plants to which the parametrization applies and the resulting parametrization is also not complete (Morari and Zafiriou, 1989).

3.2.4 Calculation of Limits of Achievable Performance via Convex Optimization

Using the result of Boyd that many performance specifications are convex in H_{zw}, it is possible to express controller synthesis as the following convex optimization problem:

$$\min_{H_{zw} \in \Omega \cap H_{\text{stab}}} \Phi(H_{zw}) \tag{3.18}$$

where Φ is a convex functional of H_{zw} and reflects a measure of closed-loop performance which is desired to be optimal. Ω is the set of all H_{zw}s that satisfy the performance constraints and H_{stab} is the set of all H_{zw} achievable with stabilizing controllers. Since H_{stab} is a convex set and Ω has been shown by Boyd and coworkers to be convex for many performance specifications, the search space is also convex. Therefore the above corresponds to a convex optimization problem, which has the property that any optimum found is global. Furthermore, if no solution is found, then no solution exists. Since Q parametrizes all stabilizing linear feedback controllers, the performance at the optimum represents a limit of performance for any such controller.

Since H_{zw} is linear in Q, the above can be transformed into a convex program in Q. This is preferable as Q is simpler to handle than H_{zw} and, for a stable plant, Q has a physical interpretation as the IMC controller. Upon transformation one obtains:

$$\begin{aligned} & \min_{Q \in \bar{\Omega}} \quad \bar{\Phi}(Q) \qquad (3.19) \\ \text{where} \quad \bar{\Omega} &= \{Q \,|\, T_1 + T_2 Q T_3 \in \Omega \,,\; Q \text{ stable}\} \\ \text{and} \quad \bar{\Phi}(Q) &= \Phi(T_1 + T_2 Q T_3) \end{aligned}$$

If $\bar{\Omega}$ is empty, then there exists *no* stabilizing linear feedback controller that results in an H_{zw} which can satisfy all the performance constraints in Ω. It is useful to note that the above problem formulation is an extension of the Fundamental Controller Design Problem since it not only requires feasibility but also optimizes a given closed-loop performance measure.

In the current form, (3.19) is not amenable to numerical solution as the set of all stable Q is infinite dimensional. To overcome this Q is approximated by a large, finite dimensional space.

3.2.5 Finite Dimensional Approximation of Q

The set of all stable transfer function matrices can be approximated in a finite dimensional manner in either the frequency domain or the discrete-time domain. Boyd *et al.* (1990 and 1991) mainly consider approximations in the frequency domain as it is easy to ensure stability by choosing a transfer function basis with poles in the left-half-plane. The approximations take the following form:

$$Q = \sum_{k=0}^{L} x_k Q_k \tag{3.20}$$

where $x_k \in \Re$ and the matrices Q_k are fixed stable maps expressed in the frequency domain.

For the convenient handling of dead-time and time-domain constraints, a discrete formulation is adopted, with the (n, m) element of Q being approximated as (Boyd *et al.*, 1988; Swartz, 1994):

$$Q_{nm} = \sum_{k=0}^{L} q_{nm}(k)\, z^{-k} \tag{3.21}$$

where L is the order of the finite dimensional approximation and is typically fairly large so as to ensure an accurate solution. The coefficients $q_{nm}(k)$ now become the search variables in the optimization problem (3.19). In addition to the size of L, the choice of sampling time used in the discretization also influences the accuracy of the solution. In this thesis it has been attempted to choose sampling times which provide a good level of accuracy without leading to excessively large optimization problems.

It should be noted that the approximation in (3.21) is not yet complete as it does not ensure that Q is stable. This may be done rigorously by requiring that all the roots of the above polynomial lie within the unit circle but this would be very complicated. Alternately, one could require $\sum_{k=0}^{L} |q_{nm}(k)| < \infty$, but this is not a practical condition given the fact that a finite dimensional approximation is being made.

In order to overcome these difficulties, stability on Q is enforced indirectly by requiring that the inputs settle out to their desired steady-state values after a specified number of time intervals. The discussion that follows shows how the above theory may be applied to dynamic operability assessment.

3.3 Application to Dynamic Operability Assessment

Morari (1983) argued that dynamic operability should be assessed as a limit of achievable closed-loop performance and should not be biased by controller type or tuning. With this in mind, it is clear that the Q-parametrization approach of Boyd for assessing limits of performance, in the context of control system design, lends itself naturally to the assessment of dynamic operability.

Since dynamic operability assessment is carried out during the process design phases, the closed-loop performance specifications are often much simpler than would be the case during a rigorous controller design. Constraints of interest typically include bounds on the input and output behavior so as to meet hard design criteria. The objective function used as a measure of closed-loop performance is often a weighted sum-of-square-errors measure. As a consequence, in the absence of model uncertainty, dynamic operability assessment may be posed as a convex quadratic programming problem. More sophisticated problem formulations can be treated within the broad setting of convex optimization but the above problem type is usually sufficient for the purposes of dynamic operability assessment. When model uncertainty is present the problem is more complicated and Chapter 4 deals with this issue.

As mentioned earlier, a discrete formulation is used to facilitate the handling of dead-time and time-domain constraints. Q is approximated in a finite dimensional manner as shown in (3.21) with the coefficients $q_{nm}(k)$ becoming the search variables in the optimization problem. If performance specifications are to be placed on the inputs and outputs, for both setpoint changes and disturbances, then z, w, u and y would be partitioned as in (3.4) and P would be as in (3.5). The processes considered in this thesis are open-loop stable, although the approach is not limited to such processes. The T_i matrices are as shown in (3.14). The dimension of z is n_z and the dimension of w is n_w. Strictly speaking, a two-degree-of-freedom controller would be used when designing for both regulatory and servo behavior. However, for notational convenience we only consider a one-degree-of-freedom controller, with extensions to the former being straightforward.

The step response coefficient $s_{ij}(i_o)$ at time increment i_o of the ith component of z to a step of size w_j in the jth component of w is a linear expression in the coefficients of Q through (3.7) and has the form (Appendix A.1):

$$s_{ij}(i_o) = w_j \sum_{k=0}^{i_o} t_{1\,ij}(k) + w_j \sum_{m=1}^{n_y} \sum_{n=1}^{n_u} \sum_{k=0}^{i_o} q_{nm}(k) \sum_{v=k}^{i_o} \sum_{\ell=k}^{v} t_{2\,in}(v-\ell) t_{3\,mj}(\ell-k) \qquad (3.22)$$

In the above equation t_1, t_2 and t_3 are the pulse response coefficients of the transfer matrices

T_1, T_2 and T_3 respectively, and n_y and n_u are the respective dimensions of y and u. If more than one element of w acts simultaneously on the system, then the overall response is the sum of the individual step responses in (3.22). For notational convenience it is assumed that the elements of w act individually and that the vector of step changes can be written as:

$$w = \left[\begin{array}{cc} y_{set}^T & d^T \end{array} \right]^T \tag{3.23}$$

By considering the form of the T_i matrices, it is possible to rewrite (3.22) in terms of the pulse response coefficients of the plant model G_P and the disturbance transfer matrix G_D (Appendix A.2). The resulting expression for the output response ($i \leq n_y$) to setpoint changes of step-size $y_{set\,j}$ ($j \leq n_y$) is:

$$s_{ij}(i_o) = y_{set\,j} \sum_{n=1}^{n_u} \sum_{k=0}^{i_o} q_{nj}(k) \sum_{v=k}^{i_o} G_{P\,in}(v-k) \tag{3.24}$$

The output response ($i \leq n_y$) to a step of size d_j in the jth disturbance is given by:

$$s_{i\,(j+n_y)}\,(i_o) = d_j \sum_{k=0}^{i_o} G_{D\,ij}(k) - d_j \sum_{m=1}^{n_y} \sum_{n=1}^{n_u} \sum_{k=0}^{i_o} q_{nm}(k) \sum_{v=k}^{i_o} \sum_{\ell=k}^{v} G_{D\,mj}(\ell-k)\, G_{P\,in}(v-\ell) \tag{3.25}$$

The expression for the input response ($i > n_y$) to a setpoint change of size $y_{set\,j}$ ($j \leq n_y$) is given by:

$$s_{ij}(i_o) = y_{set\,j} \sum_{k=0}^{i_o} q_{(i-n_y)\,j}(k) \tag{3.26}$$

The input response ($i > n_y$) to a disturbance d_j is given by:

$$s_{i\,(j+n_y)}(i_o) = -d_j \sum_{m=1}^{n_y} \sum_{k=0}^{i_o} q_{(i-n_y)\,m}(k) \sum_{v=k}^{i_o} G_{D\,mj}(v-k) \tag{3.27}$$

The step response coefficients for the outputs and inputs may be arranged into a composite vector of the form:

$$s(Q, y_{set}, d) = \left[s_{11}^T, \ldots, s_{n_y\,1}^T, \ldots, s_{n_y\,n_w}^T, s_{(n_y+1)\,1}^T, \ldots, s_{(n_y+n_u)\,1}^T, \ldots, s_{(n_y+n_u)\,n_w}^T \right]^T \tag{3.28}$$

where $s_{ij}^T = [s_{ij}(0), \ldots, s_{ij}(L)]$. Time domain bounds on the deviational response of the inputs and outputs are now simply linear constraints on Q and take the form

$$s_{\min} \leq s(Q, y_{set}, d) \leq s_{\max} \tag{3.29}$$

where $s_{\min}$ and $s_{\max}$ are partitioned in the same manner as s. Included in the above set of constraints would be the implicit enforcement of the stability of Q via the requirement for the inputs to settle out to their steady-state values.

The measure of closed-loop performance regularly used in this thesis is that of a weighted sum-of-square-errors of the outputs, y', from their setpoints and is written in terms of the above notation as:

$$\Phi = \sum_{j=1}^{n_w} \sum_{i=1}^{n_y} \sum_{k=0}^{L} W_{ij}(k) \left[s_{ij}(k) - r_{ij}(k) \right]^2 \tag{3.30}$$

In the above, $r_{ij}(k)$ is the desired value for the step response coefficient $s_{ij}(k)$ and $W_{ij}(k)$ is a weighting function used to ascribe the relative importance of the outputs and to include a time-weighting if necessary. It should be noted though that any other form of objective function could have been chosen provided that it is convex. In particular, the input action could also be penalized by including quadratic terms corresponding to the deviation of the input trajectories from some desired values.

Dynamic operability assessment may now be expressed as the following convex quadratic programming problem:

$$\begin{aligned} \min_{Q} \quad & \Phi = \sum_{j=1}^{n_w} \sum_{i=1}^{n_y} \sum_{k=0}^{L} W_{ij}(k) \left[r_{ij}(k) - s_{ij}(k) \right]^2 \\ \text{s.t.} \quad & \\ s_{\min} \quad \leq \quad & s(Q, y_{set}, d) \leq s_{\max} \end{aligned} \tag{3.31}$$

As mentioned earlier, the convexity guarantees that any optimum is global and the fact that Q parametrizes all stabilizing linear feedback controllers implies that the performance at the optimum represents the best possible performance for any controller in this class. The representation of several other constraints such as specifications on slew rate, RMS disturbance rejection and so forth are shown in Boyd *et al.* (1988, 1990). The above problem has very useful features pertaining to its structure and sparsity which may be exploited to reduce computational time. A discussion of these features and how they have been exploited may be found in Chapter 5.

3.3.1 Application Example

The approach discussed above is applied to a multivariable system containing RHPT zeros, input constraints and time delays. The process considered is from Psarris and Floudas (1991b) and involves the control of a pilot scale ethanol and water distillation column, originally modelled by Ogunnaike *et al.* (1983). The outputs to be controlled are the overhead ethanol mole fraction (y_1) and a bottom tray temperature (y_2 in °C). The manipulated inputs are the reflux flowrate (u_1 in gpm) and the reboiler steam pressure (u_2 in psig). The

nominal plant model $\tilde{P}$ has the following transfer matrix description:

$$\tilde{P}(s) = \begin{bmatrix} \frac{0.66\,e^{-6\,s}}{(6.7\,s+1)} & \frac{-0.005}{(9.06\,s+1)} \\ \frac{-34.7\,e^{-4\,s}}{(8.15\,s+1)} & \frac{0.87\,(11.6\,s+1)e^{-2\,s}}{(3.9\,s+1)\,(18.8\,s+1)} \end{bmatrix} \tag{3.32}$$

As mentioned in Chapter 2, the time delays in the above transfer matrix may limit the achievable closed-loop performance by pure delay effects, by generating infinite RHPT zeros and by causing interaction difficulties.

Psarris and Floudas (1991b) used the distribution of zeros of quasi-polynomials to show that the above plant contains an infinite number of RHPT zeros due to the distribution of time delays within the transfer matrix. They also showed that, if it were possible to increase the delays on the off-diagonal elements of $\tilde{P}$ such that the sum of these time delays exceeds eight, then all the RHPT zeros would be eliminated. Large time delays in certain elements are also sometimes beneficial with regard to reducing interaction (Holt and Morari, 1985b). These two potential benefits of larger time delays need to be traded off against the obvious disadvantage of having longer minimum response times. These trade-offs are explored by analyzing the dynamic operability of a number of alternative plants, differing only in the distribution of time delays within their transfer matrices.

Mathematical formulation of dynamic operability assessment problem

The closed-loop response of the system to individually applied setpoint changes is considered. In terms of the general feedback structure, we choose $w = [y_{set}]$. As a consequence, $n_w = n_y = 2$. Performance specifications are to be placed on both the input and output behavior and therefore z is chosen as $z = \begin{bmatrix} y'^T & u^T \end{bmatrix}^T$.

The objective function chosen as a measure of closed-loop performance is the weighted sum-of-square errors (SSE) of the outputs to steps of -0.035 and $+3$ applied individually to the setpoints of y_1 and y_2 respectively. To be consistent with the work of Psarris and Floudas (1991b), the same setpoint changes were chosen as in their study. The objective is convex and quadratic and has the following form:

$$\Phi = \sum_{j=1}^{n_w} \sum_{i=1}^{n_y} W_{ij} \sum_{k=0}^{L} [s_{ij}(k) - r_{ij}(k)]^2 \tag{3.33}$$

The problem is discretized at a sampling interval of $\Delta t = 0.5$ minutes and a time horizon of

$L = 100$ is used. The weighting matrix W is chosen as

$$W = \begin{bmatrix} 2500 & 2500 \\ 1 & 1 \end{bmatrix} \tag{3.34}$$

in order to roughly account for the difference in the size of the setpoint changes applied to y_1 and y_2. The weights on the outputs have been chosen in such a manner that the contributions of each output to the total objective value are approximately equal. No bounds are placed on the output responses, but the following bounds are placed on the deviational input responses

$$\begin{aligned} -0.112 &\leq u_1 \leq 0.065\,\text{gpm} \\ -4.4 &\leq u_2 \leq 14.0\ \text{psig} \end{aligned} \tag{3.35}$$

While no constraints are placed on the output response, it is still essential that the outputs y be included in z, since the performance specification on them takes the form of an objective function in (3.33), which is to be minimized. The above problem may be formulated as a convex quadratic programming problem, as shown in (3.31), and solved efficiently by exploiting its structure and sparsity. Chapter 5 provides more details in this regard.

Results and discussion

To explore the effect of the distribution of delays on dynamic operability, the following six alternative delay structures are considered:

$$\begin{aligned} B_1 &= \begin{bmatrix} 6 & 0 \\ 4 & 2 \end{bmatrix}, \quad B_2 = \begin{bmatrix} 6 & 0 \\ 9 & 2 \end{bmatrix}, \quad B_3 = \begin{bmatrix} 6 & 5 \\ 4 & 2 \end{bmatrix} \\ B_4 &= \begin{bmatrix} 6 & 4 \\ 5 & 2 \end{bmatrix}, \quad B_5 = \begin{bmatrix} 6 & 6 \\ 6 & 2 \end{bmatrix}, \quad B_6 = \begin{bmatrix} 6 & 0 \\ 4 & 4 \end{bmatrix} \end{aligned} \tag{3.36}$$

The rest of the process dynamics are as in (3.32). The first structure, B_1, corresponds to the original plant in (3.32). As mentioned earlier, this delay structure introduces an infinite number of RHPT zeros and poor dynamic operability is thus expected.

Structures B_2, B_3 and B_4 correspond to the intuitive choices for the optimal time delay structure assuming that it is desired to eliminate all the RHPT zeros without adding unnecessarily large delays. That is, for each of these structures the off-diagonal delay terms sum to nine.

Structures B_5 and B_6 provide optimal lower bounds for the time delay resiliency indices of Holt and Morari (1985a). These resiliency indices were defined earlier in Chapter 2 and

their significance explained. In the absence of other performance-limiting effects, dynamic decoupling for these two delay structures would be ISE-optimal. Since B_5 satisfies the requirement for eliminating the RHPT zeros, the control performance in the absence of input constraints would only be limited by the response time needed for the inputs to affect the outputs. It should be noted, however, that B_6 does not eliminate the infinite RHPT zeros. In fact, Psarris and Floudas (1991b) show that the delay structure given by B_6 shifts the RHPT zeros closer to origin. Thus, one would expect such a system to have very poor operability, despite having an optimal lower bound.

The results of the dynamic operability assessment for each of the delay structures considered are shown in Table 3.1. The objective reported is the minimum weighted SSE, and an approximate weighted ISE measure may be obtained by multiplying the results by the sampling time $\Delta t = 0.5$. Also indicated in the table are the lower and upper bounds used by Holt and Morari (1985a) as a measure of dynamic operability.

Table 3.1: Minimum achievable weighted SSE and resiliency bounds for each delay structure.

Delay structure	**RHPT Zeros**	**Lower bound**	**Upper bound**	**Objective**
B_1	Infinite	$\text{diag}(e^{-2s}, e^{-4s})$	$\text{diag}(1, e^{-2s})$	117.8
B_2	None	$\text{diag}(e^{-6s}, e^{-2s})$	$\text{diag}(1, e^{-2s})$	101.8
B_3	None	$\text{diag}(e^{-6s}, e^{-2s})$	$\text{diag}(e^{-5s}, e^{-2s})$	98.0
B_4	None	$\text{diag}(e^{-6s}, e^{-2s})$	$\text{diag}(e^{-4s}, e^{-2s})$	98.6
B_5	None	$\text{diag}(e^{-6s}, e^{-2s})$	$\text{diag}(e^{-6s}, e^{-2s})$	96.8
B_6	Infinite	$\text{diag}(1, e^{-4s})$	$\text{diag}(1, e^{-4s})$	166.0

Since a smaller objective corresponds to better dynamic operability, the following observations can be made:

1. The time delay structure of B_5 has the best dynamic operability. It thus offers the best compromise between the three competing time delay effects. This result is somewhat surprising at first, since B_5 would intuitively appear to have unnecessarily large time delays. However, it will be seen that next to the RHPT zeros, interaction is an important cause of control difficulties in this example. Structure B_5 not only eliminates the RHPT zeros but also has an achievable upper bound which facilitates decoupled behavior.

2. By looking purely at the time delay bounds and the presence or absence of RHPT zeros, structure B_2 would appear to be better than B_3, B_4 and B_5, since it has the

best upper bound and all other factors are equal. The upper bound is, however, not always achievable and is thus not a reliable measure of dynamic operability. This is evidenced by the results above, which go in exactly the reverse order as what would have been expected from the upper bound.

3. The presence of infinite RHPT zeros limits the closed-loop performance dramatically and more so when they are closer to the origin, as in system B_6.

To illustrate the first two issues above, the optimal output trajectories for some of the delay structures are studied. The optimal output trajectories of structures B_1, B_4 and B_5 are shown in Figure 3.4 for the setpoint change of -0.035 in y_1. Figure 3.5 gives the output responses for the setpoint change of $+3$ in y_2. From the figures it is clear that B_1 demonstrates significant interaction between the response of the outputs. The interaction problems experienced by B_1 are an indication that the upper bound given in Table 3.1 is not achievable. Stated in terms of the work of Holt and Morari (1985a), off-diagonal elements need to be added to $\tilde{G}_+$ in (2.27) of Chapter 2, in order for the (IMC) controller to be causal.

While delay structure B_4 has better closed-loop behavior, its upper bound is also not achievable. This may be seen by solving the dynamic operability assessment problem in the absence of input constraints. The best achievable weighted SSE is calculated to be 85.92, which is worse than the value of 72.56 obtained if the outputs tracked their setpoints according to the minimum achievable settling time, given by the upper bound in Table 3.1.

All the delay structures considered in Figures 3.4 and 3.5 initiate behavior according to the response times given by their upper bounds, but do not immediately track their setpoints thereafter. As mentioned above, this is a consequence of the upper bounds not being achievable for structures B_1 and B_4, and the presence of input constraints. It should be noted that structure B_5 responds according to the upper bound given in Table 3.1 and thereafter the control behavior is only limited by input constraints.

The above discussion has only considered the delay structures shown in (3.36). Of interest is to determine the optimal delay structure for this particular example, assuming that no delay elements may be reduced. By solving the dynamic operability assessment problem over a grid of alternative time delay structures, B_5 was found to be the optimal delay structure. The grid considered only the $(1,2)$ and $(2,1)$ elements of the time delay structures, as these are the delays which, if increased appropriately, will remove all the RHPT zeros from the system. It has already been established that the elimination of the RHPT zeros is essential for good dynamic operability and therefore no increases in the diagonal elements were considered.

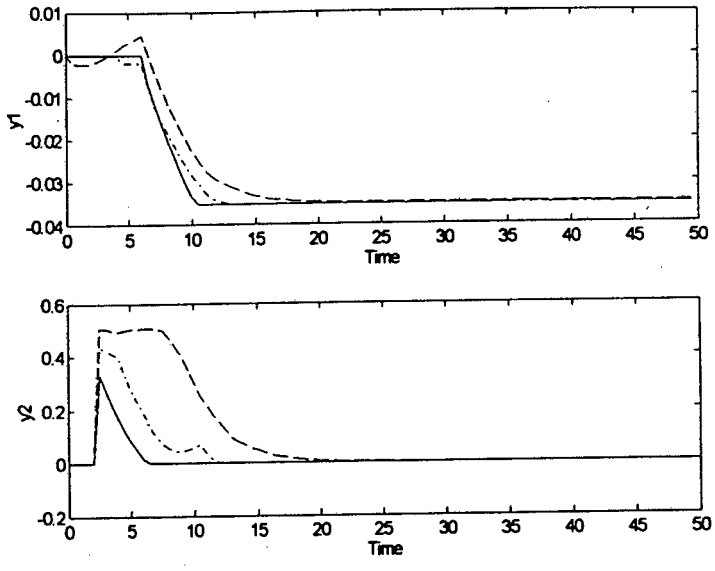

Figure 3.4: Optimal output trajectories for a setpoint change of -0.035 in y_1 for the delay structures B_1 (- -), B_4 (-·) and B_5 (-).

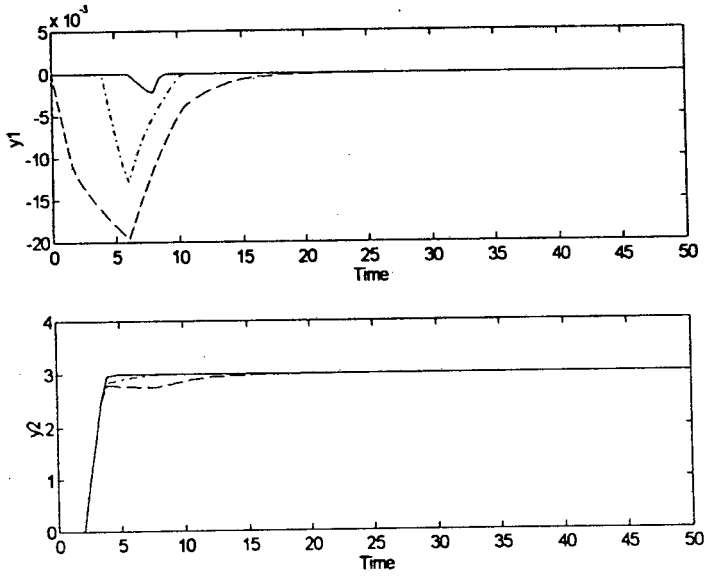

Figure 3.5: Optimal output trajectories for a setpoint change of $+3$ in y_2 for the delay structures B_1 (- -), B_4 (-·) and B_5 (-).

Only integer values for the delay elements were considered. The results are plotted in Figure 3.6, with a more refined view given in Figure 3.7.

It is interesting to note how flat the region is once the RHPT zeros have been eliminated. It is perhaps surprising that delay structures containing quite large off-diagonal delay elements still have acceptable dynamic operability, even though such delays would seriously worsen their lower bounds. It is thus clear that, for this example, the lower bound of Holt and Morari (1985b) may be very conservative when both the off-diagonal delays are large.

To summarize, in this example the performance degradation caused by the infinite RHPT zeros is the most serious. Increasing the time delays in such a manner so as to eliminate the RHPT zeros is beneficial, despite the negative aspect of having a longer response time before input action affects the output. Time delay structures which have no RHPT zeros associated with them may still have slightly inferior closed-loop behavior due to interaction problems. These interaction problems, worsened to some extent by the presence of input constraints, are an indication that the upper resiliency bound of Holt and Morari (1985b) is not achievable. In this example, the delay structure with no RHPT zeros and an achievable upper bound has little problem with interaction (caused only by the input constraints) and has the best dynamic operability.

3.4 Posing Dynamic Operability In Economic Terms

The above discussion showed how dynamic operability may be assessed at fixed operating conditions on the basis of the closed-loop response to specific setpoint and/or disturbance changes and ignored economic considerations. In this section, arbitrary step-like disturbances within a given range are considered and dynamic operability is posed in economic terms (Young *et al.*, 1996). The purpose of this approach is to enable competing designs to be compared according to a common economic basis.

The approach involves including the process setpoints as search variables together with Q and optimizing an economic objective subject to constraints on the worst-case closed-loop behavior to the given range of disturbances. The closed-loop constraints include simple bounds on the responses of the inputs and outputs as well as a bound on the weighted SSE of the outputs to the worst-case disturbances within the given range. The SSE constraint is included to ensure rapid disturbance rejection. An alternative to using the SSE constraints is to use tapered bounds on the output response. This may be more intuitive, particularly if it is not obvious what value should be used when bounding the SSE. The advantage of

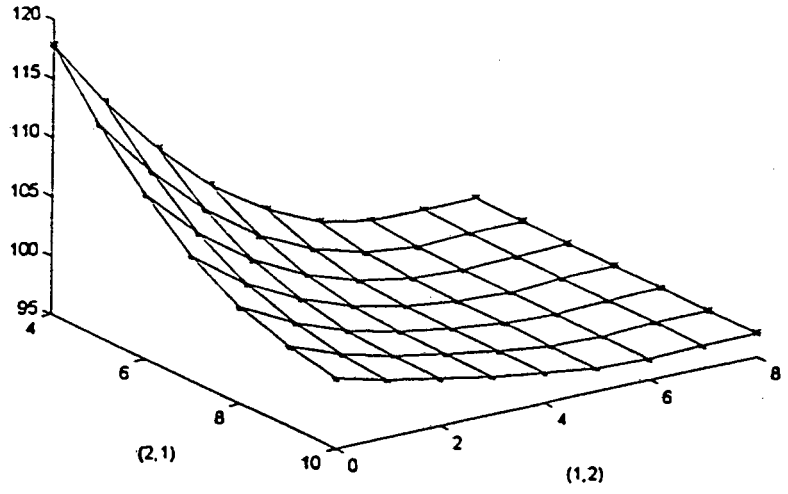

Figure 3.6: Optimal achievable SSE as a function of the delays in the $(1,2)$ and $(2,1)$ elements of the transfer matrix.

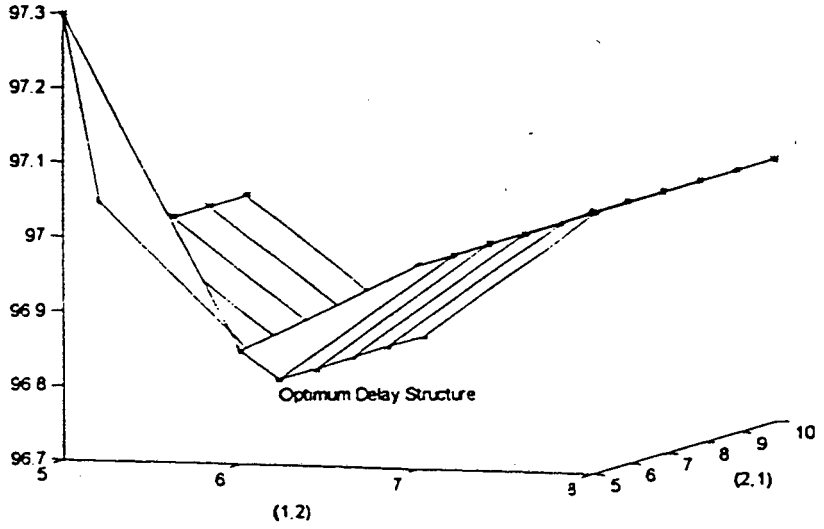

Figure 3.7: Optimal achievable SSE as a function of the delays in the $(1,2)$ and $(2,1)$ elements of the transfer matrix - a closer view.

the SSE constraints, however, is that it permits a deeper understanding of the relationship between economics and dynamic operability, since dynamic operability is typically quantified in terms of the SSE measure.

The approach allows one to explore the influence of constraint proximity on dynamic operability and steady-state economics. For a given process, as one operates closer to the limiting constraints in search of economic efficiency, the dynamic operability may be worsened in certain cases due to less input power being available for disturbance rejection. However, when comparing alternative designs, the benefit of having inherently good dynamic operability is that such a process is able to operate closer to the constraints defining its steady-state economic optimum, without violating them in the face of disturbance-induced dynamics. In this case, processes with good dynamic operability may be beneficial from an economic viewpoint.

3.4.1 Mathematical Formulation

Disturbance Regime Considered

The back-off from the constraints defining the steady-state optimum to prevent constraint violation is clearly a function of the disturbance regime. For ease of notation the discussion below is developed for a single disturbance and it is assumed that we are not concerned with setpoint responses. The disturbances are assumed to be comprised of a sequence of steps, initiated from a base value d_b with step size Δd, such that $d = d_b + \Delta d$. The frequency of the steps is uncertain but it is assumed that the time between successive steps is greater than the process settling time. It is assumed that all such disturbances lie between upper and lower bounds, d^+ and d^-, about a nominal level d_b^N. For a single disturbance, a typical disturbance trajectory which satisfies these requirements is shown in Figure 3.8.

The set of all allowable disturbances is mathematically represented by:

$$\Gamma = \{(d_b, \Delta d) \mid d = d_b + \Delta d;\ d^- \leq d \leq d^+;\ d^- \leq d_b \leq d^+\} \tag{3.37}$$

For a single disturbance, the range of values of d_b and Δd which ensure that $d \in \Gamma$ are shown in Figure 3.9. In terms of the general feedback structure discussed earlier, the set of exogenous inputs w is given by:

$$w = \{\Delta d \mid d \in \Gamma\} \tag{3.38}$$

The initial disturbance level d_b, together with the process setpoint y_{ss}, determines the initial steady-state input levels, denoted $u_{ss}(y_{ss}, d_b)$, and consequently the constraint proximity.

The notation $u_{ss}(y_{ss}, d_b)$ implies that u_{ss} is a function of y_{ss} and d_b. Since the processes considered are linear, a linear steady-state model will relate y_{ss} and $u_{ss}\,(y_{ss}, d_b)$.

Assuming that closed-loop performance constraints are to be placed on both outputs and inputs, the set of regulated variables is chosen as $z = \left[\begin{array}{cc} y'^T & u^T \end{array}\right]^T$.

Due to the linearity of H_{zw} in Q, the worst-case disturbances (critical points) correspond to the vertices of Γ (Halemane and Grossmann, 1983). Those vertices for which $\Delta d = 0$ may be neglected as they induce no dynamic fluctuations and their steady-state effect is accounted for by the disturbances making up the other two vertices. Hence, one need only consider $\{(d_{b\,1}, \Delta d_1), (d_{b\,2}, \Delta d_2)\}$ and we denote this set as Γ_C. This dramatically simplifies the solution procedure as the problem is no longer semi-infinite in nature.

3.4.2 Dynamic Operability Constraints

The processes considered in this thesis are open-loop stable and hence we have (Boyd *et al.*, 1990):

$$T_1 = \left[\begin{array}{cc} G_D & G_D \\ 0 & 0 \end{array}\right], \quad T_2 = -\left[\begin{array}{c} G_P \\ I \end{array}\right], \quad \text{and } T_3 = \left[\begin{array}{cc} G_D & G_D \end{array}\right] \tag{3.39}$$

where G_D and G_P represent the disturbance and plant transfer functions respectively.

The step response coefficient, $s_{ic}(i_o)$, at time increment i_o of the ith component of z to a step Δd_c, where c corresponds to a given critical point ($c = 1, 2$), is a linear expression in the coefficients of Q and follows from (3.22):

$$s_{ic}(i_o) = \Delta d_c \sum_{k=0}^{i_o} t_{1\,ic}(k) + \Delta d_c \sum_{m=1}^{n_y} \sum_{n=1}^{n_u} \sum_{k=0}^{i_o} q_{nm}(k) \sum_{v=k}^{i_o} \sum_{\ell=k}^{v} t_{3\,mc}(\ell - k) t_{2\,in}(v - \ell) \tag{3.40}$$

where t_1, t_2 and t_3 contain the pulse response coefficients for the transfer function matrices T_1, T_2 and T_3; and n_y and n_u are the respective dimensions of y and u.

For notational convenience, the step response coefficients for the outputs and inputs are arranged in vector form as follows:

$$s(Q, \Delta d) = \left[s_{11}^T, \ldots, s_{n_y\,1}^T, \ldots, s_{n_y\,2}^T, s_{(n_y+1)\,1}^T, \ldots, s_{(n_y+n_u)\,1}^T, \ldots, s_{(n_y+n_u)\,2}^T\right]^T \tag{3.41}$$

where $s_{ic}^T = [s_{ic}(0), \ldots, s_{ic}(L)]$.

The elements of z, and thus of $s(Q, \Delta d)$, are expressed in deviational form about the steady-state operating conditions y_{ss} and $u_{ss}(y_{ss}, d_b)$. The actual process signal for the closed-loop

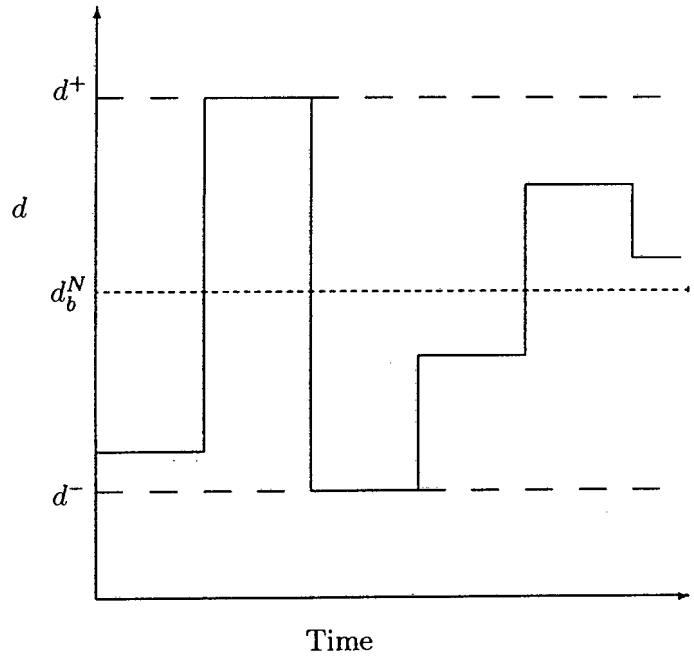

Figure 3.8: An example of a disturbance trajectory included in the set Γ.

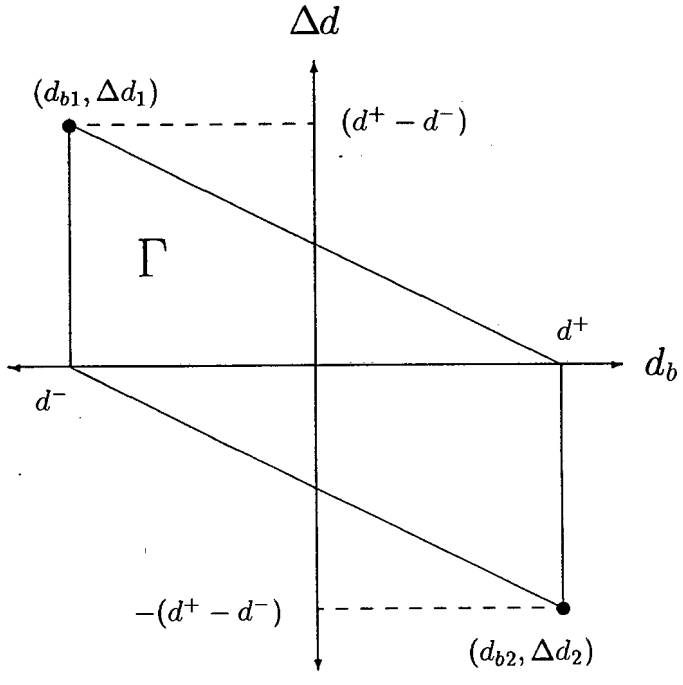

Figure 3.9: The range of possible values for d_b and Δd such that $(d_b, \Delta d) \in \Gamma$.

responses of the system are thus given by

$$S(y_{ss}, Q, d_b, \Delta d) = s(Q, \Delta d) + z_{ss}(y_{ss}, d_b) \tag{3.42}$$

where z_{ss} is a vector describing the steady-state operating conditions and is partitioned in a fashion similar to $s(Q, \Delta d)$.

The bound on the weighted SSE to the critical disturbances may be written as follows:

$$\sum_{c=1}^{2}\sum_{i=1}^{n_y}\sum_{k=0}^{L} W_{ic}(k)\left[s_{ic}(k)\right]^2 \leq \gamma \tag{3.43}$$

where γ is the desired level of dynamic operability. The weighting term $W_{ic}(k)$ is able to include time-weightings if need be. It should be noted that the reference value $r_{ic}(k)$ for the deviational output response is zero and has thus been omitted.

In order to assess the optimal operating conditions, the process setpoints y_{ss} are included as search variables with Q. Given a convex economic objective function $\Psi(y_{ss}, d_b^N)$, the following convex optimization problem needs to be solved:

$$\begin{aligned} &\min_{y_{ss}, Q} \ \Psi(y_{ss}, d_b^N) \\ &\text{s.t.} \\ &\begin{bmatrix} y_{\min} \\ u_{\min} \end{bmatrix} \leq S(y_{ss}, Q, d_b, \Delta d) \leq \begin{bmatrix} y_{\max} \\ u_{\max} \end{bmatrix} \quad \forall\, (d_b, \Delta d) \in \Gamma_C \\ &\sum_{c=1}^{2}\sum_{i=1}^{n_y}\sum_{k=0}^{L} W_{ic}(k)\left[s_{ic}(k)\right]^2 \leq \gamma \end{aligned} \tag{3.44}$$

where $y_{\min}$ and $y_{\max}$ are the respective lower and upper bounds on the actual output responses, and $u_{\min}$ and $u_{\max}$ pertain in a similar manner to the actual input responses. The above problem may be solved efficiently by exploiting its sparsity. The formulation above is an extension of Young *et al.* (1996) to include a quadratic constraint on the weighted SSE of the outputs. In contrast to the problem formulation in the previous section, here the dynamic operability is simply constrained and the aim is to determine the most economical operating conditions whilst maintaining the desired level of operability.

It is useful to note that if the process setpoints are fixed and the objective function involves the minimization of γ, then the above problem would be similar to the dynamic operability formulation considered earlier in the chapter. The only difference would be the treatment of a range of disturbances.

3.4.3 Illustrative Example

The framework discussed and presented above is applied to a simple single-input single-output (SISO) example in order to illustrate certain aspects regarding the interrelationship between economics and dynamic operability. The process considered is from Young *et al.* (1996), where the plant and disturbance transfer functions are given by:

$$G_P(s) = \frac{2}{3s+1} \quad , \quad G_D(s) = \frac{0.5}{0.5s+1} \tag{3.45}$$

A simulation horizon of 200 time intervals is used, with a sampling time of 0.05 minutes. It is assumed that the process has been linearized about an operating point and the outputs and inputs translated to give a nominal steady-state output $y_{ss}^N = 0$ and a nominal steady-state input, in the absence of disturbances, $u_{ss}^N = 0$. It is assumed that the nominal disturbance level is zero ($d_b^N = 0$) and that the upper and lower bounds on the disturbance trajectory are $d^+ = 0.4$ and $d^- = -0.4$ respectively. The critical points for the disturbance description considered are shown in Table 5.4.

Table 3.2: Critical points for the range of disturbances considered.

Critical Point	d_b	Δd
1	−0.4	0.8
2	0.4	−0.8

The following hard constraints exist on the actual input and output signals, u_{act} and y_{act} respectively:

$$| y_{\text{act}} | \leq 0.9 \quad , \quad | u_{\text{act}} | \leq 0.5 \tag{3.46}$$

In addition to the above constraints there is the requirement that the output settles to within 0.01 of its desired steady-state value within 150 time increments. Furthermore, the manipulated input is required to settle to within 1% of its desired steady-state value within 150 time increments.

The measure of closed-loop performance is taken as the SSE of the outputs to the critical point disturbances within the given range. Assuming that the process operates at the point $y_{ss} = y_{ss}^N = 0$, the minimum achievable SSE subject to the input and output constraints mentioned above is calculated to be 0.184. By taking note of the sampling time, this corresponds to an approximate ISE of 0.0092.

To demonstrate the effect of the steady-state operating conditions on dynamic operability, the operating points $y_{ss} = -0.3$ and $y_{ss} = -0.69$ are considered, for which the minimum

achievable SSEs are calculated to be 0.584 and 3.122 respectively. Figures 3.10 and 3.11 show the optimal input and output trajectories, corresponding to both critical points, at each of the three operating point considered thus far. It is clear that as y_{ss} moves toward its lower bound of -0.9, less input power is available for rejecting the disturbance corresponding to critical point 1 and consequently the closed-loop performance deteriorates.

It should also be noted from the figures that, due to the linearity of the controller, the input action to critical point 2 is limited indirectly, even though more input action is potentially available. This highlights one of the limitations imposed by assuming linear control when assessing dynamic operability. Chapter 5 will deal with this issue in further detail and will illustrate the potential benefits of nonlinear control.

The discussion above focussed on the impact that the process operating conditions have on dynamic operability. As mentioned earlier, the operating conditions have a direct bearing on the steady-state economics. This interrelationship is explored in greater detail in the remainder of this example.

Assume now that economic considerations would seek the minimization of y_{ss}. The dynamic operability and feasibility requirements include the constraints in (3.46) as well as a bound on the SSE of the outputs to the critical disturbances. The problem is posed as in (3.44), with $\Psi = y_{ss}$, and is solved for a number of different values of γ, where γ represents the bound on the SSE. Table 3.3 shows how the optimal economic measure varies as a function of the desired level of dynamic operability. Clearly the optimal achievable y_{ss} improves as the SSE bound γ is loosened. Neglecting the SSE constraint altogether shows that feasible operation, under the present assumption of linear control, can only be achieved for $y_{ss} \geq -0.69$. Due to the symmetry of the problem, y_{ss} is also required to be less that $+0.69$. This feasible range of $[-0.69, 0.69]$ differs quite substantially from the feasible range of $y_{ss} \in [-0.8, 0.8]$, as determined from the following steady-state analysis of the problem:

$$\begin{aligned} & \min_{y_{ss}} \; y_{ss} \\ & \text{subject to} \\ -0.9 \;\; &\leq \;\; y_{ss} \;\leq 0.9 \\ -0.5 \;\; &\leq \;\; u_{ss}\left(y_{ss}, d_{b\,i}\right) \;\leq 0.5 \quad \text{for } i = 1, 2 \end{aligned} \tag{3.47}$$

The steady-state input level at the base disturbance level $d_{b\,i}$ is given by:

$$u_{ss}\left(y_{ss}, d_{b\,i}\right) = \frac{y_{ss} - G_D\left(0\right) d_{b\,i}}{G_P\left(0\right)} \tag{3.48}$$

where $G_D\left(0\right) = 0.5$ and $G_P\left(0\right) = 2$ are the respective steady-state gains of the disturbance and process transfer functions. The difference between the feasible operating range as cal-

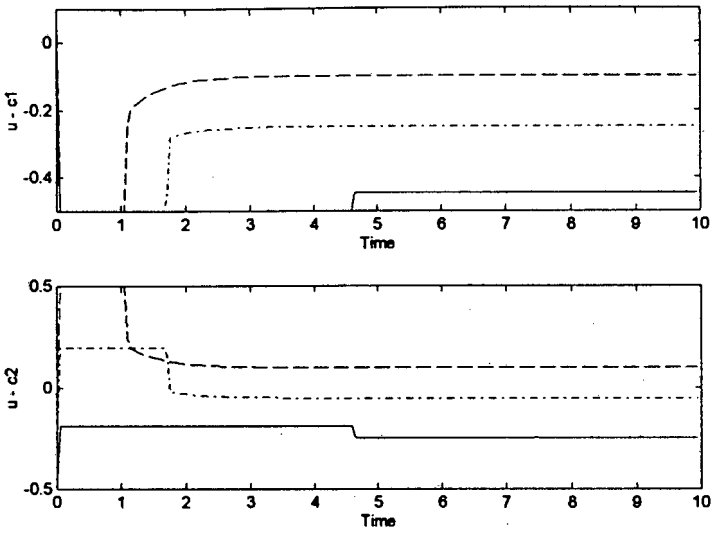

Figure 3.10: Best achievable input trajectories for operation at $y_{ss} = 0$ (- -), $y_{ss} = -0.3$ (- ·) and $y_{ss} = -0.69$ (-).

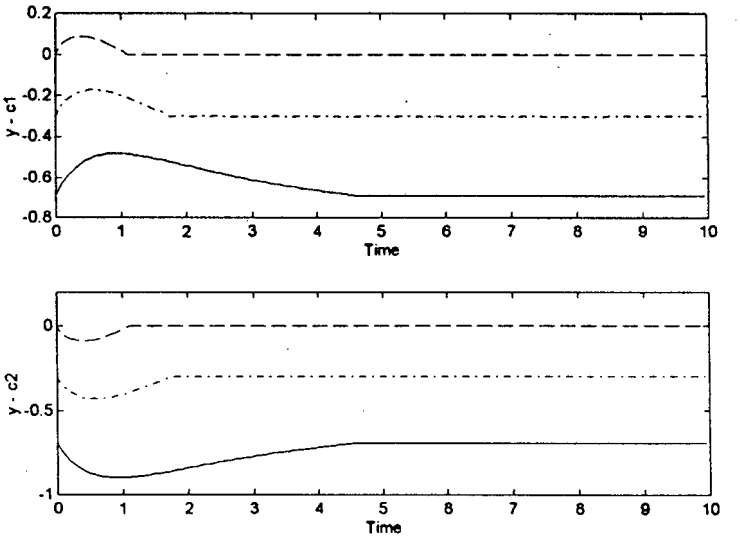

Figure 3.11: Best achievable output trajectories for operation at $y_{ss} = 0$ (- -), $y_{ss} = -0.3$ (- ·) and $y_{ss} = -0.69$ (-).

culated from (3.47) and (3.44) highlights the need to consider disturbance-induced dynamic fluctuations when selecting operating conditions and comparing alternative designs.

Table 3.3: Optimal achievable steady-state economic measure at different levels of dynamic operability.

SSE Bound	**Optimal y_{ss}**
$\gamma \leq 0.1$	infeasible
$\gamma \leq 0.5$	-0.26
$\gamma \leq 1.0$	-0.43
$\gamma \leq 1.5$	-0.53
$\gamma \leq 2.0$	-0.60
$\gamma \leq 2.5$	-0.64
$\gamma \leq 3.0$	-0.68
$\gamma < \infty$	-0.69

From the results in Table 3.3, the trade-off between economics and dynamic operability is evident. When considering a given design, dynamic operability is usually sacrificed as the process is pushed toward its steady-state economic optimum. However, when comparing competing designs, a process which is inherently operable may be able to operate closer to the constraints defining its economic optimum without violating them in the face of disturbances. To illustrate this point we consider a different plant, with the following transfer function description:

$$G_{P\,\mathrm{mod}}(s) = \frac{2(-s+1)}{(s+1)(4s+1)} \tag{3.49}$$

The disturbance transfer function, disturbance range and all other constraints are as before. The minimum achievable SSE for the above process, operating at $y_{ss} = y_{ss}^N = 0$, is calculated to be 10.813. This is considerably worse than the performance achieved by the original process (SSE$=$ 0.184) at the same operating conditions. The major cause of the poor performance is due to the zero at $+1$ in the right-half-plane.

Feasible closed-loop behavior, neglecting the SSE bound, can only be achieved for y_{ss} in the range $[-0.51, 0.51]$. This is significantly poorer than the achievable range of the original plant, highlighting the economic penalty of having poor dynamic operability. Furthermore, had a criterion been placed on the SSE for the above plant, the optimization of economic performance in (3.44) would be infeasible for all values of $\gamma \leq 10.813$. It is interesting to note that if dynamic aspects are ignored, the feasible range of operation would be as for the original plant, since both processes have the same steady-state gains. This further emphasizes the need to consider dynamic aspects in the screening of alternative process designs.

Chapter 4

Dynamic Operability Assessment in the Presence of Model Uncertainty

The simple illustrative example presented in Chapter 2.2, served as an introduction to how model uncertainty affects dynamic operability and how some designs may be inherently more sensitive to model uncertainty. The aim of this chapter is to show how modern robust control theory may be incorporated within the Q-parametrization framework in order to assess the impact of model uncertainty on the dynamic operability of a given plant design. After providing a brief background to robust control, some of the important methodologies for robustness analysis will be presented and compared. Thereafter, it will be shown how one such methodology is incorporated in a convenient fashion into the computational strategy presented in Chapter 3.

4.1 Background to Robust Control

The plant models typically used in process control are linear time invariant (LTI) models which describe the true process dynamics only approximately. Uncertainty in the plant model may have many possible sources. Typical causes of model error or model uncertainty include:

1. Unmodelled high frequency dynamics.
2. Linearization of a nonlinear model about a particular operating point.

3. Different operating conditions leading to time variation in the model parameters, even if the process is fairly linear.

4. True uncertainties, such as an imperfect knowledge of model parameters and the model order at high frequencies.

A common approach in robust control theory is to consider a model of the plant (nominal plant) and a set of plants (uncertainty set) lying within a given region about the nominal plant and thought to contain the actual plant. The plants in the uncertainty set are viewed as perturbations about the nominal plant. Plant perturbations can be broadly classified into non-parametric and parametric perturbations (Dahleh and Diaz-Bobillo, 1995). Non-parametric perturbations are perturbations of the input-output description of the process and are typically bounded in the sense of induced norms. This class of perturbations can be used to represent any of the first three sources of model uncertainty in the above list. For example, the effect of linearization or time-variation of a process can be described by a non-linear or time-varying perturbation of a LTI model. Non-parametric perturbations may have structure, to allow for the fact that the different sources of uncertainty may be independent of each other.

Parametric perturbations, on the other hand, are (real) perturbations of specific parameters in a process model. Often these parameters may have a physical meaning, but this is not always the case. Although parametric perturbations are quite natural, they are much harder to treat in a non-conservative manner than are nonparametric perturbations. The theory for controller analysis and synthesis in the presence of combinations of parametric and nonparametric perturbations is, as yet, not fully developed (Dahleh and Diaz-Bobillo, 1995; Packard and Doyle, 1993).

There is currently a wealth of literature for treating various forms of model uncertainty with more or less conservatism. Usually a trade-off exists between mathematical convenience and practical significance. It is often possible to obtain very simple robust stability criteria but these may be very misleading if the actual uncertainty is significantly different from what is assumed. On the other hand, while a detailed description of the model uncertainty will provide more meaningful results, such information is generally not known at the early design stages and, furthermore, the mathematical complexity associated with a rigorous treatment is often undesirable. What is therefore sought is a practical description of the expected model uncertainty which captures its essential features and which allows for convenient mathematical treatment (Skogestad and Morari, 1987).

4.1.1 Representation of Model Uncertainty

The most common treatment of model uncertainty involves the use of norm-bounded perturbations about a nominal model of the plant. It will be shown below that even parametric uncertainty may be approximated in this fashion. We define Π to be the set of all possible plants, P, falling within the range of the expected maximum uncertainty from the nominal plant, $\tilde{P}$.

Uncertainty description based on parametric uncertainty

Often certain parameters in the transfer function model are imprecisely known. Typically upper and lower bounds would exist on these parameters. As an example, consider the following first order SISO plant (Skogestad and Postlethwaite, 1996):

$$p(s) = \frac{ke^{-\theta s}}{\tau s + 1} \quad , \quad 2 \leq k, \theta, \tau \leq 3 \tag{4.1}$$

The parameters in the above model are thought to lie within the given ranges. By varying the model parameters over their expected ranges and plotting $p(j\omega)$ in the complex plane, the uncertainty set $\Pi(\omega)$ shown in Figure 4.1 (Skogestad and Postlethwaite, 1996) is obtained. This set clearly has a very complicated shape and a complex mathematical description. In order to simplify the mathematical treatment Π is approximated by discs centered about the nominal plant, as shown in Figure 4.2 (Skogestad and Postlethwaite, 1996).

Conservatism is clearly introduced by the disc approximation as is evidenced in Figure 4.2. While exact methods, based on complex region mapping, do exist for avoiding the disc approximation (Laughlin *et al.*, 1986), these are complicated and are best suited to the robustness analysis of simple systems. As dynamic operability assessment is mainly concerned with controller synthesis, these methods will not be considered any further.

Using the disc-shaped uncertainty description, the disc-shaped uncertainty regions may be treated as being generated by an additive complex perturbation L_A about a nominal plant:

$$\Pi_A = \{p(s) \mid p(s) = \tilde{p}(s) + w_A(s)\Delta_A(s) \quad , \quad |\Delta_A(j\omega)| \leq 1 \quad \forall \omega\} \tag{4.2}$$

In the expression above, the perturbation L_A is defined in terms of a weight $w_A(s)$ on a norm-bounded perturbation Δ_A. At each frequency $\Delta_A(j\omega)$ maps out a disc-shaped region in the complex plane centered at 0 with radius 1. Therefore, $\tilde{p}(j\omega) + w_A(j\omega)\Delta_A(j\omega)$ maps out a disc-shaped region of radius $|w_A(j\omega)|$ centered at $\tilde{p}\,(j\omega)$.

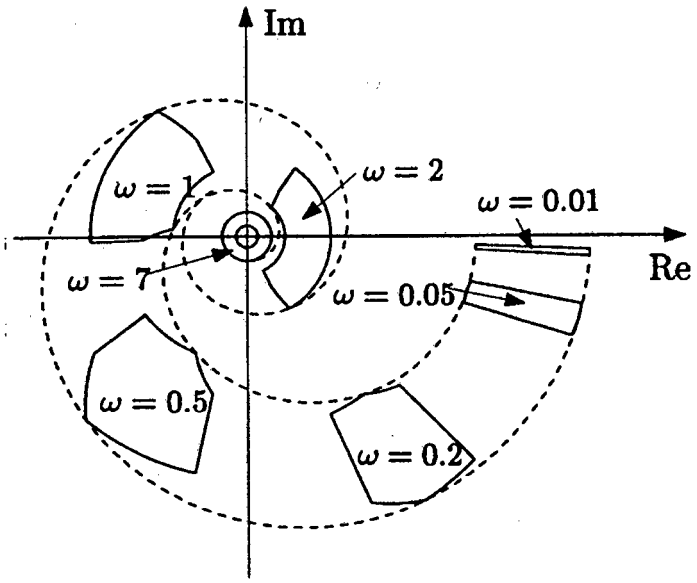

Figure 4.1: Uncertainty set for parametric uncertainty in the gain, the time constant and the dead-time of a SISO process (Skogestad and Postlethwaite, 1996).

The uncertainty weight may be determined at each frequency by finding the smallest radius which includes all the possible plants in Π:

$$|w_A(\omega)| \geq \max_{p \in \Pi} |p(j\omega) - \tilde{p}(j\omega)| \tag{4.3}$$

To simplify subsequent controller design, $w_A(s)$ is usually chosen to be stable, minimum phase and of low order.

It should be noted that when parametric uncertainty is treated in a norm-bounded fashion, the parameters of the nominal model can be chosen so as to reduce the conservatism of the disc approximation. Essentially this involves moving the centre of the disc within the uncertainty region so as to minimize the size of the disc radius. A trade-off exists between having a simple nominal model which facilitates controller synthesis but which has an overly conservative uncertainty region; and having a complicated nominal model with a tight uncertainty description. Skogestad and Postlethwaite (1996) provide further details in this regard.

Apart from being mathematically convenient, the norm-bounded disc approximation to parametric uncertainty may be more appropriate at the process design stage. The reason is that it may be unrealistic to provide a very careful description of the parametric uncertainty when in fact the model structure or model order may be poorly known as well. When multiple sources of uncertainty are present for SISO systems, these are often lumped together, and

Table 4.1: Descriptions of model uncertainty and the resulting relationship between P and $\tilde{P}$.

Type of uncertainty	**Mathematical relation**	**Common example**
Additive	$P = \tilde{P} + L_A$	nonlinearities
Multiplicative input	$P = \tilde{P}(I + L_I)$	actuator uncertainty
Multiplicative output	$P = (I + L_O)\tilde{P}$	neglected (sensor) dynamics
Inverse multiplicative	$P = (I + L_E)^{-1}\tilde{P}$	pole uncertainty

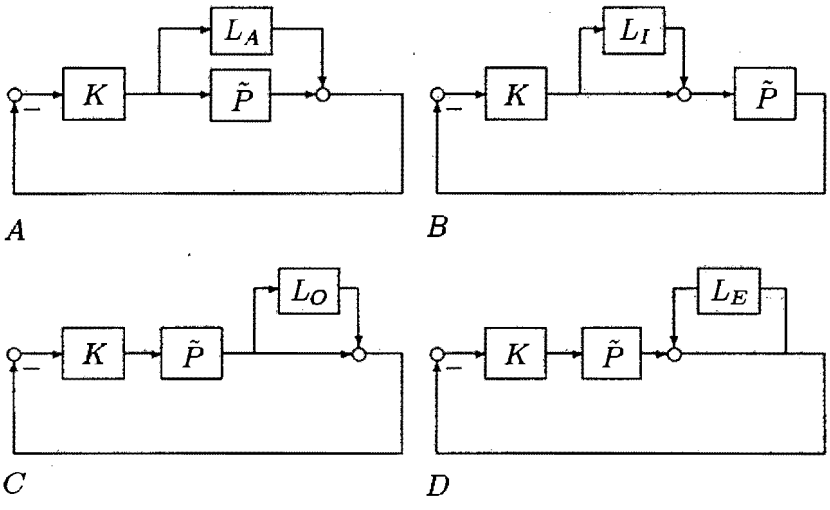

Figure 4.3: Classical block diagram representation of four common types of model uncertainty. A - additive, B - multiplicative input, C - multiplicative output and D - inverse multiplicative output uncertainty.

and will generally result in a more conservative controller design. Accurately accounting for the structure of the model uncertainty is important in robust control but also significantly complicates the mathematics involved, particularly when treating the problem of controller synthesis.

4.1.2 The M-Δ Framework for Robustness Analysis

Much of the work in robust control relies on the M-Δ framework, shown in Figure 4.4, for representing the effect of model uncertainty on the nominal plant. M is termed the interconnection matrix and is the nominal closed-loop system as "seen" from Δ, the perturbation matrix. The interconnection matrix connects the outputs of the perturbations to their inputs and typically includes the nominal plant, the (stabilizing) controller and any weighting

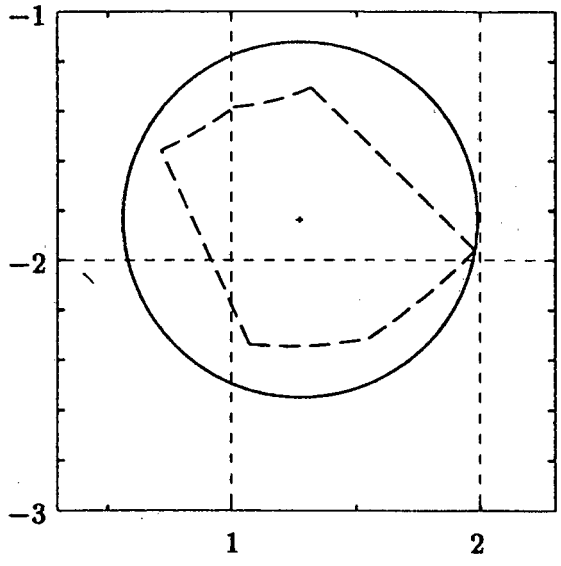

Figure 4.2: Disc approximation (–) at a given frequency ($\omega = 0.2$) to the uncertainty region (--) obtained from parametric uncertainty (Skogestad and Postlethwaite, 1996).

in this case a disc approximation is usually quite satisfactory (Skogestad and Postlethwaite, 1996).

Uncertainty description for multivariable systems

When describing model uncertainty in multivariable systems, it is important to note the location or source of the model uncertainty. Typically, model uncertainty is classed as additive, multiplicative input, multiplicative output or inverse multiplicative output, although many more types do exist (Doyle and Stein, 1981). Table 4.1 shows the relationship between the actual plant and the nominal plant model for each of these descriptions of uncertainty as well as common examples of each. Illustrations of how the above are represented in block diagram form are shown in Figure 4.3.

The perturbation matrices in Table 4.1 may have structure. For example, when considering actuator uncertainty, the different inputs are generally independent and thus L_I has a diagonal structure. If, however, L_I is treated as a full matrix (unstructured), then the model error is assumed to be spread over the entire transfer function matrix. This may introduce more sources of uncertainty than what are physically possible, making II unnecessarily large,

functions on the perturbations. Both the uncertainty weights and the nominal plant are typically linear time-invariant (LTI) and the controller is assumed to be LTI. For a stabilizing controller, M is stable. Table 4.2 lists the mathematical form of the interconnection matrix M for the four different sources of model uncertainty listed in Table 4.1. Skogestad and Morari (1987) provide many examples showing the construction of M for combinations of the uncertainties given above. One of the important features of the Q-parametrization approach is that M is generally linear in Q.

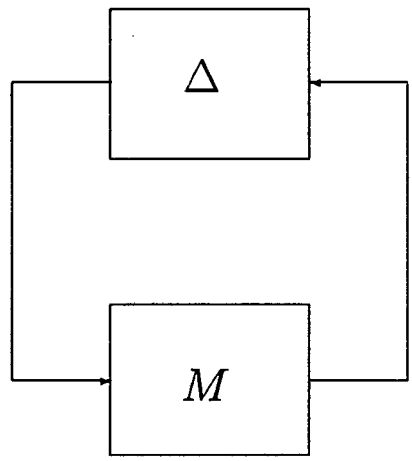

Figure 4.4: The M-Δ framework for robustness analyis.

Table 4.2: Construction of the interconnection matrix M for four common uncertainty descriptions.

Type of uncertainty	**Mathematical description of M**
Additive	$M = L_A(I + K\tilde{P})^{-1}K$
Mutiplicative input	$M = L_I(I + K\tilde{P})^{-1}K\tilde{P}$
Mutiplicative output	$M = L_O\tilde{P}K(I + \tilde{P}K)^{-1}$
Inverse mutiplicative	$M = L_E(I + \tilde{P}K)^{-1}$

The advantage of the M-Δ framework is that it is easy to see that uncertainty causes stability problems due to the extra feedback paths which are provided by the perturbations contained in Δ. A sufficient condition for the (robust) stability of the closed-loop shown in Figure 4.4 is given by the small-gain theorem. This theorem states that if $||\Delta|| \leq \gamma$ then the system is robustly stable provided $||M|| < \frac{1}{\gamma}$. Implicit in the small-gain theorem is the assumption

that the perturbation Δ is totally unstructured. The robust stability criterion may thus be conservative if the perturbation is structured.

4.1.3 Characterization of the Model Uncertainty

Apart from its structure and location in the feedback structure, little mention has been made regarding the details of the perturbation Δ. The uncertainty may be described either as parametric, linear time-invariant, nonlinear/time-varying, sector-bounded nonlinear or may be comprised of combinations of these. Each of these factors will determine the appropriate criteria to use for the analysis of robustness. Depending on the assumptions regarding the model uncertainty, more or less sophisticated criteria will be needed. In general, as one restricts the uncertainty to a smaller class, the mathematical complexity of the condition needed to test robustness increases. Thus the paradox exists that the criteria applicable to nonlinear/time-varying model uncertainty are significantly easier to test than those for real parametric uncertainty.

Another important property when characterizing uncertainty is the choice of induced norm used to bound the uncertainty magnitude. The choice of induced norm depends much on the nature of the underlying signals. Common examples of signal norms include the ℓ_2 and ℓ_∞ signal norms. Describing signals in terms of ℓ_∞ norms allows for persistent bounded signals to be considered, whereas ℓ_2 signal norms require that the signals are not only bounded in their peak magnitude, but also decay with time. The choice of signal norm in conjunction with the assumption regarding the nature of the model uncertainty will then determine the appropriate robustness conditions to use.

Some of the most widely used approaches to robust control include the structured singular value approach and the ℓ_1 approach. The structured singular value approach assumes that the model uncertainty is LTI and that the underlying signal norms are of finite energy and bounded in an ℓ_2 sense. The ℓ_1 robust control approach is best suited to nonlinear/time-varying model uncertainty and assumes the signal norms are bounded in their peak magnitude or ℓ_∞ sense.

In the remainder of the chapter these two alternative approaches to robust control are presented in greater detail. In addition, a recently proposed theoretical framework based on the passivity theorem with multipliers is presented and discussed. This framework is able to treat, in a unified manner, a number of different forms of model uncertainty and includes, as a special case, the results obtained using the structured singular value approach. The merits

of the different approaches, in the context of dynamic operability assessment, are compared. It is argued that a nonlinear/time-varying uncertainty description may be more appropriate at the early design stage. This, together with its mathematical convenience and its natural discrete-time formulation make the ℓ_1 approach well suited for implementation within the Q-parametrization approach to dynamic operability assessment developed in Chapter 3. The details regarding the incorporation of model uncertainty are presented and applied to an illustrative example. Before continuing, a brief description of signal and operator norms is given.

4.1.4 Norms of Signals and Systems

The norms described below are mainly defined for continuous time systems. In certain cases of importance, their equivalent form for discrete-time systems are given.

Norms of vector signals

In the case of vector signals $u(t)$, where $u \in \Re^n$, the L_1 vector signal norm is written as L_1^n and defined as follows:

$$\begin{aligned} ||u(t)||_1 &= \int_0^\infty \sum_{i=1}^n |u_i(t)|\, dt \\ &= \sum_{i=1}^n ||u_i||_1 \end{aligned} \tag{4.4}$$

where $||u_i||_1$ is the L_1 norm for the scalar signal $u_i(t)$.

Similarly, the L_2^n vector signal norm is defined as:

$$\begin{aligned} ||u(t)||_2 &= \left(\int_0^\infty \sum_{i=1}^n u_i(t)^2\, dt \right)^{1/2} \\ &= \left(\sum_{i=1}^n ||u_i||_2^2 \right)^{1/2} \end{aligned} \tag{4.5}$$

The L_2^n signal norm defines the total energy of a signal and is appropriate for decaying signals. Using Parseval's theorem, an equivalent frequency domain expression may be obtained:

$$||u(t)||_2 = \left(\frac{1}{2\pi} \int_{-\infty}^{\infty} u(j\omega)^* u(j\omega)\, d\omega \right)^{1/2} \tag{4.6}$$

where $u(j\omega)^*$ is the complex conjugate transpose of $u(j\omega)$.

The discrete-time equivalent of the L_2^n signal norm is given by:

$$||u(t)||_{\ell_2} = \left(\sum_{k=0}^{\infty} \sum_{i=1}^{n} |u_i(k)|^2 \right)^{1/2} \tag{4.7}$$

The L_∞^n norm is defined as:

$$\begin{aligned} ||u(t)||_\infty &= \sup_{t \geq 0} \max_{1 \leq i \leq n} |u_i(t)| \\ &= \max_{1 \leq i \leq n} ||u_i||_\infty \end{aligned} \tag{4.8}$$

The L_∞^n norm defines the peak absolute value of the signal. From the above definition it is clear that for $||u||_\infty$ to be small, *every* component of u is required to be small over *all* time. The discrete-time equivalent of the above norm is given by:

$$||u||_{\ell_\infty} = \sup_k \max_i |u_i(k)| \tag{4.9}$$

where $u_i(k)$ is the kth pulse response coefficient of the ith element of the signal vector u. Comparison of (4.7) and (4.9) reveals that signals which are ℓ_2-stable (finite energy) are ℓ_∞-stable (finite magnitude), but not vice-versa.

System or operator norms

An important notion is the gain of a system. This is a measure of the amount of amplification that a system exerts on normalized bounded signals. The gain is a function of the norms of both the input and output signals and provides a measure of the size of a system. Some important gains for LTI MIMO are given below.

For bounded L_2^n input and output signals, the gain of a stable MIMO system is given by:

$$||H||_\infty = ||H||_{L_2\text{-ind}} = \sup_{||w||_2 \neq 0} \frac{||Hw||_2}{||w||_2} \tag{4.10}$$

$$= \sup_\omega \sigma_M(H(j\omega)) \tag{4.11}$$

where σ_M is the maximum singular value of H and is calculated from the eigenvalues (λ_i) of H as follows:

$$\sigma_M = \max_i \sqrt{\lambda_i(H^*H)} \tag{4.12}$$

The peak gain of a MIMO system of dimension n is:

$$||H||_{\text{pk-gain}} = ||H||_{L_\infty\text{-ind}} = \sup_{||w||_\infty \neq 0} \frac{||Hw||_\infty}{||w||_\infty} \tag{4.13}$$

$$= \max_{1 \leq i \leq n} \int_0^\infty \sum_{j=1}^{n} |h_{ij}(t)| \, dt$$

For a SISO system, this means that L_∞-stability is guaranteed if the impulse response is in L_1. That is,

$$\int_0^\infty |h(t)|\, dt < \infty \tag{4.14}$$

In this chapter considerable attention will be given to the discrete-time equivalent of the above operator norm, namely:

$$||H||_{\ell_\infty\text{-ind}} = \max_{1 \le i \le n} \sum_{j=1}^{n} \sum_{k=0}^{\infty} |h_{ij}(k)| \tag{4.15}$$

In the above, the $h_{ij}(k)$ corresponds to the pulse response coefficients of h_{ij}.

4.2 The Structured Singular Value Framework for Robust Control

The structured singular value μ was introduced by Doyle (1982) to overcome the conservatism in the small-gain theorem introduced by lumping all the sources of model uncertainty into one full perturbation matrix Δ. The conservatism results from the fact that more perturbations are included than what may be physically possible.

In the μ-framework, each perturbation Δ_i is assumed to be stable and norm bounded ($\bar{\sigma}$ $(\Delta_i) \le 1, \quad \forall \omega$). The actual perturbation L_i is written as $L_i = W_{2i}\Delta_i W_{1i}$, where W_{1i} and W_{2i} are stable LTI weighting matrices introduced to ensure that the above bound is unity at all frequencies. Implicit in the formulation is the assumption that Δ_i is complex. Special modifications need to be made in order to restrict Δ_i to be real.

The perturbations which may occur at different points in the feedback system are collected and placed into one large block diagonal perturbation matrix:

$$\Delta = \{\text{diag}\,[\delta_1 I_{r_1}, ..., \delta_S I_{r_S}, \Delta_1, ..., \Delta_F] \mid \delta_i \in C\,,\ |\delta_i| \le 1\,,\ \Delta_j \in C^{m_j \times m_j}\,,\ \bar{\sigma}\,(\Delta_j) \le 1\} \tag{4.16}$$

where S refers to the number of repeated scalar perturbation blocks and F is the number of full perturbation blocks. For notational convenience the perturbations are assumed to be square, with r_i being the dimension of the ith repeated scalar block and m_j being the dimension of the jth full block. It can be shown that $\bar{\sigma}\,(\Delta) \le 1 \quad \forall \omega$.

The M-Δ framework, defined earlier, is used to express the effect of model uncertainty on the nominal plant. The goal is now to derive conditions on M which guarantee robust stability in the presence of structured LTI model uncertainty. Doyle (1982) showed that,

for a nominally stable system, testing robust stability is equivalent to testing the stability of the M-Δ closed-loop structure. Using the Nyquist test for stability, this is equivalent to requiring that $\det(I + \Delta M)$ does not encircle the origin as s traverses the Nyquist D contour for all possible Δ in the uncertainty set. Since the perturbations are norm-bounded, this is equivalent to:

$$\begin{aligned} \det(I + \Delta M) &\neq 0 \quad \forall \omega, \quad \forall \Delta, \quad \bar{\sigma}(\Delta) \leq 1 \\ &\Leftrightarrow \quad \rho(\Delta M) \leq 1, \quad \forall \Delta, \quad \bar{\sigma}(\Delta) \leq 1 \end{aligned} \tag{4.17}$$

The above condition is still not suitable as it must be tested for all possible perturbations Δ. What is required is a condition on M alone. This is provided by the following theorem of Doyle (1982).

Theorem 4 *Assume that the nominal system is stable. Then, the closed-loop system (Figure 4.4) is stable for all* Δ, $\bar{\sigma}(\Delta) \leq 1$, *if and only if*

$$\mu(M) \leq 1 \quad \forall \omega. \tag{4.18}$$

The above theorem may be interpreted as a "generalized small-gain theorem" which takes into account the structure of Δ. The function μ, called the structured singular value, is defined to get the tightest possible bound on M such that (4.17) is satisfied. Defining X_ν as

$$X_\nu = \{\Delta = \text{diag}\,\{\delta_1 I_{r_1}, ..., \delta_S I_{r_S}, \Delta_1, ..., \Delta_F\} \mid \quad |\delta_i| \leq \nu\,,\ \bar{\sigma}(\Delta_j) \leq \nu\}\,, \tag{4.19}$$

the structured singular value is defined formally as:

$$\mu(M)^{-1} = \min_{\nu} \{\nu \mid \det(I + \Delta M) = 0 \text{ for some } \Delta \in X_\nu\} \tag{4.20}$$

If no such Δ exists then $\mu(M) = 0$. It is important to note that μ depends both on M and on the structure of the perturbations in Δ. It may be intuitively thought of as the inverse of the smallest structured perturbation Δ that causes instability of the M-Δ structure. To emphasize that μ depends on the structure of Δ as well on M, we write $\mu_\Delta(M)$.

In general, μ is difficult to calculate exactly and is usually evaluated in terms of upper and lower bounds. Doyle (1982) showed that the following bounds exist for μ:

$$\rho(M) \leq \mu_\Delta(M) \leq \bar{\sigma}(M) \tag{4.21}$$

The lower bound is an equality when the perturbation Δ is diagonal (totally structured) and the upper bound is an equality when Δ is full (unstructured uncertainty). From this we

see that μ is a generalization of the spectral radius ρ and the maximum singular value $\bar{\sigma}$. The above set of bounds can be very conservative if the uncertainty has a block diagonal structure. To overcome this conservatism, use is made of the following tighter bounds:

$$\max_{U \in \mathcal{U}} \rho(UM) \leq \max_{\Delta \in X_{\nu=1}} \rho(\Delta M) = \mu_{\Delta}(M) \leq \inf_{D \in \mathcal{D}} \bar{\sigma}\left(DMD^{-1}\right) \tag{4.22}$$

where $\mathcal{U}$ is the set of all unitary matrices with the same structure as Δ and D is a scaling matrix which has the following structure:

$$\mathcal{D} = \text{diag}\left[D_1, ..., D_S, d_1 I_{m_1}, ..., d_{F-1} I_{m_{F-1}}, I_{m_F}\right] \tag{4.23}$$

where S, m_i and F are as defined before. The matrices D_i are complex full matrices of dimension r_i, where r_i is the dimension of the ith repeated scalar block in Δ. In addition, the matrices D_i are required to be Hermitian and positive definite ($D_i = D_i^* > 0$). The real scalars d_i are required to be positive ($d_i \in \Re, d_i > 0$).

The above bounds have some interesting advantages and disadvantages with regard to their computation. Firstly, the lower bound has been shown by Doyle (1982) to be an equality, but the function $\rho(UM)$ may have multiple local minima, making its exact computation difficult. On the other hand, the upper bound can be formulated as a convex optimization problem and solved reliably using Linear Matrix Inequality (LMI) theory and semi-definite programming. Unfortunately, the bound is potentially conservative for all cases where $2S + F > 3$. Nevertheless, the above two bounds provide a useful means for computing μ and have been employed in a number of packages such as the μ-Analysis and Synthesis Matlab Toolbox (Balas *et al.*, 1991). Further refinements to the above bounds may be made to restrict the uncertainty to purely real perturbations or to mixed real/complex perturbations. These are not discussed here since the framework of the passivity theorem with multipliers, discussed next, provides a convenient means of formulating the upper bound for these situations.

The discussion thus far has only considered the issue of robust stability analysis, and the important issues of robust performance analysis and robust controller synthesis have not been dealt with yet. Robust performance relates to the requirement that all plants in a given uncertainty set meet a certain performance specification. In other words, it is concerned with the worst-case performance achievable for any plant in the uncertainty set. Doyle (1982) showed that robust performance may be treated in a similar fashion to robust stability via the addition of fictitious perturbations which are actually performance requirements.

In the area of robust controller synthesis, a popular approach is the design of the so-called μ-optimal controller which has the feature that it optimizes a worst-case robust performance measure. Such a controller is usually of very high order and is designed using an iterative

procedure known as "D-K Synthesis" (Doyle, 1982; Doyle and Stein, 1981). This automated procedure involves alternating between finding an optimal controller (K) at fixed scales (D) and finding optimal scales for a given controller. It has been argued that the μ-optimal controller is an ideal measure of dynamic operability as it represents a closed-loop performance limit and rigorously includes the issue of model uncertainty (Morari and Perkins, 1995). There are, however, a number of difficulties associated with the use of the μ-optimal controller, namely:

1. The μ-optimal controller design methodology does not directly handle time domain specifications on the input and output behavior.
2. Designing for the worst-case controller performance may be overly conservative in many situations, particularly when the worst-case model uncertainty is highly unlikely.
3. Treating time-delay systems is complicated because the μ framework requires rational polynomial transfer functions.
4. The μ-optimal controller design problem is highly nonconvex and there is no guarantee of global optimality.

Having provided a brief introduction to the structured singular value framework for control, we now proceed to discuss a recently proposed approach (Balakrishnan *et al.*, 1994) which aims at unifying a number of seemingly unrelated robustness measures.

4.3 Robustness Analysis Using the Passivity Theorem With Multipliers

It has been shown thus far how the structured singular value framework is able to exploit information regarding the structure of LTI perturbations and thereby reduce the conservatism associated with the small-gain theorem. In general though, the perturbations may be real, nonlinear, sector-bounded nonlinear ("Popov" uncertainty), time-varying, slowly time-varying or combinations of these. In the past, a host of different sufficient conditions for the robust stability of such systems have been derived using seemingly unrelated techniques. It has recently been shown (Balakrishnan *et al.*, 1994) that many of these criteria may be rederived in the framework of the passivity theorem with multipliers and tested numerically using convex optimization over Linear Matrix Inequalities (LMIs). Details of this approach

to robustness analysis as well as an introduction to LMI theory are presented in this section. An implicit assumption of this approach is that the magnitude of the underlying signals is best described by an ℓ_2 signal norm. This is in contrast to the assumption used in the ℓ_1 robustness framework to be discussed hereafter, which assumes ℓ_∞ signals.

4.3.1 Converting from the Small-Gain Framework to that of the Passivity Theorem

The first step in the discussion is the conversion from the small-gain $(M-\Delta)$ framework to that of the passivity theorem. Given the bound on the uncertainty magnitude, $\overline{\sigma}(\Delta) \leq \gamma$, this is conveniently done by applying a so-called 'bilinear sector transformation' where we define:

$$\tilde{p} = \gamma q - p \quad \text{and} \quad \tilde{q} = \gamma q + p \tag{4.24}$$

It should be noted that γ is simply a bound on the uncertainty magnitude and should not be confused with the process condition number, defined in Chapter 2. Routine algebraic manipulation allows the system in Figure 4.4 to be written as that in Figure 4.5 (the passivity theorem framework); where G is stable, LTI and has a transfer function matrix given by:

$$G(s) = (I + \gamma M(s))^{-1}(I - \gamma M(s)), \tag{4.25}$$

and

$$\tilde{\Delta} = (\gamma I - \Delta)^{-1}(\gamma I + \Delta). \tag{4.26}$$

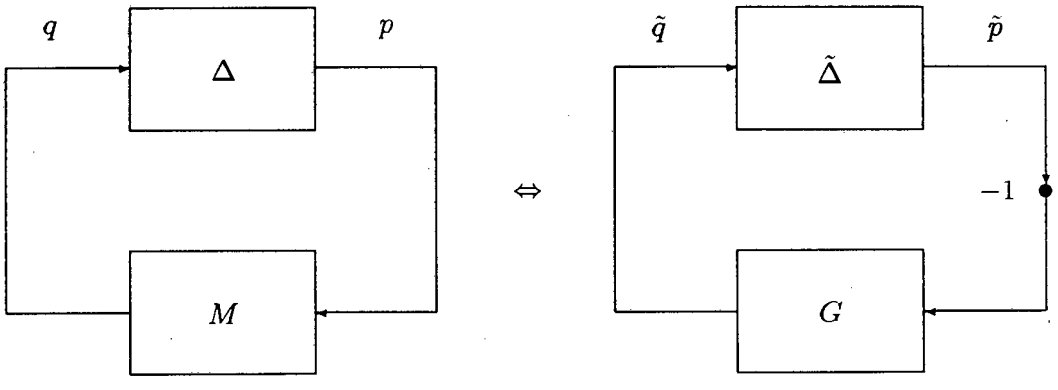

Figure 4.5: The passivity theorem framework for robustness analysis and its relation to the M-Δ framework of the small-gain theorem.

It should be noted in Figure 4.5 that negative feedback is required in the passivity theorem framework. Table 4.3 summarizes how some of the important properties in the small-gain

framework are translated to properties in the passivity theorem framework (Balakrishnan *et al.*, 1995). From the first entry in the table it is worthwhile to mention once again that the passivity framework assumes that the perturbation magnitude is bounded in terms of an ℓ_2-induced norm. It is thus applicable to systems where the signals dissipate with time.

Table 4.3: Relation between properties in the small-gain framework and those in the passivity theorem framework.

Small-gain property	**Passivity framework property**
$\|\Delta\|_{\ell_2\text{-ind}} = \overline{\sigma}(\Delta) < \gamma$	$\tilde{\Delta}$ is strictly passive
Δ is diagonal	$\tilde{\Delta}$ is diagonal
Δ is LTI	$\tilde{\Delta}$ is LTI
Δ is a constant matrix	$\tilde{\Delta}$ is a constant matrix

4.3.2 Definition of Strict Passivity

The operator $\tilde{\Delta}$ is said to be strictly passive if, for some positive real ϵ,

$$\int_0^\Gamma p(t)^T(\tilde{\Delta}p)(t)dt > \epsilon \int_0^\Gamma p(t)^T p(t)dt \quad , \quad \forall\, \Gamma \geq 0 \text{ and } \forall\, p(t)\ . \tag{4.27}$$

To illustrate the meaning of this definition, consider the case where $\tilde{\Delta}$ is LTI. Using Parseval's theorem, the requirement that $\tilde{\Delta}$ be strictly passive is equivalent to the following condition:

$$\tilde{\Delta}(j\omega) + \tilde{\Delta}^*(j\omega) > 0 \qquad \forall\, \omega \tag{4.28}$$

The inequality in the above constraint refers to positive definiteness. That is, we require $u^T\left(\tilde{\Delta} + \tilde{\Delta}^*\right)u$ to be positive for all nonzero real vectors u of appropriate dimension.

The definition for passivity is slightly relaxed and ϵ in (4.27) need only be non-negative. The result is that $\tilde{\Delta}$ need only satisfy

$$\tilde{\Delta}(j\omega) + \tilde{\Delta}^*(j\omega) \geq 0 \quad \forall\, \omega \tag{4.29}$$

The passivity theorem (Desoer and Vidyasagar, 1975) states that, given the feedback system shown in Figure 4.5, if $\tilde{\Delta}$ is strictly passive then G is passive. It will be shown subsequently how this result may be used to test the robustness of the original system in Figure 4.4. Central to the passivity theorem approach to robustness analysis is the use of Linear Matrix Inequality (LMI) theory for the efficient testing of the robustness criteria. A brief overview of LMIs and their application to process control will be provided before illustrating their use in conjunction with the passivity theorem for robustness analysis.

4.3.3 Background to Linear Matrix Inequalities in Process Control

A linear matrix inequality (LMI) has the form:

$$F(x) = F_0 + \sum_{i=1}^{m} x_i F_i > 0 \tag{4.30}$$

where $x \in \Re^m$ is the optimization/feasibility variable and $F_0, ..., F_m \in \Re^{n \times n}$ are given symmetric matrices. The inequality symbol in the above expression means that $F(x)$ is positive definite, that is $u^T F(x) u > 0$ for all nonzero $u \in \Re^n$. It often happens that the optimization/feasibility variable is a matrix as opposed to a vector. If this is the case, then it is always possible to reduce the resulting problem to the standard form given above (Boyd *et al.*, 1994).

The above constraint on x is convex, allowing LMI-based problems to be solved efficiently from a numerical standpoint, using interior-point methods, even though they may not always be solved analytically.

Many standard constraints in systems analysis may be written as LMIs. Boyd *et al.* (1994) illustrate how linear, convex quadratic and matrix norm constraints can all be expressed as LMIs. Furthermore, multiple LMIs may be expressed as a single LMI by writing them in block diagonal form. While a number of important convex constraints do not appear to be LMIs, they can be readily transformed to equivalent LMI conditions with the aid of techniques such as the Schur complement, the introduction of slack variables and the use of elimination. Boyd *et al.* (1994) provide useful examples in this regard.

History of LMIs in control system analysis

The history of LMIs in the study of the stability of dynamical systems starts in the late nineteenth century with the pioneering work of Lyapunov. He showed that the n-dimensional system described by the set of differential equations

$$\frac{d}{dt} y = Ay \tag{4.31}$$

is stable (in the sense that all trajectories converge to zero) if and only if there exists a symmetric positive definite matrix P such that

$$A^T P + PA < 0 \quad , \quad P = P^T > 0 \tag{4.32}$$

The above requirement on P is a special form of an LMI and can be written in the standard form of (4.30) by setting

$$F_0 = 0 \text{ and } F_i = -A^T P_i - P_i A \qquad \forall i = 1, ..., m \tag{4.33}$$

where $P_1, ..., P_m$ form a basis for $n \times n$ symmetric matrices ($m = n(n+1)/2$). The matrix P may be constructed from the x_i coefficients which solve (4.30) by setting $P = \sum_{i=1}^{m} x_i P_i$.

Lyapunov showed that (4.32) may be solved analytically by finding a solution of the linear equation system

$$A^T P + PA + I = 0 \tag{4.34}$$

Subsequent developments in the application of LMIs to control problems are summarized in Table 4.4 and described in greater detail in Boyd *et al.* (1994).

Table 4.4: Summary of important developments in the use of LMIs in Process Control.

Date	**Practical or theoretical devlopment**
1890	First LMI - solved analytically via Lyapunov equation.
1940s	Application to practical control problems - small LMIs, solved by hand.
1960s	Positive Real lemma provides graphical solution criteria for small LMIs.
1970s	Solution of LMIs in optimal quadratic control via algebraic Ricatti equations.
early 1980s	Solution of many LMIs in control system analysis by convex optimization.
late 1980s	Development of efficient interior-point algorithms for solving *any* LMIs.

4.3.4 Application of the Passivity Theorem to Robustness Analysis

Given the system shown in Figure 4.5 where G is a stable, LTI system and $\tilde{\Delta}$ is strictly passive, application of the passivity theorem (Desoer and Vidyasagar, 1975) shows that the system is robustly stable if G is stable and passive. Since G is LTI, this corresponds to the following frequency domain condition:

$$G(j\omega) + G(j\omega)^* \geq 0 \quad , \quad \forall \omega \in \Re \tag{4.35}$$

In order to test this condition, use is made of the Kalman-Yakubovich-Popov (KYP) lemma. This states that if G has a state-space realization (A_G, B_G, C_G, D_G), then the above condition is equivalent to testing for the existence of $P = P^T > 0$, such that the following Linear Matrix Inequality (LMI) is satisfied:

$$\begin{bmatrix} A_G^T P + PA_G & PB_G - C_G^T \\ B_G^T P - C_G & -(D_G + D_G^T) \end{bmatrix} \leq 0 \tag{4.36}$$

As is always the case with LMI constraints, the matrix to the left of the inequality is symmetric. The LMI given above may be converted into the standard form of (4.30) in a similar manner to that described for (4.32). More specifically, this involves selecting a basis $P_1, ..., P_m$ for symmetric matrices and then setting

$$F_0 = \begin{bmatrix} 0 & C_G^T \\ C_G & (D_G + D_G^T) \end{bmatrix} \quad \text{and} \quad F_i = - \begin{bmatrix} A_G^T P_i + P_i A_G & P_i B_G \\ B_G^T P_i & 0 \end{bmatrix} \tag{4.37}$$

The solution may then be constructed as before by setting $P = \sum_{i=1}^{m} x_i P_i$. The LMI feasibility problem may be solved efficiently using interior-point methods. Thus, given a realization of G, which is readily determined from that of M, the robust stability of the system is easily checked.

In the current form the passivity theorem only uses information on the magnitude of the uncertainty and does not exploit any additional information about Δ (or $\tilde{\Delta}$). The results may thus be conservative if Δ has, for example, any of the other properties given in Table 4.3. In order to exploit any such additional information, and thereby overcome this conservatism, use is made of stability multipliers. The basic idea is that instead of requiring G to be passive, a matrix W is sought such that WG is passive. Properties of the uncertainty are taken into account by requiring that $\tilde{\Delta}W$ be strictly passive. It should be noted that selecting $W = I$ is equivalent to the current robust stability condition in (4.35).

Use of multiplier theory to exploit information about the uncertainty

Balakrishnan *et al.* (1994) show, with the aid of multiplier theory (Desoer and Vidyasagar, 1975), that a tighter condition for the robust stability of the system in Figure 4.5 is that a stability multiplier $W(s)$ exists such that:

1. $W(j\omega) + W(j\omega)^* > 0\,, \quad \forall \omega \in \Re$ (W must be strictly passive).
2. $W(j\omega)^* \circ \tilde{\Delta}^* + \tilde{\Delta} \circ W(j\omega) > 0, \quad \forall \omega \in \Re$ ($\tilde{\Delta} \circ W$ must be strictly passive).
3. $W(j\omega)G(j\omega) + G(j\omega)^* W(j\omega)^* \geq 0, \quad \forall \omega \in \Re$ (WG must be passive).

The notation $\tilde{\Delta} \circ W(j\omega)$ in condition 2 above is used to refer to the composition operation, as $\tilde{\Delta}$ may be nonlinear or time-varying.

A further requirement on W, which is sometimes not explicitly stated, is that W must commute with every element of the perturbation matrix $\tilde{\Delta}$. This requirement is similar to

that used in the framework of the structured singular value where the scaling matrix D is required to be of the form in (4.23) so as to commute with the form of Δ in (4.16).

Now, by taking into account the properties of $\tilde{\Delta}$, condition 2 above may be converted to a direct constraint on W, to be used in conjunction with conditions 1 and 3 to test for robustness. Table 4.5 lists the extra conditions placed on the stability multiplier W for different types of model uncertainty (Balakrishnan *et al.*, 1995). For the cases listed where the uncertainty is structured it is assumed that the perturbations are SISO.

Table 4.5: Conditions on the stability multipliers for different forms of model uncertainty.

Structure	**Nature**	$\mathbf{W = diag\,(w_i)}$
unstructured	nonlinear	$w_i = 1$
diagonal	nonlinear	$w_i > 0\,, \quad w_i \in \Re$
diagonal	linear time-invariant	$w_i = w_i^*\,, \quad w_i \in C$
diagonal	real (parametric)	$w_i \in C$

A subtle point is that the set of allowable stability multipliers is infinite dimensional. In order to make the problem tractable, the search is restricted to a finite dimensional subspace, whereby a basis for the subspace is chosen and a vector of unknown coefficients θ effectively define W. The form of the basis depends on the commutivity requirements between W and $\tilde{\Delta}$ and the conditions in Table 4.5. It should be noted that the choice of a good basis, which introduces the least conservatism into the result, is still an active area of research (Balakrishnan *et al.*, 1995).

Having chosen a basis, the stability multiplier may be denoted by the state-space realization $(A_W, B_W, C_W(\theta), D_W(\theta))$, where $C_W(\theta)$ and $D_W(\theta)$ are linear functions of θ (Balakrishnan *et al.*, 1995). Similarly, the state-space realization of $W(s)G(s)$ is denoted as $(A_{WG}, B_{WG}, C_{WG}(\theta), D_{WG}(\theta))$.

Testing for robust stability now involves the simultaneous satisfaction of two LMIs pertaining to the requirements that W be strictly passive and that WG be passive. The requirement that $\tilde{\Delta}W$ be strictly passive is taken care of by the choice of the basis for W.

Using the KYP lemma, the condition for the strict passivity of W is equivalent to the following LMI in the matrix variable $P_1 = P_1^T$ and the vector θ:

$$\begin{bmatrix} A_W^T P_1 + P_1 A_W & P_1 B_W - C_W(\theta)^T \\ B_W^T P_1 - C_W(\theta) & -(D_W(\theta) + D_W^T(\theta)) \end{bmatrix} < 0 \tag{4.38}$$

Similarly, the condition for the passivity of WG is equivalent to the LMI in the search variables $P_2 = P_2^T$ and θ:

$$\begin{bmatrix} A_{WG}^T P_2 + P_2 A_{WG} & P_2 B_{WG} - C_{WG}(\theta)^T \\ B_{WG}^T P_2 - C_{WG}(\theta) & -(D_{WG}(\theta) + D_{WG}(\theta)^T) \end{bmatrix} \leq 0 \tag{4.39}$$

Robust stability requires the simultaneous satisfaction of both (4.38) and (4.39) using the search variables P_1, P_2 and θ. It should be noted that for the case $W = I$, the above two LMIs reduce to the LMI in (4.36).

An excellent illustration of the benefits of the passivity theorem approach to robust control is that the only difference between treating LTI and real uncertainty is the fact that the former requires W, and hence the elements comprising its basis, to be Hermitian ($W = W^*$). In contrast to this, the (equivalent) robust stability criterion developed in the framework of 'real-μ-analysis' is considerably more difficult to derive (Fan *et al.*, 1991) and the theory differs significantly from that used for LTI perturbations. However, in the passivity framework the only difference is in the properties of the multipliers used.

A further benefit of the passivity theorem framework is that *combinations* of nonlinear, LTI and parametric uncertainty may be treated in a unified setting by simply placing appropriate constraints on the stability multiplier. Furthermore, testing the resulting robust stability conditions is conveniently done by solving convex optimization problems involving LMIs. Reliable interior-point methods, such as the LMI Control Toolbox (Gahinet *et al.*, 1995), exist for this purpose.

4.3.5 Application to Robust Control Synthesis

The approach discussed above is very convenient for the purposes of robustness analysis where a given controller has been designed and its robustness is being tested. When considering the issue of controller synthesis, the problem is considerably more complicated. The reason is that the realization of G is now a function of the controller which we are seeking to find. The resulting matrix inequalities are thus bilinear and nonconvex. As a result, many of the computational benefits associated with this approach are lost. Therefore, while the passivity theorem is very useful for the purposes of robustness analysis, it is not as convenient for the purposes of controller synthesis, which is essentially what is required for dynamic operability assessment.

In the next section we introduce the ℓ_1 framework for robust control and compare it to the approaches discussed thus far. The mathematical convenience of the resulting criteria, the

discrete-time formulation and the fact that the uncertainty description may be more realistic for operability studies, make it well suited for incorporation into the Q-parametrization approach to dynamic operability assessment.

4.4 The ℓ_1 Framework for Robust Control

In this section a brief overview of the ℓ_1 robust control framework is provided. Only the issue of stability robustness is considered, as performance robustness may be treated in the same manner via the addition of fictitious perturbations.

As is the case with the structured singular value framework, ℓ_1 robust control makes use of the M-Δ closed-loop structure shown in Figure 4.4. The uncertainty weights and the nominal plant are restricted to be linear time-invariant (LTI) and the controller is assumed to be LTI. For a stabilizing controller this makes M LTI and stable. As mentioned earlier, M is linear in Q.

In ℓ_1 robust control the uncertainty Δ is assumed to be causal and belonging to the following class:

$$\mathcal{D}(NP) = \{\Delta = \text{diag}\,(\Delta_1, ..., \Delta_{NP}) \mid \|\Delta_i\|_{\ell_\infty\,-\,\text{ind}} \leq 1\} \tag{4.40}$$

where NP is the number of perturbation blocks and $\|\Delta_i\|_{\ell_\infty\,-\,\text{ind}}$ is the ℓ_∞-induced matrix norm (corresponding to bounded peak-to-peak behavior) given by:

$$\|\Delta_i\|_{\ell_\infty\,-\,\text{ind}} \equiv \sup_{p \neq 0} \frac{\|\Delta_i p\|_\infty}{\|p\|_\infty} \tag{4.41}$$

There is no requirement that Δ be LTI, and thus time-varying and/or nonlinear perturbations are allowed. This differs from the μ framework in which only LTI perturbations are allowed and where their magnitude is defined using the ℓ_2 -induced norm, corresponding to signals of bounded energy. As in the μ framework, Δ is allowed a block-diagonal structure to isolate the independent sources of model uncertainty and so reduce conservatism.

The physical significance of considering systems where the underlying signal norms are bounded in an ℓ_∞ sense lies in the fact that many process control problems have exogenous inputs which are persistent and continue acting on the system as long as it is in operation. Since these signals are persistent their ℓ_2 norm is infinite and they cannot be modelled as finite energy signals, as is required in the passivity theorem. Nevertheless, it is often possible to get an estimate on the maximum amplitude of these signals. The disturbance regime

considered in Chapter 3 and consisting of bounded step-like disturbances, fits into this category of signals. Practical examples include wind gusts in aircraft control, bumps caused by irregular road surfaces in automotive control and level fluctuations due to boiling liquid in level control. The ℓ_∞ signal norm is a natural choice for measuring the size of such signals. In the context of robust control, the perturbations present in the closed-loop act on the internal signals. Any process which is subject to persistent exogenous inputs will have persistent internal signals. Therefore a natural choice for defining the magnitude of the perturbations is in terms of the bounded $\ell_{\infty\text{-ind}}$ norm.

For notational convenience the nominal plant model is assumed to be a square transfer function matrix. In addition, each of the NP perturbations is assumed to be square, with the ith perturbation being of dimension $PS(i)$. This results in a square interconnection matrix of dimension $SM = \sum_{i=1}^{NP} PS(i)$.

The interconnection matrix M may be partitioned as:

$$M = \begin{bmatrix} M_{11} & \cdots & M_{1\,NP} \\ \vdots & & \vdots \\ M_{NP\,1} & \cdots & M_{NP\,NP} \end{bmatrix} \tag{4.42}$$

An important matrix in ℓ_1 robust control is the positive matrix M^+, defined as follows:

$$M^+ = \begin{bmatrix} \|M_{11}\|_{\ell_{\infty\text{-ind}}} & \cdots & \|M_{1\,NP}\|_{\ell_{\infty\text{-ind}}} \\ \vdots & & \vdots \\ \|M_{NP\,1}\|_{\ell_{\infty\text{-ind}}} & \cdots & \|M_{NP\,NP}\|_{\ell_{\infty\text{-ind}}} \end{bmatrix} \tag{4.43}$$

For discrete-time LTI systems, the $\ell_{\infty\text{-ind}}$ norm of a transfer matrix T may be defined as in (4.41) or equivalently as:

$$\|T\|_{\ell_{\infty\text{-ind}}} \equiv \max_i \sum_j \sum_k | T_{ij}(k) | \tag{4.44}$$

where $T_{ij}(k)$ is the kth pulse response coefficient of the (i,j) element of T.

Khammash and Pearson (1991) provide necessary and sufficient conditions for the robust stability of systems with bounded ℓ_∞ signal norms and nonlinear/time-varying uncertainty.

Theorem 5 *Given the interconnection matrix M subject to time-varying and/or nonlinear perturbations $\Delta \in \mathcal{D}(NP)$, the M-Δ closed-loop system is robustly stable if and only if any of the following equivalent conditions hold:*

1. $\rho(M^+) < 1$, where ρ denotes the spectral radius and corresponds to the magnitude of the largest eigenvalue of the positive matrix M^+.

2. $x \leq M^+ x$ and $x \geq 0$ imply that $x = 0$, where the vector inequalities are taken componentwise.

3. $\inf_R \|R^{-1}MR\|_{\ell_\infty - \text{ind}} < 1$, where R is a positive (real) scaling matrix of the form

$$R = \text{diag}\{r_1 I_{PS(1)}, ..., r_{NP} I_{PS(NP)}\} \quad , \quad r_i > 0 \,. \tag{4.45}$$

The above conditions provide simple and exact criteria for robust stability. They are necessary and sufficient irrespective of the number of perturbation blocks NP. This is contrasted with the structured singular value framework where the robust stability criteria are considerably more complicated and can only be calculated approximately for more than three perturbations.

Each of the robustness conditions in the above theorem has a particular advantage in a given context. The spectral radius is often easiest to compute, particularly when NP is large, in which case power methods may be used for efficient evaluation. The LMI condition on the other hand, provides information about the effect of individual entries of M^+ on robustness. Khammash and Pearson (1991) show how the LMI condition translates into NP algebraic conditions stated explicitly in terms of the elements of M^+. The third condition involves an optimally scaled matrix norm and is best suited when treating the robust synthesis problem. As dynamic operability assessment involves controller synthesis, this condition is used. Its advantages are that it is written directly in terms of M, and not M^+, and also extends conveniently as NP increases. This is in contrast to second condition where the NP algebraic conditions become considerably more complicated as NP increases. Finally, the third condition can be formulated into a set of differentiable constraints, the great majority of which are linear. Details of this are presented in a subsequent section.

4.5 Comparison of Alternative Robust Control Frameworks

Having presented a number of different frameworks for robustness analysis it is useful to discuss how they relate to each other and what their relative merits are in the context of dynamic operability assessment. The frameworks differ from each other with respect to the class of perturbations treated and the nature of the underlying signals. The passivity theorem with multipliers is quite general and is able to treat combinations of real, LTI and nonlinear/time-varying model uncertainty for systems where the underlying signals are of finite energy (ℓ_2-stable). The structured singular value is essentially a special case of this framework. The ℓ_1 approach, on the other hand, is best suited to systems with bounded peak

signals (ℓ_∞-stable) where the uncertainty is nonlinear time-varying (NLTV), nonlinear time-invariant (NLTI) or linear time-varying (LTV). Table 4.6 provides a comparison between three different robustness criteria and is useful to understand the suitability of a particular approach.

Table 4.6: Comparison between different robustness criteria

Perturbation class	$\mu(\mathbf{M}) < 1$	$\inf_{R\in\mathcal{R}}\|\|\mathbf{R}^{-1}\mathbf{MR}\|\|_{\ell_{2\text{-ind}}}$	$\rho(\mathbf{M}^+) < 1$
NLTV, bounded ℓ_2-gain	nec	nec and suff	suff
NLTV, bounded ℓ_∞-gain	nec	nec	nec and suff
NLTI, bounded ℓ_2-gain	nec	suff	suff
NLTI, bounded ℓ_∞-gain	nec	nec	nec and suff
LTV, bounded ℓ_2-gain	nec	nec and suff	suff
LTV, bounded ℓ_∞-gain	nec	nec	nec and suff
LTI, bounded ℓ_2-gain	nec and suff	suff	suff
LTI, bounded ℓ_∞-gain	nec and suff	suff	suff

In the table nec and suff mean necessary and sufficient respectively. It should be noted that the middle column in the table refers to the case of structured nonlinear or time-varying uncertainty with ℓ_2 signal norms, and is easily derived using the passivity theorem with multipliers. It is clear from the table that the ℓ_1 approach always provides (at least) sufficient conditions for robustness. Thus, it guarantees robustness even if the uncertainty is of a different nature to that which is assumed. This is particularly useful at the process design stage where little information regarding the nature of the model uncertainty may be available.

If, however, the model uncertainty is *known* to be linear time-invariant, then the structured singular value should be used. The results obtained using the ℓ_1 theory may then be conservative. However, since the purpose of this thesis is to use the theory for flowsheet screening at the design stage, the conservatism should not be problematic, provided the two approaches are consistent. At this stage it is an open question whether there exist examples in which the two approaches display extreme behavior (Dahleh and Khammash, 1993).

Another important aspect when considering the suitability of a particular robustness framework to dynamic operability assessment is the mathematical complexity of the robustness criteria. The robust stability criteria in both the μ framework and the passivity theorem framework are far more complicated than those using the ℓ_1 framework.

Boyd *et al.* (1990) illustrate how the Q-parametrization approach is able to assess performance limits in the presence of unstructured model LTI uncertainty. Even for the case of

unstructured LTI model uncertainty, the appropriate robust stability criterion is a bound on the maximum singular value of a matrix linear in Q. While this form of constraint is convex it is not linear and requires more sophisticated convex optimization techniques to treat it. If the uncertainty is structured then the appropriate robust stability criterion is a bound on the structured singular value of a matrix linear in Q. This constraint is nonconvex and is itself a complex optimization problem. For the robustness analysis problem it has been shown that significant computational benefits may be gained via convex approximations to μ using linear matrix inequalities. However, the problem of controller synthesis involves bilinear matrix inequalities which are nonconvex and considerably more complicated to solve. While much progress has been made in this regard, the issue of controller synthesis in the presence of structured model uncertainty still remains a challenging area of research. As yet, there are no approaches which are able to determine limits of achievable performance in the presence of structured LTI uncertainty.

It will be shown in the subsequent section that dynamic operability in the presence of unstructured ℓ_1 model uncertainty may be formulated as a convex quadratic programming problem and solved very efficiently. In the presence of structured uncertainty the problem is nonconvex but is still dealt with conveniently due to the relative simplicity of the robust stability constraints.

One further benefit of the ℓ_1 approach is that it is formulated naturally in the time-domain and can thus be incorporated into the discrete formulation currently used for dynamic operability assessment, the details of which are discussed next.

4.6 Incorporation of ℓ_1 Model Uncertainty into Q-Parametrization Framework for Dynamic Operability Assessment

When considering the performance limiting effect of model uncertainty on dynamic operability, the strategy adopted is to include the robust stability conditions as additional constraints in the optimization problem. The problem to be addressed is as follows:

> How does the requirement for robust stability limit the achievable performance of the nominal plant?

As mentioned earlier, the third robustness condition of Khammash and Pearson (1991) is best suited for incorporation into the dynamic operability assessment problem. From the

definition of the ℓ_∞-induced matrix norm (4.44) and the form of the scaling matrix R, the third robustness condition is equivalent to the following constraint:

$$\inf_R \left\{ \max_i \sum_{j=1}^{SM} \frac{r_{jpert}}{r_{ipert}} \sum_{k=0}^{L} |m_{ij}(k)| \right\} < 1 \quad , \quad r_i > 0 \tag{4.46}$$

where $m_{ij}(k)$ is the kth pulse response coefficient of the (i,j) element of the interconnection matrix and *ipert* and *jpert* refer to the sub-matrix $M_{ipert\ jpert}$ of M which contains the matrix element m_{ij}. Thus, given (i,j) one can uniquely determine $(ipert, jpert)$.

The above condition for robust stability is not directly suitable for implementation within the gradient-based scheme used for dynamic operability assessment. The key difficulties are that it is non-differentiable and is itself an optimization problem. The first step in converting (4.46) to a more manageable form involves including the r_i coefficients of the scaling matrix R as search variables together with Q.

By noting that $r_i > 0$, the constraint (4.46) may be transformed into an equivalent set of differentiable constraints by the addition of the non-negative search variables β_{ijk}, defined as follows:

$$-\beta_{ijk} \leq m_{ij}(k) \leq \beta_{ijk} \quad , \quad \beta_{ijk} \geq 0 \tag{4.47}$$

Since M is linear in Q, the constraints in (4.47) are linear in the search variables β and Q. While the inclusion of β increases the total number of search variables, it allows for the use of gradient-based optimization techniques and is consistent with other approaches involving ℓ_1-type constraints (Khammash and Pearson, 1991).

Dynamic operability assessment in the presence of structured ℓ_1 model uncertainty may now be posed as the following nonconvex optimization problem:

$$\begin{aligned} &\min_{Q,r,\beta} \Phi \\ &\text{subject to} \\ s_{\min} &\leq s(Q) \leq s_{\max} \\ m_{ij}(k) - \beta_{ijk} &\leq 0 \\ m_{ij}(k) + \beta_{ijk} &\geq 0 \\ \sum_{j=1}^{SM} \frac{r_{jpert}}{r_{ipert}} \sum_{k=0}^{L} \beta_{ijk} &< 1 \qquad \forall i = 1, ..., SM \\ r_i &> 0 \\ \beta_{ijk} &\geq 0 \end{aligned} \tag{4.48}$$

where $s_{\min}$ and $s_{\max}$ are the respective lower and upper bounds on the deviational responses of the outputs and inputs, contained in the composite vector $s(Q)$. The measure of nominal

performance Φ would typically be one of the objective functions used in Chapter 3.

The robust stability constraints contained in (4.48) guarantee the satisfaction of (4.46). It should also be noted that the optimization of Φ will, if necessary, force β_{ijk} to be a tight bound on $|m_{ij}(k)|$. Thus, no conservatism is introduced by (4.47).

The nonconvexity in the above problem is introduced by the scaling factors r, which are only needed if the uncertainty is structured. Unstructured uncertainty corresponds to a single (full) perturbation block, for which no scaling factors are needed. Dynamic operability assessment in the presence of unstructured uncertainty then involves the solution of the following convex quadratic programming problem:

$$\begin{aligned}
& \min_{Q,\beta} \Phi \\
& \text{subject to} \\
s_{\min} \;\leq\; & s(Q) \;\leq s_{\max} \\
m_{ij}(k) - \beta_{ijk} \;\leq\; & 0 \\
m_{ij}(k) + \beta_{ijk} \;\geq\; & 0 \\
\sum_{j=1}^{SM} \sum_{k=0}^{L} \beta_{ijk} \;<\; & 1 \qquad \forall i = 1, ..., SM \\
\beta_{ijk} \;\geq\; & 0
\end{aligned} \tag{4.49}$$

By exploiting the sparsity of the above constraint system and the fact that only the Q variables are involved in the objective function, it is possible to solve the dynamic operability assessment problem efficiently in the presence of unstructured model uncertainty, or when the scales are fixed.

Solving the general problem (4.48) is complicated by the nonconvexity. A hybrid solution strategy is adopted whereby the search-space associated with the positive scaling factors is firstly discretized and convex QPs are solved at each point in the grid. Once an approximate location of the optimal scaling factors is found in this manner, (4.48) is solved as a sparse nonlinear programming problem. Experience thus far has shown this to be a reliable approach (Ross and Swartz, 1997a). More sophisticated solution techniques involving global optimization theory and parametric quadratic programming are recommended for future research. Chapter 5 describes in more detail how the mathematical features of the above problem have been exploited to reduce computational time.

4.6.1 Including Economic Considerations

Including the robust stability constraints into the economic formulation of Chapter 3 is straightforward and involves the solution of the following optimization problem:

$$\begin{aligned}
&\min_{y_{ss},Q,r,\beta_{ijk}} \Psi(y_{ss}, d_b^N) \qquad (4.50)\\
&\text{s.t.}\\
&\begin{bmatrix} y_\ell \\ u_\ell \end{bmatrix} \le S(y_{ss}, Q, d_b, \Delta d) \le \begin{bmatrix} y_u \\ u_u \end{bmatrix} \qquad \forall\, (d_b, \Delta d) \in \Gamma_C\\
&\sum_{c=1}^{2}\sum_{i=1}^{n_y}\sum_{k=0}^{L} W_{ic}(k)\,[s_{ic}(k)]^2 \le \gamma\\
&m_{ij}(k) - \beta_{ijk} \le 0\\
&m_{ij}(k) + \beta_{ijk} \le 0\\
&\sum_{j=1}^{SM} \frac{r_{jpert}}{r_{ipert}} \sum_{k=0}^{L} \beta_{ijk} < 1 \qquad \forall i = 1, ..., SM\\
&r_i > 0\\
&\beta_{ijk} \ge 0
\end{aligned}$$

In the above y_ℓ and y_u are the lower and upper bounds on the actual output response and u_l and u_u pertain to the actual input response, both of which are contained in $S(y_{ss}, Q, d_b, \Delta d)$. As was the case in Chapter 3, only the regulatory problem is considered. This problem is nonconvex either if the economic objective $\Psi(y_{ss}, d_b^N)$ is nonconvex, or if the uncertainty is structured and the scaling factors r are required.

4.7 Application Example

4.7.1 Multivariable Distillation Column Control

The multivariable distillation column studied in Chapter 3 is revisited, with the performance-limiting effect of model uncertainty included into the analysis. The outputs to be controlled are the overhead ethanol mole fraction (y_1) and a bottom tray temperature (y_2 in °C). The manipulated inputs are the reflux flowrate (u_1 in gpm) and the reboiler steam pressure (u_2 in psig). The nominal plant model $\tilde{P}$ has the following transfer matrix description:

$$\tilde{P}_1(s) = \begin{bmatrix} \dfrac{0.66\,e^{-6\,s}}{(6.7\,s+1)} & \dfrac{-0.005}{(9.06\,s+1)} \\ \dfrac{-34.7\,e^{-4\,s}}{(8.15\,s+1)} & \dfrac{0.87\,(11.6\,s+1)e^{-2\,s}}{(3.9\,s+1)\,(18.8\,s+1)} \end{bmatrix} \qquad (4.51)$$

As was the case in Chapter 3, the study investigates how the distribution of time delays within the transfer matrix affects dynamic operability. To this end the following alternative delay structures are considered:

$$B_1 = \begin{bmatrix} 6 & 0 \\ 4 & 2 \end{bmatrix}, \; B_3 = \begin{bmatrix} 6 & 5 \\ 4 & 2 \end{bmatrix} \text{ and } B_5 = \begin{bmatrix} 6 & 6 \\ 6 & 2 \end{bmatrix}. \tag{4.52}$$

The problem to be addressed is as follows:

> How does the requirement for robust stability in the presence of multiplicative input uncertainty limit the achievable nominal performance of each process?

The multiplicative input uncertainty weight W_I is assumed to be the same for each process and of the form:

$$W_I = w_I\, I = \frac{0.2\,(5s+1)}{(0.5\,s+1)}\, I \tag{4.53}$$

This form of uncertainty weight corresponds to a relative input uncertainty of 0.2 at low frequencies, which increases to a value of 1 at $\omega \approx 1\text{min}^{-1}$. The increase with frequency allows for a time-delay of about 1 minute and can thus represent the effect of unmodelled (actuator) dynamics (Skogestad and Morari, 1987).

As the inputs are independent of each other, Δ has a diagonal structure with two perturbations, each relating to a particular input. For illustrative purposes, the achievable performance in the presence of totally unstructured model uncertainty (Δ full) is compared with that achievable in the presence of structured uncertainty (Δ diagonal). Using the notation introduced in the previous section, for unstructured uncertainty $NP = 1$ and $PS(1) = 2$; whereas for structured uncertainty $NP = 2$ and $PS(i) = 1$ for $i = 1, 2$.

In terms of the M-Δ framework, $M = w_I Q \tilde{P}$ and has pulse response coefficients given by:

$$m_{ij}(k) = \sum_{\ell=1}^{n_y} \sum_{r=0}^{k} \sum_{io=r}^{k} q_{i\ell}(r)\, \tilde{P}_{\ell j}(io - r)\, w_I(k - io) \tag{4.54}$$

As mentioned earlier, M is linear in Q, which would not be true of the classical controller K. The linearity of M in Q dramatically simplifies matters and is a significant benefit of using the Q-parametrization framework.

The objective function chosen as a measure of closed-loop performance is as in Chapter 3 and involves the weighted sum-of-square errors (SSE) of the outputs to steps of -0.035 and $+3$ applied individually to the setpoints of y_1 and y_2 respectively. The weighting matrix W

in the objective function is as before. The problem is discretized at a sampling interval of $\Delta t = 0.5$ minutes and a time horizon of $L = 100$ sampling periods is used. The following bounds are placed on the deviational input responses

$$\begin{aligned} -0.112 &\leq u_1 \leq 0.065\,\text{gpm} \\ -4.4 &\leq u_2 \leq 14.0\ \text{psig} \end{aligned} \tag{4.55}$$

The robust stability constraints are as in (4.48), with the pulse responses coefficients of M being given by (4.54).

The results of the dynamic operability assessment are shown in Table 4.7. Since a smaller weighted SSE corresponds to better dynamic operability, it is seen that:

1. The presence of model uncertainty and the requirement for robust stability limits the achievable nominal closed-loop performance.
2. The structure of the model uncertainty plays a significant role in determining the sensitivity of a plant to model uncertainty.
3. Delay structure B_5 has significantly better performance in the presence of unstructured uncertainty than the other two plants.
4. Both B_3 and B_5 are superior to B_1, with and without model uncertainty. In fact, B_5 with unstructured uncertainty has dynamic operability comparable to B_1 in the absence of model uncertainty.

Table 4.7: Minimum achievable weighted SSE for the alternative delay structures considered.

	No uncertainty	**Structured uncertainty**	**Unstructured uncertainty**
B_1	117.8	128.5	175.8
B_3	98.0	104.2	147.2
B_5	96.8	103.3	121.1

Global optimality for structured uncertainty

The results for structured uncertainty were obtained using the hybrid solution strategy discussed earlier. A log scale was used to efficiently sweep over a large range of positive real

numbers and convex QPs were solved at each point in the grid. Thereafter, the solution was refined using sparse nonlinear programming on (4.48).

Only the ratios of the scaling factors are important and therefore one can set $r_1 = 1$. Figures 4.6, 4.7 and 4.8 show how the optimal achievable weighted SSE varies with r_2 for delay structures B_1, B_3 and B_5 respectively. It should be noted that if $r_2 = 1$, the weighted SSE is as for the case of unstructured model uncertainty.

While the behavior shown in the figures is clearly nonconvex, obtaining the global minimum was straightforward. Despite the nonconvexity, only Figure 4.6 displays multiple local minima at $r_2 = 109$ and as $r_2 \to \infty$. Attempting to solve (4.48) directly using sparse nonlinear programming and using $r_1 = r_2 = 1$ as an initial guess for the scaling factors yielded the same solutions, for each delay structure, as those obtained using the hybrid approach. This is most likely due to the monotonic decrease of the SSE toward the global optimum, with an increase in r_2. In general though, solving (4.48) directly using sparse nonlinear programming will not guarantee global optimality. The hybrid solution strategy provides more confidence in the result but involves greater computation overall.

In Figures 4.7 and 4.8 the optimal SSE occurs as $r_2 \to \infty$. However, after $r_2 = 10^5$ there is very little decrease in the objective. For example, for delay structure B_5, at $r_2 = 10^5$ the SSE is 51.6508 whereas the SSE at $r_2 = 10^{25}$ is 51.6503. It should be noted that having a local minimum as $r_2 \to \infty$ is not uncommon for problems involving scaling factors. This may be seen by noting that the requirement in (4.46) is equivalent to:

$$\begin{aligned} & \inf_R \left\{ \max_i \sum_{j=1}^{SM} \frac{r_{jpert}}{r_{ipert}} \sum_{k=0}^{L} |m_{ij}(k)| \right\} \qquad (4.56) \\ = & \inf_R \left\{ \max_i \sum_{j=1}^{SM} \frac{r_{jpert}}{r_{ipert}} m_{ij}^+ \right\} \\ = & \inf_R \left\{ \max_i \sum_{j=1}^{SM} \left[R^{-1} M^+ R \right]_{ij} \right\} \end{aligned}$$

where $[R^{-1}M^+R]_{ij}$ is the (i,j) element of the matrix $R^{-1}M^+R$. Therefore, the robust stability condition in (4.46) corresponds to a constraint on the optimally scaled row sum of M^+.

Consider now a positive matrix M^+ of the form:

$$M^+ = \begin{bmatrix} 1 & 0 \\ 5 & 1 \end{bmatrix} \qquad (4.57)$$

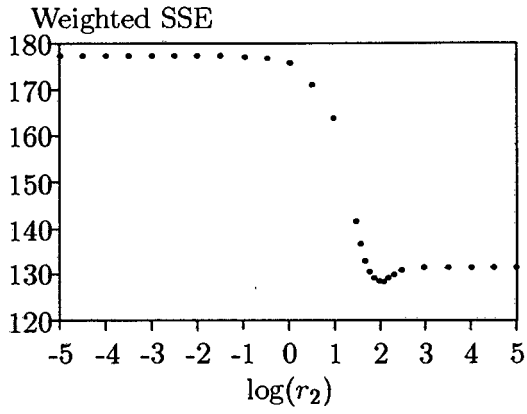

Figure 4.6: Variation of optimal weighted SSE with scaling factor r_2 for delay structure B_1.

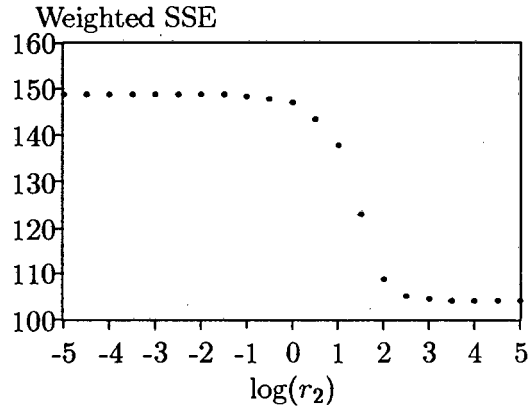

Figure 4.7: Variation of optimal weighted SSE with scaling factor r_2 for delay structure B_3.

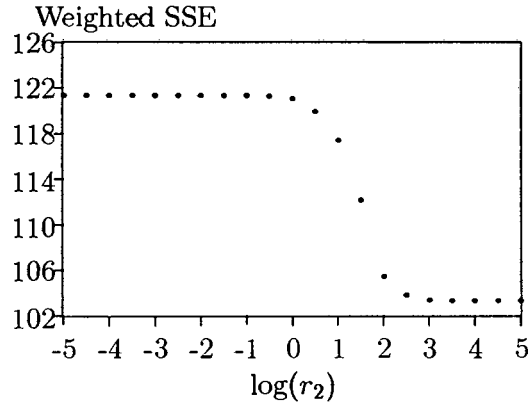

Figure 4.8: Variation of optimal weighted SSE with scaling factor r_2 for delay structure B_5.

The matrix $R^{-1}M^{+}R$ is given by:

$$R^{-1}M^{+}R = \begin{bmatrix} m_{11}^{+} & \frac{r_2}{r_1}m_{12}^{+} \\ \frac{r_1}{r_2}m_{21}^{+} & m_{22}^{+} \end{bmatrix} \tag{4.58}$$

In order to minimize the row sums of $R^{-1}M^{+}R$, the optimal scaling factor R is given by R =diag$(1, \infty)$.

Returning to the example problem; the fact that all the delay structures are likely to have optimal values for r_2 which are well in excess of unity may be understood as follows. The M^{+} matrices, determined from the optimal Q in the absence of model uncertainty, take the form:

$$M_1^{+} = \begin{bmatrix} 0.774 & 0.008 \\ 94.90 & 1.613 \end{bmatrix}, \; M_3^{+} = \begin{bmatrix} 0.801 & 0.009 \\ 86.97 & 1.682 \end{bmatrix}, \; M_5^{+} = \begin{bmatrix} 0.608 & 0.010 \\ 76.85 & 1.883 \end{bmatrix} \tag{4.59}$$

In the above, the subscripts refer to the delay structure in consideration. In the ideal case, where structured model uncertainty does not limit the achievable nominal control performance, the optimally scaled row sums would be less than unity. However, since m_{22}^{+} is larger than unity for all three cases above, the controller has to be detuned in order to achieve robustness to structured uncertainty. Despite this, it is illustrative to determine the optimal scaling factors for the M^{+} matrices in (4.59), as these give an indication of the likely magnitudes of the optimal scaling factors for the detuned controller.

The Perron-Frobenius theory for nonnegative matrices states that the scaling factors R which minimize the row sums of $R^{-1}M^{+}R$ correspond to the positive eigenvector associated with the largest eigenvalue of M^{+} (Dahleh and Khammash, 1993). As an example, for delay structure B_1 this corresponds to choosing R =diag$(0.006, 1)$. The resulting scaled matrix is as follows:

$$R^{-1}M^{+}R = \begin{bmatrix} 0.7744 & 1.4073 \\ 0.5688 & 1.6129 \end{bmatrix} \tag{4.60}$$

The ratio of the scaling factors is what is of importance. Thus, if r_1 is set to one, this corresponds to $r_2 = 166.8$, which is significantly larger than one. An interesting point is that the row sums in (4.60) are equal (to 2.182), which is a feature of such scaling problems (Dahleh and Khammash, 1993).

Computational issues

Due to the introduction of the search variables β into the problem formulation there is a significant degree of sparsity in the constraint system. Chapter 5 provides details on how this

is exploited with the aid of sparse solvers. The aim here is to demonstrate the improvements in computational efficiency that are achievable through the use of sparse solvers when solving the unstructured uncertainty problem in (4.49). The computation time required to solve the structured uncertainty problem directly with a sparse nonlinear programming routine is also reported.

The results are summarized in Table 4.8 and apply to delay structure B_1. In the presence of unstructured uncertainty, the problem was solved using LSSOL (Gill *et al.*, 1986) and SQOPT (Gill, 1996). LSSOL treats the constraint system as being dense, whereas SQOPT is able to exploit its sparsity. The structured uncertainty problem was solved using MINOS (Murtagh and Saunders, 1983), with an initial guess of $r_1 = r_2 = 1$ being chosen for the scaling factors.

From the results it is clear that the benefits of exploiting the sparsity are very significant. It should be noted that MINOS also exploits the problem sparsity, allowing for a rapid solution despite the problem being nonlinearly constrained.

Table 4.8: Comparison of computation times for the treatment of both unstructured and structured model uncertainty for delay structure B_1.

	Unstructured uncertainty	**Unstructured uncertainty**	**Structured uncertainty**
Software	LSSOL	SQOPT	MINOS
Search space dimension	800	800	800
Double precision workspace	1 294 412	539 028	523 673
Integer workspace	800	878 825	N/A
Solution time (sec)	4 560	160	240
SSE objective	175.8	175.8	128.5

Exploring the system behavior subject to unstructured uncertainty

A particularly interesting feature of the results in Table 4.7 is the fact that delay structure B_5 has significantly better dynamic operability in the presence of unstructured uncertainty than B_1 and B_3. In order to explore this further we start by considering the form of the positive matrix M^+ for each delay structure in the absence of model uncertainty, as given in (4.59).

For robust stability in the presence of unstructured uncertainty each row sum in (4.59) is

required to be less than one. From (4.59) it is clear that none of the delay structures are robustly stable using the controllers determined in the absence of model uncertainty.

In Chapter 5 it will be shown that the robust stability constraint on the ith row sum effectively constrains the behavior of the ith input (to both of the setpoint changes). Therefore, it is seen from (4.59) that, in order to achieve robustness, the input action of u_2 needs to be modified considerably.

The resulting M^+ matrices, determined from the Q which optimizes (4.49) in the presence of unstructured uncertainty, are as follows:

$$M_1^+ = \begin{bmatrix} 0.9783 & 0.0216 \\ 0.4328 & 0.5671 \end{bmatrix}, \; M_3^+ = \begin{bmatrix} 0.9762 & 0.0237 \\ 0.4206 & 0.5793 \end{bmatrix}, \; M_5^+ = \begin{bmatrix} 0.7385 & 0.0164 \\ 0.2009 & 0.7990 \end{bmatrix} \tag{4.61}$$

Robust stability requires each row sum to be *smaller* than one. As most optimization software cannot deal with strict inequality constraints, an upper bound of 0.9999 on the SM robust stability constraints has been chosen in solving the problem in (4.49).

It can be seen from (4.61), that both row sums for M_1^+ and M_3^+ are now active at their upper bounds. The robustness requirement thus directly constrains the behavior of u_1 and u_2 for these delay structures. By comparing the form of the M^+ matrices in (4.59) and (4.61) it is clear that the input power is shifted from u_2 to u_1 in order to make up for the significant restriction imposed on u_2 by the requirement for robust stability. In contrast to this, only the second row sum constraint is active for M_5^+ in (4.61). This implies that the input action of u_1 is directly constrained only by the input constraint in (4.55). Moreover, the impact of the input constraint on dynamic operability is expected not to be too severe, as it was seen in Chapter 3 that B_5 is able to achieve good closed-loop performance despite the presence of input constraints.

Figures 4.9, 4.10 and 4.11 show the behavior of u_2 with and without model uncertainty. The difference in input trajectories results from the controller being detuned to satisfy the robust stability condition. Intuitively, one would expect that the less sensitive a process is to model uncertainty, the less the input trajectories would differ from those for the perfect model case.

In the presence of unstructured uncertainty the response of u_2 to a step in $y_{set\,2}$ needs to be altered to a much lesser extent for B_5 than for the other delay structures. This, together with the fact that u_1 is not directly restricted by the robustness requirement, illustrates why B_5 has significantly better dynamic operability in the presence of unstructured uncertainty.

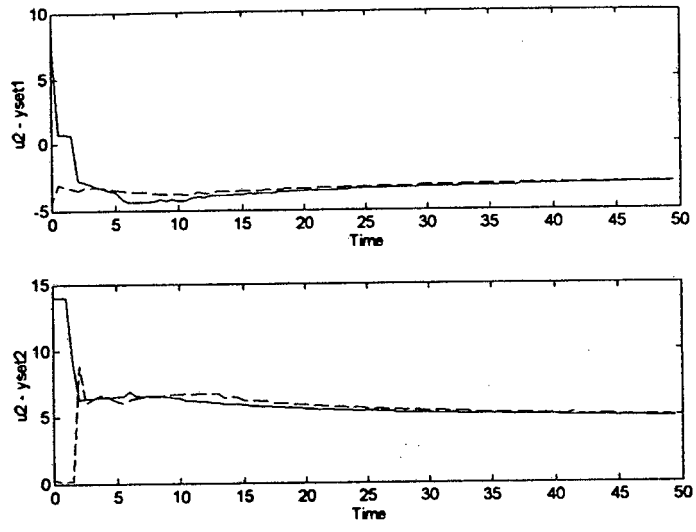

Figure 4.9: Optimal input trajectories of u_2 for delay structure B_1 in the presence of no uncertainty (-) and unstructured uncertainty (--). Figure (a) refers to the setpoint change in $y_{set\,1}$ and (b) refers to the change in $y_{set\,2}$.

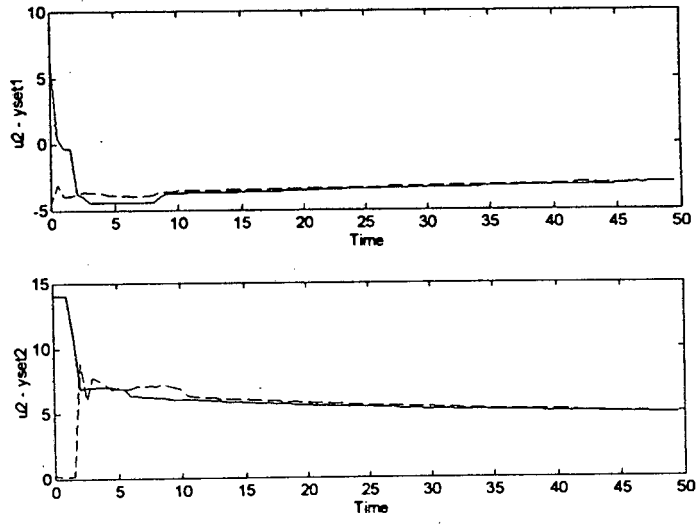

Figure 4.10: Optimal input trajectories of u_2 for delay structure B_3 in the presence of no uncertainty (-) and unstructured uncertainty (--). Figure (a) refers to the setpoint change in $y_{set\,1}$ and (b) refers to the change in $y_{set\,2}$.

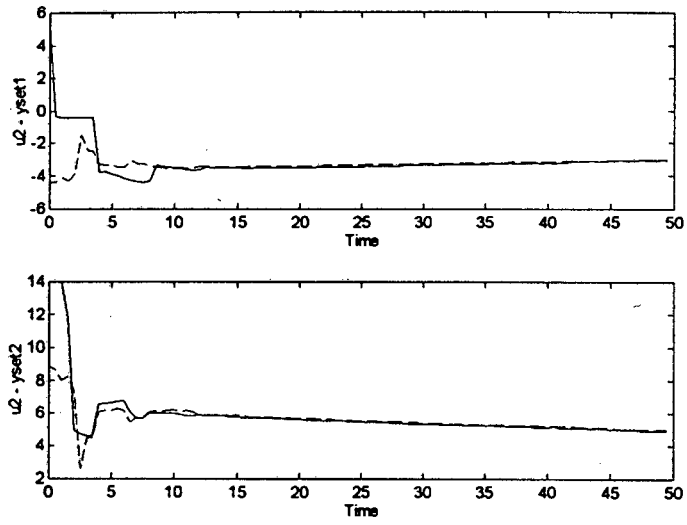

Figure 4.11: Optimal input trajectories of u_2 for delay structure B_5 in the presence of no uncertainty (-) and unstructured uncertainty (--). Figure (a) refers to the setpoint change in $y_{set\,1}$ and (b) refers to the change in $y_{set\,2}$.

Chapter 5

Formulation and Computational Issues

In Chapter 3, the basic Q-parametrization approach was outlined and its application to assessing dynamic operability in the absence of model uncertainty was presented. Chapter 4 dealt with the inclusion of model uncertainty into the formulation. In this chapter, various computational issues pertaining to these problem formulations are discussed. It will be shown how important mathematical features such as the problem structure and sparsity may be exploited to enable rapid solution of the resulting optimization problems.

In the absence of model uncertainty it is possible to transform the problem into an optimal control type problem where the goal is to seek an optimal input directly as opposed to seeking an optimal Q. The computational and theoretical implications of this are presented and discussed. Using this open-loop approach, the possible benefits of nonlinear control when treating a range of disturbances are made evident. In addition to this, the open-loop approach enables a new measure of dynamic operability, based on the maximum tolerable disturbance range, to be determined in a convenient manner.

In the presence of model uncertainty it is no longer possible to use an open-loop approach. Details of the problem structure are explored so as to allow greater insight into the effect of uncertainty on achievable performance. It is shown how the problem sparsity may be exploited in order to reduce computational time.

The computational benefits mentioned above are all achieved without any loss in accuracy. Further reductions in computational time may be achieved by developing approximate so-

lutions. One such method involves the use of a multi-rate problem formulation. In this method, small sampling periods are used initially when most of the dynamic fluctuations occur. After the majority of these transients decay, the sampling time is increased. This idea is only applied in the absence of model uncertainty and the computational benefits are explored via illustrative examples. Possible multi-rate formulations in the presence of model uncertainty are discussed briefly.

5.1 Standard Regulatory And Servo Problems

In this section, standard regulatory and servo problems are considered in the absence of model uncertainty. The treatment of a range of disturbances and the inclusion of model uncertainty are discussed in subsequent sections. An open-loop formulation to dynamic operability assessment is introduced and its computational benefits are illustrated.

5.1.1 Two-Degree-of-Freedom Controllers

Problems where both regulatory and servo control performance are important are best handled using a two-degree-of-freedom controller as shown in Figure 5.1. If performance specifications are to be placed on both y' and u, then the vectors z, w, y and u in the general feedback structure are given by:

$$z = \begin{bmatrix} y' \\ u \end{bmatrix} \quad , \quad w = \begin{bmatrix} y_{set} \\ d \end{bmatrix} \quad , \quad y = \begin{bmatrix} y_{set} \\ y' \end{bmatrix} \quad \text{and} \quad u = [u] \, . \tag{5.1}$$

The transformation of the classical control framework into the general feedback control framework is shown in Figure 5.2. The resulting matrix P is given by:

$$\left[\begin{array}{c} y' \\ u \\ \hline y_{set} \\ y' \end{array}\right] = \left[\begin{array}{cc|c} 0 & G_D & G_P \\ 0 & 0 & I \\ \hline I & 0 & 0 \\ 0 & G_D & G_P \end{array}\right] \left[\begin{array}{c} y_{set} \\ d \\ \hline u \end{array}\right] \tag{5.2}$$

where G_D and G_P refer to the disturbance and process transfer functions respectively.

The processes considered in this thesis are open-loop stable and therefore the T_i matrices in the Q-parametrization framework are as follows:

$$T_1 = \begin{bmatrix} 0 & G_D \\ 0 & 0 \end{bmatrix} \quad , \quad T_2 = -\begin{bmatrix} G_P \\ I \end{bmatrix} \quad \text{and} \quad T_3 = \begin{bmatrix} I & 0 \\ 0 & G_D \end{bmatrix} \tag{5.3}$$

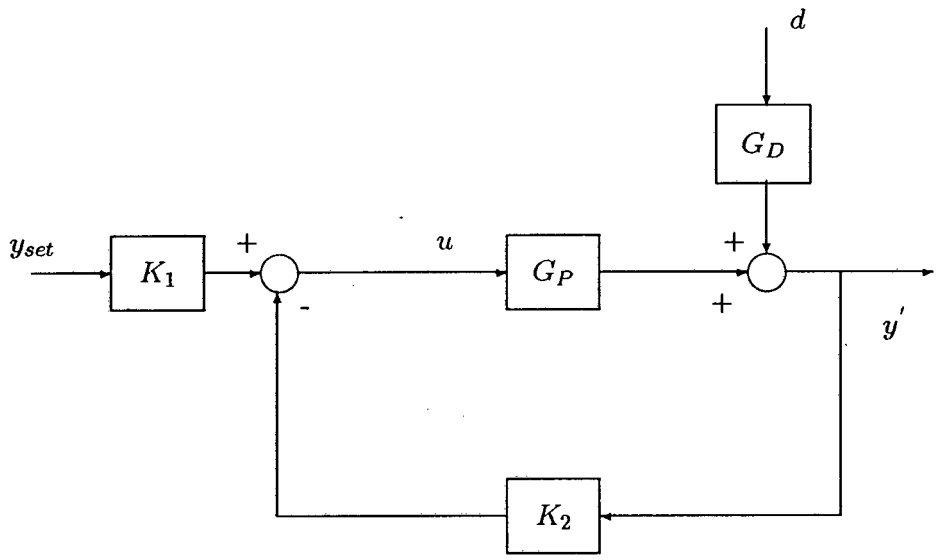

Figure 5.1: A two-degree-of-freedom controller in the clssical feedback structure.

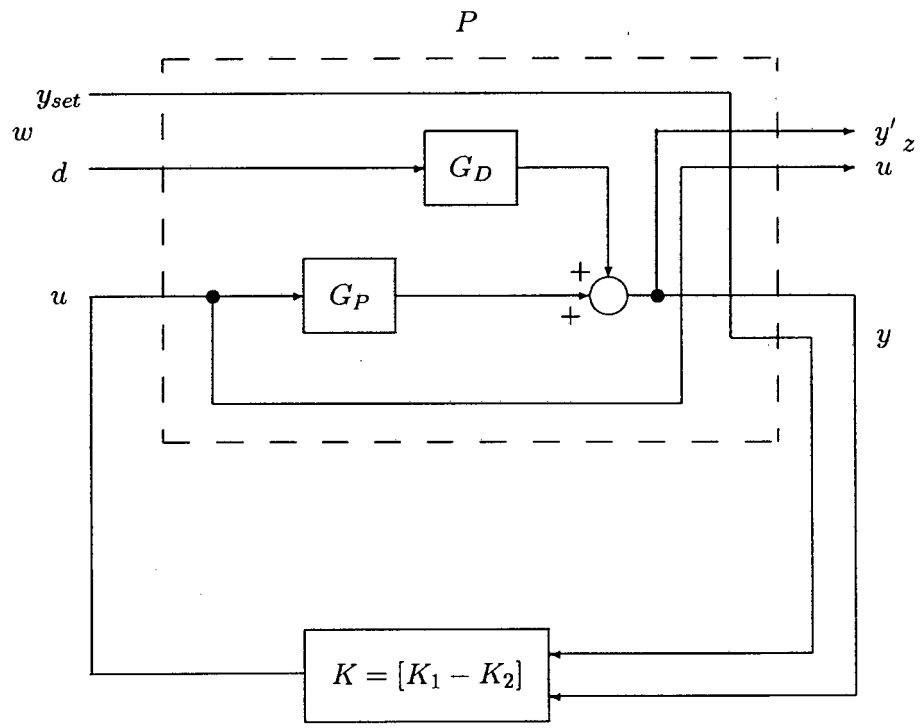

Figure 5.2: Transformation between the two-degree-of-freedom control structure and the general feedback structure used by Boyd and coworkers.

The closed-loop matrix H_{zw} thus takes the form:

$$\begin{aligned} H_{zw} &= T_1 + T_2 Q T_3 \qquad (5.4) \\ &= \begin{bmatrix} 0 & G_D \\ 0 & 0 \end{bmatrix} - \begin{bmatrix} G_P \\ I \end{bmatrix} \begin{bmatrix} Q_1 & Q_2 \end{bmatrix} \begin{bmatrix} I & 0 \\ 0 & G_D \end{bmatrix} \\ &= \begin{bmatrix} -G_P Q_1 & G_D - G_P Q_2 G_D \\ -Q_1 & -Q_2 G_D \end{bmatrix} \qquad (5.5) \end{aligned}$$

where $Q = \begin{bmatrix} Q_1 & Q_2 \end{bmatrix}$. If the setpoint changes are not made simultaneously with the disturbances, then the problem is separable. Two sub-problems may be solved *independently* whereby Q_1 is determined for good servo control performance and Q_2 for good regulatory control performance (Tebbutt, 1991). As a result, problems involving two-degree-of-freedom controllers will not be considered further. Attention will rather be given to solving the individual regulatory and servo control problems.

5.1.2 Standard Regulatory Control Problems

Basic problem formulation

In Chapter 3 it was shown that for regulatory problems, in the absence of model uncertainty, dynamic operability assessment may be posed as the following convex quadratic programming problem:

$$\begin{aligned} &\min_{Q} \quad \Phi = \sum_{j=1}^{n_w} \sum_{i=1}^{n_y} \sum_{k=0}^{L} W_{ij}(k) \left[s_{ij}(k) \right]^2 \qquad (5.6) \\ &\text{subject to} \\ s_{\min} \;&\leq\; s(Q, \Delta d) \leq s_{\max} \end{aligned}$$

In the above, the step response coefficients $s_{ij}(k)$ are arranged in the composite vector $s(Q)$ with the input responses following those of the outputs:

$$s(Q) = \left[s_{11}^T, ..., s_{n_y 1}^T, ..., s_{n_y n_w}^T, s_{(n_y+1)1}^T, ..., s_{(n_y+n_u)1}^T, ..., s_{(n_y+n_u)n_w}^T \right]^T \qquad (5.7)$$

where $s_{ij}^T = [s_{ij}(0), ..., s_{ij}(L)]$, is the response of the ith component of z to a step in the jth component of w. The reference signal vector is omitted in the above formulation since pure regulatory problems are being considered. For notational convenience, it is assumed that only one disturbance is acting on the system and thus $n_w = n_d = 1$. In light of this fact, the subscript j in the notation s_{ij} is dropped. Since performance specifications are to be placed on both the inputs and the outputs, the dimension of the set of regulated variables, z, is given by $n_z = n_y + n_u$.

Matrix representation of objective and constraints Much of the work is this chapter will rely on a different problem representation to that given in (5.6). The shorthand representation used in (5.6) does not capture certain aspects of the problem, such as its structure and sparsity. To this end, a matrix representation of the constraint system and objective function is developed in this subsection.

In Appendix A.2 it is shown that the output step response coefficient ($s_i(i_o)$ for $i \leq n_y$), at time increment i_o of the ith component of z to a step of size d in the disturbance is a linear expression in Q and takes the form:

$$s_i(i_o) = d\sum_{k=0}^{i_o} G_{D\,i}(k) - d\sum_{m=1}^{n_y}\sum_{n=1}^{n_u}\sum_{k=0}^{i_o} q_{nm}(k)\sum_{v=k}^{i_o}\sum_{\ell=k}^{v} G_{D\,m}(\ell-k)\,G_{P\,in}(v-\ell) \tag{5.8}$$

where $G_{D\,i}$ refers to the ith element of the vector G_D and $G_{P\,in}$ is the (i,n) element of G_P.

In a similar manner, the expression for the input response ($i > n_y$) is given by:

$$s_i(i_o) = -d\sum_{m=1}^{n_y}\sum_{k=0}^{i_o} q_{(i-n_y)m}(k)\sum_{v=k}^{i_o} G_{D\,m}(v-k) \tag{5.9}$$

The linear system given by the step responses of (5.8) and (5.9) may be compactly represented via the following matrix equation:

$$s = A\,q + b \tag{5.10}$$

where s is partitioned as in (5.7). For future reference, the matrix A is written in the form:

$$A = d\begin{bmatrix} A_{\text{out}} \\ A_{\text{inp}} \end{bmatrix} \tag{5.11}$$

and the vector b is written as:

$$b = d\begin{bmatrix} b_{\text{out}} \\ 0 \end{bmatrix} \quad . \tag{5.12}$$

The search variables q are arranged in vector form as follows:

$$q = \left[q_{11}^T, \ldots, q_{n_u 1}^T, \ldots, q_{1n_y}^T, \ldots, q_{n_u n_y}^T\right]^T \quad \text{where} \quad q_{ij}^T = [q_{ij}(0), \ldots, q_{ij}(L)]. \tag{5.13}$$

Appendix A.3 provides greater details on the form of the matrices A_{out}, A_{inp} and the vector b_{out}. For the case of a SISO process with one disturbance acting, A_{out} is a lower triangular Toeplitz matrix of the form:

$$A_{\text{out}} = -\begin{bmatrix} g_d(0)\,g_p(0) & 0 & \cdots & \cdots & 0 \\ \sum_{v=0}^{1}\sum_{\ell=0}^{v} g_d(\ell)\,g_p(v-\ell) & g_d(0)\,g_p(0) & & & \vdots \\ \vdots & & & \ddots & \vdots \\ \vdots & & & & 0 \\ \sum_{v=0}^{L}\sum_{\ell=0}^{v} g_d(\ell)\,g_p(v-\ell) & \sum_{v=0}^{L-1}\sum_{\ell=0}^{v} g_d(\ell)\,g_p(v-\ell) & \cdots & \cdots & g_d(0)\,g_p(0) \end{bmatrix} \tag{5.14}$$

Similarly, A_{inp} is given by:

$$A_{\text{inp}} = -\begin{bmatrix} g_d(0) & 0 & \cdots & \cdots & 0 \\ g_d(0)+g_d(1) & g_d(0) & & & \vdots \\ \vdots & & \ddots & & \vdots \\ \vdots & & & \ddots & 0 \\ \sum_{v=0}^{L} g_d(v) & \sum_{v=0}^{L-1} g_d(v) & \cdots & \cdots & g_d(0) \end{bmatrix} \tag{5.15}$$

The vector b_{out} takes the form:

$$b_{\text{out}} = \begin{bmatrix} g_d(0) \\ g_d(0)+g_d(1) \\ \vdots \\ \sum_{k=0}^{L} g_d(k) \end{bmatrix}$$

Returning to the general multivariable problem, the weighted SSE objective function in (5.6) may be written in the following form:

$$\sum_{j=1}^{n_w}\sum_{i=1}^{n_y}\sum_{k=0}^{L} W_{ij}(k)\,[s_{ij}(k)]^2 = (d\,A_{\text{out}}q + d\,b_{\text{out}})^T\Lambda(d\,A_{\text{out}}q + d\,b_{\text{out}}) \tag{5.16}$$

In the above, the weighting matrix Λ is defined in terms of W as follows:

$$\Lambda = \text{diag}\,[W_{11},...,W_{n_y 1},...,W_{1\,n_w},...,W_{n_y\,n_w}] \tag{5.17}$$

where

$$W_{ij} = [W_{ij}(0),..,W_{ij}(L)] \tag{5.18}$$

Dynamic operability assessment for a single disturbance may be posed as the following quadratic programming problem:

$$\begin{aligned} \min_{q} \quad & (d\,A_{\text{out}}\,q + d\,b_{\text{out}})^T\,\Lambda\,(d\,A_{\text{out}}\,q + d\,b_{\text{out}}) \\ \text{s.t.} \quad & \begin{bmatrix} y_\ell \\ u_\ell \end{bmatrix} - d\begin{bmatrix} b_{\text{out}} \\ 0 \end{bmatrix} \le d\begin{bmatrix} A_{\text{out}} \\ A_{\text{inp}} \end{bmatrix} q \le \begin{bmatrix} y_u \\ u_u \end{bmatrix} - d\begin{bmatrix} b_{\text{out}} \\ 0 \end{bmatrix} \end{aligned} \tag{5.19}$$

where y_ℓ and y_u are the respective lower and upper bounds on the deviational output responses, and u_l and u_u pertain in a similar manner to the deviational input responses.

The above optimization problem is typically of large dimension and its solution is computationally intensive. Two methods are presented which enable reduced computation times by exploiting certain features of the problem. The first involves formulating the problem in an

open-loop manner where an optimal input trajectory is sought directly, thereby converting the input constraints to simple bounds on the search variables. The second method involves exploiting the considerable sparsity in the objective function and constraint system. Neither method approximates the solution, but rather takes advantage of the problem structure. A method which relies on approximating the optimal Q and which enables rapid calculation of an approximate solution is presented in section 5.4 of this chapter.

Open-loop formulation

Analysis of the summation equations (5.8) and (5.9) shows that the output response may be written in terms of the input trajectory. That is, for $i \leq n_y$ we have:

$$\begin{aligned}
s_i(i_o) &= d\sum_{k=0}^{i_o} G_{D\,i}(k) - d\sum_{m=1}^{n_y}\sum_{n=1}^{n_u}\sum_{k=0}^{i_o} q_{nm}(k)\sum_{v=k}^{i_o}\sum_{\ell=k}^{v} G_{D\,m}(\ell-k)\,G_{P\,in}(v-\ell) \\
&= d\sum_{k=0}^{i_o} G_{D\,i}(k) - d\sum_{n=1}^{n_u}\sum_{\alpha=0}^{i_o} G_{P\,in}(\alpha)\sum_{m=1}^{n_y}\sum_{k=0}^{i_o-\alpha} q_{nm}(k)\sum_{v=k}^{i_o-\alpha} G_{D\,m}(v-k) \\
&= d\sum_{k=0}^{i_o} G_{D\,i}(k) + \sum_{n=1}^{n_u}\sum_{\alpha=0}^{i_o} G_{P\,in}(\alpha)\,s_{(n_y+n)}\,(i_o-\alpha) \\
&= d\sum_{k=0}^{i_o} G_{D\,i}(k) + \sum_{n=1}^{n_u}\sum_{\alpha=0}^{i_o} s_{(n_y+n)}\,(\alpha)\,G_{P\,in}(i_o-\alpha) \qquad (5.20)
\end{aligned}$$

Since the optimization problem in (5.6) involves performance specifications only on the inputs and outputs, it is possible to perform a change-of-variables and solve for the optimal input trajectory instead of Q. The advantages of solving directly for the inputs are that the input constraints are simply bounds, and a reduction in search-space is made possible (as discussed below). When robust stability constraints are present it is not possible, in general, to express them in terms of the input behavior, preventing the use of an open-loop formulation.

The input trajectories are now defined as the search variable x,partitioned as follows:

$$x = [x_1(0),\ldots,x_1(L),\ldots,x_{n_u}(0),\ldots,x_{n_u}(L)]^T\,. \qquad (5.21)$$

where $x_i(i_o) = s_{n_y+i}(i_o)$.

The notation s_{out} will refer to those elements of s corresponding to the output response, whereas s_{inp} refers to the input response. By definition of the variable transformation, $x = s_{\text{inp}} = d\,A_{\text{inp}}q$.

Remark 1 *Due to the form of A_{inp}, certain constraints need to be placed on x to ensure causality of the input behavior. These are needed because some rows of A_{inp} are structurally equal to zero due to the nature of the pulse response of G_D. If the disturbance is strictly proper or contains time-delays then one needs to set:*

$$x_i(i_o) = 0 \qquad \forall\, i = 1, \ldots, n_u \;\; and \;\; \forall\, i_o = 0, \ldots, k^* \tag{5.22}$$

where

$$k^* = \min_j \{k \,|\, G_{Dj}(k) \neq 0\} \tag{5.23}$$

Physically this corresponds to preventing any control action being taken before the disturbance hits the process. It should be noted that such constraints are not needed on q, since the q's are multiplied by G_D. Hence, q may be nonzero even if the input response is zero.

From (5.20) it is clear that the output response may be written as:

$$s_{\text{out}} = d\, A_{\text{out}} q + d\, b_{\text{out}} = \mathcal{P} x + d\, b_{\text{out}} \tag{5.24}$$

In the above, the matrix $\mathcal{P}$ is given by:

$$\mathcal{P} = \begin{bmatrix} P_{11} & \cdots & P_{1\,n_u} \\ \vdots & & \vdots \\ P_{n_y 1} & \cdots & P_{n_y n_u} \end{bmatrix} \tag{5.25}$$

where P_{ij} are lower triangular Toeplitz matrices of the form:

$$P_{ij} = \begin{bmatrix} G_{P\,ij}(0) & 0 & 0 \\ \vdots & \ddots & 0 \\ G_{P\,ij}(L) & \cdots & G_{P\,ij}(0) \end{bmatrix} \tag{5.26}$$

Application of the above to the dynamic operability assessment problem in (5.19) yields the following equivalent optimization problem:

$$\begin{aligned} & \min_x \quad (\mathcal{P} x + d\, b_{\text{out}})^T \Lambda\, (\mathcal{P} x + d\, b_{\text{out}}) \\ & \text{subject to} \\ u_\ell^{'} \;&\leq\; x \;\leq\; u_u^{'} \\ y_\ell - d\, b_{\text{out}} \;&\leq\; \mathcal{P} x \;\leq\; y_u - d\, b_{\text{out}} \end{aligned} \tag{5.27}$$

where $u_\ell^{'}$ and $u_u^{'}$ refer to the slightly modified bounds on the deviational input responses in order to account for the constraints in (5.22). For notational convenience they are from now on simply written as u_ℓ and u_u. As mentioned earlier, the input constraints in (5.27) are simply bounds on x as opposed to general linear constraints on Q. Interesting theoretical and computational features of the above problem formulation are discussed next.

Relation of open-loop formulation to the Internal Model Control framework

The first important feature of the above formulation is that, in the absence of model uncertainty, the Q-parametrization approach is equivalent to an "open-loop optimal control" approach. This is not an unexpected result since, for a stable plant, the Q-parametrization approach is equivalent to the Internal Model Control (IMC) framework (Morari and Zafiriou, 1989), and, with a perfect model, the IMC structure is effectively open-loop (García *et al.*, 1989).

This can be understood by considering the IMC structure shown in Figure 5.3, with Q being the IMC controller. In the presence of no model uncertainty ($G = G_P$), the closed-loop expression for the output is given by:

$$y = G_P Q(y_{set} - G_d\, d) + G_d\, d \tag{5.28}$$

The input u is given by:

$$u = Q(y_{set} - G_d\, d) \tag{5.29}$$

It is thus clear that $y = G_P u + G_d\, d$, which is open-loop.

The reason why it is possible to pose dynamic operability in an open-loop manner is because performance limits are determined on the basis of *specific* exogenous inputs. Since the exogenous inputs y_{set} and d are specified (and no model uncertainty is present), it is clear from (5.28) that searching for an optimal Q may be replaced by searching for the optimal input trajectory associated with that Q.

Analysis of (5.28) shows that, for no model uncertainty, the closed-loop system in Figure 5.3 may be redrawn in an open-loop manner as shown in Figure 5.4, thus illustrating some of the above points graphically and also showing why the choice of $Q = G_P^{-1}$ results in perfect control.

Relation of the open-loop formulation to the controllability analysis framework

Apart from being closely related to the IMC framework, the open-loop approach also has close ties with the concept of functional controllability, defined as follows (Russell and Perkins, 1987):

Definition 6 *A system with polynomial transfer matrix $G(s)$ will be called functionally controllable if it satisfies the following condition. Given any trajectory $y(t)$ which is zero for*

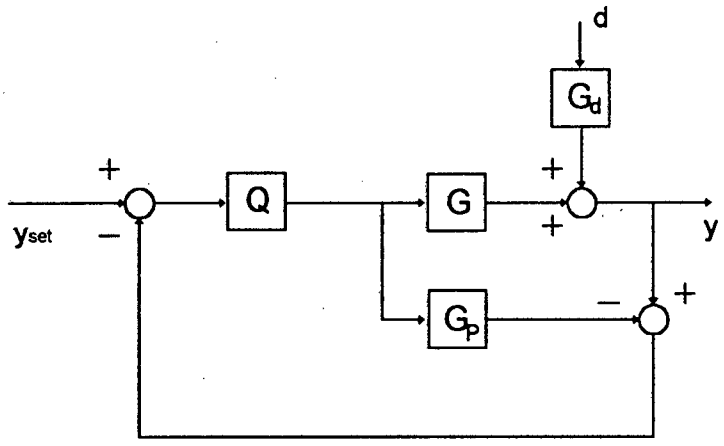

Figure 5.3: Internal Model Control (IMC) structure.

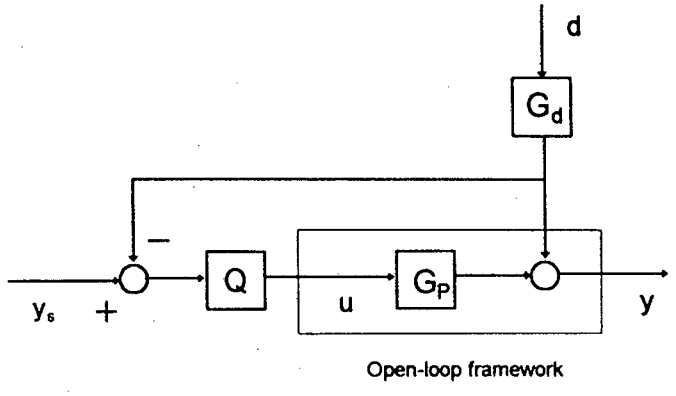

Figure 5.4: Relation between the open-loop structure and the IMC structure in absence of model uncertainty.

$t < 0$ and which satisfies certain smoothness conditions, there exists an input trajectory $u(t)$ such that with zero initial conditions on the states, u generates y.

In the open-loop framework, the aim is to determine the best achievable output trajectory, as well as to determine the input trajectory which will achieve this. The open-loop approach is thus similar to that used by Cao *et al.* (1994), discussed in Chapter 2, who treat nonlinear process models. If the models are linear and written in a discrete-time manner, then the two approaches are equivalent.

As has been mentioned earlier, the open-loop formulation applies only in the absence of model uncertainty. When model uncertainty is present, the standard Q-parametrization formulation is needed. The advantage of the open-loop formulation is that it enables rapid solution of the optimization problems needed to assess dynamic operability. Details of this are discussed next and illustrated through an application example.

Computational features

Reduction in search space dimension and number of constraints There are two important computational features associated with the problem formulation in (5.27). The first is that a reduction in the search-space dimension is achieved. Originally the number of decision variables was $n_u \times n_y \times L$. Following the change-of-variables the number of decision variables is reduced to $n_u \times L$, as seen from (5.21). Since the inputs are fixed at zero for the first k^* time increments, these need not be included as search variables and the actual number needed is $n_u \times (L - k^*)$. As computation times for quadratic programming problems often increase in a quadratic manner with problem size, this dimension reduction will typically reduce computation time by a factor of n_y^2. It should be noted that if multiple disturbances are present ($n_d > 1$), then the number of search variables needed is $n_d \times n_u \times (L - k^*)$. Clearly, for $n_d = n_y$ disturbances, there is essentially no reduction in the search space.

The second important computational feature is that there is a reduction in the number of general linear constraints. This is because the input constraints are now direct bounds on the search variables, as opposed to bounds on linear combinations of the search variables. For problems where only input constraints are present, the reduction in double precision workspace is often considerable. For example, LSSOL (Gill *et al.*, 1986) requires the double precision workspace for constrained least squares problems to be at least $2N^2 + 9N + 6NCLIN$, where N is the search-space dimension and $NCLIN$ is the number of general linear constraints. If, however, no general linear constraints are present, then the required

double precision workspace is only $9N$.

Exploiting sparsity and other aspects of the problem structure Due to the lower triangular structure of the sub-matrices contained in $\mathcal{P}$, the set of general linear constraints in (5.27) is approximately 50% sparse. The sparsity in the constraint system may be exploited by using a sparse quadratic programming package and involves no modification to the formulation given in (5.19) or (5.27) to achieve this.

Exploiting the sparsity of $\mathcal{P}$ in the objective function is slightly more complicated. The software codes available at the time of this research are only able to do this via the introduction of search variables p, defined as follows:

$$p = \mathcal{P}\,x + d\,b_{\text{out}} \tag{5.30}$$

Clearly, the new search variables are equivalent to the output response and can thus also be used to convert the output constraints to simple bounds. The resulting optimization problem takes the form:

$$\begin{aligned} & \min_{x,p} p^T \Lambda p \\ & \text{subject to} \\ u_\ell \;&\leq\; x \leq u_u \\ y_\ell \;&\leq\; p \leq y_u \\ p \;&=\; \mathcal{P}\,x + d\,b_{\text{out}} \end{aligned} \tag{5.31}$$

A disadvantage of the above formulation is that the total number of search variables needed increases and additional constraints are added. This is, however, overcome by the fact that the sparsity of $\mathcal{P}$ is exploited and the output constraints are bounds as opposed to general linear constraints. Experience thus far has proven this to be a very efficient problem formulation for dynamic operability assessment in the absence of model uncertainty.

A beta version of the SQOPT code (Gill, 1996) was used to solve the sparse quadratic programming problems. A useful feature of the code is that, in addition to exploiting sparsity, it is able to utilize the fact that only p is involved in the objective function. As a result, the Hessian is not unnecessarily large in dimension.

Finally, by taking into account the lower triangular Toeplitz nature of the submatrices in $\mathcal{P}$, the problem set-up may be coded very efficiently, allowing for an extremely rapid problem set-up.

Example 5.1

To illustrate the computational benefits of exploiting the problem structure and sparsity for regulatory problems we consider a multivariable flotation circuit. The process model is described in greater detail in Chapter 6 and corresponds to flotation circuit 3. The outputs to be controlled are the grade G and the recovery R. The manipulated inputs are the air factor k_a and the feedwater flowrate w_f. The process disturbance corresponds to changes in the total feed solids flowrate. The transfer function description of the process is given by:

$$\begin{bmatrix} G \\ R \end{bmatrix} = G_P \begin{bmatrix} k_a \\ w_f \end{bmatrix} + G_D\, d \tag{5.32}$$

where

$$G_P = \begin{bmatrix} \dfrac{-20.91\,(5.43\,s+1)}{(9.82\,s+1)(5.84\,s+1)} & \dfrac{10.36}{(7.06\,s+1)(0.287\,s+1)} \\ \dfrac{14.62\,(61.78\,s+1)}{(10.01\,s+1)(0.410\,s+1)} & \dfrac{-10.46\,(22.55\,s+1)}{(2.02s+1)(10.55\,s+1)} \end{bmatrix} \tag{5.33}$$

and

$$G_D = \begin{bmatrix} \dfrac{0.0092\,(3.32\,s+1)}{(9.33\,s+1)(9.33\,s+1)} \\ \dfrac{-0.0053\,(91.4\,s+1)}{(7.32\,s+1)} \end{bmatrix} . \tag{5.34}$$

No constraints are placed on the output responses, but the following constraints are placed on the deviational input behavior:

$$\begin{aligned} -0.1 \;&\leq\; k_a \leq 0.1 \\ -0.05 \;&\leq\; w_f \leq 0.05 \quad \text{ton.min}^{-1} \end{aligned} \tag{5.35}$$

The measure of closed-loop performance is chosen to be the time-weighted SSE of the outputs to a step of $120\,\text{kg.min}^{-1}$ in the feed disturbance, initiated from a base value of $d_b = -60\,(\text{kg.min}^{-1})$. A sampling time of 1 minute is used and a simulation horizon of $L = 200$ is chosen.

The dynamic operability assessment problem is solved using the standard Q-parametrization approach, the open-loop approach and an open-loop approach where sparsity is exploited, and the results are shown in Table 5.1. The double precision workspace, search space dimension and other important computational aspects are listed as well. Both the standard Q-parametrization approach and the standard open-loop approach were solved as constrained least squares problems using LSSOL (Gill *et al.*, 1986). The sparse open-loop formulation made use of a beta version of SQOPT (Gill, 1996), a sparse QP solver. The solution times indicated are achieved on a SUN SPARCstation 20.

Table 5.1: Important computational issues pertaining to the multivariable regulatory control problem.

	Standard approach	**Open-loop formulation**	**Sparse open-loop formulation**
Search space dimension	800	400	400
Double precision workspace	1 292 000	3 600	214 202
Integer workspace	800	400	250 001
Solution time (sec)	942	78.5	47.0
SSE objective	24.02	24.02	24.02

It is clear that exploiting the problem sparsity in addition to the dimension reduction enables significant improvements in computation time to be achieved. As expected, the solution obtained is identical using all three of the approaches listed.

The computational improvements achieved for this particular example were all gained without approximating the solution. It will be shown in a later section how a multi-rate approximation of the optimal Q may provide rapid and fairly accurate solutions to such dynamic operability assessment problems. Such an approach may be particularly beneficial when including the Q-parametrization formulation within a synthesis or retrofit algorithm, a topic which is recommended for future research.

5.1.3 Servo Control Problems Without Model Uncertainty

In this subsection, the formulation of and computational issues relating to the servo dynamic operability assessment problem are addressed. Much of the development parallels that for the regulatory problem, in which case only the pertinent details are provided.

Basic formulation

In Chapter 3, the basic problem formulation for this type of problem was established. For open-loop stable processes, the output response ($i \leq n_y$) to a step of size $y_{set\,j}$ in the setpoint of the jth output is given by:

$$s_{ij}(i_o) = y_{set\,j} \sum_{n=1}^{n_u} \sum_{k=0}^{i_o} q_{nj}(k) \sum_{v=k}^{i_o} G_{P\,in}(v-k) \tag{5.36}$$

Similarly, the expression for the input response ($i > n_y$) is given by:

$$s_{ij}(i_o) = y_{set\,j} \sum_{k=0}^{i_o} q_{(i-n_y)\,j}(k) \tag{5.37}$$

These closed-loop response summation equations in (5.36) and (5.37) may be written in matrix form as:

$$s = Aq = \begin{bmatrix} A_{\text{out}} \\ A_{\text{inp}} \end{bmatrix} q \tag{5.38}$$

where A_{out} and A_{inp} correspond to the coefficient matrices of the output and input responses respectively. The vector q is partitioned as in (5.13). Appendix A.3 provides more details on the form of the coefficient matrices.

For the case of a SISO process, A_{out} is a lower triangular matrix of the form:

$$A_{\text{out}} = y_{set\,1} \begin{bmatrix} g_p(0) & 0 & \cdots & \cdots & 0 \\ g_p(0)+g_p(1) & g_p(0) & 0 & & \vdots \\ \vdots & & & \ddots\ 0 & \vdots \\ \vdots & & & \ddots & 0 \\ \sum_{v=0}^{L} g_p(v) & \sum_{v=0}^{L-1} g_p(v) & \cdots & \cdots & g_p(0) \end{bmatrix} \tag{5.39}$$

Similarly, A_{inp} is given by:

$$A_{\text{inp}} = y_{set\,1} \begin{bmatrix} 1 & 0 & \cdots & 0 \\ \vdots & 1 & 0 & \vdots \\ \vdots & & \ddots & 0 \\ 1 & \cdots & \cdots & 1 \end{bmatrix} \tag{5.40}$$

Using a weighted SSE objective function as a measure of the closed-loop performance, dynamic operability assessment may be posed as the following convex quadratic programming problem:

$$\begin{aligned} &\min_q \left(A_{\text{out}}q - y_{set}\right)^T \Lambda \left(A_{\text{out}}q - y_{set}\right) \\ \text{s.t.} \quad &y_\ell \le A_{\text{out}}q \le y_u \\ &u_\ell \le A_{\text{inp}}q \le u_u \end{aligned} \tag{5.41}$$

For individually applied setpoint changes, the reference signal vector y_{set} is given by:

$$y_{set} = \left[\underbrace{y_{set\,1}, \cdots, y_{set\,1}}_{L+1}, \cdots, \underbrace{y_{set\,n_y}, \cdots, y_{set\,n_y}}_{L+1} \right]^T \tag{5.42}$$

The diagonal matrix Λ is a weighting matrix defined in a similar manner to that given in (5.17). The vectors u_ℓ and u_u are the respective lower and upper bounds on the deviational input responses, and y_ℓ and y_u refer similarly to the deviational output responses. In a similar manner as (5.19), (5.41) may be expressed in a sparse open-loop manner, details of which are provided next.

Open-Loop Formulation

Analysis of the summation equations (5.36) and (5.37) defining the output and input closed-loop behavior reveals that the output response may be written directly in terms of the input trajectory. That is, for $i \leq n_y$ we have:

$$\begin{aligned} s_{ij}(i_o) &= y_{set\,j} \sum_{n=1}^{n_u} \sum_{k=0}^{i_o} q_{nj}(k) \sum_{v=k}^{i_o} G_{P\,in}(v-k) \\ &= y_{set\,j} \sum_{n=1}^{n_u} \sum_{\alpha=0}^{i_o} G_{P\,in}(\alpha) \sum_{k=0}^{i_o-\alpha} q_{nj}(k) \\ &= \sum_{n=1}^{n_u} \sum_{\alpha=0}^{i_o} G_{P\,in}(\alpha)\; s_{(n_y+n)\,j}(i_o-\alpha) \\ &= \sum_{n=1}^{n_u} \sum_{\alpha=0}^{i_o} s_{(n_y+n)\,j}(\alpha)\, G_{P\,in}(i_o-\alpha) \end{aligned} \tag{5.43}$$

where $s_{(n_y+n)\,j}$ is the step response of the nth input for the setpoint change in the jth output. Since there are only input and output constraints present, it is possible to search for the optimal input trajectory directly, rather than searching for q.

The input trajectories are defined as the search variable x, which is partitioned as follows:

$$x = \left[x_{11}^T, ..., x_{n_u\,1}^T, ..., x_{1\,n_y}^T, ..., x_{n_u\,n_y}^T\right]^T \tag{5.44}$$

where $x_{ij}^T = [x_{ij}(0), ..., x_{ij}(L)] = s_{(n_y+i)\,j}$. It should be noted that no dimension reduction is achieved for servo problems. The only benefit of the open-loop formulation in this case is the fact that the input constraints are simply bounds.

By definition of the variable transformation, $x = s_{\text{inp}} = A_{\text{inp}} q$. It is clear from (5.43) that the output response may be written as:

$$s_{\text{out}} = A_{\text{out}} q = \mathcal{P}_{\text{set}} x \tag{5.45}$$

In the above, the matrix $\mathcal{P}_{\text{set}}$ is defined as follows:

$$\mathcal{P}_{\text{set}} = \begin{bmatrix} \mathcal{P} & 0 & 0 \\ 0 & \ddots & 0 \\ 0 & 0 & \mathcal{P} \end{bmatrix} \tag{5.46}$$

where the matrices $\mathcal{P}$ are as defined in (5.25) and (5.26).

Application of this variable transformation to the dynamic operability assessment problem in (5.41) results in the following optimization problem:

$$\begin{aligned} & \min_{x} \left(\mathcal{P}_{\text{set}}\, x - y_{set}\right)^T \Lambda \left(\mathcal{P}_{\text{set}}\, x - y_{set}\right) \\ \text{s.t.} \quad & u_\ell \leq x \leq u_u \\ & y_\ell \leq \mathcal{P}_{\text{set}}\, x \leq y_u \end{aligned} \tag{5.47}$$

As in (5.27), the input constraints in (5.47) are simply bounds on x as opposed to general linear constraints on Q.

It can be seen from (5.46) that the matrix $\mathcal{P}_{\text{set}}$ has significant sparsity. In an analogous manner to that used before, the sparsity is exploited by introducing additional search variables p, defined as:

$$p = \mathcal{P}_{\text{set}}\, x - y_{set} \tag{5.48}$$

The resulting optimization problem takes the form:

$$\begin{aligned} & \min_{x,p} p^T \Lambda p \\ & \text{subject to} u_\ell \leq x \leq u_u \\ & y_\ell - y_{set} \leq p \leq y_u - y_{set} \\ & p = \mathcal{P}_{\text{set}}\, x - y_{set} \end{aligned} \tag{5.49}$$

The new search variables define the error and are used to convert the linear constraints on the output response to simple bounds, as shown above. Despite the introduction of search variables, exploiting the problem sparsity leads to dramatic improvements in computational time.

As before, by taking into account both the structure of $\mathcal{P}_{\text{set}}$ and the Toeplitz nature of the submatrices in $\mathcal{P}_{\text{set}}$, the problem set up may be coded very efficiently. It should be noted that, for individually applied setpoint changes, the problem in (5.49) may be separated into $n_w = n_y$ independent sub-problems. The separable nature of the problem is evidenced by the form of $\mathcal{P}_{\text{set}}$. It has been found, perhaps surprisingly, that the computational benefits of doing this are not significant, and thus this idea is not discussed further.

Table 5.2: Computational issues pertaining to the servo multivariable distillation column dynamic operability assessment problem.

	Standard approach	**Sparse Q-parametrization formulation**	**Sparse open-loop formulation**
Search space dimension	400	400	400
Double precision workspace	326 000	280 602	154 202
Integer workspace	400	377 201	130 001
Solution time (sec)	85	30	22
SSE objective	58.91	58.91	58.91

Example 5.2

To illustrate the benefits of exploiting the structure and sparsity of servo problems, the above techniques are applied to the multivariable distillation example considered in Chapter 3. For the purposes of this example, only the original transfer matrix is considered, namely:

$$\tilde{P}(s) = \begin{bmatrix} \frac{0.66\,e^{-6\,s}}{(6.7\,s+1)} & \frac{-0.005}{(9.06\,s+1)} \\ \frac{-34.7\,e^{-4\,s}}{(8.15\,s+1)} & \frac{0.87\,(11.6\,s+1)e^{-2\,s}}{(3.9\,s+1)\,(18.8\,s+1)} \end{bmatrix} \tag{5.50}$$

The objective function and constraints are chosen as in Chapter 3 and are not repeated here as the emphasis is on the computational benefits achieved for this problem.

In the basic Q-parametrization framework, dynamic operability assessment is posed as in (5.41) and solved using standard constrained least squares codes such as LSSOL (Gill *et al.*, 1986). However, as mentioned earlier, the problem contains significant structure and sparsity which may be exploited using the formulations in (5.47) and (5.49). In this case, no dimension reduction is possible and the only benefit of the open-loop formulation, compared with the standard Q-parametrization formulation, is that the input constraints are simply bounds, as opposed to general linear constraints.

Table 5.2 shows a number of relevant computational features associated with three different problem formulations. In order to emphasize the benefits of simply exploiting sparsity, the standard Q parametrization approach is compared directly with a sparse Q-parametrization formulation. This, in turn, is compared with the further benefits of using an open-loop formulation.

From the results it is clear that there are considerable benefits to be gained by exploiting the

problem structure and sparsity. These benefits would have been even greater had the output behavior been constrained in addition to the input behavior. This would have required additional linear constraints in the standard Q-parametrization formulation. For the sparse approaches, however, no additional linear constraints would be needed since these constraints would simply take the form of bounds on p.

The above computational benefits are once again achieved without any loss in accuracy. It will be shown in section 5.4.1 how approximations to the optimal Q may considerably speed up solution time without introducing significant inaccuracy.

5.2 Regulatory Problems Involving A Range of Disturbances

In this section, regulatory problems involving a single range of disturbances in the absence of model uncertainty are treated. Attention will be given to dynamic operability assessment at fixed operating conditions and to the determination of the maximum tolerable disturbance range. The latter is an alternative measure of dynamic operability which is conveniently developed using an open-loop formulation. The potential benefits of nonlinear control when treating a range of disturbances will be discussed and demonstrated through illustrative examples. The open-loop formulation is used throughout this chapter as it facilitates much of the discussion which follows.

5.2.1 Dynamic Operability Assessment at Fixed Operating Conditions

For a single step-like disturbance, initiated from a base value d_b with step-size Δd, lying between upper and lower bounds, d^+ and d^- respectively, it was shown in Chapter 3 that the critical points are shown in Table 5.3.

Table 5.3: Critical points for the disturbance region considered.

Critical Point	$\mathbf{d}_b$	$\mathbf{\Delta d}$
1	d^-	$d^+ - d^-$
2	d^+	$d^- - d^+$

It is assumed that d^+ and d^- are symmetric about the nominal disturbance level d_b^N, which is chosen as zero. If d_b^N is not zero, it can be made so by an appropriate variable shift. Due to the assumption regarding the symmetry of the upper and lower bounds about the nominal

disturbance level d_b^N, the following relations apply:

$$\begin{aligned} d_{b\,2} &= -d_{b\,1} \\ \Delta d_2 &= -\Delta d_1 \\ \text{and} \quad d_{b\,i} &= -0.5\Delta d_i \quad \text{for } i = 1, 2 \end{aligned} \tag{5.51}$$

In Chapter 3, the treatment of a range of disturbances was in the context of an economic formulation. The bounds on the input and output behavior were expressed in terms of bounds on the actual responses as opposed to the deviational responses. In this chapter, bounds on the deviational responses will be used, noting that the bounds are functions of the operating point. A useful notational and conceptual idea is introduced which involves splitting each of the bounds in the constraint system into a part which is a function of the disturbance Δd (b_{inp} and b_{out}) and a part which is not (ℓ_{inp}, ℓ_{out}, u_{inp} and u_{out}). As an explanation of the notation, u_{out} relates to the upper bound on the output response. This simplifies the treatment of subsequent developments.

When considering a range of disturbances, the aim is to seek to determine optimal input trajectories for each disturbance direction. These trajectories are written as x^1 and x^2, where x^1 and x^2 refer to the input trajectories for critical points 1 and 2 respectively and are partitioned as in (5.21).

The output response to critical points 1 and 2 are given by:

$$\begin{aligned} s_{\text{out }1} &= \mathcal{P}x^1 + \Delta d_1\, b_{\text{out}} \\ s_{\text{out }2} &= \mathcal{P}x^2 + \Delta d_2\, b_{\text{out}} \end{aligned} \tag{5.52}$$

The measure of closed-loop performance is chosen as the weighted SSE of the outputs to the two critical point disturbances, namely:

$$\Phi = \begin{bmatrix} s_{\text{out }1} \\ s_{\text{out }2} \end{bmatrix}^T \Lambda \begin{bmatrix} s_{\text{out }1} \\ s_{\text{out }2} \end{bmatrix} \tag{5.53}$$

Determining the best achievable closed-loop behavior to the critical disturbances may thus be posed as the following optimization problem:

$$\begin{aligned} &\min_{x^1, x^2} \left(\begin{bmatrix} \mathcal{P} & 0 \\ 0 & \mathcal{P} \end{bmatrix} \begin{bmatrix} x^1 \\ x^2 \end{bmatrix} + \begin{bmatrix} \Delta d_1 b_{\text{out}} \\ \Delta d_2 b_{\text{out}} \end{bmatrix} \right)^T \Lambda \left(\begin{bmatrix} \mathcal{P} & 0 \\ 0 & \mathcal{P} \end{bmatrix} \begin{bmatrix} x^1 \\ x^2 \end{bmatrix} + \begin{bmatrix} \Delta d_1 b_{\text{out}} \\ \Delta d_2 b_{\text{out}} \end{bmatrix} \right) \\ &\text{subject to} \\ &\begin{pmatrix} \ell_{\text{out}} \\ \ell_{\text{out}} \\ \ell_{\text{inp}} \\ \ell_{\text{inp}} \end{pmatrix} - \begin{pmatrix} \Delta d_1 b_{\text{out}} \\ \Delta d_2 b_{\text{out}} \\ \Delta d_1 b_{\text{inp}} \\ \Delta d_2 b_{\text{out}} \end{pmatrix} \leq \begin{bmatrix} \mathcal{P} & 0 \\ 0 & \mathcal{P} \\ I & 0 \\ 0 & I \end{bmatrix} \begin{bmatrix} x^1 \\ x^2 \end{bmatrix} \leq \begin{pmatrix} u_{\text{out}} \\ u_{\text{out}} \\ u_{\text{inp}} \\ u_{\text{inp}} \end{pmatrix} - \begin{pmatrix} \Delta d_1 b_{\text{out}} \\ \Delta d_2 b_{\text{out}} \\ \Delta d_1 b_{\text{inp}} \\ \Delta d_2 b_{\text{inp}} \end{pmatrix} \end{aligned} \tag{5.54}$$

It should be noted that $\ell_{\text{inp}}, \ell_{\text{out}}, u_{\text{inp}}$, and u_{out} are not functions of Δd (or d_b) and thus do not take on different values at each of the critical points.

In solving (5.54), a number of options are available, depending on the assumptions made regarding the control behavior. The first option is to assume that the input trajectory is determined by a single linear controller Q. The second option is to assume that the optimal input trajectory is not determined by some underlying linear controller Q, but is free to behave in a non-linear way. The analysis of the problem for each approach will be discussed next.

Optimal linear control

Under the assumption of a single underlying linear controller Q, it is necessary to introduce the constraint that $x^2 = -x^1$. The need for this constraint is obvious from the change-of-variables described earlier, since $x = \Delta d\, A_{\text{inp}}\, q$, and $\Delta d_2 = -\Delta d_1$. With this assumption, x^2 may be eliminated from the problem to obtain:

$$\begin{aligned}
&\min_{x^1} \left(\begin{bmatrix} \mathcal{P} \\ -\mathcal{P} \end{bmatrix} x^1 + \Delta d_1 \begin{bmatrix} b_{\text{out}} \\ -b_{\text{out}} \end{bmatrix} \right)^T \Lambda \left(\begin{bmatrix} \mathcal{P} \\ -\mathcal{P} \end{bmatrix} x^1 + \Delta d_1 \begin{bmatrix} b_{\text{out}} \\ -b_{\text{out}} \end{bmatrix} \right) \\
&\text{subject to} \\
&\begin{pmatrix} \ell_{\text{out}} \\ \ell_{\text{out}} \\ \ell_{\text{inp}} \\ \ell_{\text{inp}} \end{pmatrix} - \Delta d_1 \begin{pmatrix} b_{\text{out}} \\ -b_{\text{out}} \\ b_{\text{inp}} \\ -b_{\text{inp}} \end{pmatrix} \leq \begin{bmatrix} \mathcal{P} \\ -\mathcal{P} \\ I \\ -I \end{bmatrix} x^1 \leq \begin{pmatrix} u_{\text{out}} \\ u_{\text{out}} \\ u_{\text{inp}} \\ u_{\text{inp}} \end{pmatrix} - \Delta d_1 \begin{pmatrix} b_{\text{out}} \\ -b_{\text{out}} \\ b_{\text{inp}} \\ -b_{\text{inp}} \end{pmatrix}
\end{aligned} \tag{5.55}$$

Now, careful analysis of the objective function and constraint system shows that the above problem is equivalent to:

$$\begin{aligned}
&\min_{x^1} \quad 2\left(\mathcal{P}x^1 + \Delta d_1 b_{\text{out}}\right)^T \Lambda' \left(\mathcal{P}x^1 + \Delta d_1 b_{\text{out}}\right) \\
&\text{subject to} \\
&\begin{pmatrix} \ell^*_{\text{out}} \\ \ell^*_{\text{inp}} \end{pmatrix} - \Delta d_1 \begin{pmatrix} b_{\text{out}} \\ b_{\text{inp}} \end{pmatrix} \leq \begin{bmatrix} \mathcal{P} \\ I \end{bmatrix} x^1 \leq \begin{pmatrix} u^*_{\text{out}} \\ u^*_{\text{inp}} \end{pmatrix} - \Delta d_1 \begin{pmatrix} b_{\text{out}} \\ b_{\text{inp}} \end{pmatrix}
\end{aligned} \tag{5.56}$$

where Λ has been appropriately truncated to give Λ', and where

$$\begin{aligned}
\ell^*_{\text{out}} &= \max(\ell_{\text{out}}, -u_{\text{out}}) \\
u^*_{\text{out}} &= \min(u_{\text{out}}, -\ell_{\text{out}}) = -\ell^*_{\text{out}} \\
\ell^*_{\text{inp}} &= \max(\ell_{\text{inp}}, -u_{\text{inp}}) \\
u^*_{\text{inp}} &= \min(u_{\text{inp}}, -\ell_{\text{inp}}) = -\ell^*_{\text{inp}}
\end{aligned} \tag{5.57}$$

The bounds in (5.57) are a consequence of the constraint asymmetry and the fact that, except for its sign, the coefficient matrix is identical for each critical point.

It should be noted that the above analytical insight enables the number of constraints and search variables to be halved when treating a range of disturbances under the assumption of linear control. In fact, the number of search variables and general linear constraints is as for the case of a single disturbance. Thus, under linear control, the computation time should essentially be the same whether one treats a single range of disturbances or just a single disturbance. Clearly the sparsity in the above optimization problem would be exploited as in (5.31).

Optimal nonlinear control

If the linearity constraint ($x^2 = -x^1$) is not enforced, then it is possible in most cases to obtain significantly better control performance. The problem in (5.54) has a separable structure which may be used to reduce computation time. This is done by splitting (5.54) into two *independent* problems, namely:

$$\min_{x^1} \quad \left(\mathcal{P}\,x^1 + \Delta d_1 b_{\text{out}}\right)^T \Lambda' \left(\mathcal{P}\,x^1 + \Delta d_1 b_{\text{out}}\right) \tag{5.58}$$

subject to

$$\begin{pmatrix} \ell_{\text{out}} \\ \ell_{\text{inp}} \end{pmatrix} - \begin{pmatrix} \Delta d_1 b_{\text{out}} \\ \Delta d_1 b_{\text{inp}} \end{pmatrix} \leq \begin{bmatrix} \mathcal{P} \\ I \end{bmatrix} x^1 \leq \begin{pmatrix} u_{\text{out}} \\ u_{\text{inp}} \end{pmatrix} - \begin{pmatrix} \Delta d_1 b_{\text{out}} \\ \Delta d_1 b_{\text{inp}} \end{pmatrix}$$

and

$$\min_{x^2} \quad \left(\mathcal{P}\,x^2 + \Delta d_2 b_{\text{out}}\right)^T \Lambda' \left(\mathcal{P}\,x^2 + \Delta d_2 b_{\text{out}}\right) \tag{5.59}$$

subject to

$$\begin{pmatrix} \ell_{\text{out}} \\ \ell_{\text{inp}} \end{pmatrix} - \begin{pmatrix} \Delta d_2 b_{\text{out}} \\ \Delta d_2 b_{\text{inp}} \end{pmatrix} \leq \begin{bmatrix} \mathcal{P} \\ I \end{bmatrix} x^2 \leq \begin{pmatrix} u_{\text{out}} \\ u_{\text{inp}} \end{pmatrix} - \begin{pmatrix} \Delta d_2 b_{\text{out}} \\ \Delta d_2 b_{\text{inp}} \end{pmatrix}$$

The overall computation time will typically be halved by exploiting the separable nature of the problem. The reason is because each of the problems (5.58) and (5.59) will require roughly a quarter of the time needed to solve (5.54). The sparsity in both (5.58) and (5.59) would be exploited as mentioned before in (5.31).

The only difference between these two problems is the fact that $\Delta d_2 = -\Delta d_1$. The minimum objective value in (5.54) is the sum of (5.58) and (5.59). It should be noted that this value is always less than or equal to the value obtained from the optimal linear control formulation (5.56). Only in the case where $u_{\text{out}} = -\ell_{\text{out}}$ and $u_{\text{inp}} = -\ell_{\text{inp}}$ will one obtain the same

performance. Physically, this corresponds to the situation where the process is operating at a setpoint where the actual steady-state input level, with $d = 0$, lies exactly half-way between the upper and lower bounds on the actual input signal.

An important point to note is that the above equality in performance between a linear and a nonlinear controller is a consequence of the choice of objective function, where performance is assessed on the basis of the response to the critical disturbances (which are equal in absolute magnitude). However, if the control performance is compared for a number of disturbances of different sizes within the given range, then linear control will always be inferior to nonlinear control. The reason for this is because the input action for a disturbance of size Δd will be halved for a disturbance of size $0.5\,\Delta d$. In this way, the input action is made unnecessarily conservative, resulting in sub-optimal control performance.

Another point to note is that the measure of dynamic operability determined from (5.58) and (5.59) may not necessarily be achievable by a single feedback controller. The determination of an *achievable* limit of performance for nonlinear controllers is a topic which is recommended for future research.

Example 5.3

Many of the important features mentioned above may be highlighted by considering the SISO regulatory example of Chapter 3. The aim here is to illustrate the potential benefits of nonlinear control when treating a range of disturbances. The plant and disturbance transfer functions are given by:

$$G_P(s) = \frac{2}{3\,s+1} \quad , \quad G_D(s) = \frac{0.5}{0.5\,s+1} \tag{5.60}$$

A simulation horizon of $L = 200$ time intervals is used, with a sampling time of 0.05 minutes. The process is assumed to have been linearized about the operating point given by $\left(y_{ss}^N = 0, u_{ss}^N = 0\right)$, with the nominal disturbance level d_0^N assumed to be zero. The upper and lower bounds on the disturbance trajectory are $d^+ = 0.4$ and $d^- = -0.4$ respectively. The corresponding critical points for the disturbance description considered are shown in Table 5.4.

The following hard constraints exist on the actual input and output signals:

$$| y_{\text{act}} | \leq 0.9 \quad , \quad | u_{\text{act}} | \leq 0.5 \tag{5.61}$$

The notation y_{act} and u_{act} is introduced here to emphasize that the bounds are on the actual responses and not on the deviational responses. In addition to the above constraints, there

Table 5.4: Critical points for the range of disturbances considered.

Critical Point	d_b	Δd
1	-0.4	0.8
2	0.4	-0.8

is the requirement that the output settles to within 0.01 of its desired steady-state value within 150 time increments. Furthermore, the manipulated input is required to settle to within 1% of its desired steady-state value within 150 time increments.

The measure of closed-loop performance is taken as the SSE of the outputs to the critical disturbances within the given range. Assuming that the process operates at the conditions given by $\left(y_{ss}^N, u_{ss}^N\right)$, the minimum achievable SSE subject to the input and output constraints mentioned above, under the assumption of linear control, is calculated to be 0.184. The same objective is achieved under nonlinear control due to the symmetry of the constraints about the nominal operating point and the symmetry of the critical point disturbances.

However, as the process setpoint is pushed towards its lower bound of -0.9, in search of improved economics, the constraints become skewed and the benefit of nonlinear control becomes more apparent. In order to illustrate the potential benefits of nonlinear control, Figures 5.5 and 5.6 show the system behavior at an operating point of $y_{ss} = -0.69$ under linear and nonlinear control respectively. From these figures it is clear that the assumption of linear control indirectly limits the input power available for rejecting the disturbance corresponding to critical point 2. As a consequence, the output behavior for critical point 2 is not as tight as is possible, preventing operation closer to the desired steady-state economic optimum.

This issue is further illustrated in Figure 5.7 where the minimum achievable SSE is plotted as a function of the process setpoint y_{ss}, for both linear and nonlinear control. In Chapter 3 it was shown that linear control allows for feasible operation over the range $y_{ss} \in [-0.69, 0.69]$. Nonlinear control, on the other hand, potentially allows for feasible operation over the range $y_{ss} \in [-0.77, 0.77]$ and enables operation closer to the desired steady-state economic optimum.

A steady-state analysis in Chapter 3 revealed that feasible operation is possible for y_{ss} in the range $y_{ss} \in [-0.8, 0.8]$. It is therefore clear that, even with a level of nonlinear control performance which may not be achievable, a back-off is required in order to cope with the disturbances-induced dynamic fluctuations. This again emphasizes the importance of considering dynamic aspects in such an analysis.

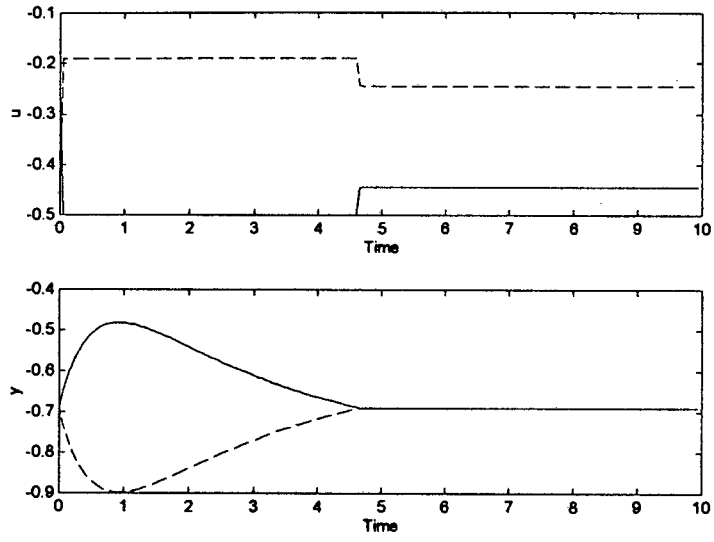

Figure 5.5: Optimal input and output trajectories under the assumptions of linear control at an operating point of $y_{ss} = -0.69$, for critical point 1 (—) and critical point 2 (--).

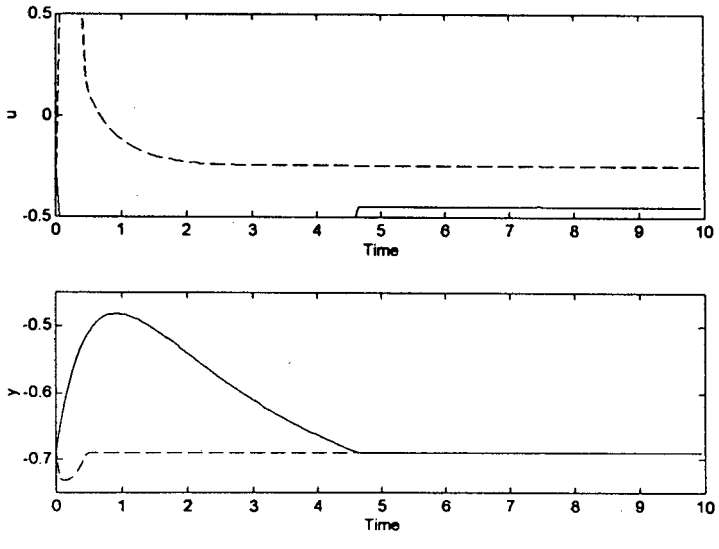

Figure 5.6: Optimal input and output trajectories under the assumptions of nonlinear control at an operating point of $y_{ss} = -0.69$, for critical point 1 (—) and critical point 2 (--).

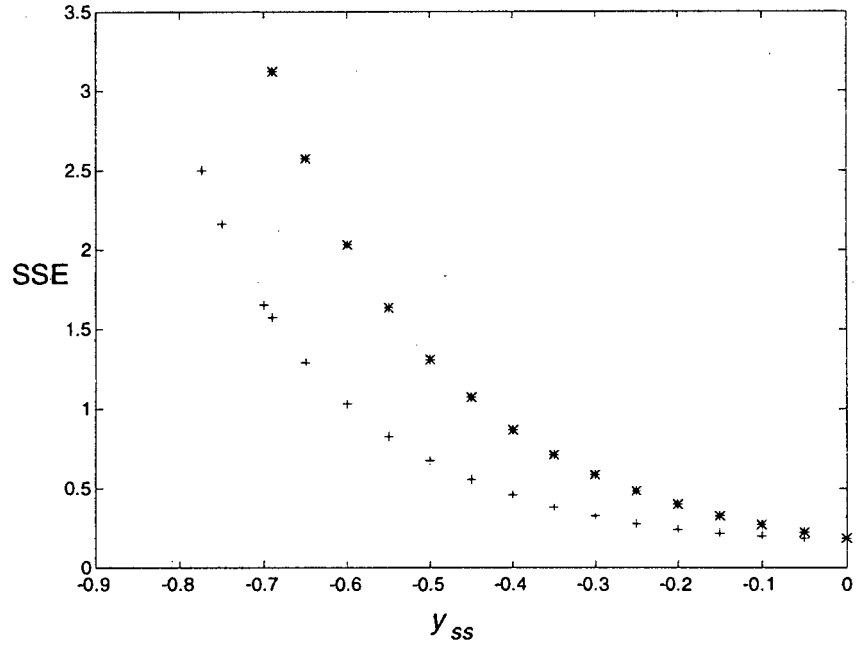

Figure 5.7: Variation of the minimum achievable SSE with the operating point y_{ss} for the cases of linear control (*) and nonlinear control (+).

5.2.2 Determination of Maximum Disturbance Range for Dynamic Feasibility

Using the open-loop formulation, it is possible to conveniently determine an alternative measure of dynamic operability based on the largest range of disturbances that a process can tolerate without violating dynamic feasibility requirements. Such a measure has been studied in a different context by a number of researchers in both the time domain (Pearson and Bamieh, 1990) and the frequency domain (Sobhani and Jayasuriya, 1994). The approach discussed below also has similarities with the approach of Dimitriadis and Pistikopoulos (1995) who address the issue of dynamic flexibility. In terms of their approach, the disturbance may be thought of as an uncertain parameter for which it is desired to determine the largest variation that be tolerated without violating dynamic feasibility constraints. The discussion below considers both linear and nonlinear control performance limits.

In order to determine the maximum possible disturbance range, the term Δd is included together with the input trajectories as search variables. It is thus necessary to augment the constraint coefficient matrix to include the terms involving Δd (and d_b). The notation

adopted earlier enables this to be done in a transparent fashion.

Determining the maximum disturbance range possible whilst ensuring dynamic feasibility may be formulated as a linear programming problem:

$$\begin{aligned} &\min_{x^1,\, x^2,\, \Delta d} -\Delta d \\ &\text{subject to} \\ x_j^1(k) &= 0 \quad \forall\, j = 1, \ldots, n_u \text{ and } \forall\, k = 1, \ldots, k^* \\ x_j^2(k) &= 0 \quad \forall\, j = 1, \ldots, n_u \text{ and } \forall\, k = 1, \ldots, k^* \\ \begin{pmatrix} \ell_{\text{out}} \\ \ell_{\text{out}} \\ \ell_{\text{inp}} \\ \ell_{\text{inp}} \end{pmatrix} &\leq \begin{bmatrix} \mathcal{P} & 0 \\ 0 & \mathcal{P} \\ I & 0 \\ 0 & I \end{bmatrix} \begin{bmatrix} x^1 \\ x^2 \end{bmatrix} + \begin{pmatrix} b_{\text{out}} \\ -b_{\text{out}} \\ b_{\text{inp}} \\ -b_{\text{inp}} \end{pmatrix} \Delta d \leq \begin{pmatrix} u_{\text{out}} \\ u_{\text{out}} \\ u_{\text{inp}} \\ u_{\text{inp}} \end{pmatrix} \end{aligned} \tag{5.62}$$

The constraints on x^1 and x^2 setting them to zero over the first k^* increments are to enforce causality, as in (5.22). To ensure that the outputs settle out to their desired values, the bounds ℓ_{out} and u_{out} are adjusted accordingly, and may also be tapered to ensure a given settling time is achieved. Considering (5.62), one is again faced with the two options of linear and nonlinear control, both of which are discussed below.

Optimal linear control

Under the assumption of a single underlying linear controller Q, it is necessary to impose the constraint that $x^2 = -x^1$. Eliminating x^2 from the optimization problem in (5.62) and utilizing the form of the constraint system, one obtains:

$$\begin{aligned} &\min_{x^1,\, \Delta d} -\Delta d \\ &\text{subject to} \\ x_j^1(k) &= 0 \quad \forall\, j = 1, \ldots, n_u \text{ and } \forall\, k = 1, \ldots, k^* \\ \begin{pmatrix} \ell^*_{\text{out}} \\ \ell^*_{inp} \end{pmatrix} &\leq \begin{bmatrix} \mathcal{P} \\ I \end{bmatrix} x^1 + \begin{pmatrix} b_{\text{out}} \\ b_{\text{inp}} \end{pmatrix} \Delta d \leq \begin{pmatrix} u^*_{out} \\ u^*_{inp} \end{pmatrix} \end{aligned} \tag{5.63}$$

where ℓ^*_{out}, ℓ^*_{inp}, u^*_{out} and u^*_{inp} are as in (5.57). It is thus possible to use the modified bounds so as to halve the number of constraints which need to be checked. Unfortunately, the constraints relating to the input trajectory are now general linear constraints due to the inclusion of Δd in the search variables. Nevertheless, they are efficiently handled by exploiting the considerable sparsity of the problem.

Optimal nonlinear control

By not enforcing the constraint $x^2 = -x^1$ it is possible, in many cases, to tolerate a greater disturbance range. The problem in (5.62) can be solved efficiently by utilizing the separable problem structure and splitting it into two *independent* optimization problems, namely:

$$\begin{aligned} & \min_{x^1,\,\Delta d} -\Delta d \qquad (5.64) \\ & \text{subject to} \\ x_j^1(k) &= 0 \quad \forall\, j = 1,\ldots,n_u \text{ and } \forall\, k = 1,\ldots,k^* \\ \begin{pmatrix} \ell_{out} \\ \ell_{inp} \end{pmatrix} &\leq \begin{bmatrix} \mathcal{P} \\ I \end{bmatrix} x^1 + \begin{pmatrix} b_{\text{out}} \\ b_{\text{inp}} \end{pmatrix} \Delta d \leq \begin{pmatrix} u_{\text{out}} \\ u_{\text{inp}} \end{pmatrix} \end{aligned}$$

and

$$\begin{aligned} & \min_{x^2,\,\Delta d} -\Delta d \qquad (5.65) \\ & \text{subject to} \\ x_j^2(k) &= 0 \quad \forall\, j = 1,\ldots,n_u \text{ and } \forall\, k = 1,\ldots,k^* \\ \begin{pmatrix} \ell_{out} \\ \ell_{inp} \end{pmatrix} &\leq \begin{bmatrix} \mathcal{P} \\ I \end{bmatrix} x^2 - \begin{pmatrix} b_{\text{out}} \\ b_{\text{inp}} \end{pmatrix} \Delta d \leq \begin{pmatrix} u_{\text{out}} \\ u_{\text{inp}} \end{pmatrix} \end{aligned}$$

The solution to (5.62) is then given by the smaller of the solutions to (5.64) and (5.65). It should once again be noted that only in the case where $u_{\text{out}} = -\ell_{out}$ and $u_{\text{inp}} = -\ell_{inp}$ will one obtain the same result for linear and nonlinear control. As mentioned above, exploiting the sparsity of the above problem will reduce the computation time considerably.

Example 5.4

The above theory is applied to the SISO example considered in section 5.2.1 of this chapter. The constraints on the input and output are as before. The maximum tolerable disturbance range under linear and nonlinear control is plotted in Figure 5.8 as a function of the operating point y_{ss}. Also indicated is the maximum disturbance range $\Delta d_{\max\ ss}$, as determined from a steady-state analysis of the problem.

The determination of $\Delta d_{\max\ ss}$ involves the solution of the following problem:

$$\begin{aligned} \Delta d_{\max\ ss} &= \max_{\Delta d} \Delta d \qquad (5.66) \\ & \text{subject to} \\ u_{\min} &\leq u_{ss}(y_{ss}, d_{b\,i}) \leq u_{\max} \quad , \quad \text{for } i = 1,2 \end{aligned}$$

The steady-state input at the base disturbance level d_{bi} is determined from the steady-state linear process model as follows:

$$u_{ss}\left(y_{ss}, d_{bi}\right) = G_P\left(0\right)^{-1}\left(y_{ss} - G_D\left(0\right) d_{bi}\right) \tag{5.67}$$

where $G_P\left(0\right) = 2$ and $G_D\left(0\right) = 0.5$ are the respective steady-state gains of the process and the disturbance. Now, due to the assumptions regarding the symmetry of the upper and lower bounds on the disturbance about a nominal value of zero, we have that $d_{b1} = -d_{b2}$ and $d_{bi} = -0.5\Delta d_i$. Therefore, the optimization problem takes the form:

$$\begin{aligned} \Delta d_{\max\ ss} &= \max_{\Delta d} \Delta d \\ &\text{subject to} \\ u_{\min} &\leq G_P(0)^{-1}(y_{ss} + 0.5 G_D\left(0\right) \Delta d\,) \leq u_{\max} \\ u_{\min} &\leq G_P(0)^{-1}(y_{ss} - 0.5 G_D\left(0\right) \Delta d\,) \leq u_{\max} \end{aligned} \tag{5.68}$$

where $u_{\max} = 0.5$ and $u_{\min} = -0.5$.

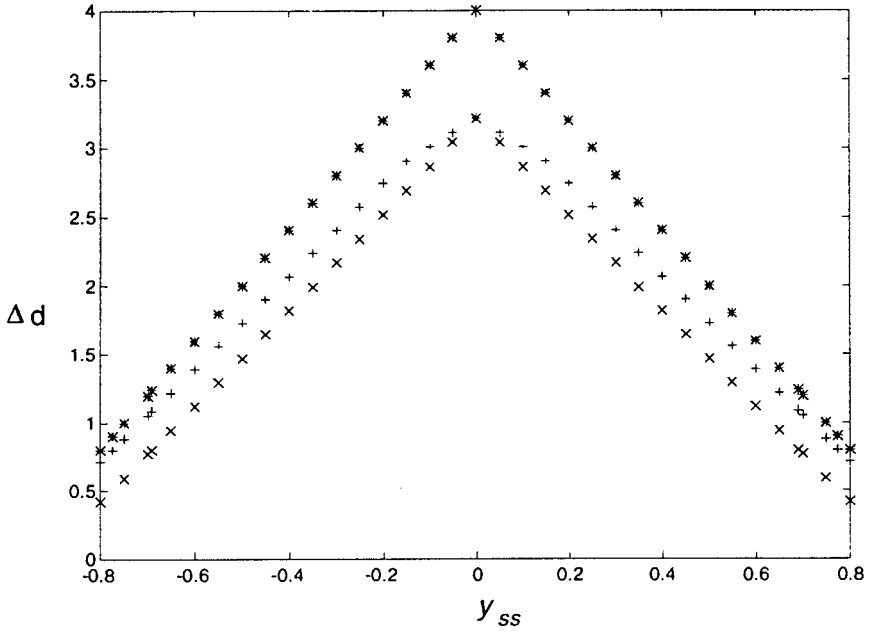

Figure 5.8: Variation of the maximum tolerable disturbance range with the operating point y_{ss} for both linear ($\times$) and nonlinear control ($+$), as well as the steady-state case ($*$).

It should be noted in Figure 5.8 that, for linear control, $\Delta d_{\max} = 0.8$ at $y_{ss} = -0.69$. This result is closely related to the economic formulation used in Chapter 3, where it was determined that, with $\Delta d = 0.8$, the minimum achievable value for y_{ss}, in the absence of a

quadratic performance constraint, is given by $y_{ss} = -0.69$. A similar agreement exists for nonlinear control where $\Delta d_{\max} = 0.8$ for $y_{ss} = -0.77$.

As in the case of the SSE measure of dynamic operability, the potential benefits achievable via nonlinear control are clear from Figure 5.8, particularly when operating close to the input constraints. A useful feature of the maximum disturbance measure is that the problem always has a feasible solution, provided that the steady-state operating conditions are feasible, and it therefore always provides quantitative information. It may sometimes also be more intuitive for a design engineer to make decisions based on the maximum tolerable disturbance range as opposed to an SSE measure.

5.3 Problems Involving Model Uncertainty

In Chapter 4 it was shown how dynamic operability may be assessed in the presence of structured nonlinear/time-varying model uncertainty. In this section further details of the problem formulation are presented, with the view of highlighting how reductions in computational time may be achieved. Only the servo problem will be considered, with the principles being identical for regulatory problems. As an example of the insights that can be gained by analyzing the problem structure it will be shown how the robust stability constraints impact on the input behavior.

5.3.1 Basic Formulation for Servo Problems

Using a weighted least squares objective function as a measure of the closed-loop performance, dynamic operability assessment in the presence of structured ℓ_1 model uncertainty may be posed as the following nonconvex optimization problem:

$$\min_{Q,r,\beta} (A_{\text{out}} q - y_{set})^T \Lambda \, (A_{\text{out}} q - y_{set}) \tag{5.69}$$

subject to

$$\begin{aligned}
y_\ell &\leq A_{\text{out}} q \leq y_u \\
u_\ell &\leq A_{\text{inp}} q \leq u_u \\
m_{ij}(k) - \beta_{ijk} &\leq 0 \\
m_{ij}(k) + \beta_{ijk} &\geq 0 \\
\sum_{j=1}^{SM} \frac{r_{jpert}}{r_{ipert}} \sum_{k=0}^{L} \beta_{ijk} &< 1 \quad \forall i = 1, ..., SM
\end{aligned}$$

$$
\begin{aligned}
r_i &> 0 \\
\beta_{ijk} &\geq 0
\end{aligned}
$$

For individually applied setpoint changes the vector y_{set} is given by:

$$
y_{set} = \left[\underbrace{y_{set\,1}, \ldots, y_{set\,1}}_{L+1}, \ldots, \underbrace{y_{set\,n_y}, \ldots, y_{set\,n_y}}_{L+1} \right]^T \tag{5.70}
$$

The diagonal matrix Λ is a weighting matrix, u_ℓ and u_u are the respective lower and upper bounds on the deviational input responses, and y_ℓ and y_u refer similarly to the deviational output responses.

The nonconvexity introduced by the scaling factors r is dealt with by using a combination of convex quadratic programming and standard nonlinear programming. The above problem has significant sparsity in the objective function and constraint system. In order to exploit the sparsity in the objective function, additional search variables are introduced as follows:

$$
p = A_{\text{out}} q - y_{set} \tag{5.71}
$$

The constraints on the output behavior may now written as bounds on p and take the form:

$$
y_\ell - y_{set} \leq p \leq y_u - y_{set} \tag{5.72}
$$

As a result, the dynamic operability assessment problem may be posed as follows:

$$
\min_{Q,r,\beta,p} p^T \Lambda p \tag{5.73}
$$

subject to

$$
\begin{aligned}
p &= A_{\text{out}} q - y_{set} \\
u_\ell &\leq A_{\text{inp}} q \leq u_u \\
m_{ij}(k) - \beta_{ijk} &\leq 0 \\
m_{ij}(k) + \beta_{ijk} &\geq 0 \\
\sum_{j=1}^{SM} \frac{r_{jpert}}{r_{ipert}} \sum_{k=0}^{L} \beta_{ijk} &< 1 \quad \forall i = 1, \ldots, SM \\
r_i &> 0 \\
\beta_{ijk} &\geq 0 \\
y_\ell - y_{set} &\leq p \leq y_u - y_{set}
\end{aligned}
$$

Certain valuable insights may be gained by analyzing the structure of the above optimization problem. As an example of this, it was mentioned in Chapter 4 that for multiplicative input uncertainty, each of the SM robustness constraints relate directly to a particular input. An explanation of this is provided below.

5.3.2 Analysis of Problem Structure

For multiplicative input uncertainty, the interconnection matrix $M = w_i Q \tilde{P}$ has pulse response coefficients given by:

$$m_{ij}(k) = \sum_{\ell=1}^{NY} \sum_{r=0}^{k} \sum_{io=r}^{k} q_{i\ell}(r)\, \tilde{P}_{\ell j}(io - r)\, w_i(k - io) \tag{5.74}$$

By noting the form of the robust stability conditions

$$\sum_{j=1}^{SM} \frac{r_{jpert}}{r_{ipert}} \sum_{k=0}^{L} \beta_{ijk} < 1 \quad \forall i = 1, ..., SM \tag{5.75}$$

It is seen that the ith robust stability constraint relates only to β_{i**}, and consequently only to $m_{i*}(*)$. The notation β_{i**} means that all those elements of β for which the first subscript is i are present in the ith robust stability constraint. From (5.74), we see that the ith robust stability constraint relates only to q_{i*}. This is due to the type of model uncertainty assumed and a different relation would hold if the uncertainty had been multiplicative output uncertainty.

Now, for setpoint changes applied individually, the input response at time increment i_o of the ith input to the jth setpoint change is given by:

$$s_{(n_y+i)\,j}(i_o) = y_{set\,j} \sum_{k=0}^{i_o} q_{i\,j}(k) \tag{5.76}$$

From the above it is clear that the behavior of ith input is determined only by q_{i*}. The notation $s_{(i+n_y)\,j}$ is used to define the ith input response since s_{ij} for $i \leq n_y$ refers to the ith output response. Combining this result with the earlier one it is seen that the ith robust stability constraint has a direct impact only on behavior of the ith input (albeit to both setpoint changes and not one unique setpoint change).

It should also be noted, that for servo problems with model uncertainty, it is possible to implement a type of open-loop formulation due to the form of (5.76). This can be done because it is possible to define the $q_{ij}(k)$ coefficients in terms of the input response. From (5.76) it can be seen that:

$$\begin{aligned} q_{ij}(0) &= \frac{s_{(n_y+i)\,j}(0)}{y_{set\,j}} \\ q_{ij}(k) &= \frac{s_{(n_y+i)\,j}(k) - s_{(n_y+i)\,j}(k-1)}{y_{set\,j}} \qquad \forall\, k = 1, ..., L \end{aligned} \tag{5.77}$$

By performing the above change-of-variables, the input constraints are transformed to simple bounds, which will reduce the computation time even further. Such a procedure is not

possible if multiple setpoint changes are made simultaneously, neither is possible for regulatory problems. In both these instances $s_{ij}(i_o)$ is a function of q_{i*}, which prevents one from writing q_{ij} in terms of s_{ij}. For example, the input responses for regulatory problems with a single disturbance, take the form:

$$s_i(i_o) = -d \sum_{m=1}^{n_y} \sum_{k=0}^{i_o} q_{(i-n_y)\,m}(k) \sum_{v=k}^{i_o} G_{D\,m}(v-k) \tag{5.78}$$

which clearly does not allow the coefficients of q to be expressed uniquely in terms of the input response.

Stated differently, the robust stability constraints cannot be factorized into a part which relates to the input trajectory. For this reason the open-loop approach has not been implemented for problems with model uncertainty but is simply noted here for completeness.

5.4 Multi-Rate Problem Formulations

The computational benefits achievable thus far have been gained without any loss in accuracy. The structure and sparsity of the problems have been exploited to reduce computation. In the absence of model uncertainty it has been shown how dynamic operability assessment may be posed in an open-loop optimal control manner. The computational benefits of this formulation have been explained and presented through application examples.

In this section it is shown how the open-loop formulation allows an additional insight into the problem which may significantly improve computational times. In contrast to the discussions of the earlier sections, the optimal solution is approximated in some manner. It will nevertheless be shown that a high degree of accuracy may still be obtained.

The basic premise involves keeping the input behavior constant for more than one sampling period. In this way the number of search variables required is dramatically reduced. This idea is illustrated graphically in Figure 5.9 where an arbitrary input trajectory is plotted as a function of time. The behavior of the input is such that it is vigorous initially but then gradually settles out to its steady-state value. After L_1 sampling periods it is clear that if the input action were held constant for more than one time increment, the difference in the output trajectory would be negligible. Since the inputs are held constant for more than one time increment it is not necessary to include the "redundant" inputs in the optimization problem. As a result, considerable reduction in the search-space dimension may be achieved. This improvement is gained at the expense of a slightly conservative solution. It should be

noted that the sampling time for the output response should be kept constant, at its original value, in order to prevent additional approximations to the solution from being introduced.

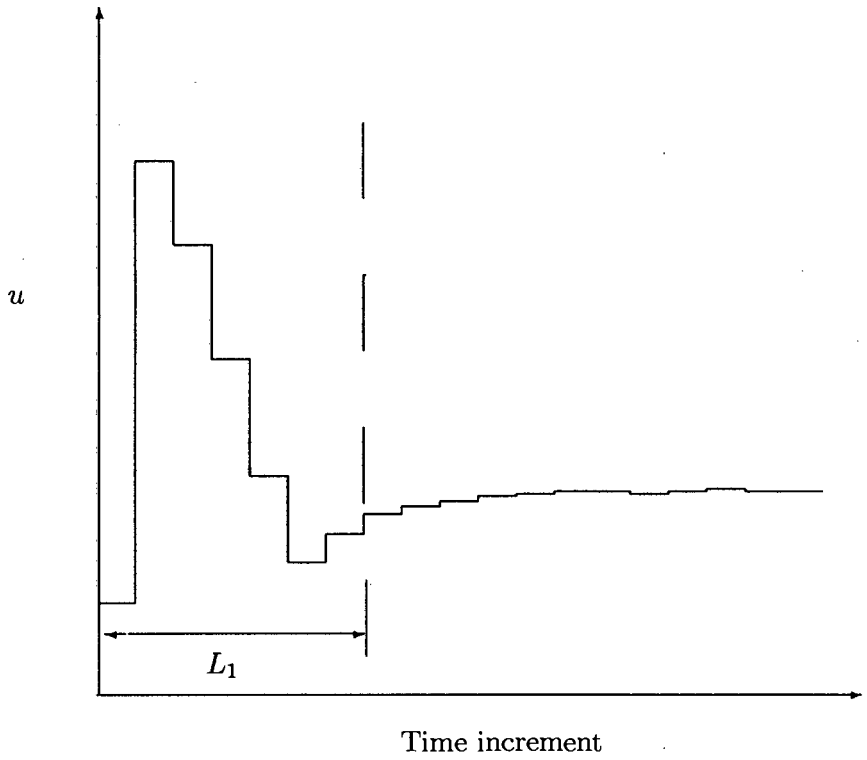

Figure 5.9: Arbitrary input trajectory to illustrate the benefits achievable by using a multi-rate problem formulaion for dynamic operability assessment.

Therefore, what is done is to split the simulation horizon of L time increments into two parts. The first part contains L_1 sampling points where the sampling time is as for the original problem formulation. The second part contains L_2 sampling points, where the sampling time is $(L-L_1)/L_2$ times larger than the original sampling period. The number of sampling periods for which the input action is held constant denoted as *nsteps*. In other words, the simulation horizon $L = L_1 + nsteps * L_2$.

In terms of the open-loop formulation introduced in this chapter, the following constraints are placed on the response of the ith input to the jth element of w:

$$x_{ij}(k) = x_{ij}(k+1) = ... = x_{ij}(k+nsteps-1) \quad \forall\, k \in K \tag{5.79}$$

where

$$K = \left\{ \underbrace{L_1, L_1 + nsteps, ..., L_1 + nsteps.\,(L_2 - 1)}_{L_2} \right\} \tag{5.80}$$

5.4.1 Application to Servo Control Problems

The multi-rate technique is applied to the multivariable distillation column servo control problem considered in section 5.1.3 of this chapter. The results are summarized in Table 5.5, where the minimum achievable SSE and computation time are shown for a number of different choices of L_1 and L_2. The number of sampling periods for which the input is held constant is given by $(L - L_1)/L_2$.

Table 5.5: Minimum achievable SSE and solution time for various combinations of L_1 and L_2 using the multi-rate formulation for servo problems.

L_1	L_2	**Objective function**	**Solution time (sec)**
0	100	58.91	22.0
0	50	58.98	6.4
0	25	59.08	2.1
0	20	59.69	1.8
20	20	58.91	4.7
10	30	58.91	5.9
10	15	58.91	2.5
10	9	58.92	1.1

From Table 5.5, it is seen that the objective function is relatively insensitive to the multi-rate approximation and that a considerable reduction in computation is achievable without significant loss in accuracy. In fact, choosing $L_1 = 10$ and $L_2 = 9$ allows for great accuracy to be achieved concurrently with an 80-fold reduction in computation time as compared to the standard Q-parametrization approach (shown in Table 5.2).

5.4.2 Application to Regulatory Control Problems

The multi-rate technique is applied to the flotation circuit regulatory control problem considered in section 5.1.2 of this chapter. The results are summarized in Table 5.6 for various combinations of L_1 and L_2.

Table 5.6: Minimum achievable SSE and solution time for various combinations of L_1 and L_2 using the multi-rate formulation for regulatory problems.

L_1	L_2	**Objective function**	**Solution time (sec)**
0	200	24.02	47.0
100	50	23.97	28.5
50	50	24.00	15.8
40	40	24.02	10.5
20	20	24.37	3.5
10	19	25.21	1.6

As was the case with the servo problem, considerable reduction in computation time is possible without sacrificing significant accuracy.

5.4.3 Application to Problems with Model Uncertainty

When model uncertainty is present, it is not possible, in general, to use the open-loop formulation presented through much of this chapter. As a result, the multi-rate formulation considered thus far is not directly applicable.

An approach which, at least for servo problems, is equivalent in concept to the multi-rate idea used thus far, is to set every alternate element of q to zero after the first L_1 time increments. This may be seen from the expression for the input response to individually applied setpoint changes:

$$s_{ij}(i_o) = y_{set\,j} \sum_{k=0}^{i_o} q_{(i-n_y)j}(k) \tag{5.81}$$

Clearly, setting $q_{(i-n_y)j}(i_o+1) = 0$ results in

$$\begin{aligned} s_{ij}(i_o+1) &= y_{set\,j} \sum_{k=0}^{i_o+1} q_{(i-n_y)j}(k) \\ &= y_{set\,j} \sum_{k=0}^{i_o} q_{(i-n_y)j}(k) \\ &= s_{ij}(i_o) \end{aligned} \tag{5.82}$$

which is required by the multi-rate formulation (for $n_{steps} = 2$).

Unfortunately, the same idea cannot be applied to regulatory problems. This is because the requirement for the input action to remain constant over two time increments *does not*

correspond to setting a particular element of q to zero. For example, even for a SISO process, the input action at consecutive increments is given by:

$$s_i(i_o) = -d\sum_{k=0}^{i_o} q(k) \sum_{v=k}^{i_o} G_D(v-k) \tag{5.83}$$

$$s_i(i_o+1) = -d\sum_{k=0}^{i_o+1} q(k) \sum_{v=k}^{i_o+1} G_D(v-k) \tag{5.84}$$

Setting $q(i_o+1)=0$ results in

$$\begin{aligned} s_i(i_o+1) &= -d\sum_{k=0}^{i_o} q(k) \sum_{v=k}^{i_o+1} G_D(v-k) \\ &\neq s_i(i_o) \end{aligned} \tag{5.85}$$

As a consequence of the above, the multi-rate formulation discussed thus far is not used for problems with model uncertainty.

Despite this, it may be possible to obtain significant reductions in computation time by applying a multi-rate type of idea to the robustness constraints (as opposed to the input response). The motivation behind this is the fact that often the elements of $m_{ij}(k)$, and thus β_{ijk}, are mainly zero after the initial transients have died out.

To illustrate this point, Figure 5.10 is a plot of the elements of β for the problem considered in Chapter 4, with delay structure B_1 and unstructured model uncertainty. The subplots have been laid out in a fashion which is consistent with the constraints on the row sums. That is, the sum of the elements of β_{11} and β_{12} needs to be less than or equal to unity; and similarly for β_{21} and β_{22}. Clearly the majority of the elements of β_{ijk} are zero, particularly after the first 40 time increments.

This feature may be exploited by doubling the sampling time used in the robustness constraints after the first L_1 sampling periods. This decreases the dimension of β and correspondingly reduces the number of robust stability constraints needed. The robust stability constraints then take the form:

$$\inf_R \left\{ \max_i \sum_{j=1}^{SM} \frac{r_{jpert}}{r_{ipert}} \left[\sum_{k=0}^{L_1-1} |m_{ij}(k)| + \sum_{k\in K} |m_{ij}(k)+m_{ij}(k+1)| \right] \right\} < 1 \quad , \quad r_i > 0 \tag{5.86}$$

where

$$K = \left\{ \underbrace{L_1, L_1+2, ..., L_1+2(L_2-1)}_{L_2} \right\} \tag{5.87}$$

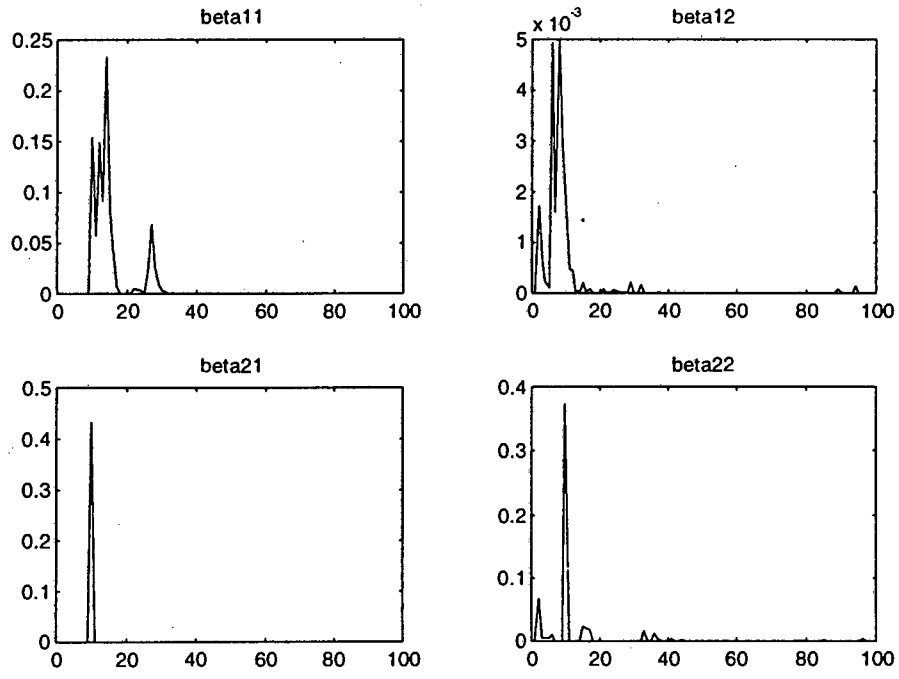

Figure 5.10: The elements of β for the multivariable distillation example considered in Chapter 4.

Strictly speaking, the robustness constraints are actually being *loosened* because of the fact that:

$$|m_{ij}(k)| + |m_{ij}(k+1)| \geq |m_{ij}(k) + m_{ij}(k+1)| \qquad \text{for } k \in K \tag{5.88}$$

However, since the values of $m_{ij}(k)$ are generally very small later on in the simulation horizon, the error introduced is should be not significant. Preliminary experience has shown that such an idea may have potential for reducing the computational time required to treat problems involving model uncertainty. This issue is, however, recommended for future research and is not considered further in this thesis.

Chapter 6

Case Study - The Dynamic Operability of Alternative Flotation Circuit Designs

In this section the Q-parametrization approach is applied to the screening of alternative three-bank flotation circuit designs. The circuits were considered first in a study by Barton *et al.* (1991). Two different implementations of the Q-parametrization approach are presented and applied to the problem. The first involves determining the best achievable closed-loop performance of each of the flowsheets at fixed operating conditions, for a range of disturbances. Use of these results in conjunction with a steady-state economic measure enables the generation of a noninferior set of flowsheets. This set has the property that no circuit in it has both better dynamic operability and steady-state economics than another circuit in the set. In this manner, inherently inferior circuits are screened from further consideration.

The second approach presented involves determining the operating conditions which maximize some economic measure subject to constraints on the quality of the closed-loop performance. This enables a comparison of alternative circuits according to a common economic basis and permits screening in this manner. The two approaches are closely related and the results obtained with each are compared and discussed.

6.1 Flotation Circuit Modelling

Flotation circuits are mainly used in the minerals processing industry to separate valuable minerals from gangue material. The separation is achieved in a flotation cell, where a slurry of gangue (worthless) material and valuable material is pumped into an air-sparged tank, shown schematically in Figure 6.1. The notation used in Figure 6.1 will be adopted in the subsequent model development and is described in greater detail there.

Various chemicals are added to the slurry to promote a stable froth layer and to make the surface of the valuable material more hydrophobic than the gangue material. Being more hydrophobic, the valuable particles preferentially adhere to the air bubbles and are carried into the froth layer, producing a concentrate stream of higher grade than the feed. Conversely, the tailing stream is of lower grade than the feed and is withdrawn from the lower or pulp zone of the tank. In industrial flotation processes, a number of cells are physically joined together to form a flotation bank, with the concentrate and tailings from a bank comprising of the concentrates and tailings from the individual cells in the bank.

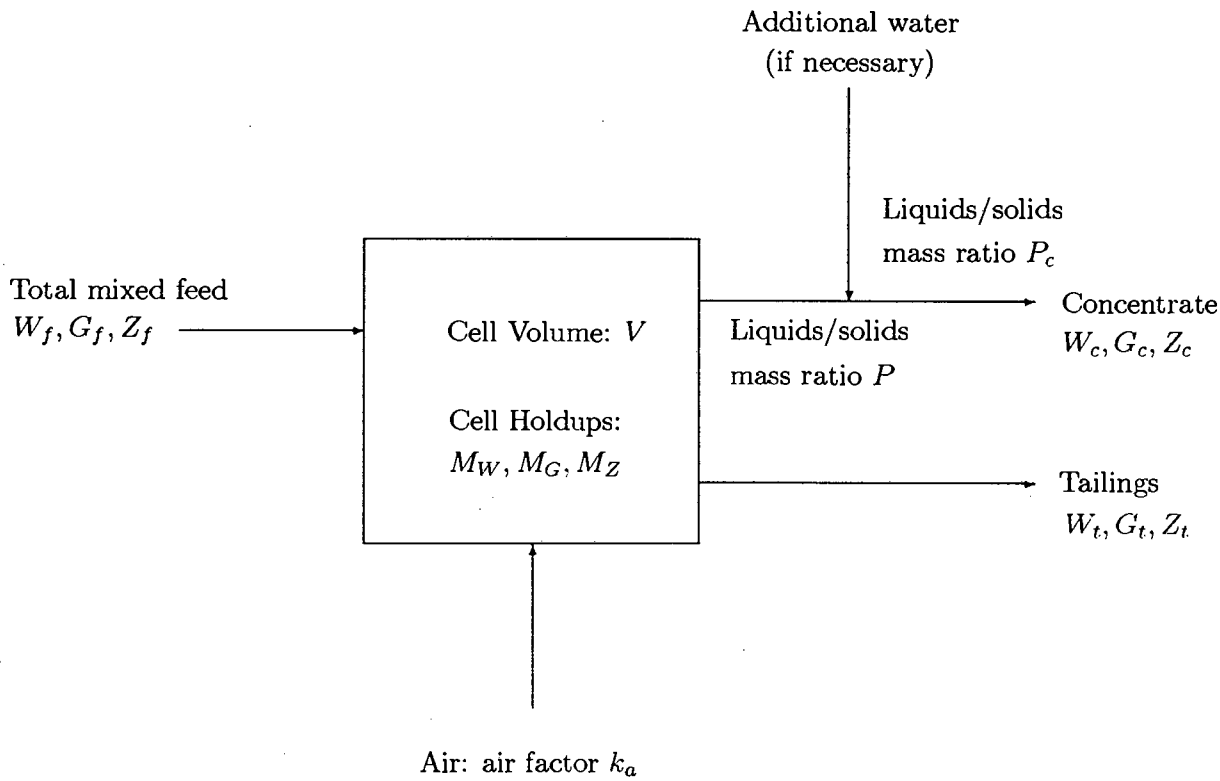

Figure 6.1: Air-sparged flotation cell for the separation of gangue and valuable material.

6.1.1 Mathematical Model of the Flotation Circuit

As the dynamic operability analysis is to be carried out at the early design stages, a fairly simple dynamic model of the flotation circuit is used, with the main aim being to capture the essential dynamic features present in a flotation circuit. The model assumptions used are those of Barton *et al.* (1991) and are as follows:

1. The various minerals present in the ore can be classified, for simplicity, in terms of gangue and valuable material.
2. Each bank in the circuit is modelled as a single flotation cell.
3. Perfect level control is maintained within each cell.
4. The contents of a cell are well-mixed.
5. The flotation rates of the gangue and valuable material are modelled using first-order kinetics.
6. The effect of air flowrate on the flotation kinetics is modelled by an air factor, k_a, which increases the flotation rate of both the gangue and the valuable material.
7. The air flowrate to each bank in the circuit is the same.

The above assumptions are consistent with other assumptions used in the literature (Lynch *et al.*, 1981) and are appropriate for the nature of the study. The weakest assumption is that of perfect level control, as this is seldom achieved in practice (Schubert, 1996).

Using the assumptions given above, the following differential-algebraic model equation system may be developed. The equation system developed below is for a single cell/bank and thus the equation system for the entire circuit would involve three such sets of equations connected appropriately. The nomenclature is based on that of Figure 6.1, where W, G and Z refer to water, gangue and valuable material respectively.

Unsteady-state mass balances around the cell lead to:

$$\begin{aligned} \frac{dM_G}{dt} &= G_f - G_c - G_t \\ \frac{dM_Z}{dt} &= Z_f - Z_c - Z_t \end{aligned} \tag{6.1}$$

where M_i refers to the mass holdup of component i in the cell. The subscript f refers to the mass flow of a particular component in the feed stream and c and t apply in a similar manner to the concentrate and tailings streams respectively.

By definition of the cell volume (V) one obtains:

$$\frac{M_W}{\rho_W} + \frac{M_G}{\rho_G} + \frac{M_Z}{\rho_Z} = V \tag{6.2}$$

From the assumption of perfect level control, one obtains:

$$\left[\frac{W_f}{\rho_W} + \frac{G_f}{\rho_G} + \frac{Z_f}{\rho_Z}\right] - \left[\frac{P(Z_c + G_c)}{\rho_W} + \frac{G_c}{\rho_G} + \frac{Z_c}{\rho_Z}\right] - \left[\frac{W_t}{\rho_W} + \frac{G_t}{\rho_G} + \frac{Z_t}{\rho_Z}\right] = 0 \tag{6.3}$$

where P is defined as the liquids to solids mass ratio of the concentrate stream exiting the cell, prior to water addition.

The assumption of a well-mixed cell gives:

$$\begin{aligned} \frac{G_t}{W_t + G_t + Z_t} &= \frac{M_G}{M_W + M_G + M_Z} \\ \frac{Z_t}{W_t + G_t + Z_t} &= \frac{M_Z}{M_W + M_G + M_Z} \end{aligned} \tag{6.4}$$

The assumptions regarding the flotation kinetics and the effect of the air factor on the flotation rate lead to:

$$\begin{aligned} G_c &= k_a K_G M_G \\ Z_c &= k_a K_Z M_Z \end{aligned} \tag{6.5}$$

where K_G and K_Z refer to the flotation rates of the gangue and valuable material. From the above two relations it is clear that changes in the air flowrate result in instantaneous changes in the concentrate flows of the gangue and valuable material. This may perhaps seem unrealistic, but Schubert (1996) reports this to be fairly typical behavior for industrial plants, where the response time between air flowrate and concentrate flow is generally only one or two minutes.

Specification of the pulp density of the concentrate stream, after the addition of water, sets the water content of that stream as follows:

$$W_c = P_c(Z_c + G_c) \tag{6.6}$$

where P_c is the liquids to solids mass ratio of the concentrate stream after water addition.

6.2 Flotation Circuits Considered

Barton *et al.* (1991) considered eleven alternative three-bank flotation circuits in their dynamic operability analysis; about half of these being similar in layout to circuits used industrially and the rest being more unconventional.

In the current study, a preliminary screening of the eleven flowsheets was performed and only those flowsheets having steady-state recoveries (defined as the ratio of valuable material in the final concentrate stream to that in the feed) in excess of 90% were considered for further analysis. This reduced the number of flowsheets under consideration from eleven to the six shown in Figure 6.2, with the original numbering being maintained. In the figure, the upper stream leaving a bank is the concentrate stream, with the lower stream being the tailings.

Indicated on the figure are the cell volumes for each bank within a given circuit. These volumes were determined by Barton *et al.* (1991) by optimizing the steady-state recovery (R) of a given flowsheet at the operating conditions and material physical properties shown in Table 6.1. The constraints placed on the optimization are the requirement of a 60% grade (dry mass fraction of valuable material) for the final concentrate stream and a maximum total plant capacity of 54m^3.

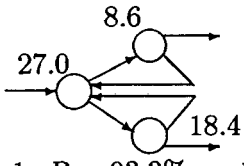

Flowsheet 1: $R = 93.3\%$

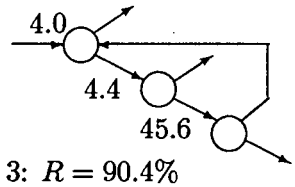

Flowsheet 3: $R = 90.4\%$

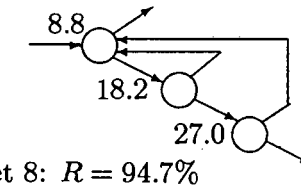

Flowsheet 8: $R = 94.7\%$

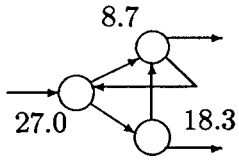

Flowsheet 2: $R = 93.6\%$

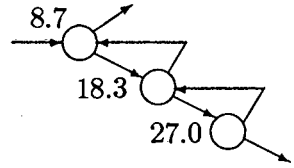

Flowsheet 4: $R = 94.4\%$

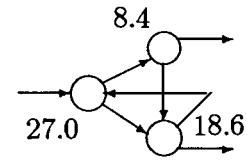

Flowsheet 9: $R = 91.1\%$

Figure 6.2: Alternative three bank flotation circuits considered.

As mentioned, the optimization of cell volumes was performed at fixed operating conditions. A more refined procedure would include the operating conditions, with their associated bounds and their impact on the steady-state economics, as search variables together with the cell volumes in the optimization. This was not done in Barton *et al.* (1991) and is thus not considered here, for the purpose of being consistent with their study. It will be seen that many important issues pertaining to the interrelationship between steady-state

economics and dynamic operability may be considered without the complications introduced by the inclusion of the effect of cell volumes into the problem formulation.

Table 6.1: Material physical properties and operating conditions for the flotation circuits considered.

	Water	**Gangue**	**Valuable**
Feed flowrate ($kg.min^{-1}$)	1022	1056	144
Density ($kg.m^{-3}$)	1000	3100	4000
Rate constant (h^{-1})	—	0.8	12.0
Liquids to solids mass ratios:	$P = P_c = 0.852$ (no water addition)		
Steady-state air factor:	$k_a = 1.0$		

From Figure 6.2 it is clear that flowsheets 1, 2 and 9 are of the rougher/cleaner/scavenger type while flowsheets 3, 4 and 8 are of the rougher/scavenger/re-scavenger type. Intuitively, one would expect the latter set to have difficulties coping with a feed disturbance as each of their first banks is small and the final product is taken directly from the first bank (except for circuit 3 where the product is a mixture of the concentrate from the first two banks).

6.3 Development of Transfer Function Models

It is assumed that the function of the control system is to provide good regulatory control of the final concentrate grade (G) and the recovery (R) of valuable material. The manipulated inputs to be used are the air factor k_a (which amounts to varying the air flowrate to a bank) and the feedwater flowrate w_f. As mentioned earlier, it is assumed that k_a is the same for each bank in the circuit. A single disturbance is considered, corresponding to step variations in the total feed solids flowrate within the range of -5% to $+5\%$ of the nominal total feed solids flowrate of $1200\,kg.\,min^{-1}$. The nominal disturbance level d_0^N, in deviational terms, is assumed to be zero.

To develop the transfer function models, step tests were performed and the dynamic responses of the grade and recovery were simulated by numerical integration of the differential-algebraic model equation system. The actual step sizes applied were a 0.1 increase in k_a, a $0.1\,ton.min^{-1}$ increase in w_f and a $120\,kg.min^{-1}$ increase in the total feed solids ($Z_c + G_c$). The resulting responses were converted to deviational form before fitting second-order lag with a first-order lead transfer functions to them.

As an example of the form of the transfer function models, the process transfer matrix for

flotation circuit 8 is given by:

$$\begin{bmatrix} G \\ R \end{bmatrix} = G_P \begin{bmatrix} k_a \\ w_f \end{bmatrix} + G_D\, d \tag{6.7}$$

where

$$G_P = \begin{bmatrix} \frac{-22.35\,(18.62\,s+1)}{(15.06\,s+1)(15.01\,s+1)} & \frac{11.52\,(14.23\,s+1)}{(11.53\,s+1)(11.53\,s+1)} \\ \frac{10.09\,(106.88\,s+1)}{(11.09\,s+1)(0.069\,s+1)} & \frac{-7.67\,(28.32\,s+1)}{(9.42\,s+1)(2.28\,s+1)} \end{bmatrix} \tag{6.8}$$

and

$$G_D = \begin{bmatrix} \frac{0.0087\,(5.72\,s+1)}{(11.76\,s+1)(11.76\,s+1)} \\ \frac{-0.0038\,(176.8\,s+1)}{(9.79\,s+1)} \end{bmatrix} . \tag{6.9}$$

The second-order transfer function model above fits the actual step response data with reasonable accuracy, as evidenced in Figures 6.3 to 6.8. The major difficulty is modeling the initial behavior accurately. Appendix B provides transfer matrix descriptions for the remaining circuits.

6.4 Dynamic Operability of Alternative Designs

6.4.1 Dynamic Operability at Fixed Operating Conditions

The approach adopted in this section is to use a measure of dynamic operability in conjunction with steady-state economic considerations to generate a noninferior set of flowsheets. The objective function used to measure the quality of closed-loop performance is chosen to be the time-weighted sum-of-square-errors of the outputs to the critical step-like feed disturbances in the range $[-60, 60]$ kg.min^{-1}. This form of objective function is convex and is chosen so as to penalize those flowsheets which are not able to rapidly reject the effect of the feed disturbance. The outputs are initially assumed to be equally weighted, but a different weighting is considered later on and its implications on the results are analyzed.

The two critical points to be considered are given in Table 6.2.

Table 6.2: Critical points for the range of disturbances considered.

Critical Point	d_b (kg.min^{-1})	Δd (kg.min^{-1})
1	-60	120
2	60	-120

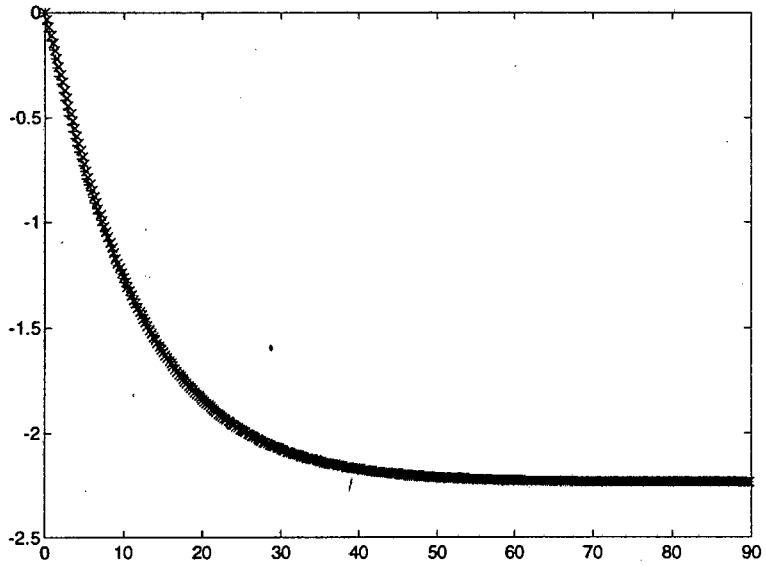

Figure 6.3: Flotation circuit 8: Actual (×) and model-fitted (+) responses of the grade to a step of 0.1 in the air factor k_a.

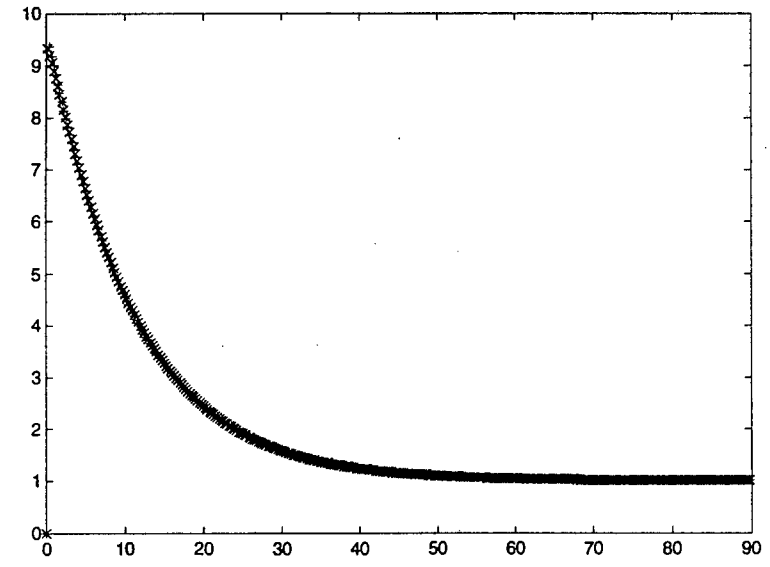

Figure 6.4: Flotation circuit 8: Actual (×) and model-fitted (+) responses of the recovery to a step of 0.1 in the air factor k_a.

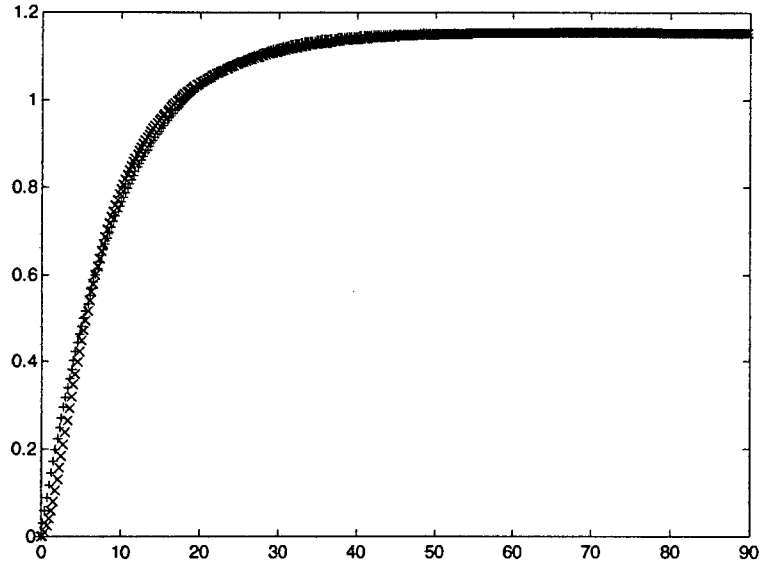

Figure 6.5: Flotation circuit 8: Actual (×) and model-fitted (+) responses of the grade to a step of 0.1 in the feedwater flowrate w_f.

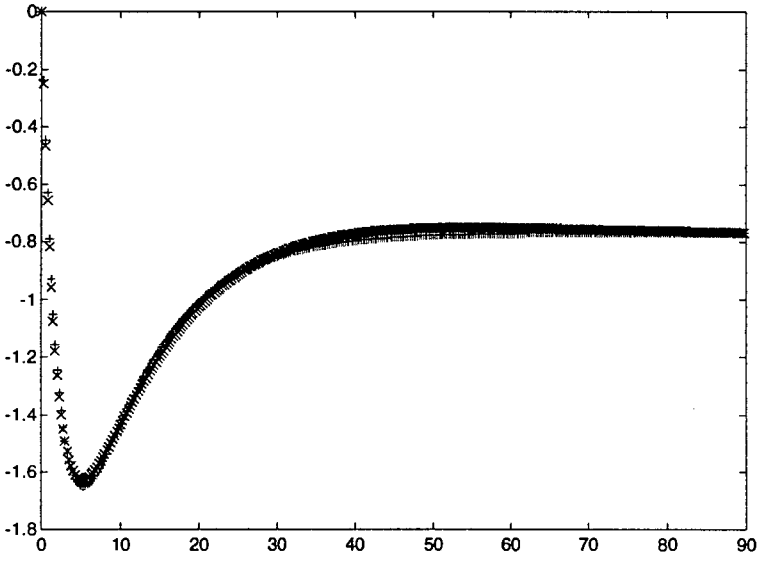

Figure 6.6: Flotation circuit 8: Actual (×) and model-fitted (+) responses of the recovery to a step of 0.1 in the feedwater flowrate w_f.

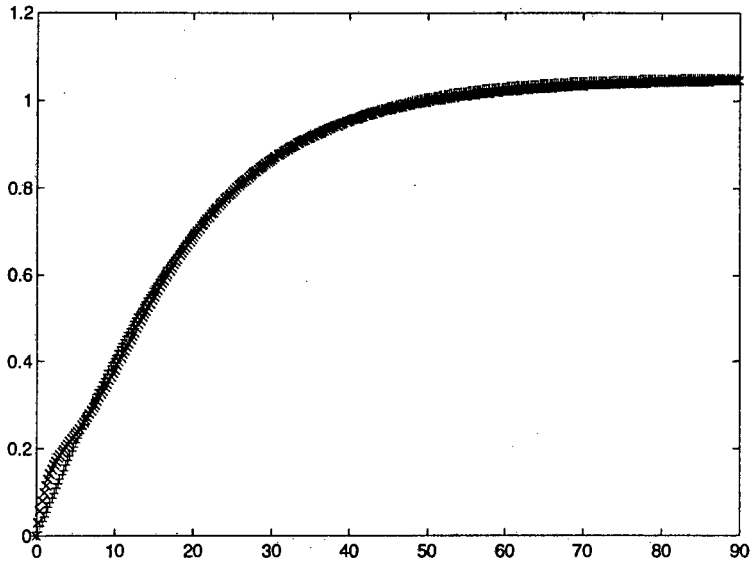

Figure 6.7: Flotation circuit 8: Actual (×) and model-fitted (+) of the grade to a step of 120 kg.min^{-1} in the feed disturbance.

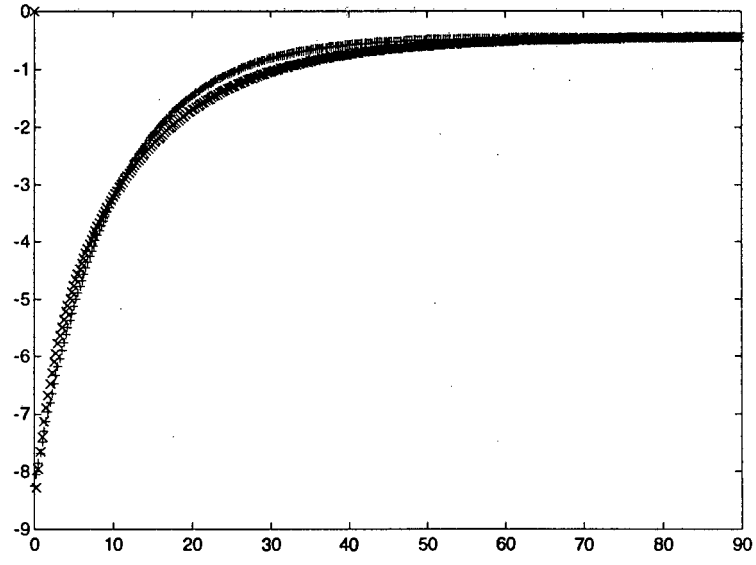

Figure 6.8: Flotation circuit 8: Actual (×) and model-fitted (+) of the recovery to a step of 120 kg.min^{-1} in the feed disturbance.

No bounds are placed on the output behavior, but the actual responses of the manipulated inputs are required to satisfy certain bounds. In particular, the actual value of the air factor k_a is constrained as follows:

$$0.9 \leq k_a \leq 1.1 \tag{6.10}$$

A number of different constraints on the actual feedwater flowrate w_f are considered, namely:

$$|w_f - 1.022| \leq \delta \quad \text{ton.min}^{-1} \tag{6.11}$$

where $\delta \in \{0.05\ ,\ 0.10\ ,\ 0.15\ ,\ 0.20\}$. The idea behind this is to determine how sensitive the results are to the level of input constraint on w_f. A similar treatment for k_a was found to be unnecessary as the air factor typically rises to its required steady-state value without any "overshoot". This is contrasted with w_f which was found to firstly move to an upper or lower bound before settling to its required steady-state level.

It should be noted that the units of the feed water flowrate have been scaled for convenience, in order that the inputs are of similar magnitudes. In many approaches to dynamic operability assessment scaling of the inputs is essential, but this is not the case here.

A sampling time of $\Delta t = 1$ minute and a simulation horizon of $L = 200$ minutes were chosen for the study. The mathematical formulation for the dynamic operability assessment problem at fixed operating conditions, for a range of disturbances, is as shown in Chapters 3 and 5 and is not repeated here. Table 6.3 shows the results achieved for each of the six flowsheets at different values of δ. Also indicated is the steady-state recovery and the value of any RHPT zeros, if such zeros are present in the process transfer function model $G_P(s)$.

Table 6.3: Dynamic operability measure (at different levels of input constraints), steady-state recovery and right-half-plane transmission (RHPT) zeros for the six flowsheets considered.

Flowsheet:	**1**	**2**	**3**	**4**	**8**	**9**
$\delta = 0.20$	7.6 e-7	1.8 e-4	44.3	581	209	3.0 e-7
$\delta = 0.15$	7.7 e-7	2.1 e-3	45.1	592	212	3.0 e-7
$\delta = 0.10$	8.7 e-7	1.5 e-2	46.3	606	216	3.2 e-7
$\delta = 0.05$	6.7 e-1	9.5 e-2	48.1	640	222	1.2 e-1
Recovery (%)	93.3	93.6	90.4	94.4	94.7	91.1
RHPT zero	—	—	0.0116	0.0065	0.0070	—

None of the flowsheets contain time delays and the effect of model uncertainty is only considered later on in this investigation. Thus, the only theoretical causes of poor dynamic operability at this stage are the presence of RHPT zeros and the fact that certain flowsheets may be more sensitive to input constraints than others.

Holt and Morari (1985b) have shown that RHPT zeros near the origin may cause serious control difficulties. The results in Table 6.3 illustrate this effect clearly, with the dynamic operability of those flowsheets containing RHPT zeros becoming progressively worse as the RHPT zeros become smaller in size. The results also confirm the intuition that the rougher/scavenger/re-scavenger circuits would be difficult to control. However, this kind of intuitive reasoning is not always possible, and furthermore, it provides one with no quantitative information as to how difficult the circuits are to control.

For the rougher/cleaner/scavenger circuits, which do not contain RHPT zeros, the ranking of the flowsheets, based on their dynamic operability, is a function of the level of input constraints considered. This is because the dynamic operability of circuit 2 does not worsen noticeably as the input constraints are tightened and is eventually better than, for example, circuit 1 when $\delta = 0.1$. This is a very beneficial property as it enables such a flowsheet to operate close to its constraints, and thus close to its economic optimum, without significant degradation in the quality of the closed-loop performance. This idea is given greater attention in the following subsection.

From the results in Table 6.3, it is possible to generate a set of 'noninferior' flowsheets where a pareto-optimal trade-off exists between dynamic operability and steady-state economics. This set has the property that no flowsheet in it has both better dynamic operability and steady-state economics, measured in terms of recovery, than any other flowsheet in the set. Figure 6.9 shows how the noninferior set is determined for the case where $\delta = 0.2$. In theory, the noninferior set is comprised of flowsheets 1, 2, 8 and 9. Common sense, however, would eliminate flowsheet 9 from this set due to its significantly poorer steady-state economics as compared to flowsheet 1, which has essentially the same dynamic operability.

An interesting point to note is that the elements comprising the noninferior set depends on the level of the input constraints. For $\delta = 0.20$ or greater, flowsheets 1, 2, 8 and 9 are all members, whereas for $\delta = 0.05$, only flowsheets 2 and 8 belong to the noninferior set. As mentioned earlier, this is because flowsheet 2 is not as sensitive to the input constraints as flowsheet 1 and 9.

Having determined the noninferior set, any further screening is made very difficult by the fact that it is hard to quantify the economic benefits of good control performance using the current formulation. One convenient means of doing this is presented by Young *et al.* (1996) and involves the optimization of an economic objective subject to constraints on the closed-loop behavior. In their approach only time domain bounds on the input and output behavior are considered, but the method readily allows for the inclusion of quadratic bounds on the

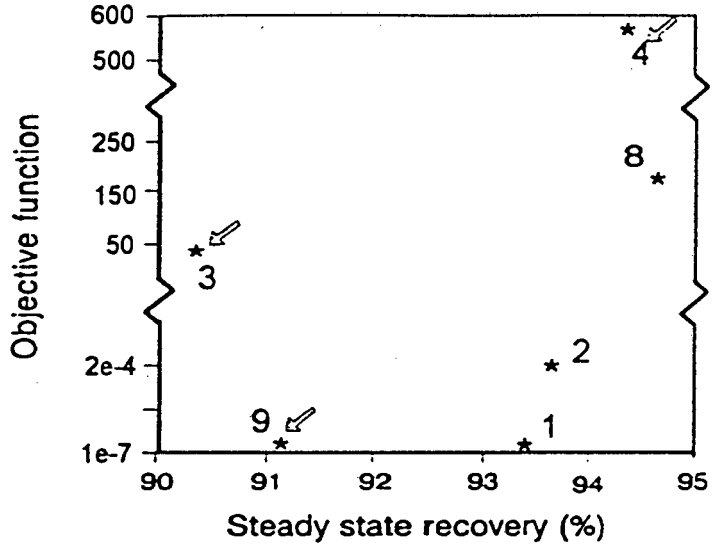

Figure 6.9: Trade-off between steady-state economics and dynamic operability for the six alternative flotation circuits considered. The inferior circuits are indicated with an arrow.

quality of the output behavior, as shown in Chapter 3. This is particularly beneficial as it ensures both bounded peak behavior and rapid settling. If a constraint were not enforced on the (weighted) SSE of the outputs then it is possible that the outputs may take very long to settle out, despite not deviating much in a peak sense from their desired steady-state value. Application of this approach to the flotation circuit case study is presented next.

6.4.2 Optimizing Steady-State Economics at a Specified Level of Dynamic Operability

The results of the previous section were obtained at fixed operating conditions. In practice the goal will be to drive the process as close as is possible to its economic optimum without significant degradation in control quality. Such degradation would result if the inputs are more tightly constrained when operating in close proximity to the steady-state economic optimum.

For simplicity, the economic performance measure is chosen to be the maximization of the steady-state recovery whilst maintaining the steady-state grade at 60%. Before considering the dynamic aspects of the problem, a purely steady-state analysis is adopted first, with

Table 6.4: Steady-state maximization of recovery subject to steady-state grade and input constraints.

Flotation Circuit	**Optimal R from steady-state analysis**	**Nominal steady-state recovery (%)**	**Maximum actual steady-state recovery (%)**
1	1.27	93.3	94.6
2	1.02	93.6	94.6
3	0.45	90.4	90.9
4	0.42	94.4	94.8
8	0.36	94.7	95.1
9	1.06	91.1	92.2

$\delta = 0.20$. The steady-state problem is posed as follows:

$$\max_{R,G} \; R \tag{6.12}$$

$$\text{s.t.} \quad \begin{bmatrix} -0.1 \\ -0.2 \end{bmatrix} \leq G_P(0)^{-1} \left(\begin{bmatrix} G \\ R \end{bmatrix} - G_D(0)\, d \right) \leq \begin{bmatrix} 0.1 \\ 0.2 \end{bmatrix} \quad \text{for } d = -60,\, 60$$

$$G = 0$$

where R and G are the recovery and grade at steady-state, expressed in deviational form about the nominal steady-state values used in the previous section. The steady-state gain matrix of the process is given by $G_P(0)$, and $G_D(0)$ is the disturbance gain matrix.

Using the steady-state gains given in Appendix B, the above problem may be solved for each of the six flowsheets, with the results being reported in Table 6.4. The actual recovery is given by the sum of the optimal R determined by solution of (6.12) and the nominal steady-state recovery indicated in Figure 6.2.

The results in Table 6.4 are slightly unexpected since circuits 3, 4 and 8 all required small steady-state inputs for the dynamic operability assessment considered in the previous section. Intuitively one might expect them to be able to handle a larger change in R before being limited by the input constraints. However, the nature of their steady-state gain matrices is such that the required steady-state input levels are very sensitive to changes in the steady-state recovery. The limiting constraint for circuits 1, 2 and 9 is the lower bound on w_f when $d = -60$. For circuits 3, 4 and 8 the limiting constraint is the lower bound on k_a when $d = -60$. Even if the bound on k_a is loosened these three circuits can still only achieve values of R in the range 0.5 to 0.6 before the lower bound on w_f at $d = -60$ becomes limiting.

This simple calculation is very useful as it gives one some indication of the potential economic benefits which may be derived if a process is able to operate near to its economic limit. The next step in the analysis is to quantify the extent to which this can be done when dynamic considerations are included. The theoretical background for treating such problems was provided in Chapter 3. A mathematical optimization is posed where the maximum achievable steady-state recovery is determined for each of the six flowsheets, subject to the former bounds on the input responses (with $\delta = 0.20$), together with the additional quadratic performance constraint:

$$\Phi = \sum_{c=1}^{2} \sum_{r=1}^{n_y} W_r \sum_{k=0}^{L} k \left[s_{r,c}(k) \right]^2 \leq \gamma \tag{6.13}$$

In the above constraint, W is a vector defining the relative importance of the outputs, with W_r being the rth element of this vector. For the case of equal weighting of the outputs, $W = \begin{bmatrix} 1 & 1 \end{bmatrix}^T$.

A number of different values of γ are considered in this study, namely $\gamma \in \{0.1,\ 1,\ 45,\ 210\}$, corresponding to needs ranging from tight control to fairly loose control. Table 6.5 shows the maximum actual recovery, based on dynamic considerations, for each flowsheet at the different values of γ, for the case where $\delta = 0.20$. As expected, none of the rougher/scavenger/re-scavenger circuits could satisfy the dynamic operability constraints for $\gamma = 0.1$ and $\gamma = 1$. It should also be noted that, for $\gamma = 0.1$, circuits 1, 2 and 9 need to 'back-off' from the maximum recovery given in Table 6.4 in order to satisfy the dynamic operability criterion.

Table 6.5: Maximum achievable steady-state recovery at various levels of dynamic operability for the six flowsheets considered.

Flowsheet:	**1**	**2**	**3**	**4**	**8**	**9**
$\gamma = 0.1$	94.3	94.5	—	—	—	92.0
$\gamma = 1$	94.6	94.6	—	—	—	92.1
$\gamma = 45$	94.6	94.6	90.8	—	—	92.1
$\gamma = 210$	94.6	94.6	90.9	—	95.0	92.1

The results show that if very tight control is essential, then flowsheet 2 appears to be the best choice, although flowsheet 1 should not be neglected. In fact, the economic performance of these two circuits is similar to that of flowsheet 8 and there is the additional benefit of very good control performance. This is because flowsheets 1 and 2 are inherently easy to control, thus enabling them to operate closely to their economic optima without significant degradation in control quality. If, however, it can be established that tight control is not essential, and say $\gamma = 210$ is acceptable, then flowsheet 8 is the best choice, as would be expected from the results of the previous section.

Determining the importance of good control depends on the problem at hand and, in particular, on the requirements of the downstream processes. For example, large fluctuations in the recovery from the flotation circuit correspond to feed disturbances in the subsequent unit operation, which may or may not influence the success of the overall plant operation.

Another important factor in the analysis that was alluded to earlier is the relative weighting of the outputs. In the above formulations the grade and recovery have been equally weighted in the quadratic control performance measure shown in (6.13). In practice it is more likely that only the grade will be required to be controlled tightly and therefore it may be appropriate to reduce the relative importance of the recovery in (6.13). This will enable more control effort to be geared toward achieving good grade control. Stated in terms of the research of Holt and Morari (1985b), one is effectively shifting the effect of the RHPT zero onto the least important output.

Using a weighting matrix $W = \begin{bmatrix} 1 & 10^{-3} \end{bmatrix}^T$ and resolving the dynamic operability assessment problems at constants operating conditions, the results are shown in Table 6.6 (for $\delta = 0.2$). The optimal output responses of flowsheet 8 for the two weightings considered are shown in Figures 6.10 and 6.11. From these responses it is clear that the grade control is significantly improved without seriously worsening the recovery control. In fact, the quality of grade control achievable for circuit 8, together with its high steady-state recovery means that such a circuit may often be a sensible choice in a practical environment.

Table 6.6: Minimum achievable time weighted SSE for each flowsheet using a modified weighting on the outputs.

Flowsheet:	**1**	**2**	**3**	**4**	**8**	**9**
Weighted SSE	3.0 e-7	8.0 e-5	9.4 e-2	9.2 e-1	3.0 e-1	3.0 e-7

6.4.3 Analyzing the Sensitivity of the Circuits to Model Uncertainty

Thus far the issue of model uncertainty has not been treated in this application example. As mentioned in Chapter 4, model uncertainty may have many possible sources ranging from poor model assumptions and poorly understood process dynamics, to measurement inaccuracies and imperfectly known model parameters, such as rate constants.

In terms of flotation circuits, a typical cause of model error would be uncertainty in the flotation rate constants K_G and K_Z, together with uncertainty on the exact manner in which the air flowrate affects the flotation kinetics. The major reason for this uncertainty typically

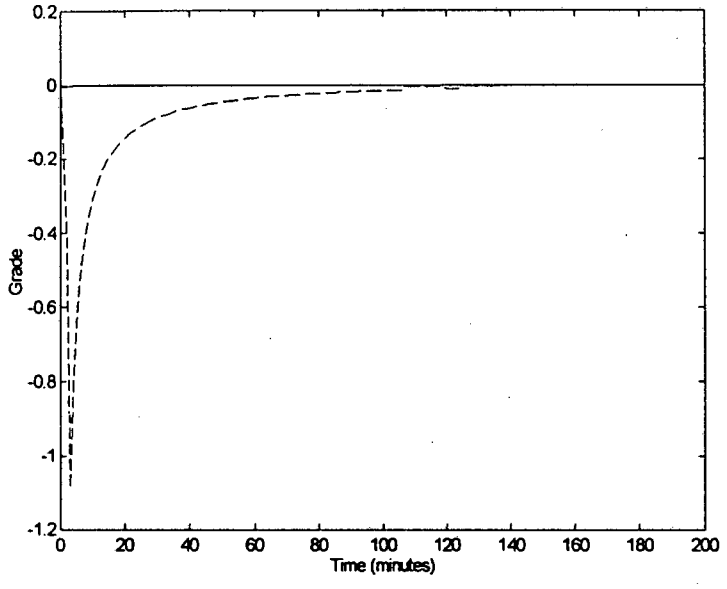

Figure 6.10: Optimal responses of the grade of circuit 8 to the feed disturbance for the cases where the outputs are equally weighted (--) and where the recovery weighting is reduced (-).

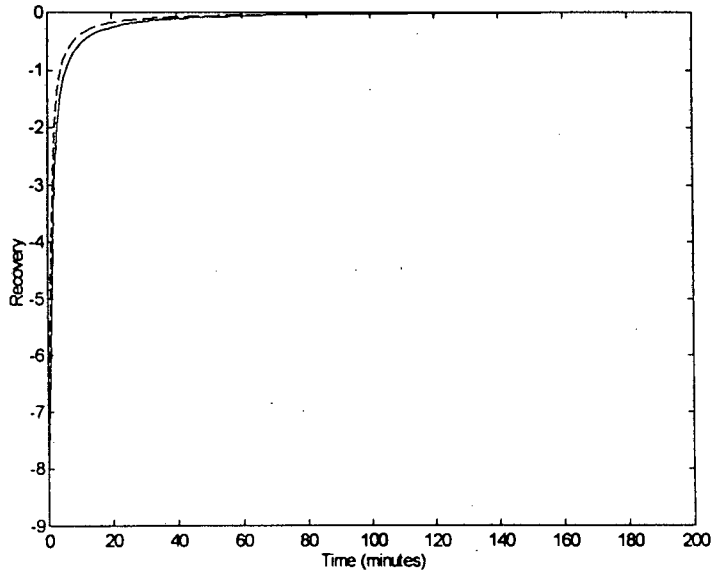

Figure 6.11: Optimal responses of the recovery of circuit 8 to the feed disturbance for the cases where the outputs are equally weighted (--) and where the recovery weighting is reduced (-).

lies in the scale-up of batch flotation results to the full-scale plant.

Another source of model uncertainty is due to the neglected dynamics associated with the immediate response of the concentrate streams to a change in the air factor, as shown in (6.5). Furthermore, the assumption of perfect level control will certainly introduce error into the model. To rigorously derive an estimate of the magnitude of the expected model uncertainty may be unrealistic and therefore an assumption has been made regarding the magnitude and source of the uncertainty. It is assumed that the uncertainty is associated with the inputs and that the uncertainty weight takes the following form for each flowsheet:

$$\begin{aligned} W_I &= w_I I \\ &= \frac{\left(1+\frac{r_k}{2}\right)\theta_{\max} s + 1}{\frac{\theta_{\max}}{2} s + 1} I \end{aligned} \tag{6.14}$$

In the above, $r_k = 0.2$ is the relative uncertainty at steady-state and $\theta_{\max} = 1$ represents the magnitude of the neglected time delay. The above weight is developed in Skogestad and Postlethwaite (1996) and assumes a first-order Padé approximation for the neglected time delay. The unmodelled delay is an attempt to compensate for the neglected lag in the response of the concentrate flows to a change in the air factor. Clearly the uncertainty Δ is structured since the inputs are independent of each other.

Strictly speaking, a different weight w_I should be derived for each circuit and should be a function of the properties of that circuit. This has not been done but is a recommended area of future research. Despite these simple assumptions it will be seen that certain circuits are inherently more sensitive to model uncertainty than others.

Due to the nonlinearity of the model equations describing the flotation circuit and the likely time variation in the process, it becomes clear that the assumptions used in the ℓ_1 robust control framework are very appropriate for this sort of study.

In assessing the impact of model uncertainty on closed-loop performance it is assumed that the measure of nominal performance is as in (6.13), with $W = \begin{bmatrix} 1 & 1 \end{bmatrix}^T$. In Chapter 4 it was shown how dynamic operability may be assessed in the presence of structured model uncertainty at fixed operating conditions. Table 6.7 shows the results achieved through application of this approach to each of the circuits. The constraint on the behavior of w_f corresponds to the case where $\delta = 0.2$ in (6.11).

From the results in Table 6.7 it is clear that circuits 1 and 9 are considerably more sensitive to the model uncertainty than the other circuits. These results further support the motivation for selecting either circuit 2 or circuit 8, as neither of these are very sensitive to the

Table 6.7: Minimum achievable time-weighted SSE for each flowsheet, both with and without structured multiplicative input uncertainty.

Flowsheet:	**1**	**2**	**3**	**4**	**8**	**9**
Structured uncertainty	13.9	1.9 e-4	48.4	584	210	1.2
No uncertainty	7.6 e-7	1.8 e-4	44.3	581	209	3.0 e-7

source of model uncertainty considered. Clearly this type of information is not intuitively obvious and requires a study of the type performed here to quantify these characteristics of the different designs.

6.5 Conclusion

The impact of a plant's design on its achievable performance has prompted research into methodologies for plant operability assessment. In this chapter two different implementations of the Q-parametrization approach to dynamic operability assessment have been applied to the design of three-bank flotation circuits.

The first implementation involved calculating the dynamic operability of alternative circuit designs at a fixed operating point. The results show that plants with right-half-plane zeros near the origin may have serious control difficulties. It was also seen that the dynamic operability of a process is a function of the level of input constraints and that different processes have different sensitivities to the level of input constraints. Furthermore, it was shown that the measure of dynamic operability is essentially multiobjective and depends on the relative weights of the outputs. Careful thought is thus needed by the designer when determining the control objectives for a particular circuit. If good recovery control is not critical, then the weighting of the recovery term in the objective should be reduced. In this manner more control effort is focussed on the grade control, and flowsheets 3, 4 and 8 are able to perform acceptably despite having RHPT zeros present.

Use of the dynamic operability measure in conjunction with steady-state recovery enabled the generation of a noninferior set of flowsheets and allowed for inherently poor designs to be screened. Unfortunately, further screening is complicated by the fact that it is difficult to quantify the economic benefits associated with good control.

A second implementation of the Q-parametrization approach involved determining the economically optimal operating conditions which allow for a specified quality of closed-loop

performance to be achieved. In this manner, designs were compared according to a common economic basis. Unfortunately, the problem is still multiobjective, as the economic performance depends on the level of dynamic operability required. Using the different problem formulations presented in this chapter allows greater insight into the trade-offs involved and equips the design engineer with useful information with which to make a good decision.

In addition to the above, the impact of model uncertainty on the achievable closed-loop performance has been quantified. It was seen that the dynamic performance of circuits 1 and 9 is inherently more sensitive to the source of model error assumed in the study. This type of information is certainly not intuitively obvious and requires a formal investigation of the type considered in this chapter.

Conclusions and Recommendations

The ability to guarantee high product quality, in terms of low variability, is emerging as a defining factor when distinguishing between suppliers in the modern production environment. The extent to which this can be done is termed a plant's dynamic operability and is a function of both the plant design and the control system design. Taken to the limit, it is a function of the inherent properties of the plant. Factors known to limit the achievable closed-loop performance of a process are the presence of right-half-plane zeros, time delays, input constraints and uncertainty in the plant model.

The interrelationship between a plant design and its ability to be controlled has been noted in the literature as early as 1943 (Ziegler and Nichols, 1943). Despite this early realization, it has not always been considered essential to include dynamic operability as a formal objective in process design; the main reason for this being the fact that processes were not always pushed to their limits. However, increases in raw material and energy costs and the need for tighter design margins have resulted in highly integrated designs with little spare capacity to handle process upsets. This, together with the requirements for low product variability and stricter environmental regulations, has placed considerable pressure on plant control systems and has necessitated the development of systematic techniques for the screening of designs with inherently inferior dynamic operability.

In this thesis, one such approach, based on the Q-parametrization of stabilizing linear feedback controllers, has been presented. The method involves posing a (convex) mathematical programming problem through which a limit of achievable closed-loop performance is calculated for any controller in this class. The ability to quantify a limit of performance independent of controller type or tuning makes the approach well suited to dynamic operability

assessment. Furthermore, the approach enables the simultaneous treatment of combinations of performance-limiting factors, a feature which has not been possible with the earlier analytical approaches presented in the literature.

The interrelationship between steady-state economics and dynamic operability is explored in this thesis with the aid of a problem formulation which includes economic considerations. These two issues are linked because the proximity of the steady-state operating condition to the process constraints impacts on both the steady-state economics and the dynamic operability. For example, operating close to the input constraints, which is often favorable from a steady-state economic viewpoint, limits the input power available for achieving good regulatory and servo control behavior.

The incorporation of economic considerations is treated formally by including the process setpoints as decision variables together with Q and optimizing an economic performance measure subject to constraints on the quality of the closed-loop behavior. The constraints include both time-domain bounds on the responses of the inputs and outputs as well as a bound on the weighted sum-of-square errors of the output response. In this manner competing designs may be compared according to a common economic basis. An interesting feature of this formulation is that processes which are inherently easy to control are generally able to operate closer to their economic optimum than processes which have poor dynamic operability. In this way the unfavorable economic consequences of having poor dynamic operability may be quantified.

Another important aspect of this research has been the treatment of structured multivariable model uncertainty. Such a treatment is necessary since the linear time-invariant (LTI) models used in process control only represent the true process dynamics approximately. Typical sources of model error include unmodelled dynamics, the linearization of nonlinear models, time-variation in the process and imperfectly known model parameters. The purpose of robust control theory is to design controllers which provide acceptable closed-loop performance within an environment of uncertainty. In the context of dynamic operability assessment, one seeks designs which are inherently insensitive or less sensitive to model uncertainty.

In attempting to quantify the impact of model uncertainty on achievable closed-loop performance, certain assumptions need to be made regarding the nature of the uncertainty. Two of the most popular assumptions are that the uncertainty is LTI and, on the other hand, that the uncertainty is nonlinear/time-varying. The former assumption forms the basis of the structured singular value framework, while the latter is used in the ℓ_1 robust control framework. Both these approaches have been reviewed in this thesis. Clearly, the appli-

cability of any such assumption depends on the process and application at hand. It has been argued that the ℓ_1 approach is well suited to dynamic operability assessment, since it is mathematically convenient and its assumptions regarding the nature of the model uncertainty may be more appropriate at the design stage. In other words, allowing for possibly nonlinear/time-varying uncertainty is a safe option when little is known regarding the nature of the model uncertainty. Furthermore, the ℓ_1 approach is formulated naturally in the discrete-time domain, facilitating its incorporation into the Q-parametrization formulation.

The basic strategy for quantifying the impact of model uncertainty on dynamic operability involves determining the optimal achievable nominal control performance, subject to the requirement that the closed-loop system be stable in the presence of a given amount and type of model uncertainty. Mathematically this corresponds to augmenting the basic optimization strategy, used in the absence of model uncertainty, with additional constraints enforcing robust stability.

The robust stability criteria of the ℓ_1 approach are not directly suitable for use within a gradient-based optimization scheme. They are converted, without loss of accuracy, to an equivalent set of differentiable constraints, with the addition of search variables. When treating structured model uncertainty, additional scaling factors are required in the robustness constraints. These scaling factors introduce nonconvexity into the problem and complicate the solution procedure. A hybrid solution strategy, consisting of a combination of convex quadratic programming and standard nonlinear programming, has been adopted in this thesis to deal with this issue.

The computational approaches developed in this thesis have been applied to a number of illustrative examples. The results highlight the importance of simultaneously considering the effect of combinations of performance-limiting factors. Application to a multivariable distillation column containing all four performance limitations revealed a number of non-intuitive results. It was found that designs which have large time delays in certain elements of their transfer matrices may actually have superior dynamic operability, as these delays often reduce interaction and may prevent the occurrence of infinite RHPT zeros. Other examples explored the relationship between steady-state economics and dynamic operability as well as the economic benefits of inherently operable plants.

A detailed case study involving the application of the Q-parametrization approach to the screening of alternative flotation circuit designs was presented. The study explored the trade-off between the performance-limiting effects of right-half-plane zeros, input constraints and model uncertainty. By incorporating economic considerations into the formulation,

greater insight was gained into the interrelationship between dynamic operability and steady-state economics. Those flotation circuits which are inherently easy to control are able to maintain good control performance whilst operating in close proximity to their desired steady-state economic optimum.

As the optimization problems required in the above formulations are typically of large dimension, methods were presented to improve computational efficiency. Particular attention was paid to exploiting the problem structure and sparsity in order to reduce computation time. It has been shown that, in the absence of model uncertainty, dynamic operability assessment may be posed in an open-loop optimal-control manner. The theoretical and computational consequences of this are explored and illustrated through application examples. Using the open-loop formulation, an alternative measure of dynamic operability is conveniently formulated. This measure involves determining the largest possible disturbance range that can be tolerated without violating dynamic feasibility requirements. Application of this procedure was illustrated on an example problem and the results were compared to those obtained using the previously described formulations for dynamic operability assessment.

When treating a range of disturbances, it has been shown that the assumption of linear control may be conservative. This results from the fact that, when a process operates close to a particular input constraint, additional input power is available in the other direction and should be exploited when possible. However, due to the linearity of the controller, this input power cannot be utilized and control performance is degraded unnecessarily. The potential benefits of nonlinear control have been explored briefly using the open-loop problem formulation. It is, however, recommended that future research in this field should target the issue of nonlinear control and explore in greater detail the benefits of handling input saturation in a nonconservative manner. In particular, the ability of nonlinear controllers to improve both the dynamic operability and the steady-state economics of given designs should be addressed.

The treatment of other forms of model uncertainty is also an area for future research. What will be of particular benefit for both dynamic operability analysis and robust control is a quantification of the sensitivity of the achievable closed-loop performance to the assumptions regarding the model uncertainty. Furthermore, the use of global optimization techniques to treat problems involving structured (ℓ_1) model uncertainty should be explored.

This thesis has mainly addressed the issue of dynamic operability *analysis*, with the process design being predetermined. An extension of the approaches developed in this thesis to treat retrofit problems is a necessary avenue of research. Methods should be sought whereby the

dynamic operability of a given design may be improved by appropriate design modifications. This will involve both detecting process bottlenecks and determining how they may be removed without seriously worsening the steady-state economics. Finally, research is needed which is targeted at the development of systematic techniques for the synthesis of designs which are both operable and economical.

References

Anderson, J.S., "A Practical Problem in Dynamic Heat Transfer", *Chem. Engr.*, CE97-CE103 (1966).

Arkun, Y., "Dynamic Process Operability. Important Problems, Recent Results and New Challenges", In M. Morari and T.J. McAvoy (editors), *Proceedings of Third International Conference on Chemical Process Control CPC III*, Elsevier, Amsterdam, The Netherlands, 323-367 (1986).

Arkun, Y., B. Manousiouthakis, A. Palazoglu, V. Guruswamy and P. Putz, "Computer-Aided Analysis and Design of Robust Multivariable Control Systems for Chemical Processes", *Comp. Chem. Engng.*, **9**(1), 27-59 (1985).

Asbjornsen, O.A., "Control and Operability of Process Plants", *Comp. Chem. Engng.*,**13** (4/5), 351-364 (1989).

Bahri, P.A., "An Integrated Strategy for Operability Analysis of Chemical Plants", *Proceedings: Volume 2, Chemeca '96, 24th Australian and New Zealand Chemical Engineering Conference*, Sydney, Australia, 133-138 (1996).

Bahri, P.A., J.A. Bandoni and J.A. Romagnoli, "An Integrated Procedure for Flexibility and Controllability Analysis in Design and Control of Chemical Processes", *AIChE Annual Meeting*, Miami, USA, November 12-17 (1995).

Balakrishnan, V., E. Feron and S. Hall, "Practical Methods for Robust Control", Summer Professional Program 16.30s presented at the Massachusetts Institute of Technology, Boston, Massachusetts, USA, July 17-21 (1995).

Balakrishnan, V., Y. Huang, A. Packard and J. Doyle, "Linear Matrix Inequalities In Analysis With Multipliers", *Proceedings of the American Control Conference,* Baltimore, Maryland, USA, Vol. 2, 1228-1232 (1994).

Balas, G.J., J.C. Doyle, K. Glover, A. Packard and R. Smith, *μ-Analysis and Synthesis Toolbox User's Guide*, MuSyn Inc. and the Math Works Inc., Natick, Massachusetts, USA (1991).

Bandoni, J.A. and J.A. Romagnoli, "Uncertainty in Linear Programming", *Numerical and Applied Mathematics*, 635-640 (1989).

Bandoni, J.A., J.A. Romagnoli and G.W. Barton, "On Optimizing Control and the Effect of Disturbances: Calculation of Open-loop Back-offs", *Comp. Chem. Engng.*, **18**, S506-S509 (1994).

Barton, G.W., W.K. Chen and J.D. Perkins, "Interaction Between Process Design and Process Control: The Role of Open-Loop Indicators", *J. of Proc. Cont.*, **1**, 161-170 (1991).

Bellman, R. and K.L. Cook, *Differential-difference Equations*, Academic Press, New York (1963).

Benson, R.S., "The State of Chemical Process Control: An Industrialist's View", *Chem. Eng. Res. Des.*, **65**, 451-452 (1987).

Biss, D. and J.D. Perkins, "Application of Input-Output Controllability Analysis to Chemical Processes", In: *ECC-93 Proc.*, Gronigen, The Netherlands, 1056-1059 (1993).

Boyd, S.P., V. Balakrishnan, C.H. Barratt, N.M. Khraishi, X. Li, D.G. Meyer and S.A. Norman, "A New CAD Method and Associated Architectures for Linear Controllers", *IEEE Trans. on Autom. Control*, **AC-33**(3), 268-282 (1988).

Boyd, S.P., C.H. Barratt and S.A. Norman, "Linear Controller Design : Limits of Achievable Performance Via Convex Optimisation", *Proceedings of the IEEE*, **78**(3), 529-564 (1990).

Boyd, S.P. and C.H. Barratt, *Linear Controller Design: The Limits of Performance*, Prentice Hall, Englewood Cliffs, New Jersey, USA (1991).

Boyd, S.P., L. El Ghaoui, E. Feron and V. Balakrishnan, *Linear Matrix Ineqaulities System and Control Theory*, Siam Studies in Applied Mathematics, Vol. 15 (1994).

Bristol, E.H., "On a New Measure of Interaction for Multivariable Process Control", *IEEE Trans. Autom. Control*, **AC-11**, 133-134 (1966).

Bristol, E.H.., "A New Process Interaction Concept: Pinned Zeros", Internal Report of the Foxboro Co., Boston, Massachusetts, USA (1980).

Cao, Y., D. Biss and J.D. Perkins, "Assessment of Input-Output Controllability in the Presence of Control Constraints", *Proceedings of the IFAC Workshop on Integration of Process Design and Control*, Baltimore, 35-40 (1994).

Chacon-Mondragon, O.L. and D.M. Himmelblau, "A New Definition of Flexibility for Chemical Process Design", *Comp. Chem. Engng.*, **12**(5), 383-387 (1988).

Chacon-Mondragon, O.L. and D.M. Himmelblau, "Integration of Flexibility and Control in Process Design", *Proceedings of the IFAC Workshop on Integration of Process Design and Control*, Baltimore, 111-116 (1994).

Dahleh, M.A. and I.J. Diaz-Bobillo, *Control of Uncertain Systems*, Prentice Hall, Englewood Cliffs, New Jersey, USA (1995).

Dahleh, M.A. and M.H. Khammash, "Controller Design for Plants with Structured Uncertainty", *Automatica*, **29**(1), 37-56 (1993).

Desoer, C.A. and M. Vidyasagar, *Feedback Systems: Input-Output Properties*, Academic Press, New York, USA (1975).

Dhillon, B.S. and S.N. Rayapati, "Chemical-System Reliability: A Review", *IEEE Trans. Reliability*, **37**, 199 (1988).

Dimitriadis, V.D. and E.N. Pistikopoulos, "Flexibility Analysis of Dynamic Systems", *Ind. Eng. Chem. Res.*, **34**(12), 4451-4462 (1995).

Douglas, J.M., "A Hierarchical Decision Procedure for Process Synthesis", *AIChE J.*, **31**, 353 (1985).

Downs, J.J. and J.E. Doss, "Present Status and Future Needs - A View from North American Industry", In Y. Arkun and W.H. Ray (editors), *Proceedings of Fourth International Conference on Chemical Process Control CPC IV*, Elsevier, Amsterdam, The Netherlands, 297-318 (1991).

Downs, J.J. and B. Ogunnaike, "Design for Control and Operability: An Industrial Perspective", In L.T. Biegler and M.F. Doherty (editors), *Fourth International Conference on the Foundations of Computer-Aided Process Design*, AICHE Symposium Series, Vol. **91** No. 304, 115-123 (1995).

Doyle, J.C., "Analysis of Feedback Systems with Structured Uncertainty", *IEEE Proceedings*, **129**, 242-250 (1982).

Doyle, J.C. and G. Stein, "Multivariable Feedback Design : Concepts for a Classical Modern Synthesis", *IEEE Trans. on Autom. Control*, **AC-26**(1), 4-16 (1981).

Edwards, D.W. and D. Lawrence, "Assessing the Inherent Safety of Chemical Process Routes: Is There a Relation Between Plant Costs and Inherent Safety?", *Trans IChemE*, **71**, Part B, November, 252-258 (1993).

Fan, M.K.H., A.L. Tits and J.C. Doyle, "Robustness in the Presence of Mixed Parametric Uncertainty and Unmodeled Dynamics", *IEEE Trans. on Autom. Control*, **36**(1), 25-38 (1991).

Fararooy, S., J.D. Perkins, T.I. Malik, M.J. Oglesby and S. Williams, "Process Controllability Toolbox (PCTB)", *Comp. Chem. Eng.*, **17**(5/6), 617-625 (1993).

Figueroa, J.L., P.A. Bahri, J.A. Bandoni and J.A. Romagnoli, "Economic Impact of Disturbances and Uncertain Parameters in Chemical Processes: A Dynamic Back-off Analysis", *Comp. Chem. Engng.*, **20**(4), 453-461 (1996).

Figueroa, J.L., P.A. Bahri, G.W. Barton and J.A. Romagnoli, "The Economic Assessment of Alternatives in Optimizing Control", *IChemE Symposium Series*, No. 133 (1994a).

Figueroa, J.L., P.A. Bahri and J.A. Romagnoli, "Economic Impact of Disturbances in Chemical Processes - A Dynamic Analysis", *Proceedings of the IFAC Workshop on Integration of Process Design and Control*, Baltimore, Maryland, USA (1994b).

Fisher, W.R., M.F. Doherty and J.M. Douglas, "Steady-State Control as a Prelude to Dynamic Control", *Chem. Eng. Res. Des.*, **63**, 353-357 (1985).

Fisher, W.R., M.F. Doherty and J.M. Douglas, "The Interface Between Design and Control. 1. Process Controllability", *Ind. Eng. Chem. Res.*, **27**, 597-605 (1988a).

Fisher, W.R., M.F. Doherty and J.M. Douglas, "The Interface Between Design and Control. 2. Process Operability", *Ind. Eng. Chem. Res.*, **27**, 606-611 (1988b).

Fisher W.R., M.F. Doherty and J.M. Douglas, "The Interface Between Design and Control. 3. Selecting a Set of Controlled Variables", *Ind. Eng. Chem. Res.*, **27**, 611-615 (1988c).

Francis, B.A., *A Course in $\mathcal{H}_\infty$ Control Theory*, Springer-Verlag, Berlin, Germany (1987).

Frank, P.M., "Entwurf von Regelkreisen mit Vorgeschrieben Verhalten", G. Braun, Karlsruhe (1974).

Freudenberg, J.S., D.P. Looze and B.J. Cruz, "Robustness Analysis Using Singular Value Sensitivities", *Int. J. Control*, **35**(1), 95-116 (1982).

Gahinet, P., A. Nemirovski, A.J. Laub and M. Chilali, *LMI Control Toolbox User's Guide*, The Math Works Inc., Natick, Massachusetts, USA (1995).

García, C.E., D.M. Prett and M. Morari, "Model Predictive Control: Theory and Practice - A Survey", *Automatica*, **25**(3), 335-348 (1989).

Georgakis, C. and D.J. Worthey, "On Dynamical Methods of Heat Integration Design", *AIChE J.*, **24**(6), 976-984 (1978).

Gill, P.E., Department of Mathematics, University of California, San Diego, U.S.A., Personal communication (1996).

Gill, P.E., S.J. Hammerling, W. Murray, M.A. Saunders and M.H. Wright, *User's Guide for LSSOL (Version 1.0): A Fortran Package for Constrained Least-Squares And Convex Quadratic Programming*, Systems Optimization Laboratory, Department of Operations Research, Stanford University, California, USA (1986).

Gonzaga, C. and E. Polak, "On Constraint Dropping Schemes and Optimality Functions for a Class of Outer Approximation Algorithms", *SIAM J. Control and Optimization*, **17**(4) (1979).

Grossmann, I.E. and C.A., Floudas, "Active Constraint Strategy for Flexibility Analysis in Chemical Processes", *Comp. Chem. Engng.*, **11**(6), 675-693 (1987).

Grossmann, I.E., K.P. Halemane and R.E. Swaney, "Optimization Strategies for Flexible Chemical Processes", *Comp. Chem. Engng.* **7**, 439 (1983).

Grossmann, I.E. and M. Morari, "Operability, Resiliency and Flexibility — Process Design Objectives for a Changing World", In A.W. Westerberg and H.H. Chien (editors), *Proceedings of the Second International Conference on Foundations of Computer-Aided Process Design*, Snowmass, Colorado, USA, 931-1030 (1984).

Guruswamy, V., "Use of Singular Values in Process Design and Control: New Computational Techniques and Applications in Chemical Engineering", *M.S. Thesis*, Rensselare Polytechnic Institute, Troy, New York, USA (1983).

Haimes, Y., W.A. Hall and H.T. Freedman, *Multiobjective Optimization in Water Resource Systems: The Surrogate Worth Trade-off Method*, Elsevier, Amsterdam, The Netherlands (1975).

Halemane, K.P. and I.E. Grossmann, "Optimal Process Design Under Uncertainty", *AIChE J.*, **29**, 425-433 (1983).

Heikkila, A., M. Hurme and M. Jarvelainen, "Safety Considerations in Process Synthesis", *Comp. Chem. Engng.*, **20**, S115-S120 (1996).

Holt, B.R. and M. Morari, "Design of Resilient Processing Plants - V. Effect of Deadtime on Dynamic Resilience", *Chem. Eng. Sci.*, **40**(7), 1229-1237 (1985a).

Holt, B.R. and M. Morari, "Design of Resilient Processing Plants - VI. Effect of Right-Half-Plane Zeros on Dynamic Resilience", *Chem. Eng. Sci.*, **40**(1), 59-74 (1985b).

Hovd, M. and S. Skogestad, "Simple Frequency-dependent Tools for Control System Analysis, Structure Selection and Design", *Automatica*, **28**, 989-996 (1992).

Khammash, M. and J.B. Pearson, "Performance Robustness of Discrete-Time Systems with Structured Uncertainty", *IEEE Trans. on Autom. Control*, **36**(4), 398-412 (1991).

Kletz, T., *Plant Design for Safety*, Hemisphere, New York, USA (1991).

Klema, V.C. and A.J. Laub, "The Singular Value Decomposition: Its Computation and Some Applications" *IEEE Trans. Autom. Control*, **AC-25**, 164 (1980).

Kuo, D.H., D.S. Hsu and C.T. Chang, "A Prototype for Integrating Automatic Fault Tree/Event Tree/HAZOP Analysis", *Comp. Chem. Engng.*, **21**, S923-S928 (1997).

Kwakernaak, H. and R. Sivan, *Linear Optimal Control Systems*, Wiley, New York, USA (1972).

Langer, R.E., "On the Zeros of Exponential Sums and Integrals", *Bull. Amer. Math. Soc.*, **37**, 213-239 (1931).

Laub, A.J. and B.C. Moore, "Calculation of Transmission Zeros using QZ Techniques", *Automatica*, **14**, 557-566 (1978).

Laughlin, D.L., K.G. Jordan and M. Morari, "Internal Model Control and Process Uncertainty - Mapping Uncertainty Regions for SISO Controller-Design", *Int. J. Control*, **44**(6), 1675-1698 (1986).

Lear, J.B., G.W. Barton and J.D. Perkins, "Interaction Between Process Design and Process Control: The Impact of Disturbances and Uncertainty on Estimates of Achievable Economic Performance", *J. Proc. Cont.*, **5**(1), 49-62 (1995).

Lee, H.H., L.B. Koppel and H.C. Lim, "Integrated Approach to Design and Control of a Class of Counter-Current Processes", *Ind. Eng. Chem. Process Des. Dev.*, **11**, 376-382 (1972).

Lenhoff, A.M. and M. Morari, "Design of Resilient Processing Plants — I. Process Design Under Consideration of Dynamic Aspects", *Chem. Eng. Sci.*, **37**(2), 245-258 (1982).

Lin, C.T., "Structural Controllability", *IEEE Trans. Auto. Control*, **AC-19**(3), 201-208 (1974).

Luyben, M.L. and C.A. Floudas, "Analyzing the Interaction of Design and Control – 1. A Multiobjective Framework and Application to Binary Distillation Synthesis", *Comp. Chem. Engng.*, **18**(10), 933-969 (1994a).

Luyben, M.L. and C.A. Floudas, "Analyzing the Interaction of Design and Control – 2. Reactor-Separator-Recycle System", *Comp. Chem. Engng.*, **18**(10), 971-994 (1994b).

Luyben, W.L., "Trade-Offs Between Design and Control in Chemical Reactor Systems", *J. Proc. Cont.*, **3**(1), 17-41 (1993).

Lyapunov, A.M., *Problème Général de la Stabilité du Mouvement*, Volume 17 of *Annals of Mathematics Studies*, Princeton University Press, Princeton, New Jersey, USA (1947).

Lynch, A.J., N.W. Johnson, E.V. Manlapig and C.G. Thorne, *Mineral and Coal Flotation Circuits*, Elsevier, New York, USA (1981).

MacFarlane, A.G.J. and N. Karcanias, "Poles and Zeros of Linear Multivariable Systems: A Survey of the Algebraic, Geometric and Complex-Variable Theory", *Int. J. Control*, **24**, 33 (1976).

Maciejowski, J.M., *Multivariable Feedback Design*, Addison-Wesley, United Kingdom (1989).

Mathisen, K.W. and S. Skogestad, "Design, Operation and Control of Resilient Heat Exchanger Networks", *Presented at AIChE Annual Meeting*, Miami Beach, USA, November 1-6 (1992).

Mohideen, M.J., J.D. Perkins and E.N. Pistikopoulos, "Optimal Synthesis and Design of Dynamic Systems under Uncertainty", *Comp. Chem. Eng.*, **20**, S895-S900 (1996).

Moler, C.B. and G.W. Stewart, "An Algorithm for Generalized Matrix Eigenvalue Problems", *SIAM J. Numer. Anal.*, **10**, 241-256 (1973).

Morari, M., "Design of Resilient Processing Plants — III. A General Framework for the Assessment of Dynamic Resilience", *Chem. Eng. Sci.*, **38**(11), 1881-1891 (1983).

Morari, M. and J.D. Perkins, "Design for Operations", In L.T. Biegler and M.F. Doherty (editors), *Fourth International Conference on the Foundations of Computer-Aided Process Design*, AICHE Symposium Series, Vol. **91** No. 304, 105-114 (1995).

Morari M. and E. Zafiriou, *Robust Process Control,* Prentice Hall, Englewood Cliffs, New Jersey, USA (1989).

Morari, M., E. Zafiriou and B.R. Holt, "Design of Resilient Processing Plants. New Characterization of the Effect of RHP Zeros", *Chem. Eng. Sci.*, **42**(10), 2425-2428 (1987).

Murtagh, B.A. and M.A. Saunders, *MINOS 5.4 User's Guide*, Systems Optimization Laboratory, Department of Operations Research, Stanford University, California, USA (1983).

Narraway, L.T., "Selection of Process Control Structure Based on Economics", *PhD Thesis*, University of London, United Kingdom (1992).

Narraway, L.T. and J.D. Perkins, "Selection of Process Control Structure Based on Linear Dynamic Economics", *Ind. Eng. Chem. Res.*, **32**, 2681-2692 (1993a).

Narraway, L.T. and J.D. Perkins, "Selection of Control Structure Based on Economics", *Comp. Chem. Eng.*, **18**, S511-S515 (1993b).

Narraway, L.T., J.D. Perkins and G.W. Barton, "Interaction Between Process Design and Control: Economic Analysis of Process Dynamics", *J. Proc. Cont.*, **1**, 243-250, November (1991).

Nishida, N. and A. Ichikawa, "Synthesis of Optimal Dynamic Process Systems by a Gradient Method", *Ind. Eng Chem. Proc. Des. Dev.*, **14**(3), 236-242 (1975).

Nishida, N., Y.A. Liu and A. Ichikawa, "Studies in Chemical Process Design and Synthesis. 2. Optimal Synthesis of Dynamic Process Systems Under Uncertainty", *AIChE J.*, **22**(3), 539-549 (1976).

Ogunnaike, B.A., J.P. Lemaire, M. Morari and W.H. Ray, "Advanced Multivariable Control of a Pilot Scale Distillation Column", *AIChE J.*, **29**, 632-640 (1983).

Oglesby, M.J., T.I. Malik, S. Fararooy and V. Geake, "Early Stage Process Controllability Assessment", In J.D. Perkins (editor), *Interaction Between Process Design and Control*, Pergamon, Oxford, United Kingdom, 145-150 (1992).

Ovstrovsky, G.M., Y.M. Volin and D.V. Golovahkin, "Evaluation of Chemical Process Flexibility", *Comp. Chem. Engng.*, **20**, S617-S622 (1996).

Packard, A. and J.C. Doyle, "The Complex Structured Singular Value", *Automatica*, **29**(1), 71-109 (1993).

Palazoglu, A., B. Manousiouthakis and Y. Arkun, "Design of Chemical Plants with Improved Dynamic Operability in an Uncertain Environment, " *Ind. Eng. Chem. Proc. Des. Dev.*, **24**, 802-813 (1985).

Palazoglu, A. and Y. Arkun, "A Multiobjective Approach to Design Chemical Plants with Robust Dynamic Operability Characteristics", *Comp. Chem. Engng.*, **10**(6), 567-575 (1986).

Paules, G.E. and C.A. Floudas, "APROS: Algorithmic Development Methodology for Disctrete-Continuous Optmization Problems", *Operations Research*, **37**, 902-915 (1989).

Pearson, J.B. and B. Bamieh, "On minimizing maximum errors", *IEEE Trans. Autom. Control*, **AC-35**, 598-601 (1990).

Perkins, J.D., "Interaction Between Process Design and Control", *Proceedings of DYCORD+ 1989*, Maastricht, The Netherlands (1989).

Perkins, J.D. and S.P.K. Walsh, "Optimization as a Tool for Design/Control Integration", *IFAC Workshop on Integration of Process Design and Control*, Baltimore, Maryland, USA, 1-10 (1994).

Perkins, J.D. and M.P.F. Wong, "Assessing Controllability of Chemical Plants", *Chem. Eng. Res. Des.*, **63**, 358-362 (1985).

Pistikopoulos, E.N. and T.A. Mazzuchi, "A New Flexibility Analysis Approach for Processes with Stochastic Parameters", *AIChE Annual Meeting*, San Francisco, USA *(1989).*

Pistikopoulos, E.N. and T.A. Mazzuchi, "A Novel Flexibility Analysis Approach for Processes with Stochastic Parameters", *Comp. Chem. Engng.*, **14**(9), 991-1000 (1990).

Pontryagin, L.S., "On the Zeros of Some Elementary Transcendental Functions", *Izv. Akad. Nauk. SSSR, Ser. Mat.*, **6**, 115-134 (1942). Translation in *Amer. Math. Soc. Transl. Ser. 2*, **1** 95-110 (1955).

Pradubsripetch, D., S. Lee, A. Adriani and Y. Naka, "Real Time Generation of Operating Procedures to Support Flexible Start-up Operation", *Comp. Chem. Engng.*, **20**, S1203-S1208 (1996).

Preston, M.L., D.C Richards and A.G. Rushton, "CAPE - Crusading for Process Safety: An Industrial Perspective", *Comp. Chem. Engng.*, **20**, S1533-1538 (1996).

Psarris, P. and C.A. Floudas, "Improving Dynamic Operability of MIMO Systems with Time Delays", *Chem. Eng. Sci.*, **45**, 3505-3524 (1990).

Psarris, P. and C.A. Floudas, "Dynamic Operability of MIMO Systems with Time Delays and Transmission Zeroes — I. Assessment", *Chem. Eng. Sci.*, **46**(10), 2691-2707 (1991a).

Psarris, P. and C.A. Floudas, "Dynamic Operability of MIMO Systems with Time Delays and Transmission Zeroes — II. Enhancement", *Chem. Eng. Sci.*, **46**(10), 2709-2728 (1991b).

Roat, S., J. Downs, E. Vogel and J. Doss, "The Integration of Rigorous Dynamic Modelling and Control System Synthesis for Distillation Columns: An Industrial Approach", *CPC III*, M. Morari and T.J. McAvoy editors, Elsevier, Amsterdam, The Netherlands, 99-138 (1986).

Rosenbrock, H.H., *State-space and Multivariable Theory*, Nelson, London, United Kingdom (1970).

Ross, R. and C.L.E. Swartz, "Inclusion of Model Uncertainty in a Computational Framework for Dynamic Operability Assessment", *7th European Symposium on Computer-Aided Process Engineering*, Trondheim, Norway (1997a).

Ross, R. and C.L.E. Swartz, "An Overview of a Computational Approach to Dynamic Operability Assessment", *8th National Meeting of the South African Institution of Chemical Engineers*, Cape Town, South Africa (1997b).

Russell, L.W. and J.D. Perkins, "Towards a Method for Diagnosis of Controllability Problems in Chemical Plants", *Chem. Eng. Res. Des.*, **65**, 453-461 (1987).

Schubert, J., Measurement and Control Division, Mintek, Randburg, South Africa, Personal communication (1996).

Silverstein, J. and R. Shinnar, "Stabilization of reactors operating at an unstable steady-state", *70th AIChE Annual Meeting*, New York, USA (1977).

Skogestad, S., M. Hovd and P. Lundstorm, "Towards Integrating Design and Control: Use of Frequency-dependent Tools for Controllability Analysis", *PSE '91 4th International Symposium on Process Systems Engineering*, Montebello, Quebec, Canada, III.3.1-III.3.15 (1991).

Skogestad, S., E.W. Jacobsen and M. Morari, "Inadequacy of Steady-State Analysis for Feedback Control: Distillate Bottom Control of Distillation Columns", *Ind. Eng. Chem. Res.*, **29** 2339-2346 (1990).

Skogestad, S. and M. Morari, "Design of Resilient Processing Plants — IX. Effect of Model Uncertainty on Dynamic Resilience", *Chem. Eng. Sci.*, **42**(7), 1765-1780 (1987).

Skogestad, S., M. Morari and J.C. Doyle, "Robust Control of Ill-Conditioned Plants: High-Purity Distillation", *IEEE Trans. Autom. Control*, **33**(12), 1092-1105 (1988).

Skogestad, S. and I. Postlethwaite, *Multivariable Feedback Control: Analysis and Design*, John Wiley and Sons, London, United Kingdom (1996).

Sobhani, M. and S. Jayasuriya, "Controller Design for Maximizing the Size of a Step Disturbance in Non-Minimum Phase, Unstable Uncertain Systems", *Int. J. Control*, **59** (2), 561-581 (1994).

Sourlas, D.D. and V. Manousiouthakis, "Best Achievable Decentralized Performance", *IEEE Trans. Autom. Control*, **AC-40**(11), 1858-1871 (1995).

Srinophakhun, T. and P.A. Lant, "A Prototype Package for Control, Design and Evaluation based on a Structural Model", *Proceedings: Volume 2, Chemeca '96, 24th Australian and New Zealand Chemical Engineering Conference*, Sydney, Australia, 133-138 (1996).

Stanley, G., M. Marino-Galarraga and T.J. McAvoy, "Shortcut Operability Analysis. 1. The Relative Disturbance Gain", *Ind. Eng. Chem. Proc. Des. Dev.*, **24**, 1181-1188 (1985).

Straub, D.A. and I.E. Grossmann, "Integrated Stochastic Metric of Flexibility for Systems with Discrete State and Continuous Parameter Uncertainties", *Comp. Chem. Engng.*, **14**(9), 967-985 (1990).

Swaney, R.E. and I.E. Grossmann, "An Index for Operational Flexibility in Chemical Process Design. Part I : Formulation and Theory", *AIChE J.*, **31**(4), 621-630 (1985a).

Swaney, R.E. and I.E. Grossmann, "An Index for Operational Flexibility in Chemical Process Design. Part II : Computational Algorithms", *AIChE J.*, **31**(4), 631-641 (1985b).

Swartz, C.L.E., "A Computational Framework for Dynamic Operability Assessment", *IFAC Workshop on Integration of Process Design and Control*, Baltimore, Maryland, USA, 153-158 (1994). Also *Comput. Chem. Engng.*, **20**(4), 365-371 (1996).

Tebbutt, C.D., "Control System Design Using Artificial Intelligence", *PhD Thesis*, Department of Electrical and Electronic Engineering, University of Cape Town, South Africa (1991).

Uppal, A., W.H. Ray and A.B. Poore, "On the Dynamic Behavior of Continuous Stirred Tanks", *Chem. Eng. Sci.*, **29**, 967 (1974).

Vassiliadis, V.S., "DAEOPT - A Differential-Algebraic Optimal Control Problem Solver, version 1.0", IRC for Process Systems Engineering, ICSTM, London, United Kingdom (1992).

Vassiliadis, V.S., R.W.H. Sargent and C.C. Pantelides, "Solution of a Class of Multistage Dynamic Optimization Problems. 1. Problems Without Path Constraints", *Ind. Eng. Chem. Res.*, **33**, 2111-2122 (1994a).

Vassiliadis, V.S., R.W.H. Sargent and C.C. Pantelides, "Solution of a Class of Multistage Dynamic Optimization Problems. 2. Problems With Path Constraints", *Ind. Eng. Chem. Res.*, **33**, 2123 (1994b).

Venkatasubramanian, V., and R. Vaidhyanathan, "A Knowledge-Based Franework for Automating HAZOP Analysis", *AIChE J.*, **40**, 496 (1994).

Vidyasagar, M., *Control System Synthesis : A Factorisation Approach*, MIT Press, Cambridge, Massachusetts, USA (1985).

Viswanathan, J. and I.E. Grossmann, "A Combined Penalty Function and Outer Approximation Method for MINLP Optimization", *Comp. Chem. Engng.*, **14**, 769-782 (1990).

Youla, D.C., J.J. Bongiorna J.R. and H.A. Jabr, "Modern Wiener-Hopf Design of Optimal Controllers. Part I: The Single-Input-Output Case", *IEEE Trans. Autom. Control*, **AC-21**(1), 3-13 (1976a).

Youla, D.C., J.J. Bongiorna J.R. and H.A. Jabr, "Modern Wiener-Hopf Design of Optimal Controllers. Part II: The Multivariable Case", *IEEE Trans. Autom. Control*, **AC-21**(3), 319-338 (1976b).

Young, J.C.C.Y., C.L.E. Swartz and R. Ross, "On the Effects of Constraints, Economics and Uncertain Disturbances on Dynamic Operability Assessment", *Comput. Chem. Engng.*, **20**, S677-S682 (1996).

Zafiriou, E. and H. Chiou, "On the Dynamic Resiliency of Constrained Processes", *Proceedings of the IFAC Workshop on Integration of Process Design and Control*, Baltimore, Maryland, USA, 35-40 (1994).

Ziegler, J.G. and N.B. Nichols, "Process Lags in Automatic-Control Circuits", *Transactions of the A.S.M.E.*, **65**, 433-444 (1943).

Appendix A

Details of Mathematical Formulation

A.1 Development of Step Response Equations

The closed-loop matrix H_{zw} in the general feedback framework used by Boyd and coworkers is

$$H_{zw} = T_1 + T_2 Q T_3 \quad , \; Q \text{ stable} \tag{A.1}$$

Using standard rules of matrix multiplication, and noting that Q is an $n_u \times n_y$ matrix, the (i,j) element of T_2QT_3 is given by:

$$[T_2QT_3]_{ij} = \sum_{m=1}^{n_y} \sum_{n=1}^{n_u} t_{2\,in} . q_{nm} . t_{3\,mj} \tag{A.2}$$

The transfer function between the ith element of z to the j element of w, namely H_{ij}, has a discrete-time representation,

$$H_{ij}(z) = \sum_{k=0}^{L} h_{ij}(k)\, z^{-k} \quad . \tag{A.3}$$

From (A.1) and (A.2), the pulse response coefficients, $h_{ij}(k)$, take the form:

$$h_{ij}(k) = t_{1\,ij}(k) + \sum_{m=1}^{n_y} \sum_{n=1}^{n_u} [T_2QT_3]_{ij}\,(k) \tag{A.4}$$

where $[T_2QT_3]_{ij}\,(k)$ is the kth pulse response coefficient of (i,j) element of T_2QT_3. It is determined as follows from the convolution of the pulse response coefficients of t_2, q and t_3:

$$[T_2QT_3]_{ij}\,(k) \;=\; \sum_{\alpha=0}^{k} q_{nm}(\alpha)\; [t_{2\,in} . t_{3\,mj}]\,(k-\alpha) \tag{A.5}$$

$$= \sum_{\alpha=0}^{k} q_{nm}(\alpha) \sum_{\beta=0}^{k-\alpha} t_{2\,in}(k-\alpha-\beta)\, t_{3\,mj}(\beta)$$

The step response may now be determined from the pulse response,

$$s_{ij}(i_o) = w_j \sum_{k=0}^{i_o} h_{ij}(k) \tag{A.6}$$

where $s_{ij}(i_o)$ is the step response coefficient at time increment i_o to a step of size w_j in the jth element of w. Using the developments above, $s_{ij}(i_o)$ is given by:

$$s_{ij}(i_o) = w_j \sum_{k=0}^{i_o} t_{1\,ij}(k) + w_j \sum_{m=1}^{n_y} \sum_{n=1}^{n_u} \sum_{k=0}^{i_o} \sum_{\alpha=0}^{k} q_{nm}(\alpha) \sum_{\beta=0}^{k-\alpha} t_{2\,in}(k-\alpha-\beta)\, t_{3\,mj}(\beta) \tag{A.7}$$

It is desirable to rearrange the summations above so that each nm combination of q occurs just once in the composite sum. This facilitates writing the summations in matrix form.

An intuitive way of doing this is to differentiate the equation above with respect to $q_{nm}(\gamma)$. Essentially this involves setting $\alpha = \gamma$, removing the summation over α (since α is fixed) and realizing that $k - \gamma$ must be greater than zero ($k \geq \gamma$ in the summation over k). This will give the coefficient associated with $q_{nm}(\gamma)$. The result is as follows:

$$\begin{aligned} \frac{\partial}{\partial\, q_{nm}(\gamma)} s_{ij}(i_o) &= w_j \sum_{k=\gamma}^{i_o} \sum_{\beta=0}^{k-\gamma} t_{2\,in}(k-\gamma-\beta)\, t_{3\,mj}(\beta) \\ &= w_j \sum_{k=\gamma}^{i_o} \sum_{\beta=\gamma}^{k} t_{2\,in}(k-\beta)\, t_{3\,mj}(\beta-\gamma) \end{aligned} \tag{A.8}$$

Using the above, the step response coefficients may now be re-written as follows:

$$s_{ij}(i_o) = w_j \sum_{k=0}^{i_o} t_{1\,ij}(k) + w_j \sum_{m=1}^{n_y} \sum_{n=1}^{n_u} \sum_{k=0}^{i_o} q_{nm}(k) \sum_{v=k}^{i_o} \sum_{\ell=k}^{v} t_{2\,in}(v-\ell)\, t_{3\,mj}(\ell-k) \tag{A.9}$$

Constraints on the step response, of the form:

$$s_{\min\,ij}(i_o) \leq s_{ij}(i_o) \leq s_{\max\,ij}(i_o) \tag{A.10}$$

are simply linear constraints on q through (A.9).

A.2 Simplifying Step Response Equations

In terms of coding the optimization problem formulation, it is very inefficient to store the entire arrays of t_1, t_2 and t_3. This is particularly so since these arrays have large portions which are structurally equal to zero. For a one-degree-of freedom controller where performance specifications are placed on the response of the outputs and inputs to setpoint changes and disturbances, P is given by:

$$\left[\begin{array}{c} y' \\ u \\ \hline -e \end{array}\right] = \left[\begin{array}{cc|c} 0 & G_D & G_P \\ 0 & 0 & I \\ \hline -I & G_D & G_P \end{array}\right] \left[\begin{array}{c} y_{set} \\ d \\ \hline u \end{array}\right] \tag{A.11}$$

For stables processes, the T_i matrices in (A.1) take the form:

$$T_1 = \left[\begin{array}{cc} 0 & G_D \\ 0 & 0 \end{array}\right] \quad , \quad T_2 = -\left[\begin{array}{c} G_P \\ I \end{array}\right] \quad \text{and } T_3 = \left[\begin{array}{cc} -I & G_D \end{array}\right] \tag{A.12}$$

Using the form of the T_i matrices above, it is possible to simplify the form of the expressions for the step response coefficients in (A.9). Details of this are given below.

A.2.1 Output response to setpoint changes ($i \leq n_y$ and $j \leq n_y$)

In this case we have:

$$\begin{aligned} t_{1\,ij}(k) &= 0 \\ t_{2\,in}(k) &= -G_{P\,in}(k) \\ t_{3\,mj}(k) &= \begin{cases} -1 & \text{if } m = j \text{ and } k = 0 \\ 0 & \text{otherwise} \end{cases} \end{aligned} \tag{A.13}$$

As a result, (A.9) reduces to:

$$s_{ij}(i_o) = y_{set\,j} \sum_{n=1}^{n_u} \sum_{k=0}^{i_o} q_{nj}(k) \sum_{v=k}^{i_o} G_{P\,in}(v-k) \quad . \tag{A.14}$$

A.2.2 Input response to setpoint changes ($i > n_y$ and $j \leq n_y$)

In this case,

$$\begin{aligned} t_{1\,ij}(k) &= 0 \\ t_{2\,in}(k) &= \begin{cases} -1 & \text{if } i - n_y = n \text{ and } k = 0 \\ 0 & \text{otherwise} \end{cases} \\ t_{3\,mj}(k) &= \begin{cases} -1 & \text{if } m = j \text{ and } k = 0 \\ 0 & \text{otherwise} \end{cases} \end{aligned} \tag{A.15}$$

As a result, (A.9) reduces to:

$$s_{ij}(i_o) = y_{set\,j} \sum_{k=0}^{i_o} q_{(i-n_y)\,j}(k) \quad . \tag{A.16}$$

A.2.3 Output response to disturbances ($i \leq n_y$ and $j > n_y$)

In this case we have:

$$\begin{aligned} t_{1\,ij}(k) &= G_{D\,i(j-n_y)}(k) \\ t_{2\,in}(k) &= -G_{P\,in}(k) \\ t_{3\,mj}(k) &= G_{D\,m(j-n_y)}(k) \end{aligned} \tag{A.17}$$

As a result, (A.9) reduces to:

$$s_{ij}\ (i_o) = d_{(j-n_y)} \sum_{k=0}^{i_o} G_{D\,i(j-n_y)}\,(k) - d_{(j-n_y)} \sum_{m=1}^{n_y} \sum_{n=1}^{n_u} \sum_{k=0}^{i_o} q_{nm}(k) \sum_{v=k}^{i_o} \sum_{\ell=k}^{v} G_{D\,m(j-n_y)}(\ell-k)\, G_{P\,in}(v-\ell) \tag{A.18}$$

A.2.4 Input response to disturbances ($i > n_y$ and $j > n_y$)

In this case we have:

$$\begin{aligned} t_{1\,ij}(k) &= 0 \\ t_{2\,in}(k) &= \begin{cases} -1 & \text{if } i - n_y = n \text{ and } k = 0 \\ 0 & \text{otherwise} \end{cases} \\ t_{3\,mj}(k) &= G_{D\,m(j-n_y)}(k) \end{aligned} \tag{A.19}$$

As a result, (A.9) reduces to:

$$s_{ij}(i_o) = -d_{(j-n_y)} \sum_{m=1}^{n_y} \sum_{k=0}^{i_o} q_{(i-n_y)\,m}(k) \sum_{v=k}^{i_o} G_{D\,m(j-n_y)}(v-k) \tag{A.20}$$

A.3 Representing Constraints In Matrix Form

Having simplified the form of the step responses, the next step is to arrange them into matrix form, as required by the optimization software. To simplify matters and to be consistent with the approach adopted in Chapter 5, the regulatory and servo problems are considered independently.

A.3.1 Regulatory problems

In order to simplify matters even further, in the development below it is assumed that only a single disturbance is acting. As a result, the subscript j in s_{ij} is dropped. To recap, the output response to a step of size d in the disturbance is given by:

$$s_i(i_o) = d \sum_{k=0}^{i_o} G_{D\,i}(k) - d \sum_{m=1}^{n_y} \sum_{n=1}^{n_u} \sum_{k=0}^{i_o} q_{nm}(k) \sum_{v=k}^{i_o} \sum_{\ell=k}^{v} G_{D\,m}(\ell-k)\, G_{P\,in}(v-\ell) \tag{A.21}$$

The input response takes the form:

$$s_i(i_o) = -d \sum_{m=1}^{n_y} \sum_{k=0}^{i_o} q_{(i-n_y)\,m}(k) \sum_{v=k}^{i_o} G_{D\,m}(v-k) \tag{A.22}$$

The step responses are arranged in composite vector form as follows:

$$s = [s_1(0), ..., s_1(L), ..., s_{n_z}(0), ..., s_{n_z}(L)]^T \tag{A.23}$$

The coefficients of q are arranged as follows:

$$q = \left[q_{11}^T, \ldots, q_{n_u 1}^T, \ldots, q_{1n_y}^T, \ldots, q_{n_u n_y}^T\right]^T \quad \text{where} \quad q_{ij}^T = [q_{ij}(0), \ldots, q_{ij}(L)]. \tag{A.24}$$

Now, the linear system given by the step responses in (A.21) and (A.22) may be compactly represented as follows:

$$\begin{aligned} s = \begin{bmatrix} s_{\text{out}} \\ s_{\text{inp}} \end{bmatrix} &= A\,q + b \\ &= \begin{bmatrix} d\,A_{\text{out}} \\ d\,A_{\text{inp}} \end{bmatrix} q + \begin{bmatrix} d\,b_{\text{out}} \\ 0 \end{bmatrix} \end{aligned} \tag{A.25}$$

For a single disturbance, the coefficient matrix A_{out} has $n_y.(L+1)$ rows and $n_u.n_y.(L+1)$ columns. Similarly, A_{inp} has $n_u.(L+1)$ rows and the same number of columns. In order to get an idea of the structure of A_{out} and A_{inp}, both of these matrices will be shown in greater detail for the case where $n_y = n_u = 2$. Extensions to higher dimensions are immediate.

The matrix A_{out} may be viewed as being comprised by a number of submatrices which are each formed by different combinations of the elements of G_D and G_P. For a 2×2 system, A_{out} may be written in a symbolic fashion as follows:

$$A_{\text{out}} = - \begin{bmatrix} G_{P11}G_{D1} & G_{P12}G_{D1} & G_{P11}G_{D2} & G_{P21}G_{D2} \\ G_{P21}G_{D1} & G_{P22}G_{D1} & G_{P21}G_{D2} & G_{P22}G_{D2} \end{bmatrix} \tag{A.26}$$

In the above, each of the submatrices $G_{Pin}G_{Dm}$ is a lower triangular Toeplitz matrix of the form:

$$\begin{bmatrix} G_{Dm}(0)\,G_{Pin}(0) & 0 & \cdots & \cdots & 0 \\ \sum_{v=0}^{1}\sum_{\ell=0}^{v} G_{Dm}(\ell)\,G_{Pin}(v-\ell) & G_{Dm}(0)\,G_{Pin}(0) & & & \vdots \\ \vdots & & \ddots & & \vdots \\ \vdots & & & \ddots & 0 \\ \sum_{v=0}^{L}\sum_{\ell=0}^{v} G_{Dm}(\ell)\,G_{Pin}(v-\ell) & \sum_{v=0}^{L-1}\sum_{\ell=0}^{v} G_{Dm}(\ell)\,G_{Pin}(v-\ell) & \cdots & \cdots & G_{Dm}(0)\,G_{Pin}(0) \end{bmatrix} \tag{A.27}$$

The Toeplitz nature in the above matrix arises from the fact that in (A.21),

$$\begin{aligned} & \sum_{v=k+1}^{i_o+1}\sum_{\ell=k+1}^{v} G_{Dm}(\ell-k-1)\,G_{Pin}(v-\ell) \qquad (A.28) \\ = & \sum_{v'=k}^{i_o}\sum_{\ell'=k}^{v'} G_{Dm}(\ell'-k)\,G_{Pin}(v'-\ell') \\ = & \sum_{v=k}^{i_o}\sum_{\ell=k}^{v} G_{Dm}(\ell-k)\,G_{Pin}(v-\ell) \end{aligned}$$

The coefficient matrix A_{inp} has the following structure for a 2×2 process:

$$A_{\text{inp}} = - \begin{bmatrix} G_{D1} & 0 & G_{D2} & 0 \\ 0 & G_{D1} & 0 & G_{D2} \end{bmatrix} \tag{A.29}$$

where the submatrix G_{Dm} is a lower triangular Toeplitz matrix of the form:

$$G_{Dm} = \begin{bmatrix} G_{Dm}(0) & 0 & \cdots & \cdots & 0 \\ G_{Dm}(0) + G_{Dm}(1) & G_{Dm}(0) & & & \vdots \\ \vdots & & \ddots & & \vdots \\ \vdots & & & \ddots & 0 \\ \sum_{v=0}^{L} G_{Dm}(v) & \sum_{v=0}^{L-1} G_{Dm}(v) & \cdots & \cdots & G_{Dm}(0) \end{bmatrix} \tag{A.30}$$

It is straightforward to see from (A.21) that the vector b_{out} takes the form:

$$b_{\text{out}} = \begin{bmatrix} G_{D1}(0) \\ G_{D1}(0) + G_{D1}(1) \\ \vdots \\ \sum_{k=0}^{L} G_{D1}(k) \\ G_{D2}(0) \\ G_{D2}(0) + G_{D2}(1) \\ \vdots \\ \sum_{k=0}^{L} G_{D2}(k) \end{bmatrix} \tag{A.31}$$

A.3.2 Servo problems

In the discussion below it is assumed that the setpoints act individually. This is not a necessary assumption but simplifies the development. To recap, the output response to a step in the jth setpoint is given by:

$$s_{ij}(i_o) = y_{set\,j} \sum_{n=1}^{n_u} \sum_{k=0}^{i_o} q_{nj}(k) \sum_{v=k}^{i_o} G_{P\,in}(v-k) \quad . \tag{A.32}$$

Similarly, the input response is given by ($i > n_y$):

$$s_{ij}(i_o) = y_{set\,j} \sum_{k=0}^{i_o} q_{(i-n_y)\,j}(k) \tag{A.33}$$

The step response coefficients are arranged in composite vector form as follows:

$$s = \left[s_{11}^T, ..., s_{n_z\,1}^T, ..., s_{1\,n_w}^T, ..., s_{n_z\,n_w}^T \right]^T \tag{A.34}$$

where $n_z = n_y + n_u$, $n_w = n_y$ and $s_{ij}^T = [s_{ij}(0), ..., s_{ij}(L)]$.

The coefficients of q are arranged as follows:

$$q = \left[q_{11}^T, \ldots, q_{n_u 1}^T, \ldots, q_{1 n_y}^T, \ldots, q_{n_u n_y}^T\right]^T \quad \text{where} \quad q_{ij}^T = [q_{ij}(0), \ldots, q_{ij}(L)]. \tag{A.35}$$

Now, the linear system given by the step responses in (A.32) and (A.33) may be compactly represented as follows:

$$\begin{aligned} s = \begin{bmatrix} s_{\text{out}} \\ s_{\text{inp}} \end{bmatrix} &= Aq \\ &= \begin{bmatrix} A_{\text{out}} \\ A_{\text{inp}} \end{bmatrix} q \end{aligned} \tag{A.36}$$

The coefficient matrix A_{out} has $n_w.n_y.(L+1)$ rows and $n_u.n_y.(L+1)$ columns. Similarly, A_{inp} has $n_w.n_u.(L+1)$ rows and the same number of columns. To understand the structure of A_{out} and A_{inp}, these matrices will be shown in greater detail for the case where $n_y = n_u = 2$. Extensions to higher dimensions are straightforward.

The matrix A_{out} may be written in shorthand form for a 2×2 system as follows:

$$A_{\text{out}} = \begin{bmatrix} G_{P11}Y_{set\,1} & G_{P12}Y_{set\,1} & 0 & 0 \\ G_{P21}Y_{set\,1} & G_{P22}Y_{set\,1} & 0 & 0 \\ 0 & 0 & G_{P11}Y_{set\,2} & G_{P12}Y_{set\,2} \\ 0 & 0 & G_{P21}Y_{set\,2} & G_{P22}Y_{set\,2} \end{bmatrix} \tag{A.37}$$

The lower triangular submatrix $G_{P\,in}Y_{set\,j}$ takes the form:

$$G_{P\,in}Y_{set\,j} = y_{set\,j} \begin{bmatrix} G_{P\,in}(0) & 0 & \cdots & \cdots & 0 \\ G_{P\,in}(0) + G_{P\,in}(1) & G_{P\,in}(0) & 0 & & \vdots \\ \vdots & & \ddots & 0 & \vdots \\ \vdots & & & \ddots & 0 \\ \sum_{v=0}^{L} G_{P\,in}(v) & \sum_{v=0}^{L-1} G_{P\,in}(v) & \cdots & \cdots & G_{P\,in}(0) \end{bmatrix} \tag{A.38}$$

In a similar manner, the coefficient matrix A_{inp} may be written as follows for a 2×2 system:

$$A_{\text{inp}} = \begin{bmatrix} Y_{set\,1} & 0 & 0 & 0 \\ 0 & Y_{set\,1} & 0 & 0 \\ 0 & 0 & Y_{set\,2} & 0 \\ 0 & 0 & 0 & Y_{set\,2} \end{bmatrix} \tag{A.39}$$

where the lower triangular Toeplitz submatrix $Y_{set\,j}$ is takes the form:

$$Y_{set\,j} = y_{set\,j} \begin{bmatrix} 1 & 0 & \cdots & 0 \\ \vdots & 1 & 0 & \vdots \\ \vdots & & \ddots & 0 \\ 1 & \cdots & \cdots & 1 \end{bmatrix} \tag{A.40}$$

Clearly, there is considerable sparsity in both A_{out} and A_{inp}. By exploiting the structure and sparsity of the constraint system it is possible to obtain significant reductions in computational time. Chapter 5 provides details on how this has been done and includes illustrative examples demonstrating the reductions possible.

Appendix B

Transfer Function Model Parameters For Flotation Study

The transfer functions used to model the dynamic behavior of the circuit are second-order-plus-zero transfer functions of the form:

$$G_{ij}(s) = \frac{k_{ij}(\tau_{a\,ij}\,s + 1)}{(\tau_{1\,ij}\,s + 1)(\tau_{2\,ij}\,s + 1)} \tag{B.1}$$

The model parameters for the (1,1) element of $G_P(s)$, relating grade to the air factor, are as follows:

Flowsheet	1	2	3	4	8	9
k_{11}	-22.311	-22.630	-20.912	-21.774	-22.354	-21.841
$\tau_{a\,11}$	0.0498	0	5.428	20.319	18.621	0.0021
$\tau_{1\,11}$	7.275	7.178	9.817	16.826	15.061	3.300
$\tau_{2\,11}$	3.947	3.031	5.842	16.826	15.010	7.901

The model parameters for the (1,2) element of $G_P(s)$ relating grade to the feed water flowrate, are as follows:

Flowsheet	1	2	3	4	8	9
k_{12}	-2.000	-1.625	10.364	13.656	11.52	-1.621
$\tau_{a\,12}$	0	0	0	17.177	14.232	0
$\tau_{1\,12}$	9.480	18.601	7.059	13.911	11.525	6.101
$\tau_{2\,12}$	0.290	2.129	0.287	13.911	11.525	0.983

Of interest in the above table is the fact that the gains for flowsheets 3,4 and 8 are approximately an order of magnitude larger than those for flowsheets 1,2 and 9 and are of opposite sign.

The model parameters for the (2,1) element of $G_P(s)$, relating recovery to the air factor, are as follows:

Flowsheet	1	2	3	4	8	9
k_{21}	10.026	8.991	14.619	12.082	10.089	11.430
$\tau_{a\ 21}$	103.25	112.55	61.799	102.40	106.88	91.748
$\tau_{1\ 21}$	9.569	10.054	10.011	12.901	11.090	10.798
$\tau_{2\ 21}$	0.1365	0.0891	0.4097	0.0614	0.0687	0.0847

The model parameters for the (2,2) element of $G_P(s)$, relating recovery to the feed water flowrate, are as follows:

Flowsheet	1	2	3	4	8	9
k_{22}	-7.062	-5.679	-10.461	-10.625	-7.669	-5.600
$\tau_{a\ 22}$	0	0	22.547	36.333	28.315	63.029
$\tau_{1\ 22}$	9.437	17.347	2.0206	13.859	9.421	66.432
$\tau_{2\ 22}$	0.292	2.511	10.546	2.733	2.283	6.358

The model parameters for the (1,1) element of $G_D(s)$, relating grade to the feed disturbance, are as follows:

Flowsheet	1	2	3	4	8	9
k_{11}	1.97e-2	1.97 e-2	9.18 e-3	5.89 e-3	8.73 e-3	1.90 e-2
$\tau_{a\ 11}$	0	0	3.316	5.971	5.724	0
$\tau_{1\ 11}$	8.847	8.703	9.326	14.209	11.764	8.916
$\tau_{2\ 11}$	2.844	2.548	9.326	14.209	11.764	2.560

The model parameters for the (2,1) element of $G_D(s)$, relating recovery to the feed disturbance, are as follows:

Flowsheet	1	2	3	4	8	9
k_{21}	-3.55 e-3	-3.68 e-3	-5.28 e-3	-3.47 e-3	-3.75 e-3	-6.08 e-3
$\tau_{a\,21}$	266.936	250.122	91.392	191.123	176.758	145.656
$\tau_{1\,21}$	12.990	12.567	7.318	9.740	9.685	12.442
$\tau_{2\,21}$	0	0	0	0	0	0